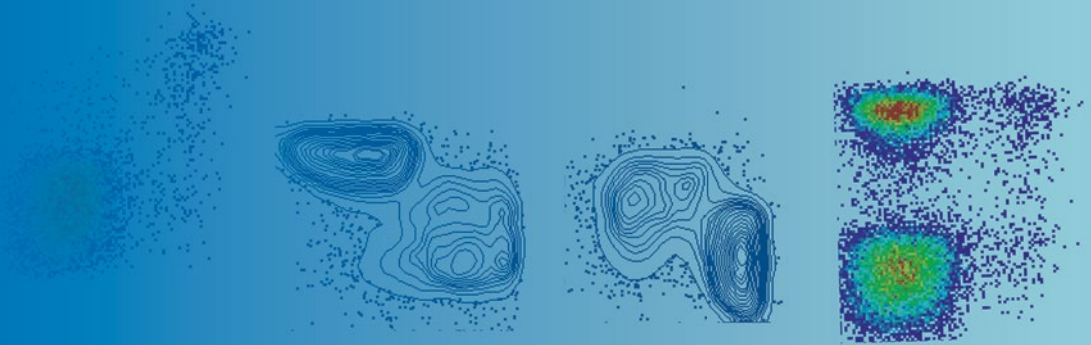


Methods in  
Molecular Biology 1514

Springer Protocols



Enrico Lugli *Editor*

# T-Cell Differentiation

Methods and Protocols

**EXTRAS ONLINE**

 Humana Press

# METHODS IN MOLECULAR BIOLOGY

*Series Editor*  
**John M. Walker**  
**School of Life and Medical Sciences**  
**University of Hertfordshire**  
**Hatfield, Hertfordshire, AL10 9AB, UK**

For further volumes:  
<http://www.springer.com/series/7651>

# **T-Cell Differentiation**

## **Methods and Protocols**

Edited by

**Enrico Lugli**

*Laboratory of Translational Immunology, Humanitas Clinical & Research Center, Rozzano, Italy*

 **Humana Press**

*Editor*

Enrico Lugli  
Laboratory of Translational Immunology  
Humanitas Clinical & Research Center  
Rozzano, Italy

ISSN 1064-3745                      ISSN 1940-6029 (electronic)  
Methods in Molecular Biology  
ISBN 978-1-4939-6546-5            ISBN 978-1-4939-6548-9 (eBook)  
DOI 10.1007/978-1-4939-6548-9

Library of Congress Control Number: 2016952630

© Springer Science+Business Media New York 2017

This work is subject to copyright. All rights are reserved by the Publisher, whether the whole or part of the material is concerned, specifically the rights of translation, reprinting, reuse of illustrations, recitation, broadcasting, reproduction on microfilms or in any other physical way, and transmission or information storage and retrieval, electronic adaptation, computer software, or by similar or dissimilar methodology now known or hereafter developed.

The use of general descriptive names, registered names, trademarks, service marks, etc. in this publication does not imply, even in the absence of a specific statement, that such names are exempt from the relevant protective laws and regulations and therefore free for general use.

The publisher, the authors and the editors are safe to assume that the advice and information in this book are believed to be true and accurate at the date of publication. Neither the publisher nor the authors or the editors give a warranty, express or implied, with respect to the material contained herein or for any errors or omissions that may have been made.

Printed on acid-free paper

This Humana Press imprint is published by Springer Nature  
The registered company is Springer Science+Business Media LLC  
The registered company address is: 233 Spring Street, New York, NY 10013, U.S.A.

---

## Preface

T cells are important effectors of the adaptive immune system. Potent T cell responses with superior quality can mediate cancer regression or control chronic viral infections while, on the other hand, exacerbated immune responses may lead to the development of autoimmune diseases. Hence, T cells are not equal in different pathological conditions; rather the T cell compartment is characterized by extreme heterogeneity, with dozens of subsets displaying differential cytokine production, metabolic activity, tissue tropism, immune reconstitution potential, or persistence in the long term. Characterization of context-specific heterogeneity is fundamental to understand the biological basis of disease pathogenesis or to exploit T cell-based responses in immunotherapeutic approaches.

This volume reports the description of established and cutting-edge technologies that are helpful to characterize the biology of T cells at sufficient depth. After reviewing the diversity of the memory T cell compartment (Pedro Romero and colleagues) and the heterogeneity of the T helper cell pool (Gagliani and Huber), I give ample space to the presentation of technologies that are capable of determining T cell features at single cell level. Flow cytometry and fluorescence-activated cell sorting (FACS; described in this volume by my group) are the best example of quantitative single cell analysis that helped very much the identification of naïve and memory T cell subsets. Additional technologies were implemented more recently and now allow to determine the behavior of single T cells after adoptive cell transfer (ACT) *in vivo* in real time (the intravital microscopy described by Matteo Iannacone and colleagues), the dynamics of intracellular proteins (the confocal imaging approach described by Larghi and colleagues), and single cell gene expression by multiplex PCR of preselected genes or by sequencing of the whole transcriptome (Chattopadhyay and colleagues and Villani and Kerkar, respectively).

T cells display their effector functions following activation of the T cell receptor (TCR) by their cognate peptide. Antigen-specific T cells with the same phenotype but different affinities/avidities of the TCR may display differential downstream effector functions. Kvistborg and colleagues describe a protocol to analyze dozens, potentially hundreds, of specificities by using combinatorial MHC class I tetramer staining by flow cytometry, thus allowing to monitor antigen-specific T cell responses with a limited amount of patient material. Antigen-specific T cells are now used in certain clinical protocols to mediate tumor regression or control chronic viral infections following adoptive T cell transfer *in vivo*. These approaches have definitively demonstrated, after decades of preclinical evaluations, that the immune system can effectively respond against tumors in humans *in vivo*. Lentiviral transduction approaches such as that described by Davila and colleagues confer a single specificity to a given T cell subset (or T cell product) through the transfer of antitumor TCRs or chimeric antigen receptors (CARs) before ACT. Importantly, not all T cell subsets are suitable in this regard: indeed, more differentiated T cells, such as effector memory or terminal effector T cells, are more exhausted (analysis of T cell exhaustion described by Boswell and Yamamoto) and display weaker effector functions overall compared to less differentiated T memory stem cells or central memory cells. To this purpose, Zanon and I describe a protocol to derive large numbers of early-differentiated memory T cells by

using dedicated cytokine cocktails, while Alessio Lanna describes an approach to measure telomerase activity in terminally differentiated, senescent T cells. Similarly, Annunziato and Maggi report approaches to differentiate subsets of CD4<sup>+</sup> T helper cells from naïve precursors and to evaluate their functional capacity. Among these CD4<sup>+</sup> T cells, a subset of cells called regulatory T (Treg) cells inhibits effector T cell responses. Such regulation is beneficial in the context of autoimmune diseases but can be detrimental in cancer patients. Piconese and colleagues describe approaches to define Treg cells at the phenotypic and functional level.

MicroRNAs and long noncoding RNAs (lncRNAs) are emerging as important regulators of T cell gene expression, differentiation, and function. Indeed, different T helper cell subsets may display differential microRNA profiles while specific microRNAs have been shown to regulate effector vs. memory differentiation. Trifari and colleagues and Pagani and colleagues report qPCR and next-generation sequencing approaches as well as bioinformatic workflows to quantify microRNAs and lncRNAs in purified T cell subsets, respectively.

The final part of the book is dedicated to the analysis of the differentiation and effector functions of innate T cells, namely the well-known CD3<sup>+</sup>CD4<sup>-</sup>CD8<sup>-</sup>  $\gamma\delta$  T cells (Silva-Santos and colleagues) and the recently identified CD8<sup>+</sup> mucosal associated invariant T (MAIT) cells (Leeansyah and colleagues). These lineages are involved in antitumor and antimicrobial immune responses both in mice and in humans; therefore it is important to define protocols to correctly identify these cells and to determine their effector functions *ex vivo*.

The recent success of checkpoint inhibitors blockade and ACT immunotherapy instilled new hope for the treatment of cancers and viral infections. Similarly, many biological therapies influence directly or indirectly the function of the immune system, which in turn favors the success of the treatment. I am confident that the protocols provided here will be important to monitor the T cell compartment at the level of single cells in pathological and immunotherapy conditions.

*Milan, Italy*

*Enrico Lugli*

---

# Contents

<i>Preface</i> . . . . .	<i>v</i>
<i>Contributors</i> . . . . .	<i>ix</i>
1 The Vast Universe of T Cell Diversity: Subsets of Memory Cells and Their Differentiation . . . . .	1
<i>Camilla Jandus, Amaia Martínez Usatorre, Selena Viganò, Lianjun Zhang, and Pedro Romero</i>	
2 Basic Aspects of T Helper Cell Differentiation . . . . .	19
<i>Nicola Gagliani and Samuel Huber</i>	
3 FACS Analysis of Memory T Lymphocytes . . . . .	31
<i>Enrico Lugli, Veronica Zanon, Domenico Mavilio, and Alessandra Roberto</i>	
4 Intravital Microscopy Analysis of Hepatic T Cell Dynamics . . . . .	49
<i>Alexandre Pierre Benechet, Lucia Ganzer, and Matteo Iannacone</i>	
5 Analysis of T Cell Activation by Confocal Microscopy . . . . .	63
<i>Paola Larghi, Antonella Viola, and Barbara Molon</i>	
6 Phenotypic and Functional Analysis of Antigen-Specific T Cell Exhaustion . . .	83
<i>Kristin L. Boswell and Takuya Yamamoto</i>	
7 pMHC Multiplexing Strategy to Detect High Numbers of T Cell Responses in Parallel . . . . .	93
<i>Daisy Philips, Marlous van den Braber, Ton N. Schumacher, and Pia Kvistborg</i>	
8 Differentiation of Diverse Progenies of Memory T Cells from Naïve CD8 <sup>+</sup> T Cell Precursors . . . . .	103
<i>Veronica Zanon and Enrico Lugli</i>	
9 Gammaretroviral Production and T Cell Transduction to Genetically Retarget Primary T Cells Against Cancer . . . . .	111
<i>Gongbo Li, Kyungho Park, and Marco L. Davila</i>	
10 Measuring Telomerase Activity in Senescent Human T Cells Upon Genetic Modification . . . . .	119
<i>Alessio Lanna</i>	
11 Strategies for T Helper Cell Subset Differentiation from Naïve Precursors . . .	127
<i>Francesco Annunziato and Laura Maggi</i>	
12 Phenotypic and Functional Analysis of the Suppressive Function of Human Regulatory T Cells . . . . .	139
<i>Eleonora Timperi, Vincenzo Barnaba, and Silvia Piconese</i>	
13 Approaches to Detect microRNA Expression in T Cell Subsets and T Cell Differentiation . . . . .	153
<i>Silvia Monticelli, Tarmo Äijö, and Sara Trifari</i>	

14 Next-Generation Sequencing Analysis of Long Noncoding RNAs  
in CD4+ T Cell Differentiation . . . . . 173  
*Valeria Ranzani, Alberto Arrigoni, Grazisa Rossetti, Ilaria Panzeri,  
Sergio Abrignani, Raoul J. P. Bonnal, and Massimiliano Pagani*

15 Highly Multiplexed, Single Cell Transcriptomic Analysis  
of T-Cells by Microfluidic PCR . . . . . 187  
*Maria Dominguez, Mario Roederer, and Pratip K. Chattopadhyay*

16 Single-cell RNA Sequencing of Human T Cells . . . . . 203  
*Alexandra-Chloé Villani and Karthik Shekhar*

17 Extensive Phenotypic Analysis, Transcription Factor Profiling, and Effector  
Cytokine Production of Human MAIT Cells by Flow Cytometry . . . . . 241  
*Joana Dias, Johan K. Sandberg, and Edwin Leeansyah*

18 Developmental and Functional Assays to Study Murine  
and Human  $\gamma\delta$  T Cells . . . . . 257  
*Julie C. Ribot, Karine Serre, and Bruno Silva-Santos*

*Index* . . . . . 269

---

## Contributors

FRANCESCO ANNUNZIATO • *Department of Experimental and Clinical Medicine, University of Florence, Florence, Italy; Regenerative Medicine Unit, Careggi University Hospital, Florence, Italy*

SERGIO ABRIGNANI • *Istituto Nazionale Genetica Molecolare ‘Romeo ed Enrica Invernizzi’, Milan, Italy; Department of Clinical Sciences and Community Health, Università degli Studi di Milano, Milano, Italy*

TARMO ÄIJÖ • *Simons Center for Data Analysis, Simons Foundation, New York, NY, USA*

ALBERTO ARRIGONI • *Istituto Nazionale Genetica Molecolare ‘Romeo ed Enrica Invernizzi’, Milan, Italy*

VINCENZO BARNABA • *Dipartimento di Medicina Interna e Specialità Mediche, Sapienza Università di Roma, Rome, Italy; Istituto Pasteur-Fondazione Cenci Bolognetti, Rome, Italy*

ALEXANDRE PIERRE BENECHET • *Division of Immunology, Transplantation and Infectious Diseases, IRCCS San Raffaele Scientific Institute, Milan, Italy*

RAOUL J.P. BONNAL • *Istituto Nazionale Genetica Molecolare ‘Romeo ed Enrica Invernizzi’, Milan, Italy*

KRISTIN L. BOSWELL • *Immunology Laboratory, Vaccine Research Center, NIAID, NIH, Bethesda, MD, USA*

PRATIP K. CHATTOPADHYAY • *Immunotechnology Section, Vaccine Research Center, NIH, Bethesda, MD, USA*

MARCO L. DAVILA • *H. Lee Moffitt Cancer Center and Research Institute, Tampa, FL, USA*

JOANA DIAS • *Center for Infectious Medicine, Department of Medicine, Karolinska Institutet, Karolinska University Hospital Huddinge, Stockholm, Sweden*

MARIA DOMINGUEZ • *Immunotechnology Section, Vaccine Research Center, NIH, Bethesda, MD, USA*

NICOLA GAGLIANI • *Department of General, Visceral and Thoracic Surgery, University Medical Center Hamburg-Eppendorf, Hamburg, Germany; I Medical Department, University Medical Center Hamburg-Eppendorf, Hamburg, Germany*

LUCIA GANZER • *Division of Immunology, Transplantation and Infectious Diseases, IRCCS San Raffaele Scientific Institute, Milan, Italy*

SAMUEL HUBER • *I Medical Department, University Medical Center Hamburg-Eppendorf, Hamburg, Germany*

MATTEO IANNAcone • *Division of Immunology, Transplantation and Infectious Diseases, IRCCS San Raffaele Scientific Institute, Milan, Italy; Vita-Salute San Raffaele University, Milan, Italy; Experimental Imaging Center, IRCCS San Raffaele Scientific Institute, Milan, Italy*

CAMILLA JANDUS • *Translational Tumor Immunology group, Ludwig Cancer Research Center, University of Lausanne, Lausanne, Switzerland*

PIA KVISTBORG • *Division of immunology, The Netherlands Cancer Institute, Amsterdam, The Netherlands*

ALESSIO LANNA • *Division of Infection and Immunity, University College London, London, UK; Kennedy Institute of Rheumatology, NDORMS, University of Oxford, Oxford, UK*

- PAOLA LARGHI • *Department of Pathophysiology and Transplantation, University of Milan, Milan, Italy; Istituto Nazionale Genetica Molecolare ‘Romeo ed Enrica Invernizzi’, INGM, Milan, Italy*
- EDWIN LEEANSYAH • *Center for Infectious Medicine, Department of Medicine, Karolinska Institutet, Karolinska University Hospital Huddinge, Stockholm, Sweden; Program in Emerging Infectious Diseases, Duke–National University of Singapore Medical School, Singapore, Singapore*
- GONGBO LI • *H. Lee Moffitt Cancer Center and Research Institute, Tampa, FL, USA*
- ENRICO LUGLI • *Laboratory of Translational Immunology, Humanitas Clinical and Research Center, Rozzano, Milan, Italy*
- LAURA MAGGI • *Department of Experimental and Clinical Medicine, University of Florence, Florence, Italy; Regenerative Medicine Unit, Careggi University Hospital, Florence, Italy*
- DOMENICO MAVILIO • *Unit of Clinical and Experimental Immunology, Humanitas Clinical and Research Center, Rozzano, Milan, Italy; Department of Medical Biotechnologies and Translational Medicine (BioMeTra), University of Milan, Milan, Italy*
- BARBARA MOLON • *Department of Biomedical Sciences, University of Padua, Padua, Italy; Venetian Institute of Molecular Medicine, VIMM, Padua, Italy*
- SILVIA MONTICELLI • *Institute for Research in Biomedicine, Università della Svizzera italiana (USI), Bellinzona, Switzerland*
- MASSIMILIANO PAGANI • *Istituto Nazionale Genetica Molecolare ‘Romeo ed Enrica Invernizzi’, Milan, Italy; Department of Medical Biotechnology and Translational Medicine, Università degli Studi di Milano, Milano, Italy*
- ILARIA PANZERI • *Istituto Nazionale Genetica Molecolare ‘Romeo ed Enrica Invernizzi’, Milan, Italy*
- KYUNGHO PARK • *H. Lee Moffitt Cancer Center and Research Institute, Tampa, FL, USA*
- DAISY PHILIPS • *Division of Immunology, The Netherlands Cancer Institute, Amsterdam, The Netherlands*
- SILVIA PICONESE • *Dipartimento di Medicina Interna e Specialità Mediche, Sapienza Università di Roma, Rome, Italy; Istituto Pasteur-Fondazione Cenci Bolognetti, Rome, Italy*
- VALERIA RANZANI • *Istituto Nazionale Genetica Molecolare ‘Romeo ed Enrica Invernizzi’, Milan, Italy*
- JULIE C. RIBOT • *Instituto de Medicina Molecular, Faculdade de Medicina, Universidade de Lisboa, Lisboa, Portugal*
- ALESSANDRA ROBERTO • *Laboratory of Translational Immunology, Humanitas Clinical and Research Center, Rozzano, Milan, Italy*
- MARIO ROEDERER • *Immunotechnology Section, Vaccine Research Center, NIH, Bethesda, MD, USA*
- PEDRO ROMERO • *Translational Tumor Immunology Group, Ludwig Cancer Research Center, University of Lausanne, Lausanne, Switzerland*
- GRAZISA ROSSETTI • *Istituto Nazionale Genetica Molecolare ‘Romeo ed Enrica Invernizzi’, Milan, Italy*
- JOHAN K. SANDBERG • *Center for Infectious Medicine, Department of Medicine, Karolinska Institutet, Karolinska University Hospital Huddinge, Stockholm, Sweden*
- TON N. SCHUMACHER • *Division of Immunology, The Netherlands Cancer Institute, Amsterdam, The Netherlands*
- KARINE SERRE • *Instituto de Medicina Molecular, Faculdade de Medicina, Universidade de Lisboa, Lisboa, Portugal*

- KARTHIK SHEKHAR • *Broad Institute of MIT and Harvard, Cambridge, MA, USA*
- BRUNO SILVA-SANTOS • *Instituto de Medicina Molecular, Faculdade de Medicina, Universidade de Lisboa, Lisboa, Portugal*
- ELEONORA TIMPERI • *Dipartimento di Medicina Interna e Specialità Mediche, Sapienza Università di Roma, Rome, Italy*
- SARA TRIFARI • *La Jolla Institute for Allergy and Immunology, San Diego, CA, USA*
- AMAIA MARTÍNEZ USATORRE • *Translational Tumor Immunology Group, Ludwig Cancer Research Center, University of Lausanne, Lausanne, Switzerland*
- MARLOUS VAN DEN BRABER • *Division of immunology, The Netherlands Cancer Institute, Amsterdam, The Netherlands*
- SELENA VIGANÒ • *Translational Tumor Immunology Group, Ludwig Cancer Research Center, University of Lausanne, Lausanne, Switzerland*
- ALEXANDRA-CHLOÉ VILLANI • *Broad Institute of MIT and Harvard, Cambridge, MA, USA; Center for Cancer Immunotherapy, Massachusetts General Hospital, Boston, MA, USA*
- ANTONELLA VIOLA • *Department of biomedical Sciences, University of Padua, Padua, Italy; Venetian Institute of Molecular Medicine, VIMM, Padua, Italy*
- TAKUYA YAMAMOTO • *Immunology Laboratory, Vaccine Research Center, NIAID, NIH, Bethesda, MD, USA; Laboratory of Adjuvant Innovation, National Institutes of Biomedical Innovation, Health and Nutrition, Osaka, Japan; Laboratory of Vaccine Science, Immunology Frontier Research Center, World Premier Institute, Osaka University, Osaka, Japan; Center for AIDS Research, Kumamoto University, Kumamoto, Japan*
- VERONICA ZANON • *Laboratory of Translational Immunology, Humanitas Clinical and Research Center, Rozzano, Milan, Italy*
- LIANJUN ZHANG • *Translational Tumor Immunology Group, Ludwig Cancer Research Center, University of Lausanne, Lausanne, Switzerland*

# Chapter 1

## The Vast Universe of T Cell Diversity: Subsets of Memory Cells and Their Differentiation

Camilla Jandus, Amaia Martínez Usatorre, Selena Viganò, Lianjun Zhang, and Pedro Romero

### Abstract

The T cell receptor confers specificity for antigen recognition to T cells. By the first encounter with the cognate antigen, reactive T cells initiate a program of expansion and differentiation that will define not only the ultimate quantity of specific cells that will be generated, but more importantly their quality and functional heterogeneity. Recent achievements using mouse model infection systems have helped to shed light into the complex network of factors that dictate and sustain memory T cell differentiation, ranging from antigen load, TCR signal strength, metabolic fitness, transcriptional programs, and proliferative potential. The different models of memory T cell differentiation are discussed in this chapter, and key phenotypic and functional attributes of memory T cell subsets are presented, both for mouse and human cells. Therapeutic manipulation of memory T cell generation is expected to provide novel unique ways to optimize current immunotherapies, both in infection and cancer.

**Key words** T cell, Differentiation, Memory, Subsets, Antigen, TCR, Vaccine

---

## 1 T Cell Memory

### 1.1 Introduction

Immunological memory, characterized by the ability to respond more rapidly and efficiently to antigens that have been encountered previously, is a unique hallmark of adaptive immunity, and provides the basis for vaccine development.

The concept of immunological memory has existed for several centuries. In the late eighteenth century, it was already well noticed that dairy maids were naturally protected from smallpox after having suffered from cowpox [1, 2]. Edward Jenner has long been recognized for his innovative attempt to control smallpox infection by use of vaccination. Over the past decades, a lot of efforts have thus been made to understand the mechanisms behind the acquired protection by Jenner's vaccination scheme and the acquisition of immunological memory.

CD8 T cells play a crucial role in immunity against infections and cancer [3–9].

In a primary response, naïve CD8 T cells are instructed by antigen, co-stimulatory molecules, and cytokines delivered by mature dendritic cells to undergo clonal expansion and functional differentiation into effector or memory lineages. While the vast majority of the antigen-specific effector T cells undergoes apoptosis soon after antigen clearance, a tiny subset of long lived memory T cells survives and is maintained for long periods of time at relatively high frequencies [10–12].

Herein, we discuss the heterogeneity of CD8 memory T cell populations and how the different subsets are defined based on distinct phenotypic marker expression, migration patterns, and effector functions, both in mouse and human. We also present the models leading to CD8 memory T cell differentiation and describe how these differentiation processes are controlled by TCR signaling and at transcriptional and metabolic levels.

## 1.2 Kinetics of Specific CD8 T Cell Responses

Three phases can be distinguished in CD8 T cell responses: expansion, contraction, and memory phases. Upon infection, pathogen derived antigens are delivered directly or carried by dendritic cells to draining lymph nodes. There, antigen-presenting cells such as dendritic cells will present those antigens to naïve CD8 T cells leading to their activation, differentiation, and **expansion**. Many of those pathogen specific CD8 T cells will then enter the blood and migrate to sites of infection. Following the elimination of the pathogen, CD8 T cells will undergo a massive **contraction**. Most effector CD8 T cells will die and only a small percentage (~5–10%) will survive and form the **memory** CD8 T cell pool that will protect the individual from a secondary infection.

## 1.3 T Cell Memory: Background and Significance

Memory CD8 T cells can provide long time protection against cancers or viral infection, which depends on their enhanced proliferative capacity, their metabolic fitness, their higher transcriptional plasticity, and their life-lasting maintenance [6, 10].

### 1.3.1 T Cell Differentiation Models

Two mechanisms can explain the formation of effector and memory T cells during an immune response (Fig. 1):

“*One cell one fate*”: In this model, memory and effector CD8 T cells derive from different precursors. Naïve T cells are predetermined during thymic development to give rise to effector or memory T cells. However, little evidence supports this model; cellular barcoding experiments have shown that single naïve T cells can give rise to both effector and memory T cells [13] (Fig. 1a).

“*One cell multiple fates*”: Effector and memory T cells can derive from a single naïve T cell clone. The fate decision is taken during T cell priming or in later stages during the T cell response. In that regard, three different models have been proposed to explain effector and memory T cell differentiation and are depicted in Fig. 1b–d.

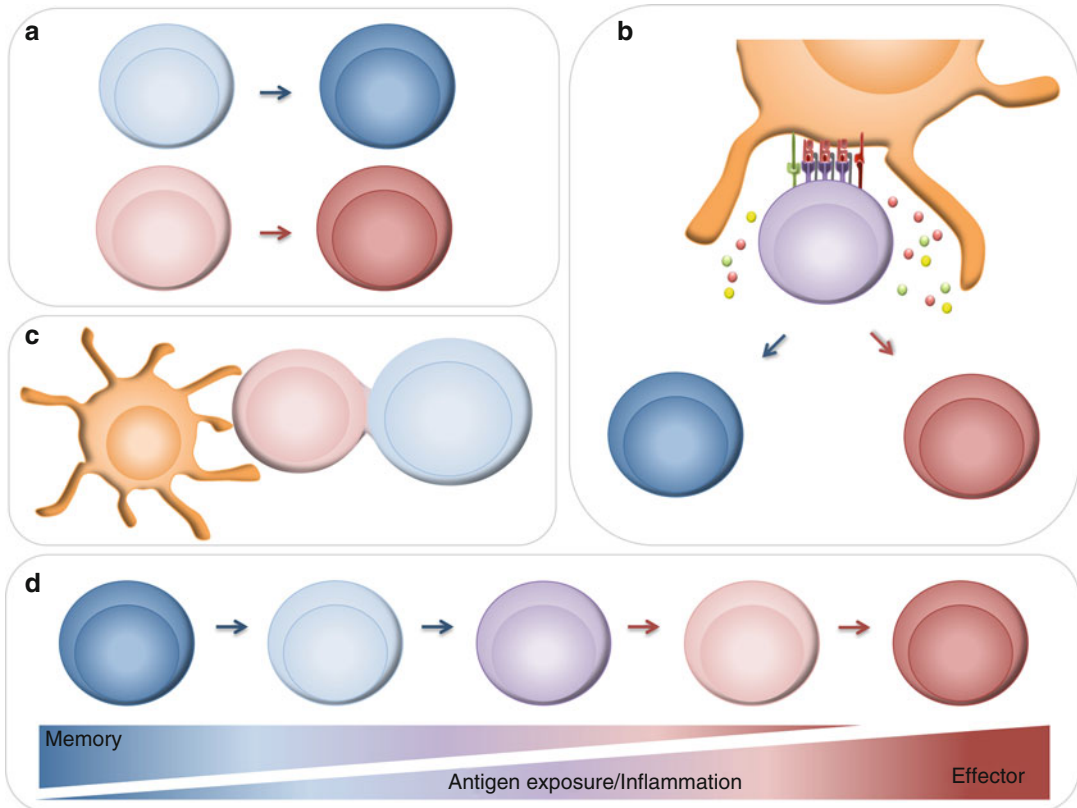


**Fig. 1** Models of CD8 memory T cell differentiation. Schematic representation of the “one cell one fate” (a) and the “one cell multiple fates” models (b–d). Fate decision in the second model might depend, in a non-mutually exclusive manner, on the strength of the signals received during priming (b), on asymmetric cell division at the immunological synapse (c) or on the effect of repetitive antigenic stimulation/inflammation (d)

- *Asymmetric division model:* During the immunological synapse between the antigen presenting cell and the T cell, asymmetric cell division allows the generation of two different daughter cells. Hence, asymmetric inheritance of fate determinants allows the generation of effector and memory T cells not only from naïve T cells in primary responses [14] but also upon pathogen rechallenge of memory T cells [15] (Fig. 1c).
- *Signal strength model:* T cells receive three key signals during T cell priming: antigen recognition (signal 1), co-stimulation (signal 2), and pro-inflammatory cytokines stimulation (signal 3). According to this model the strength of the three signals will determine the expansion amplitude and the fate of the primed T cell [16]. Increased inflammation promotes generation of short lived or terminally differentiated CD8 T cells [17], whereas deficiency in type I interferon signaling promotes IL-7R $\alpha^{\text{high}}$  memory precursor CD8 T cells following infection [18]. Similarly, deficiency of IFN- $\gamma$  or IL-12 increased

the proportion of memory precursor CD8 T cells following lymphocytic choriomeningitis virus (LCMV) and *L. monocytogenes* infection [19] (Fig. 1b).

- *Decreasing-potential model*: Upon repetitive antigen encounter and exposure to pro-inflammatory cytokines, T cells differentiate towards terminal effector T cells. These terminal effector T cells retain their cytolytic capacity but lose memory cell properties such as longevity, proliferative potential, and IL-7R $\alpha$  expression [20]. Therefore, the differentiation state of a T cell depends on the history of signals that it has encountered during infection. Antibiotic treatment after *L. monocytogenes* infection accelerated the production of memory CD8<sup>+</sup> T cells and this could be reverted by CpG-induced inflammation [21] (Fig. 1d).

It must be considered that T cell differentiation models are not mutually exclusive and the combination of them may explain the great T cell diversity.

### 1.3.2 T Cell Memory

*Subsets: Effector Memory T Cells; Central Memory T Cells; Tissue Resident Memory T Cells; Stem Cell Like Memory T Cell*

#### Memory T Cell Subsets

#### T<sub>CM</sub> and T<sub>EM</sub> Paradigm

Memory T cells exhibit considerable heterogeneity in terms of phenotypic, functional, anatomic and developmental perspectives [22–24]. So far, at least four distinct subsets of memory T lymphocytes have been described: central memory T cells (T<sub>CM</sub> cells), effector memory T cells (T<sub>EM</sub> cells), tissue-resident memory T cells (T<sub>RM</sub> cells), and stem cell like memory T cells (T<sub>SCM</sub> cells) [23–26] (Fig. 2).

It has long been recognized that CD8 T<sub>CM</sub> and T<sub>EM</sub> cells differ in their surface marker expression, trafficking properties and localization pattern as well as acquisition of immediate effector function or long term persistence. Fifteen years ago, Sallusto et al. first described the existence of two distinct human memory T cell subsets with different tissue distribution pattern and functional characteristics, termed central memory (T<sub>CM</sub>) and effector memory (T<sub>EM</sub>) populations [27]. T<sub>CM</sub> cells express CD62L and CCR7 and are restricted to the secondary lymphoid tissues. On the other hand, T<sub>EM</sub> cells migrate between peripheral tissues and circulate between the blood and the spleen [23, 24, 27]. T<sub>CM</sub> cells show superior proliferative potential and interleukin-2 (IL-2)-producing capacity whereas T<sub>EM</sub> cells have increased secretion of effector cytokines including IFN- $\gamma$  and show poor persistence when transferred in vivo.

The use of model infection systems such as LCMV [28, 29], ovalbumin expressing *Listeria monocytogenes* (Listeria) and the development of P14 and OT-1 TCR transgenic mouse lines against LCMV epitope gp33-41 and ovalbumin, respectively [4, 30–32], have been key to the great progress made in the past decade towards understanding the cellular and molecular mechanisms underlying CD8 T cell differentiation. Meanwhile, technological

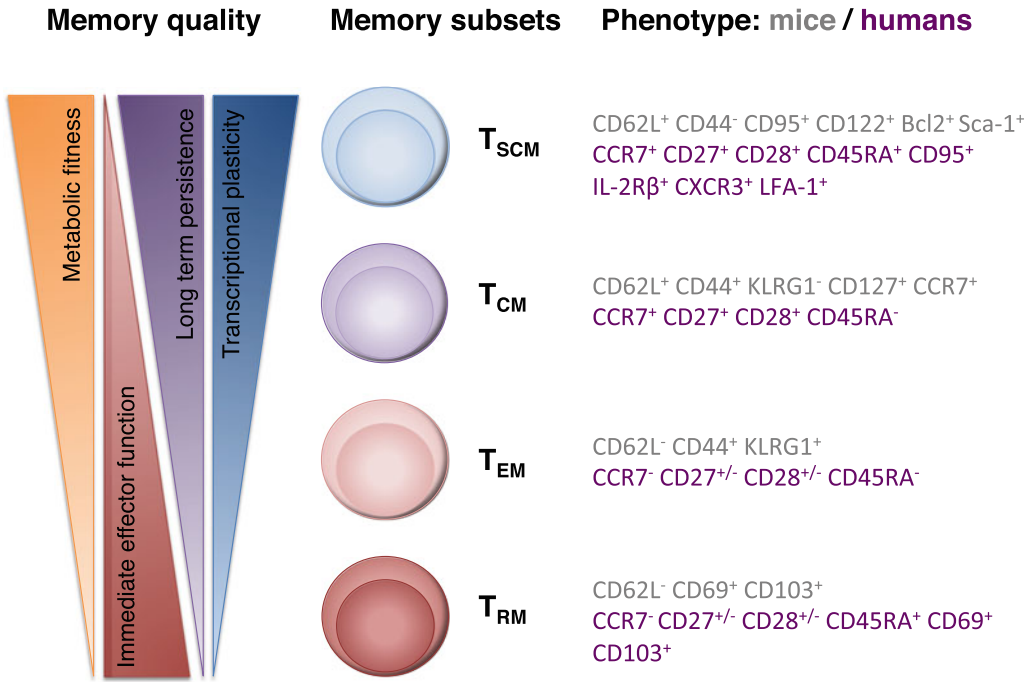


**Fig. 2** CD8 memory T cell subsets. Schematic representation showing the four main CD8 memory T cell subsets (*central panel*), with their respective quality attributes (*left panel*) and the cell surface biomarkers used for their phenotypic characterization in mice (*right panel, grey*) or in humans (*right panel, purple*).  $T_{SCM}$ : stem cell like memory T cells;  $T_{CM}$ : central memory T cells;  $T_{EM}$ : effector memory T cells;  $T_{RM}$ : tissue-resident memory T cells

advances like multicolor flow cytometry analysis, gene arrays as well as peptide/major histocompatibility complex p(MHC) multimer reagents greatly facilitated the progress of this field. Altogether, these techniques have enabled us to directly identify, isolate, quantify and characterize these antigen-specific T cells throughout the entire immune response.

Upon acute microbial infection, CD8 T cells primed by antigen undergo differentiation into SLECs and MPECs, as defined in mouse models of acute infections. SLECs, defined as KLRG1<sup>hi</sup> CD127<sup>lo</sup>, undergo massive apoptosis during the contraction phase once the infection cleared, whereas KLRG1<sup>lo</sup> CD127<sup>hi</sup> MPECs show increased potential to further differentiate into long lived memory lineage cells. Reexposure to antigen by a challenge infection results in the rapid expansion of antigen-specific memory CD8 T cells which differentiate into secondary effector T cells with potent cytokine and lytic responses that can rapidly and efficiently eliminate the pathogen.

#### New Players in the Memory Club

##### $T_{RM}$ Cells

Over the past decade, it has become evident that an important subset of memory T cells—tissue resident memory T ( $T_{RM}$ ) cells—exist in non-lymphoid tissues (NLT), while are absent from blood [25, 33–37]. Thus,  $T_{RM}$  cells reside in barrier tissues at interfaces

with the environment, such as the gastrointestinal (GI) tract, respiratory tract, reproductive tract, skin, and lungs, where they provide the front line response against infections and accelerate pathogen clearance [25, 33–39]. Interestingly, they have also been found in brain, kidney, joints, and other non-barrier tissues in mice and humans [40, 41].

The traditional view is that CD69 is a marker of early T cell activation. However, it is now clear that this marker is extensively expressed in virtually all CD4 and CD8  $T_{RM}$  cells, even if no evidence suggests that these  $T_{RM}$  cells have been recently activated with antigens. CD69 seems rather to be important for peripheral tissue retention of  $T_{RM}$  cells by blocking the surface expression and function of sphingosine 1 phosphate 1 (S1P1) [25, 34, 36, 42]. In line with these observations, the expression of the transcription factor Kruppel-like factor 2 (KLF2), which drives S1P1 expression, is downregulated in  $T_{RM}$  cells. The integrin CD103 is another surface molecule predominantly expressed in CD8  $T_{RM}$  cells in the GI tract and lungs, and also in  $T_{RM}$  cells of the brain after viral infection. It has been shown that CD103<sup>+</sup>  $T_{RM}$  cells have less proliferative potential but significantly increased effector cytokine production capacity than do CD103<sup>-</sup> counterparts.

$T_{RM}$  cells are characterized by their inability to recirculate back into blood or lymph nodes from barrier tissues. Indeed,  $T_{RM}$  cells are not simply memory T cells in the epithelial barriers but rather transcriptionally distinct from the  $T_{CM}$  or  $T_{EM}$  cells. Accumulating evidence suggest that the TCR repertoire may widely differ in  $T_{RM}$  cells from one location to the others. For example, the TCR repertoire in gut  $T_{RM}$  cells is largely different from that of  $T_{RM}$  cells from either the skin or lungs. Intriguingly,  $T_{RM}$  cells from different anatomic locations share common core transcriptomic features.

### *T<sub>SCM</sub> Cells*

$T_{SCM}$  cells represent the most recently identified memory T cell subset in mice, nonhuman primates and in humans [43–45].  $T_{SCM}$  cells have been put at the top of the hierarchy of all memory T cell subsets in a model of progressive T cell differentiation, leading from naïve T ( $T_{naïve}$ ) cells over  $T_{SCM}$  cells and  $T_{CM}$  cells to  $T_{EM}$  cells and  $T_{EFF}$  cells. These cells harbor key therapeutic value by their self-renewal capacity and ability to generate  $T_{CM}$  cells and  $T_{EM}$  cells [43–46].

Gattinoni et al. have shown that CD8  $T_{SCM}$  cells could be generated in the presence of TWS119, a proposed Wnt activator, during priming. TWS119-induced CD8  $T_{SCM}$  cells express high levels of stem cell antigen-1 (Sca-1), CD122, and B-cell lymphoma 2 whereas they remain in the CD44<sup>-</sup>CD62L<sup>+</sup> naïve fraction [43–45]. They display superior persistence and antitumor effects when transferred in vivo, as compared to  $T_{CM}$  or  $T_{EM}$  cells [45]. However, the signaling pathways controlling  $T_{SCM}$  cell formation remain incompletely understood. We have recently unraveled that CD4  $T_{SCM}$  cells can be induced from highly purified naïve cells by pharmacological inhibition of mTORC1 by either rapamycin or, surprisingly, by TWS119

[47]. Moreover, we showed that both compounds can also induce the differentiation of CD8 T<sub>SCM</sub> cells if added in vitro during naïve CD8 T cell activation. Consistently, we prove that these drugs switch T cell metabolism to fatty acid oxidation as favored metabolic program for T<sub>SCM</sub> cell generation. Of note, pharmacologically induced T<sub>SCM</sub> cells possess superior functional features, as long-term repopulation capacity after adoptive transfer. Thus, targeted induction of T<sub>SCM</sub> cells by pharmacological means is highly relevant for the design of novel immunotherapeutic approaches.

In the conditions prevailing in the course of chronic microbial infections or cancer progression, antigen-specific CD8 T cells are thought to undergo differentiation into an “exhausted” state [48], which is characterized by upregulating surface expression of inhibitory molecules like PD-1 and diminished cytokine production. This topic is not discussed here, since it is reviewed by T. Yamamoto and K. Boswell in another chapter of this book.

### 1.3.3 Metabolic Regulation of T Cell Differentiation

Metabolic requirements of T cells change during activation and T cell differentiation. It has recently been described that cytokines and transcription factors that regulate T cell differentiation do also regulate T cell metabolism (reviewed in refs. [49, 50]).

Naïve T cells are arrested at the G<sub>0</sub> stage of the cell cycle, and their energy requirements are relatively low. Therefore, they exhibit basal nutrient uptake levels and use mitochondrial oxidative phosphorylation and fatty acid oxidation for the production of energy in the form of ATP.

Activated T cells, in contrast, are highly proliferative and upregulate anabolic pathways. T cell activation results in increased expression of the glucose transporter GLUT1 to increase glucose influx [51]. The main energy source of activated T cells is aerobic glycolysis. This metabolic pathway allows proliferating T cells to generate the intermediate substrates for nucleotide and fatty acid synthesis in order to meet the demands of cellular division. Moreover, T cell activation leads to a facilitated amino acid transport and amino acid synthesis [52].

Memory T cells, in contrast to effector T cells, mainly use oxidative phosphorylation and fatty acid oxidation. They have higher spare respiratory capacity than effector T cells as they upregulate mitochondrial biogenesis pathways. Moreover, it was shown that the spare respiratory capacity is critical for cell survival under energetic stress [52].

### 1.3.4 Transcriptional Control of Effector and Memory CD8 T Cell Differentiation

Multiple transcription factors have been identified to control CD8 effector or memory differentiation [23, 24, 53]. T-box transcription factors T-bet and Eomesodermin (Eomes) represent two key transcription factors in orchestrating the effector or memory fate decision [17, 23, 24] and the fate decision between SLECs and MPECs [54, 55]. Higher T-bet–Eomes ratio drives terminal

effector differentiation whereas higher Eomes/T-bet favors memory formation. In addition, B lymphocyte induced maturation protein 1 (Blimp-1) and B cell lymphoma 6 (Bcl-6) are reciprocal regulators of CD8 T cell effector and memory differentiation. Blimp-1 enhances the formation of terminally differentiated effectors by directly binding to Bcl-6 to repress its expression [56]. Moreover, Id2- or Id3-deficient mice fail to generate short-lived effector or long-lived memory cells, respectively [57, 58]. Tcf-1, the downstream target of Wnt signaling pathway, is required for CD8 T cell memory generation and recall responses.

## 1.4 T Cell Affinity, Avidity, and Function

### 1.4.1 Definitions and Readouts

TCR pMHC recognition is essential for the activation and differentiation of T cells. Thus, it is not surprising that the strength of the interaction between the TCR and pMHC is directly correlated with the T cell expansion amplitude [32, 59].

Three terms can be defined to describe the T cell–antigen presenting cell/target cell interaction strength: T cell affinity, avidity, and functional avidity (Fig. 3). To assess each of these parameters, different techniques have been developed and are described below.

- *T cell receptor for antigen affinity:*

It is the physical binding strength between a single TCR and pMHC molecule (Fig. 2, left panel). The dissociation constant ( $K_D$ ) between soluble TCR–pMHC measured by surface plasmon resonance (SPR) is the parameter that has mainly been used to define T cell affinity.  $K_D$  measures the tendency of two molecules to dissociate. Therefore, the higher the  $K_D$  the lower it is the T cell affinity.

More recently, NTA-His tag-containing multimers (NTAmers) have been developed. These multimers, as conventional multimers, bind TCRs, but upon imidazole addition they rapidly dissociate into pMHC monomers allowing the measurement of monomeric TCR–pMHC dissociation rates ( $K_{off}$  and  $t_{1/2}$ ). However, unlike SPR experiments, NTAmers measure TCR–pMHC interactions on the cell surface. Therefore, NTAmers but not SPR measure the contribution of the CD8 co-receptor, known to stabilize TCR–pMHC complexes. Nonetheless, NTamer based dissociation kinetics correlate with SPR measured  $K_{off}$  and affinities [60].

- *T cell avidity:*

It is the interaction strength between several TCRs and pMHC molecules (Fig. 2, middle panel). It can be measured by pMHC multimer staining on the cell surface of T cells. The binding of multimeric pMHC to T cells correlates with monomeric TCR–pMHC affinity [11]. Therefore, the fluorescence intensity of pMHC multimer staining can be used to have an idea of the affinity of a T cell for its ligand, avoiding the laborious and expensive production of soluble TCRs for SPR experiments.

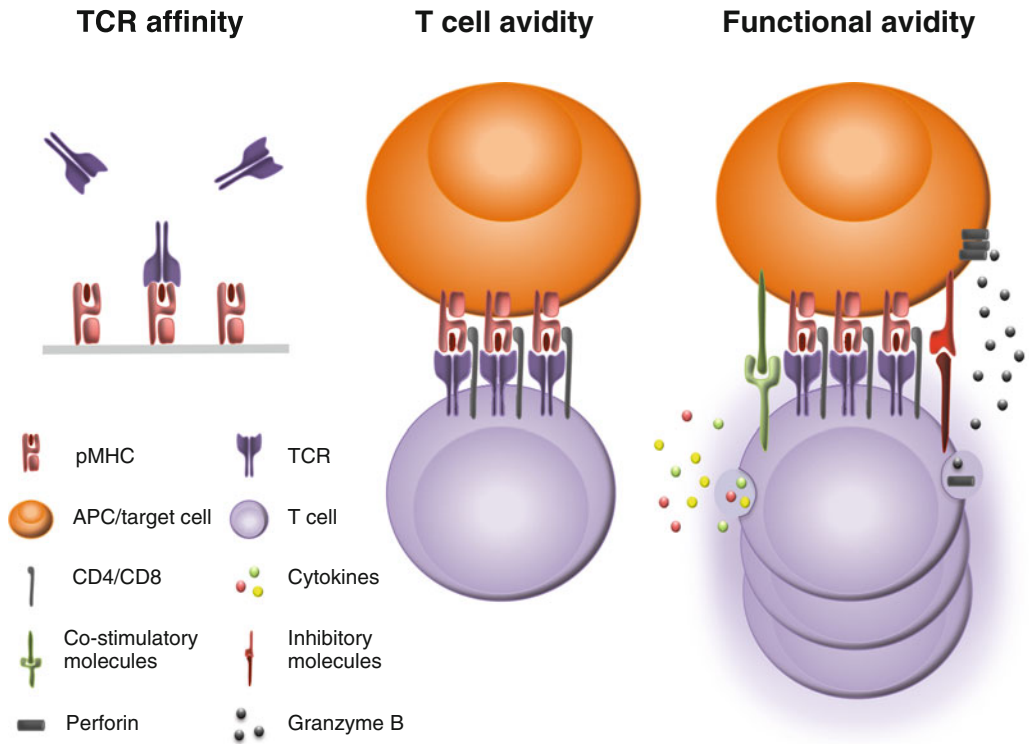


**Fig. 3** Parameters defining TCR affinity, T cell avidity, and functional avidity. Illustration of TCR affinity (*left panel*), defined as physical binding strength between a single pMHC and TCR, T cell avidity (*middle panel*) determined by the interaction between several TCR and pMHC molecules and functional avidity (*right panel*), a quality whose readouts, such as cytokine release or relative target cell killing activity, are influenced by multiple parameters including expression of TCR, pMHC, co-receptors, and adhesion molecules

pMHC multimer staining also reflects the contribution of the CD8 co-receptor molecules [11].

– *Functional avidity of a T cell:*

It is the sensitivity of a T cell to the antigen (Fig. 2, right panel). It inversely correlates with the antigen dose needed for the triggering of a T-cell response. The antigen concentration needed to reach half of a maximum response ( $EC_{50}$ ) is the parameter used to define the functional avidity of a T cell. The main functional readouts are the  $EC_{50}$  for proliferation, cytokine production, and target cell lysis.

As the functional avidity is a cellular, and not an *in silico* measurement, it is influenced by many cellular parameters. T cell affinity normally correlates with functional avidity, yet not always. Expression levels of the TCR, the co-receptors, and the adhesion molecules, also influence the binding strength between a T cell and an antigen presenting cell/target cell. Moreover, expression of inhibitory and co-stimulatory molecules modulates the T cell response and sensitivity to the antigen.

#### 1.4.2 Importance of Functional Avidity

High functional avidity T cell responses mediate efficient virus clearance [61]. In addition, since many tumors are characterized by low antigen presentation and absence of co-stimulatory signals, higher-avidity CD8 T cells promote more efficient tumor rejection [62]. However, low avidity antigen recognition may be useful to better discriminate self-antigens overexpressing tumors from healthy tissues [63], thus preventing autoimmunity. Moreover, when T cells are chronically exposed to the antigen as in chronic infections, low functional avidity T cells may be less sensitive to activation induced cell death, exhaustion, and senescence [64].

#### 1.5 Phenotypic and Functional Characterization of Human Memory T Cells

Similarly to the murine system, a large number of surface markers have been used over time to define populations of human memory T cells (Fig. 3). These markers include CD45RO, CD45RA, CD62L, CD28, CD27, CD7, CD57, CD127, KLRG1, and CCR7. However the two main human memory CD8 T cell subsets are commonly defined using four markers:  $T_{CM}$ : CCR7<sup>+</sup>/CD27<sup>+</sup>/CD28<sup>+</sup>/CD45RA<sup>-</sup>,  $T_{EM}$ : CCR7<sup>-</sup>/CD27<sup>+</sup>/CD28<sup>+</sup>/CD45RA<sup>-</sup> [65–67]. The recently described  $T_{SCM}$  cells in humans are identified among Naïve T cells, but express CD95, IL-2R $\beta$ , CXCR3, and LFA-1, were shown to display functional attributes and transcriptional profile distinctive of memory cells [43, 44] and to persist and preserve their precursor potential for up to 12 years after lymphocyte infusion [68]. Human  $T_{SCM}$  cells are specific to multiple viral and self-tumor antigens [44, 69, 70].

The above-described memory subsets have been mainly characterized in the peripheral blood of healthy individuals and patients. Additional markers have been used to define the resident memory populations present in tissues. Similarly to their murine counterpart, human  $T_{RM}$  cells have been described to express CD69, CD103 and to downregulate CCR7, preventing their migration to secondary lymphoid tissues [35].

The proportions of subsets at different maturation stages vary in healthy individuals depending on the age. In correlation with this observation, aging individuals present several altered immune functions that may explain the development of age-related life-threatening disorders including infections, cancers, and atherosclerosis. Generally, the most striking effect of aging on T cell phenotypes is an increase in the number of differentiated CD28<sup>-</sup> T cells and especially in the T effector cell subset. Among the driving mechanisms for the impaired immune function in the elderly are the repeated and cumulative exposure to pathogens some of which persist throughout life [71] and the concomitant loss of thymic capacity to generate naïve T cells over time [72].

Immunosenescence and exhaustion can however not necessarily be caused by aging of the individual, but are also observed during infections with some pathogens, in cancer and in patients with chronic diseases [73].

### 1.5.1 Characterization of Antigen-Specific T Cell Differentiation in Humans

The most direct and unbiased technique to detect, quantify, and analyze antigen specific T cells by flow cytometry is their labeling by fluorescent MHC-peptide multimers. However, this technique relies on the molecular HLA typing and on the knowledge of which epitopes are recognized by T cells, representing a barrier when working with limited patient's material in the context of immunization. In that regard, using combinatorial peptide-MHC I tetramer staining it has recently been possible to simultaneously identify and thoroughly analyze T cells specific for many epitopes, in a single human blood or tissue-dissociated sample [74, 75]. At the same time, the differentiation phenotype can also be evaluated.

Another way to identify antigen specific T cells, albeit indirect, is to evaluate cytokine production after stimulation with a specific antigen. This has become the method of choice in settings when: (a) multimers cannot be used because of technical issues of production, or HLA restriction is unknown; (b) the biological question requires evaluating the multiple functional properties of the response (phenotype, cytokine production, cytotoxic molecules); (c) the interest is to determine the global T cell response, and not an epitope-specific activity.

Finally, an elegant approach for identification and further characterization of antigen-specific cells relies on combining multimer staining, extracellular staining for differentiation markers, and intracellular staining for cytokines/cytotoxic molecules. This approach allows the most comprehensive analysis of antigen-specific cells, including those unable to produce any cytokines (i.e., exhausted cells). At the same time, the functional profile and phenotype can also be evaluated.

### 1.5.2 T Cell Differentiation Signatures in Distinct Disease Settings

Circulating human antigen-specific T cells are composed of variable proportions of naïve and differentiated cells.

In viral responses, phenotypic profiling of virus-specific CD8 T cells has revealed that antigen-specific T cells are composed of memory cells with heterogeneous differentiation profile that reflects differences in the duration of antigen exposure and persistence, and in the levels of antigen load. Influenza virus infection has been described as a model of antigen clearance and Flu-specific CD8 T cell responses are characterized by high frequency of  $T_{CM}$  cells and lack/low frequency of  $T_{EM}$  cells and T effector cells. Models of protracted antigen exposure, but low antigen load include instead chronic infection with CMV, EBV, HSV, and non-progressive HIV-1 infection, where specific CD8 T cells are principally composed by effector memory and T effector ( $T_{EMRA}$ ) cells.

Finally, progressive HIV-1 infection in untreated patients represent a model of antigen persistence with high antigen load; antigen specific “memory” CD8 T cells in the chronic infection are composed almost exclusively by  $T_{EM}$  cells, a phenotype resembling the one at the effector phase of the response during early infection; however, in this last model the presence and the definition of memory cells are still under debate since the antigen is always detectable [48]. Similarly, in the context of an intracellular bacteria infection such as *Mycobacterium tuberculosis* (Mtb), specific CD8 T cells are mostly  $T_{EMRA}$  and  $T_{EM}$  during latent and acute infection, respectively [76, 77]. In addition to this classification, the differentiation of antigen specific T cells can be dependent on the epitope considered. A striking example is the distinction between the differentiation of lytic and latent EBV epitope-specific populations. Latent epitope-specific T cells mostly lay within the  $T_{CM}$  subset, whereas lytic epitope-specific populations are more skewed toward the  $T_{EM}/T_{EMRA}$  phenotype consistent with the antigenic challenge from lytic epitopes driving some memory cells to reexpress CD45RA [78].

Regarding tumor-specific CD8 T cells, in healthy individuals, their frequency is far below the limit of detection of conventional immune-monitoring techniques. An exquisite exception is made by the unusual large repertoire of circulating Melan-A/MART1 specific CD8 T cells that has been documented in HLA-A2+ individuals, being on average 0.07% of total CD8 T cells [79]. In sharp contrast to viral-specific cells, in healthy donors, Melan-A/MART1-specific CD8 T cells display a naïve phenotype. Their presence has been associated both with a high thymic output due to lack of expression of the immunodominant Melan-A epitope by medullary thymic epithelial cells in the thymus [80], impairing negative selection, combined with a slow in vivo turnover. The only situation where priming of these cells is consistently observed is in malignant melanoma patients, where Melan-A/MART1-specific T cells display effector and memory phenotypes. Similarly, memory CD8 T cells specific for a large number of tumor-associated antigens can be readily identified ex vivo in peripheral blood and tumor-infiltrated tissues in patients. Their phenotype is only rarely associated with a  $T_{CM}$  status, bearing more often  $T_{EM}$  (either expressing CD28 or not) or  $T_{EMRA}$  characteristics [81].

**1.5.3 T Cell  
Differentiation and Its  
Correlates to Function  
in Distinct Disease Settings**

The depicted differentiation stage of antigen-specific CD8 T cells corresponds to T-cell populations with distinct homing and function potential (i.e., cytokine production, proliferation, cytotoxicity). Indeed, memory T cell subsets differ in their capacity to bear high cytotoxic potential or to produce IL-2 and proliferate. For example, Flu-specific CD8 T cells, which are mostly found in the  $T_{CM}$  compartment, are characterized by their ability to produce IL-2 (IL-2/IFN- $\gamma$  secreting cells) and retain proliferative capacities in vitro. Inversely, CMV-specific CD8 T cells that contain high frequency of

$T_{EMRA}$  are rich in granzyme and perforin [82]. Finally, HIV-1-specific CD8 T cells from untreated progressive patients, being mostly  $T_{EM}$ , are mainly single IFN- $\gamma$ -secreting cells [83]. Similarly, tumor antigen-specific CD8 T cells in cancer patients show impaired functional properties once they reside in tumor-infiltrated tissues, with decreased ability to secrete effector cytokines and degranulate, and by upregulating inhibitory molecules [84, 85]. Thus, in pathogenic conditions such as chronic infections (i.e., HIV-1, HCV, Mtb) or cancer, antigen-specific T cells are considered functionally exhausted due to their reduced polyfunctionality; this phenomenon is dependent on both the skewing of the differentiation toward a  $T_{EM}$  phenotype and on an intrinsic dysfunction (exhaustion) induced by protracted exposure to persisting antigens [86, 87]. The stage of the disease and the clinical presentation also determine the distinct profiles of specific CD8 T cell responses [77]. The control of pathogen replication by the immune system or therapeutic interventions in cancer patients partially restores the T cell functionality as well as the presence of  $T_{CM}$  and  $T_{EMRA}$  subsets [88].

## References

- Bloch H (1993) Edward Jenner (1749–1823). The history and effects of smallpox, inoculation, and vaccination. *Am J Dis Child* 147(7):772–774
- Riedel S (2005) Edward Jenner and the history of smallpox and vaccination. *Proc (Bayl Univ Med Cent)* 18(1):21–25
- Kaech SM, Hemby S, Kersh E, Ahmed R (2002) Molecular and functional profiling of memory CD8 T cell differentiation. *Cell* 111(6):837–851
- Wherry EJ, Ahmed R (2004) Memory CD8 T-cell differentiation during viral infection. *J Virol* 78(11):5535–5545. doi:10.1128/JVI.78.11.5535-5545.2004
- Wherry EJ, Ha SJ, Kaech SM, Haining WN, Sarkar S, Kalia V, Subramaniam S, Blattman JN, Barber DL, Ahmed R (2007) Molecular signature of CD8+ T cell exhaustion during chronic viral infection. *Immunity* 27(4):670–684. doi:10.1016/j.immuni.2007.09.006
- Harty JT, Badovinac VP (2008) Shaping and reshaping CD8+ T-cell memory. *Nat Rev Immunol* 8(2):107–119. doi:10.1038/nri2251
- Araki K, Turner AP, Shaffer VO, Gangappa S, Keller SA, Bachmann MF, Larsen CP, Ahmed R (2009) mTOR regulates memory CD8 T-cell differentiation. *Nature* 460(7251):108–112. doi:10.1038/nature08155, nature08155 [pii]
- Bannard O, Kraman M, Fearon D (2009) Pathways of memory CD8+ T-cell development. *Eur J Immunol* 39(8):2083–2087. doi:10.1002/eji.200939555
- Kalia V, Sarkar S, Ahmed R (2010) CD8 T-cell memory differentiation during acute and chronic viral infections. *Adv Exp Med Biol* 684:79–95
- Prlic M, Williams MA, Bevan MJ (2007) Requirements for CD8 T-cell priming, memory generation and maintenance. *Curr Opin Immunol* 19(3):315–319. doi:10.1016/j.coi.2007.04.010
- Crawford F, Kozono H, White J, Marrack P, Kappler J (1998) Detection of antigen-specific T cells with multivalent soluble class II MHC covalent peptide complexes. *Immunity* 8(6):675–682
- D'Cruz LM, Rubinstein MP, Goldrath AW (2009) Surviving the crash: transitioning from effector to memory CD8+ T cell. *Semin Immunol* 21(2):92–98. doi:10.1016/j.smim.2009.02.002
- Gerlach C, van Heijst JW, Swart E, Sie D, Armstrong N, Kerkhoven RM, Zehn D, Bevan MJ, Schepers K, Schumacher TN (2010) One naive T cell, multiple fates in CD8+ T cell differentiation. *J Exp Med* 207(6):1235–1246. doi:10.1084/jem.20091175
- Chang JT, Palanivel VR, Kinjyo I, Schambach F, Intlekofer AM, Banerjee A, Longworth SA, Vinup KE, Mrass P, Oliaro J, Killeen N, Orange JS, Russell SM, Weninger W, Reiner SL (2007) Asymmetric T lymphocyte division in the initiation of adaptive immune responses. *Science* 315(5819):1687–1691. doi:10.1126/science.1139393

15. Ciocca ML, Barnett BE, Burkhardt JK, Chang JT, Reiner SL (2012) Cutting edge: asymmetric memory T cell division in response to rechallenge. *J Immunol* 188(9):4145–4148. doi:[10.4049/jimmunol.1200176](https://doi.org/10.4049/jimmunol.1200176)
16. Lanzavecchia A, Sallusto F (2002) Progressive differentiation and selection of the fittest in the immune response. *Nat Rev Immunol* 2(12):982–987. doi:[10.1038/nri959](https://doi.org/10.1038/nri959)
17. Joshi NS, Cui W, Chandele A, Lee HK, Urso DR, Hageman J, Gapin L, Kaech SM (2007) Inflammation directs memory precursor and short-lived effector CD8(+) T cell fates via the graded expression of T-bet transcription factor. *Immunity* 27(2):281–295. doi:[10.1016/j.immuni.2007.07.010](https://doi.org/10.1016/j.immuni.2007.07.010)
18. Wiesel M, Crouse J, Bedenikovic G, Sutherland A, Joller N, Oxenius A (2012) Type-I IFN drives the differentiation of short-lived effector CD8+ T cells in vivo. *Eur J Immunol* 42(2):320–329. doi:[10.1002/eji.201142091](https://doi.org/10.1002/eji.201142091)
19. Obar JJ, Jellison ER, Sheridan BS, Blair DA, Pham QM, Zickovich JM, Lefrancois L (2011) Pathogen-induced inflammatory environment controls effector and memory CD8+ T cell differentiation. *J Immunol* 187(10):4967–4978. doi:[10.4049/jimmunol.1102335](https://doi.org/10.4049/jimmunol.1102335)
20. Yuzefpolskiy Y, Baumann FM, Kalia V, Sarkar S (2015) Early CD8 T-cell memory precursors and terminal effectors exhibit equipotent in vivo degranulation. *Cell Mol Immunol* 12(4):400–408. doi:[10.1038/cmi.2014.48](https://doi.org/10.1038/cmi.2014.48)
21. Badovinac VP, Harty JT (2007) Manipulating the rate of memory CD8+ T cell generation after acute infection. *J Immunol* 179(1):53–63
22. Youngblood B, Hale JS, Ahmed R (2015) Memory CD8 T cell transcriptional plasticity. *F1000Prime Rep* 7:38. doi:[10.12703/P7-38](https://doi.org/10.12703/P7-38)
23. Chang JT, Wherry EJ, Goldrath AW (2014) Molecular regulation of effector and memory T cell differentiation. *Nat Immunol* 15(12):1104–1115. doi:[10.1038/ni.3031](https://doi.org/10.1038/ni.3031)
24. Kaech SM, Cui W (2012) Transcriptional control of effector and memory CD8+ T cell differentiation. *Nat Rev Immunol* 12(11):749–761. doi:[10.1038/nri3307](https://doi.org/10.1038/nri3307)
25. Schenkel JM, Masopust D (2014) Tissue-resident memory T cells. *Immunity* 41(6):886–897. doi:[10.1016/j.immuni.2014.12.007](https://doi.org/10.1016/j.immuni.2014.12.007)
26. Gattinoni L (2014) Memory T cells officially join the stem cell club. *Immunity* 41(1):7–9. doi:[10.1016/j.immuni.2014.07.003](https://doi.org/10.1016/j.immuni.2014.07.003)
27. Sallusto F, Lenig D, Forster R, Lipp M, Lanzavecchia A (1999) Two subsets of memory T lymphocytes with distinct homing potentials and effector functions. *Nature* 401(6754):708–712. doi:[10.1038/44385](https://doi.org/10.1038/44385)
28. Jamieson BD, Ahmed R (1989) T cell memory. Long-term persistence of virus-specific cytotoxic T cells. *J Exp Med* 169(6):1993–2005
29. Oldstone MB, Ahmed R, Byrne J, Buchmeier MJ, Riviere Y, Southern P (1985) Virus and immune responses: lymphocytic choriomeningitis virus as a prototype model of viral pathogenesis. *Br Med Bull* 41(1):70–74
30. Wherry EJ, Teichgraber V, Becker TC, Masopust D, Kaech SM, Antia R, von Andrian UH, Ahmed R (2003) Lineage relationship and protective immunity of memory CD8 T cell subsets. *Nat Immunol* 4(3):225–234. doi:[10.1038/ni889](https://doi.org/10.1038/ni889)
31. Kaech SM, Tan JT, Wherry EJ, Konieczny BT, Surh CD, Ahmed R (2003) Selective expression of the interleukin 7 receptor identifies effector CD8 T cells that give rise to long-lived memory cells. *Nat Immunol* 4(12):1191–1198. doi:[10.1038/ni1009](https://doi.org/10.1038/ni1009)
32. Zehn D, Lee SY, Bevan MJ (2009) Complete but curtailed T-cell response to very low-affinity antigen. *Nature* 458(7235):211–214. doi:[10.1038/nature07657](https://doi.org/10.1038/nature07657)
33. Schluns KS, Klonowski KD (2015) Protecting the borders: tissue-resident memory T cells on the front line. *Front Immunol* 6:90. doi:[10.3389/fimmu.2015.00090](https://doi.org/10.3389/fimmu.2015.00090)
34. Shin H, Iwasaki A (2013) Tissue-resident memory T cells. *Immunol Rev* 255(1):165–181. doi:[10.1111/imr.12087](https://doi.org/10.1111/imr.12087)
35. Mackay LK, Rahimpour A, Ma JZ, Collins N, Stock AT, Hafon ML, Vega-Ramos J, Lauzurica P, Mueller SN, Stefanovic T, Tschärke DC, Heath WR, Inouye M, Carbone FR, Gebhardt T (2013) The developmental pathway for CD103(+)CD8+ tissue-resident memory T cells of skin. *Nat Immunol* 14(12):1294–1301. doi:[10.1038/ni.2744](https://doi.org/10.1038/ni.2744)
36. Cauley LS, Lefrancois L (2013) Guarding the perimeter: protection of the mucosa by tissue-resident memory T cells. *Mucosal Immunol* 6(1):14–23. doi:[10.1038/mi.2012.96](https://doi.org/10.1038/mi.2012.96)
37. Schenkel JM, Fraser KA, Beura LK, Pauken KE, Vezyz V, Masopust D (2014) T cell memory. Resident memory CD8 T cells trigger protective innate and adaptive immune responses. *Science* 346(6205):98–101. doi:[10.1126/science.1254536](https://doi.org/10.1126/science.1254536)
38. Wakim LM, Gupta N, Mintern JD, Villadangos JA (2013) Enhanced survival of lung tissue-resident memory CD8(+) T cells during infection with influenza virus due to selective expression of IFITM3. *Nat Immunol* 14(3):238–245. doi:[10.1038/ni.2525](https://doi.org/10.1038/ni.2525)
39. Turner DL, Bickham KL, Thome JJ, Kim CY, D'Ovidio F, Wherry EJ, Farber DL

- (2014) Lung niches for the generation and maintenance of tissue-resident memory T cells. *Mucosal Immunol* 7(3):501–510. doi:[10.1038/mi.2013.67](https://doi.org/10.1038/mi.2013.67)
40. Frost EL, Kersh AE, Evavold BD, Lukacher AE (2015) Cutting edge: resident memory CD8 T cells express high-affinity TCRs. *J Immunol* 195(8):3520–3524. doi:[10.4049/jimmunol.1501521](https://doi.org/10.4049/jimmunol.1501521)
41. Wakim LM, Woodward-Davis A, Liu R, Hu Y, Villadangos J, Smyth G, Bevan MJ (2012) The molecular signature of tissue resident memory CD8 T cells isolated from the brain. *J Immunol* 189(7):3462–3471. doi:[10.4049/jimmunol.1201305](https://doi.org/10.4049/jimmunol.1201305)
42. Gebhardt T, Mackay LK (2012) Local immunity by tissue-resident CD8(+) memory T cells. *Front Immunol* 3:340. doi:[10.3389/fimmu.2012.00340](https://doi.org/10.3389/fimmu.2012.00340)
43. Lugli E, Dominguez MH, Gattinoni L, Chattopadhyay PK, Bolton DL, Song K, Klatt NR, Brenchley JM, Vaccari M, Gostick E, Price DA, Waldmann TA, Restifo NP, Franchini G, Roederer M (2013) Superior T memory stem cell persistence supports long-lived T cell memory. *J Clin Invest* 123(2):594–599. doi:[10.1172/JCI66327](https://doi.org/10.1172/JCI66327)
44. Gattinoni L, Lugli E, Ji Y, Pos Z, Paulos CM, Quigley MF, Almeida JR, Gostick E, Yu Z, Carpenito C, Wang E, Douek DC, Price DA, June CH, Marincola FM, Roederer M, Restifo NP (2011) A human memory T cell subset with stem cell-like properties. *Nat Med* 17(10):1290–1297. doi:[10.1038/nm.2446](https://doi.org/10.1038/nm.2446)
45. Gattinoni L, Zhong XS, Palmer DC, Ji Y, Hinrichs CS, Yu Z, Wrzesinski C, Boni A, Cassard L, Garvin LM, Paulos CM, Muranski P, Restifo NP (2009) Wnt signaling arrests effector T cell differentiation and generates CD8+ memory stem cells. *Nat Med* 15(7):808–813. doi:[10.1038/nm.1982](https://doi.org/10.1038/nm.1982)
46. Lugli E, Gattinoni L, Roberto A, Mavilio D, Price DA, Restifo NP, Roederer M (2013) Identification, isolation and in vitro expansion of human and nonhuman primate T stem cell memory cells. *Nat Protoc* 8(1):33–42. doi:[10.1038/nprot.2012.143](https://doi.org/10.1038/nprot.2012.143)
47. Scholz G, Jandus C, Zhang L, Grandclement C, Lopez-Mejia IC, Sonesson C, Delorenzi M, Fajas L, Held W, Dormond O, Romero P (2016) Modulation of mTOR signalling triggers the formation of stem cell-like memory T cells. *EBioMedicine* 4:50–61. doi:[10.1016/j.ebiom.2016.01.019](https://doi.org/10.1016/j.ebiom.2016.01.019)
48. Speiser DE, Utzschneider DT, Oberle SG, Munz C, Romero P, Zehn D (2014) T cell differentiation in chronic infection and cancer: functional adaptation or exhaustion? *Nat Rev Immunol* 14(11):768–774. doi:[10.1038/nri3740](https://doi.org/10.1038/nri3740)
49. Man K, Kallies A (2015) Synchronizing transcriptional control of T cell metabolism and function. *Nat Rev Immunol* 15(9):574–584. doi:[10.1038/nri3874](https://doi.org/10.1038/nri3874)
50. Park BV, Pan F (2015) Metabolic regulation of T cell differentiation and function. *Mol Immunol* 28:497–506. doi:[10.1016/j.molimm.2015.07.027](https://doi.org/10.1016/j.molimm.2015.07.027)
51. Frauwirth KA, Riley JL, Harris MH, Parry RV, Rathmell JC, Plas DR, Elstrom RL, June CH, Thompson CB (2002) The CD28 signaling pathway regulates glucose metabolism. *Immunity* 16(6):769–777
52. van der Windt GJ, Pearce EL (2012) Metabolic switching and fuel choice during T-cell differentiation and memory development. *Immunol Rev* 249(1):27–42. doi:[10.1111/j.1600-065X.2012.01150.x](https://doi.org/10.1111/j.1600-065X.2012.01150.x)
53. Bottcher J, Knolle PA (2015) Global transcriptional characterization of CD8+ T cell memory. *Semin Immunol* 27(1):4–9. doi:[10.1016/j.smim.2015.03.001](https://doi.org/10.1016/j.smim.2015.03.001)
54. Rao RR, Li Q, Gubbels Bupp MR, Shrikant PA (2012) Transcription factor Foxo1 represses T-bet-mediated effector functions and promotes memory CD8(+) T cell differentiation. *Immunity* 36(3):374–387. doi:[10.1016/j.immuni.2012.01.015](https://doi.org/10.1016/j.immuni.2012.01.015)
55. Intlekofer AM, Takemoto N, Wherry EJ, Longworth SA, Northrup JT, Palanivel VR, Mullen AC, Gasink CR, Kaech SM, Miller JD, Gapin L, Ryan K, Russ AP, Lindsten T, Orange JS, Goldrath AW, Ahmed R, Reiner SL (2005) Effector and memory CD8+ T cell fate coupled by T-bet and eomesodermin. *Nat Immunol* 6(12):1236–1244. doi:[10.1038/ni1268](https://doi.org/10.1038/ni1268)
56. Kallies A, Xin A, Belz GT, Nutt SL (2009) Blimp-1 transcription factor is required for the differentiation of effector CD8(+) T cells and memory responses. *Immunity* 31(2):283–295. doi:[10.1016/j.immuni.2009.06.021](https://doi.org/10.1016/j.immuni.2009.06.021)
57. Ji Y, Pos Z, Rao M, Klebanoff CA, Yu Z, Sukumar M, Reger RN, Palmer DC, Borman ZA, Muranski P, Wang E, Schrumpp DS, Marincola FM, Restifo NP, Gattinoni L (2011) Repression of the DNA-binding inhibitor Id3 by Blimp-1 limits the formation of memory CD8+ T cells. *Nat Immunol* 12(12):1230–1237. doi:[10.1038/ni.2153](https://doi.org/10.1038/ni.2153)
58. Rutishauser RL, Martins GA, Kalachikov S, Chandele A, Parish IA, Meffre E, Jacob J, Calame K, Kaech SM (2009) Transcriptional repressor Blimp-1 promotes CD8(+) T cell terminal differentiation and represses the acquisition of central memory T cell properties. *Immunity* 31(2):296–308. doi:[10.1016/j.immuni.2009.05.014](https://doi.org/10.1016/j.immuni.2009.05.014)
59. Vigano S, Utzschneider DT, Perreau M, Pantaleo G, Zehn D, Harari A (2012) Functional avidity: a measure to predict the

- efficacy of effector T cells? *Clin Dev Immunol* 2012;153863. doi:[10.1155/2012/153863](https://doi.org/10.1155/2012/153863)
60. Hebeisen M, Schmidt J, Guillaume P, Baumgaertner P, Speiser DE, Luescher I, Rufer N (2015) Identification of rare high-avidity, tumor-reactive CD8+ T cells by monomeric TCR-ligand off-rates measurements on living cells. *Cancer Res* 75(10):1983–1991. doi:[10.1158/0008-5472.CAN-14-3516](https://doi.org/10.1158/0008-5472.CAN-14-3516)
  61. Berger CT, Frahm N, Price DA, Mothe B, Ghebremichael M, Hartman KL, Henry LM, Brenchley JM, Ruff LE, Venturi V, Pereyra F, Sidney J, Sette A, Douek DC, Walker BD, Kaufmann DE, Brander C (2011) High-functional-avidity cytotoxic T lymphocyte responses to HLA-B-restricted Gag-derived epitopes associated with relative HIV control. *J Virol* 85(18):9334–9345. doi:[10.1128/JVI.00460-11](https://doi.org/10.1128/JVI.00460-11)
  62. Dutoit V, Rubio-Godoy V, Dietrich PY, Quiques AL, Schnuriger V, Rimoldi D, Lienard D, Speiser D, Guillaume P, Bataard P, Cerottini JC, Romero P, Valmori D (2001) Heterogeneous T-cell response to MAGE-A10(254–262): high avidity-specific cytolytic T lymphocytes show superior antitumor activity. *Cancer Res* 61(15):5850–5856
  63. Morgan DJ, Kreuwel HT, Fleck S, Levitsky HI, Pardoll DM, Sherman LA (1998) Activation of low avidity CTL specific for a self epitope results in tumor rejection but not autoimmunity. *J Immunol* 160(2):643–651
  64. Anderton SM, Radu CG, Lowrey PA, Ward ES, Wraith DC (2001) Negative selection during the peripheral immune response to antigen. *J Exp Med* 193(1):1–11
  65. Sallusto F, Geginat J, Lanzavecchia A (2004) Central memory and effector memory T cell subsets: function, generation, and maintenance. *Annu Rev Immunol* 22:745–763. doi:[10.1146/annurev.immunol.22.012703.104702](https://doi.org/10.1146/annurev.immunol.22.012703.104702)
  66. Sathaliyawala T, Kubota M, Yudanin N, Turner D, Camp P, Thome JM, Bickham KL, Lerner H, Goldstein M, Sykes M, Kato T, Farber DL (2013) Distribution and compartmentalization of human circulating and tissue-resident memory T cell subsets. *Immunity* 38(1):187–197. doi:[10.1016/j.immuni.2012.09.020](https://doi.org/10.1016/j.immuni.2012.09.020)
  67. Romero P, Zippelius A, Kurth I, Pittet MJ, Touvrey C, Iancu EM, Corthesy P, Devivre E, Speiser DE, Rufer N (2007) Four functionally distinct populations of human effector-memory CD8+ T lymphocytes. *J Immunol* 178(7):4112–4119
  68. Biasco L, Scala S, Basso Ricci L, Dionisio F, Baricordi C, Calabria A, Giannelli S, Cieri N, Barzaghi F, Pajno R, Al-Mousa H, Scarselli A, Cancrini C, Bordignon C, Roncarolo MG, Montini E, Bonini C, Aiuti A (2015) In vivo tracking of T cells in humans unveils decade-long survival and activity of genetically modified T memory stem cells. *Sci Transl Med* 7(273):273ra213. doi:[10.1126/scitranslmed.3010314](https://doi.org/10.1126/scitranslmed.3010314)
  69. Vigano S, Negron J, Ouyang Z, Rosenberg ES, Walker BD, Lichterfeld M, Yu XG (2015) Prolonged antiretroviral therapy preserves HIV-1-specific CD8 T cells with stem cell-like properties. *J Virol* 89(15):7829–7840. doi:[10.1128/JVI.00789-15](https://doi.org/10.1128/JVI.00789-15)
  70. Fuertes Marraco SA, Soneson C, Cagnon L, Gannon PO, Allard M, Abed Maillard S, Montandon N, Rufer N, Waldvogel S, Delorenzi M, Speiser DE (2015) Long-lasting stem cell-like memory CD8+ T cells with a naive-like profile upon yellow fever vaccination. *Sci Transl Med* 7(282):282ra248. doi:[10.1126/scitranslmed.aaa3700](https://doi.org/10.1126/scitranslmed.aaa3700)
  71. Brunner S, Herndler-Brandstetter D, Weinberger B, Grubeck-Loebenstien B (2011) Persistent viral infections and immune aging. *Ageing Res Rev* 10(3):362–369. doi:[10.1016/j.arr.2010.08.003](https://doi.org/10.1016/j.arr.2010.08.003)
  72. Aspinall R, Andrew D (2000) Thymic involution in aging. *J Clin Immunol* 20(4):250–256
  73. Kim PS, Ahmed R (2010) Features of responding T cells in cancer and chronic infection. *Curr Opin Immunol* 22(2):223–230. doi:[10.1016/j.coi.2010.02.005](https://doi.org/10.1016/j.coi.2010.02.005)
  74. Hadrup SR, Bakker AH, Shu CJ, Andersen RS, van Veluw J, Hombrink P, Castermans E, Thor Straten P, Blank C, Haanen JB, Heemskerck MH, Schumacher TN (2009) Parallel detection of antigen-specific T-cell responses by multidimensional encoding of MHC multimers. *Nat Methods* 6(7):520–526. doi:[10.1038/nmeth.1345](https://doi.org/10.1038/nmeth.1345)
  75. Newell EW, Klein LO, Yu W, Davis MM (2009) Simultaneous detection of many T-cell specificities using combinatorial tetramer staining. *Nat Methods* 6(7):497–499. doi:[10.1038/nmeth.1344](https://doi.org/10.1038/nmeth.1344)
  76. Jeong YH, Jeon BY, Gu SH, Cho SN, Shin SJ, Chang J, Ha SJ (2014) Differentiation of antigen-specific T cells with limited functional capacity during Mycobacterium tuberculosis infection. *Infect Immun* 82(1):132–139. doi:[10.1128/IAI.00480-13](https://doi.org/10.1128/IAI.00480-13)
  77. Rozot V, Vigano S, Mazza-Stalder J, Idrizi E, Day CL, Perreau M, Lazor-Blanchet C, Petruccioli E, Hanekom W, Goletti D, Bart PA, Nicod L, Pantaleo G, Harari A (2013) Mycobacterium tuberculosis-specific CD8+ T cells are functionally and phenotypically different between latent infection and active disease. *Eur J Immunol* 43(6):1568–1577. doi:[10.1002/eji.201243262](https://doi.org/10.1002/eji.201243262)

78. Hislop AD, Annels NE, Gudgeon NH, Leese AM, Rickinson AB (2002) Epitope-specific evolution of human CD8(+) T cell responses from primary to persistent phases of Epstein-Barr virus infection. *J Exp Med* 195(7):893–905
79. Pittet MJ, Valmori D, Dunbar PR, Speiser DE, Lienard D, Lejeune F, Fleischhauer K, Cerundolo V, Cerottini JC, Romero P (1999) High frequencies of naive Melan-A/MART-1-specific CD8(+) T cells in a large proportion of human histocompatibility leukocyte antigen (HLA)-A2 individuals. *J Exp Med* 190(5):705–715
80. Pinto S, Sommermeyer D, Michel C, Wilde S, Schendel D, Uckert W, Blankenstein T, Kyewski B (2014) Misinitiation of intrathymic MART-1 transcription and biased TCR usage explain the high frequency of MART-1-specific T cells. *Eur J Immunol* 44(9):2811–2821. doi:[10.1002/eji.201444499](https://doi.org/10.1002/eji.201444499)
81. Romero P, Cerottini JC, Speiser DE (2006) The human T cell response to melanoma antigens. *Adv Immunol* 92:187–224. doi:[10.1016/S0065-2776\(06\)92005-7](https://doi.org/10.1016/S0065-2776(06)92005-7)
82. Celleraï C, Perreau M, Rozot V, Bellutti Enders F, Pantaleo G, Harari A (2010) Proliferation capacity and cytotoxic activity are mediated by functionally and phenotypically distinct virus-specific CD8 T cells defined by interleukin-7R{alpha} (CD127) and perforin expression. *J Virol* 84(8):3868–3878. doi:[10.1128/JVI.02565-09](https://doi.org/10.1128/JVI.02565-09)
83. Hersperger AR, Martin JN, Shin LY, Sheth PM, Kovacs CM, Cosma GL, Makedonas G, Pereyra F, Walker BD, Kaul R, Deeks SG, Betts MR (2011) Increased HIV-specific CD8+ T-cell cytotoxic potential in HIV elite controllers is associated with T-bet expression. *Blood* 117(14):3799–3808. doi:[10.1182/blood-2010-12-322727](https://doi.org/10.1182/blood-2010-12-322727)
84. Zippelius A, Batard P, Rubio-Godoy V, Bioley G, Lienard D, Lejeune F, Rimoldi D, Guillaume P, Meidenbauer N, Mackensen A, Rufer N, Lubenow N, Speiser D, Cerottini JC, Romero P, Pittet MJ (2004) Effector function of human tumor-specific CD8 T cells in melanoma lesions: a state of local functional tolerance. *Cancer Res* 64(8):2865–2873
85. Baitsch L, Baumgaertner P, Devevre E, Raghav SK, Legat A, Barba L, Wiecekowski S, Bouzourene H, Deplancke B, Romero P, Rufer N, Speiser DE (2011) Exhaustion of tumor-specific CD8(+) T cells in metastases from melanoma patients. *J Clin Invest* 121(6):2350–2360. doi:[10.1172/JCI46102](https://doi.org/10.1172/JCI46102)
86. Kaufmann DE, Kavanagh DG, Pereyra F, Zaunders JJ, Mackey EW, Miura T, Palmer S, Brockman M, Rathod A, Piechocka-Trocha A, Baker B, Zhu B, Le Gall S, Waring MT, Ahern R, Moss K, Kelleher AD, Coffin JM, Freeman GJ, Rosenberg ES, Walker BD (2007) Upregulation of CTLA-4 by HIV-specific CD4+ T cells correlates with disease progression and defines a reversible immune dysfunction. *Nat Immunol* 8(11):1246–1254. doi:[10.1038/ni1515](https://doi.org/10.1038/ni1515)
87. Lichterfeld M, Mou D, Cung TD, Williams KL, Waring MT, Huang J, Pereyra F, Trocha A, Freeman GJ, Rosenberg ES, Walker BD, Yu XG (2008) Telomerase activity of HIV-1-specific CD8+ T cells: constitutive upregulation in controllers and selective increase by blockade of PD ligand 1 in progressors. *Blood* 112(9):3679–3687. doi:[10.1182/blood-2008-01-135442](https://doi.org/10.1182/blood-2008-01-135442)
88. Larkin J, Chiarion-Sileni V, Gonzalez R, Grob JJ, Cowey CL, Lao CD, Schadendorf D, Dummer R, Smylie M, Rutkowski P, Ferrucci PF, Hill A, Wagstaff J, Carlino MS, Haanen JB, Maio M, Marquez-Rodas I, McArthur GA, Ascierto PA, Long GV, Callahan MK, Postow MA, Grossmann K, Sznol M, Dreno B, Bastholt L, Yang A, Rollin LM, Horak C, Hodi FS, Wolchok JD (2015) Combined nivolumab and ipilimumab or monotherapy in untreated melanoma. *N Engl J Med* 373(1):23–34. doi:[10.1056/NEJMoa1504030](https://doi.org/10.1056/NEJMoa1504030)

## Basic Aspects of T Helper Cell Differentiation

Nicola Gagliani and Samuel Huber

### Abstract

CD4<sup>+</sup> T helper cells orchestrate the immune response and play a pivotal role during infection, chronic inflammatory, autoimmune diseases, and carcinogenesis. CD4<sup>+</sup> T helper cells can be subdivided into different subsets, which are characterized by a specific network of transcriptional regulators and unique cytokine profiles: Th17 cells express ROR $\gamma$ t that in turn promotes the transcription of *Il17a*, *Il17f*; Th1 cells, expresses T-bet and produces IFN- $\gamma$ , IL-2, and TNF- $\alpha$ ; Th2 cells express GATA-3 and secrete IL-4, IL-5, and IL-13. The two most studied regulatory T cell subtypes are Foxp3<sup>+</sup> regulatory T cells, which can be generated either in the thymus (tTreg) or induced in peripheral lymphoid organs (pTregs) and type 1 regulatory T cells (Tr1), which are induced in the periphery. These T helper cell subsets can be differentiated from naïve T cells. In addition, recent findings indicate that some T helper cell subsets can emerge from other T helper cells, suggesting a certain degree of plasticity. Here we report basic aspects of T helper cell differentiation and function while underlining some still open questions.

**Key words** CD4 T helper cells, Cytokines, Transcriptional regulators, Differentiation, T helper cell plasticity

---

### 1 Introduction

Naïve T cells, which are functionally immature, can be differentiated into different subsets of effector T cells upon activation. Cytokines play a key role during this process. They signal via different members of the STAT family protein, which induce master transcriptional regulators. Most of these transcriptional factors then bind to the effector cytokine gene, thereby inducing gene activation, repression or epigenetic modification [1]. These different T helper cells have been thought to be stable, as first proposed by Mosmann and Coffman [2]. This model of stable T helper cell lineages has been absolutely fundamental to conceptualize the differentiation of CD4<sup>+</sup> T helper cells. However, the existing of T-cell heterogeneity within one T helper cell subset, which has been observed *in vivo*, cannot be fully explained by this model. The one cell multiple fate theory has been proposed [3], which means that different T helper cell subsets can differentiate from one common

T cell precursor, which can either be a naive T cells or already primed T cells. In line with this theory we learned that some cells of each T helper cell subset are plastic and can acquire a different fate. Further studies are needed to validate this hypothesis and to identify mechanisms regulating the fate of T cells.

### **1.1 Differentiation and Function of Th1 Cells**

Th1 cells are particularly important for the defense against intracellular bacteria, such as *Listeria* and *Mycobacterium tuberculosis*. Th1 cells express CXCR3 and IFN- $\gamma$  is their signature cytokine. Th1 cells also secrete IL-2 and/or TNF- $\alpha$ . Naive T cells upon T cell receptor (TCR) stimulation in the presence of IL-12 differentiate in Th1 cells [4]. IL-12 signals via STAT4 promote the expression of T-bet, which transcribes the *Ifng* gene [5, 6]. T-bet is the master transcriptional regulator of Th1 cells, which is essential for the IFN- $\gamma$  production [7]. Accordingly, T-bet deficient mice have a defective Th1 differentiation [8]. Another important function of T-bet is the inhibition of GATA-3 expression, the master transcriptional regulator of Th2 cells [5]. In line with these results, the Th1 and Th2 molecular programs oppose each other. Thus Th1 cells seem to be less prone to acquire features characteristic of other effector phenotypes. This is in line with the epigenetic status of in vitro differentiated Th1 cells, which maintain an inaccessible status in the key transcriptional factor of the other T helper cell subsets [9]. However, an interesting study challenged the hypothesis of stable Th1 cells, as in vivo-generated mouse Th1 cells were shown to acquire Th2 cell features in response to *Nippostrongylus brasiliensis* [10]. Moreover, it was shown in vitro that human Th1 cells are able to acquire the ability to produce IL-4, a signature cytokine of Th2 cells [11]. A recent study further supports the plasticity of Th1 cells showing that a 98% pure population of in vitro generated flagellin specific Th1 cells become Th17 cells upon migration to the intestine. TGF- $\beta$  stimulation by activating Runx1 was proposed as the possible mechanism for the conversion of these in vitro-generated Th1 into Th17 cells [12].

Th1 cells can also acquire the expression of the anti-inflammatory cytokines IL-10 [13]. Recently, it has been shown that Th1 cells can acquire a Tr1-like phenotype and prevent a variety of autoimmune mediated diseases in mouse models.

### **1.2 Differentiation and Function of Th2 Cells**

Th2 cells and their effector cytokines IL-4, IL-5, and IL-13 are essential to control helminth infections. The cytokines leading to Th2 differentiation are IL-2 and IL-4. The signature cytokines of Th2 cells are IL-4, IL-5, and IL-13. Therefore, the signature cytokine of Th2 cells, IL-4 also promotes the differentiation of Th2 cells [14–16]. Th2 cells express chemokine receptor CCR4, and STAT6, which is the major signaling pathway of IL-4-mediated Th2 differentiation, and induces GATA-3 expression [17–21]. GATA-3 is the master transcriptional regulator of Th2 cells [22, 23]

and the differentiation of these cells is indeed dependent on the induction of this master transcriptional regulator [24]. GATA-3 binds to the promoters of *Il5* and *Il13*, and the enhancer of *Il4*, thereby promoting their transcription [1]. In addition, STAT5, which can be activated by IL-2, is important for Th2 differentiation and for the maintenance of GATA-3 expression [25]. Furthermore, a recent paper suggested the receptor NLRP3 as a transcriptional regulator of Th2 differentiation [26]. In addition, it was shown that IL-25 binds to IL-17RA and IL-17RB and promotes Th2 cells differentiation. Interestingly this effect of IL-25 is mediated via STAT5 [27].

Th2 cells have also been shown to have a certain degree of plasticity. In vitro-induced Th2 can acquire a functional Th1 phenotype in response to LCMV infection, a process that involved interferons type 1 and 2 as well as IL-12 [28]. Th2 cells, which were generated in vivo in response to *H. polygyrus*, could also acquire Th1 cell properties when encountered with *Plasmodium chabaudi* [29]. In line with these murine data, also some human Th2 cells can acquire a Th1 cell phenotype [11]. Finally, Th2 cells can also be converted into regulatory Foxp3 Treg cells when stimulated in vitro with TGF- $\beta$  in the presence of all *trans* retinoic acid and rapamycin [30]. Whether Th2 plasticity can be therapeutically targeted is unknown.

### 1.3 Differentiation and Function of Th17 Cells

In the absence of pathology, Th17 cells are mainly restricted to the gastrointestinal tract. However, they expand upon infection with bacteria (i.e., *Citrobacter rodentium* or *Klebsiella pneumoniae*) and fungi (i.e., *Candida albicans*) [31–35]. Accordingly adherent bacteria can induce Th17 cells in mice and humans [36]. Th17 cells are critical for the defense against various infections. Therefore, patients with defect in IL-17 signaling develop chronic infection with *Candida albicans* [37]. The signature cytokines of Th17 cells are IL-17A and IL-17F. Th17 cells also produce IL-22 and TNF- $\alpha$ . TGF- $\beta$ , IL-1 $\beta$ , IL-6, and IL-23 are the cytokines, which are important for Th17 cell differentiation. IL-6 can activate STAT3, which induces IL-23R and ROR $\gamma$ t [38–40], the master transcriptional regulator of Th17 cells. This master transcriptional regulator leads to the production of IL-17A and IL-17F [41–44]. In the presence of IL-23, CD4<sup>+</sup> ROR $\gamma$ t<sup>+</sup> IL-17A<sup>+</sup> T cells can expand and fully mature into Th17 cells [45, 46]. Furthermore, epithelium derived serum amyloid A (SAA1/2), which is produced in response to IL-22 stimulation, can induce Th17 cells [47]. On the contrary, IL-2 activates STAT5, which blocks STAT3 and consequently reduces IL-17A expression [48]. Of note, IL-1 $\beta$  rather than IL-6 is essential for Th17 differentiation in the intestine [49].

A complex network of transcriptional factors controls Th17 cell identity. This has been studied extensively in murine systems: STAT3, BATF, IRF4, and cMAF support ROR $\gamma$ t, which is the pivotal player in Th17 differentiation. New factors have recently

been identified to be important for Th17 cell differentiation. Tsc22d3 negatively regulates Th17 differentiation and favors regulatory expression, while Fosl2, MINA, Fas, and Pou2af1 maintain Th17 specification by blocking alternative fates, such as Th1 or Treg [50, 51]. Interestingly, Th17 cells can have a pro-inflammatory or anti-inflammatory phenotype. Recently CD5L has been shown to be fundamental in attenuating the pathogenicity of Th17 cells. CD5L mediates this effect by modulating the intracellular lipi-dome of Th17 cells [52, 53]. Circadian rhythm also influences Th17 cell differentiation. In the dark, NFIL3 increases and consequently blocks ROR $\gamma$ t. An alteration of the light cycle increases intestinal Th17 cells and favors intestinal inflammation [54]. Melatonin, which is usually produced in the night, blocks Th17 development by inducing NFIL3, which blocks ROR $\gamma$ t [55].

The phenotype of Th17 cells is influenced by TGF- $\beta$ 1 and IL-1 $\beta$  [48]. Th17 cells, which have been differentiated in the presence of TGF- $\beta$ 1 are less pathogenic, produce more IL-10, and are more likely to acquire a Tr1 cell phenotype compared to Th17 cell differentiated in the presence of IL-1 $\beta$  [56–58]. However, we want to point out that pro-inflammatory and anti-inflammatory Th17 cells are not synonymous with pathogenic and protective Th17 cells. The outcome depends on the environment in which Th17 cells are present. Accordingly, pro-inflammatory Th17 cells will be protective during infection, while they are pathogenic in autoimmunity and in chronic inflammatory diseases.

In humans, it was shown that the phenotype of Th17 cells can be influenced by certain pathogens. Th17-cell clones stimulated with *Staphylococcus aureus* produce IL-10. On the contrary, Th17 cells produce IFN- $\gamma$ , when stimulated with *Candida albicans* [48]. Interestingly, some human Th17 cells share the TCRs with Th1 and Th2 cells and can also acquire their phenotype, suggesting that human Th17 cells are also plastic [11]. In line with this murine studies show that Th17 cells can acquire a Th1, Tfh, Treg or Tr1 cell phenotype [58–62].

In conclusion, the Th17 cell population reflects a dynamic state of T cells, which fluctuates between pathogenic and suppressive states according to the environment. It remains to be clarified whether this fluctuation is completely stochastic or whether some Th17 cells are actually more predisposed than others to acquire a different fate.

#### **1.4 Differentiation and Function of Foxp3<sup>+</sup> Treg Cells**

In 1995, Sakaguchi et al. first described a subpopulation of regulatory T cells characterized by the constitutive expression of the IL-2 receptor  $\alpha$ -chain (CD25). These regulatory T cells were called CD4<sup>+</sup>CD25<sup>+</sup> Treg [63]. Foxp3 was identified later on as the master transcriptional regulator of CD4<sup>+</sup>CD25<sup>+</sup> Treg cells, which have been called Foxp3<sup>+</sup> Treg cells thereafter [64, 65]. According to the literature Foxp3 Treg cells are now defined as those cells that

express Foxp3, since the overexpression of Foxp3 can confer a regulatory activity to CD4+ T cells [66–68].

Foxp3+ Treg cells can be generated within the thymus (tTreg) [63]. However, Foxp3+ Treg cell numbers are also regulated in peripheral lymphoid organs both by expansion of preexisting Foxp3+ Treg and by de novo generation of induced regulatory T cells (pTreg). The combination of the cytokines IL-2 and TGF- $\beta$ 1 are a key factor for the differentiation of naïve T cells into Foxp3+ pTreg cells [69–74]. Foxp3+ Treg cells are essential to control auto-reactive T cells, which can react to self-antigens and cause damage to the host. The key role of Foxp3+ Treg cells in the peripheral immune response is evident in murine models [75] and in humans [76]: scurfy mice [75] and IPEX (immunodysregulation polyendocrinopathy enteropathy X-linked syndrome) patients [76] lacking the master transcriptional factor of regulatory T cells—Foxp3—, develop strong autoimmune disorders. Importantly, a severe form of autoimmune enteropathy is characteristic for scurfy mice and IPEX patients [76]. This underlines the importance of Foxp3+ Treg cells for controlling the immune response in the intestine. Foxp3+ Treg cells have different mechanism to suppress effector T cells. Some of these are mediated via soluble factors (i.e., IL-10, TGF- $\beta$ 1 [77, 78]) and others are cell contact dependent (i.e., CTLA-4, cAMP [79, 80]).

Foxp3+ Treg cells are largely plastic and by adapting their phenotype to different effectors T cells, they execute their regulatory activity at their best. However, whether this phenomenon can lead to lineage instability is still discussed (for review *see ref.* [81]).

### **1.5 Differentiation and Function of Tr1 Cells**

In 1994, T regulatory type 1 (Tr1) cells were isolated from severe combined immunodeficiency (SCID) patients transplanted with allogeneic haematopoietic stem cells (HSCT). Tr1 cells are induced in the periphery, and they respond selectively to persistent foreign and self-antigens under steady-state conditions [82]. Tr1 cells are currently defined as IL-10 positive, Foxp3 negative cells with immune-suppressive properties. Tr1 cells secrete high levels of IL-10 as compared to IL-4 and IL-17A, the hallmark cytokines of Th2 and Th17 cells respectively. Depending on the milieu, Tr1 cells can produce variable levels of IFN- $\gamma$ , the key cytokine produced by Th1 cells [83]. However, Tr1 cells have the capacity to suppress inflammatory T-cell responses and, therefore, are distinct from bona fide Th1, Th2, and Th17 cells that largely promote, rather than suppress the inflammatory responses. This control is mainly mediated through the secretion of the immunosuppressive cytokines IL-10 and TGF- $\beta$ 1 [84]. The antigen-specific activation of Tr1 cells is important to potentiate their regulatory function [85]. IL-10 acts by limiting the magnitude of immune responses, as proved by mice that lack IL-10 and that exhibit spontaneous enterocolitis. IL-10 downregulates the expression of co-stimulatory molecules, such as

CD80, CD86, MHC Class II and pro-inflammatory cytokine production by APCs, and inhibits the secretion of IL-2, TNF, and IL-17 by effector T cells [86]. In particular, Tr1-cell supernatant diminishes the capacity of monocytes to stimulate Th1-cell responses and blocks the differentiation and maturation of DCs via IL-10 [87]. TGF- $\beta$  downregulates the functions of APCs [88] and inhibits the proliferation and cytokine production by T cells [89]. Therefore, the suppressive effects of Tr1 cells are reversed by the addition of anti-IL10 and anti-TGF- $\beta$  neutralizing antibodies [90–92], but additional mechanisms may also contribute. Human Tr1 cells generated in vitro by crosslinking CD3 with CD46 can kill target cells through a granzyme B/perforin-dependent mechanism [93, 94]. Accordingly human Tr1 cells selectively kill myeloid cells (i.e., DC and monocytes) through granzyme B/perforin [95]. This selective cell-killing effect is mediated by CD226, which is highly expressed on Tr1 cells. Only myeloid cells express the CD226-ligand (CD155). Thus, this type of regulatory mechanism by Tr1 cells requires a cell–cell contact with APCs.

Recently, LAG-3 and CD49b have been identified as surface markers for Tr1 cells [96–100]. Another set of marker for human Tr1 cells is CCR5 and PD1 [101]. Additionally, other markers have been shown to be expressed on mouse IL-10 secreting cells, such as PD1, TIM-3, and TIGIT [102]. However, further studies are needed to test if these markers identify the same population of cells, or alternatively, if Tr1 cells per se represent a rather heterogeneous population, which is dependent on the cellular origin (e.g., naïve T cells, memory T cells, Th17, Th1 cells) and/or environmental factors. IL-10 has been considered to be the driving force for Tr1-cell generation on the basis of experiments in which antigen-specific Tr1 cells are induced in vitro by repeated TCR stimulation in the presence of high doses of IL-10 [85, 90]. However, the frequency of Tr1 cells in IL-10 deficient mice is not altered. Several publications have demonstrated a key role of IL-27, which can even synergize with TGF- $\beta$ , in the induction of Tr1 cells [103].

After the discovery of Foxp3 as the master transcriptional regulator of Foxp3+ Treg cells, a key point was whether Tr1 cells also express a master regulator. The double reporter mouse model for IL-10 and Foxp3 was instrumental in order to demonstrate that these two types of regulatory T cells are distinct. Indeed, Tr1 cells do not constitutively express Foxp3 [104, 105] and can be induced from IPEX patients who lack Foxp3 [106]. Several transcriptional regulators have been shown to be expressed by Tr1 cells, such as Hif1 $\alpha$ , Ahr, c-Maf, Egr2, Blimp-1, and Ror $\alpha$  [55, 99, 107]. During the induction of Tr1 cells by IL-27, the ligand-activated transcription factor hydrocarbon receptor (AhR) physically associates with avian musculoaponeurotic fibrosarcoma v-maf (c-Maf) and transactivates the *Il10* and *Il21* promoters. The secretion of IL-21 acts as an autocrine growth factor for Tr1 cells (reviewed in ref. [108]).

Therefore, while IL-10 is sufficient to induce Tr1 cells in vitro and in vivo, it is not necessary when IL-27 is present. Interestingly, the overexpression of Blimp-1 promotes the induction of IL-10 and the expression of LAG-3 and CD49b in vitro [97]. In addition, Blimp1 requires EGR-2 activity to promote the production of IL-10 and expression of LAG-3 in response to IL-27 [107]. In summary, the signaling network responsible for IL-10 regulatory T cells is also emerging gradually.

## 2 Concluding remarks

CD4+ T helper cells can be subdivided into several subsets according to the expression of transcriptional factors and the cytokine profile. This classification, based on limited parameters has been and still is instrumental in simplifying the complexity of immunological responses. However, this simplified model has obvious limitations, especially when it comes to explaining T-cell heterogeneity and plasticity. The technologies emerging now such as multi-parameter measurement at single cell level combined with bioinformatics analysis will allow us to comprehend the immune system in its complexity in the future.

## References

1. Zhu J, Yamane H, Paul WE (2010) Differentiation of effector CD4 T cell populations (\*). *Annu Rev Immunol* 28:445–489. doi:[10.1146/annurev-immunol-030409-101212](https://doi.org/10.1146/annurev-immunol-030409-101212)
2. Mosmann TR, Cherwinski H, Bond MW, Giedlin MA, Coffman RL (1986) Two types of murine helper T cell clone. I. Definition according to profiles of lymphokine activities and secreted proteins. *J Immunol* 136(7):2348–2357
3. Reiner SL, Adams WC (2014) Lymphocyte fate specification as a deterministic but highly plastic process. *Nat Rev Immunol* 14(10):699–704. doi:[10.1038/nri3734](https://doi.org/10.1038/nri3734)
4. Hsieh CS, Macatonia SE, Tripp CS et al (1993) Development of TH1 CD4+ T cells through IL-12 produced by Listeria-induced macrophages. *Science* 260(5107):547–549
5. Usui T, Preiss JC, Kanno Y et al (2006) T-bet regulates Th1 responses through essential effects on GATA-3 function rather than on IFNG gene acetylation and transcription. *J Exp Med* 203(3):755–766. doi:[10.1084/jem.20052165](https://doi.org/10.1084/jem.20052165), jem.20052165 [pii]
6. Usui T, Nishikomori R, Kitani A, Strober W (2003) GATA-3 suppresses Th1 development by downregulation of Stat4 and not through effects on IL-12Rbeta2 chain or T-bet. *Immunity* 18(3):415–428. doi:[10.1016/S1074-7613\(03\)00057-8](https://doi.org/10.1016/S1074-7613(03)00057-8), S1074761303000578 [pii]
7. Szabo SJ, Kim ST, Costa GL et al (2000) A novel transcription factor, T-bet, directs Th1 lineage commitment. *Cell* 100(6):655–669. doi:[10.1016/S0092-8674\(00\)80702-3](https://doi.org/10.1016/S0092-8674(00)80702-3), S0092-8674(00)80702-3 [pii]
8. Szabo SJ, Sullivan BM, Stemann C et al (2002) Distinct effects of T-bet in TH1 lineage commitment and IFN-gamma production in CD4 and CD8 T cells. *Science* 295(5553):338–342. doi:[10.1126/science.1065543](https://doi.org/10.1126/science.1065543), 295/5553/338 [pii]
9. Wei G, Wei L, Zhu J et al (2009) Global mapping of H3K4me3 and H3K27me3 reveals specificity and plasticity in lineage fate determination of differentiating CD4+ T cells. *Immunity* 30(1):155–167. doi:[10.1016/j.immuni.2008.12.009](https://doi.org/10.1016/j.immuni.2008.12.009)
10. Panzer M, Sitte S, Wirth S et al (2012) Rapid in vivo conversion of effector T cells into Th2 cells during helminth infection. *J Immunol* 188(2):615–623. doi:[10.4049/jimmunol.1101164](https://doi.org/10.4049/jimmunol.1101164)
11. Becattini S, Latorre D, Mele F et al (2015) T cell immunity. Functional heterogeneity of human memory CD4(+) T cell

- clones primed by pathogens or vaccines. *Science* 347(6220):400–406. doi:[10.1126/science.1260668](https://doi.org/10.1126/science.1260668)
12. Clemente-Casares X, Blanco J, Ambalavanan P, Yamanouchi J, Singha S, Fandos C, Tsai S, Wang J, Garabatos N, Izquierdo C, Agrawal S, Keough MB, Yong VW, James E, Moore A, Yang Y, Stratmann T, Serra P, Santamaria P (2016) Expanding antigenspecific regulatory networks to treat autoimmunity. *Nature* 530(7591):434–40. doi:[10.1038/nature16962](https://doi.org/10.1038/nature16962), Epub 2016 Feb 17
  13. Saraiva M, Christensen JR, Veldhoen M et al (2009) Interleukin-10 production by Th1 cells requires interleukin-12-induced STAT4 transcription factor and ERK MAP kinase activation by high antigen dose. *Immunity* 31(2):209–219. doi:[10.1016/j.immuni.2009.05.012](https://doi.org/10.1016/j.immuni.2009.05.012)
  14. Le Gros G, Ben-Sasson SZ, Seder R, Finkelman FD, Paul WE (1990) Generation of interleukin 4 (IL-4)-producing cells in vivo and in vitro: IL-2 and IL-4 are required for in vitro generation of IL-4-producing cells. *J Exp Med* 172(3):921–929
  15. Seder RA, Boulay JL, Finkelman F et al (1992) CD8+ T cells can be primed in vitro to produce IL-4. *J Immunol* 148(6):1652–1656
  16. Swain SL, Weinberg AD, English M, Huston G (1990) IL-4 directs the development of Th2-like helper effectors. *J Immunol* 145(11):3796–3806
  17. Kaplan MH, Schindler U, Smiley ST, Grusby MJ (1996) Stat6 is required for mediating responses to IL-4 and for development of Th2 cells. *Immunity* 4(3):313–319. doi:[S1074-7613\(00\)80439-2](https://doi.org/10.1074-7613(00)80439-2) [pii]
  18. Shimoda K, van Deursen J, Sangster MY et al (1996) Lack of IL-4-induced Th2 response and IgE class switching in mice with disrupted Stat6 gene. *Nature* 380(6575):630–633. doi:[10.1038/380630a0](https://doi.org/10.1038/380630a0)
  19. Takeda K, Tanaka T, Shi W et al (1996) Essential role of Stat6 in IL-4 signalling. *Nature* 380(6575):627–630. doi:[10.1038/380627a0](https://doi.org/10.1038/380627a0)
  20. Kurata H, Lee HJ, O'Garra A, Arai N (1999) Ectopic expression of activated Stat6 induces the expression of Th2-specific cytokines and transcription factors in developing Th1 cells. *Immunity* 11(6):677–688. doi:[10.1016/S1074-7613\(00\)80142-9](https://doi.org/10.1016/S1074-7613(00)80142-9), [S1074-7613\(00\)80142-9](https://doi.org/10.1074-7613(00)80142-9) [pii]
  21. Zhu J, Guo L, Watson CJ, Hu-Li J, Paul WE (2001) Stat6 is necessary and sufficient for IL-4's role in Th2 differentiation and cell expansion. *J Immunol* 166(12):7276–7281
  22. Zheng W, Flavell RA (1997) The transcription factor GATA-3 is necessary and sufficient for Th2 cytokine gene expression in CD4 T cells. *Cell* 89(4):587–596. doi:[10.1016/S0092-8674\(00\)80240-8](https://doi.org/10.1016/S0092-8674(00)80240-8), [S0092-8674\(00\)80240-8](https://doi.org/10.1016/S0092-8674(00)80240-8) [pii]
  23. Zhang DH, Cohn L, Ray P, Bottomly K, Ray A (1997) Transcription factor GATA-3 is differentially expressed in murine Th1 and Th2 cells and controls Th2-specific expression of the interleukin-5 gene. *J Biol Chem* 272(34):21597–21603
  24. Zhu J, Min B, Hu-Li J et al (2004) Conditional deletion of Gata3 shows its essential function in T(H)1-T(H)2 responses. *Nat Immunol* 5(11):1157–1165. doi:[10.1038/ni1128](https://doi.org/10.1038/ni1128), [ni1128](https://doi.org/10.1038/ni1128) [pii]
  25. Zhu J, Cote-Sierra J, Guo L, Paul WE (2003) Stat5 activation plays a critical role in Th2 differentiation. *Immunity* 19(5):739–748. doi:[10.1016/S1074-7613\(03\)00292-9](https://doi.org/10.1016/S1074-7613(03)00292-9), [S1074761303002929](https://doi.org/10.1016/S1074-7613(03)00292-9) [pii]
  26. Bruchard M, Rebe C, Derangere V et al (2015) The receptor NLRP3 is a transcriptional regulator of TH2 differentiation. *Nat Immunol* 16(8):859–870. doi:[10.1038/ni.3202](https://doi.org/10.1038/ni.3202)
  27. Wu L, Zepp JA, Qian W et al (2015) A novel IL-25 signaling pathway through STAT5. *J Immunol* 194(9):4528–4534. doi:[10.4049/jimmunol.1402760](https://doi.org/10.4049/jimmunol.1402760)
  28. Hegazy AN, Peine M, Helmstetter C et al (2010) Interferons direct Th2 cell reprogramming to generate a stable GATA-3(+)T-bet(+) cell subset with combined Th2 and Th1 cell functions. *Immunity* 32(1):116–128. doi:[10.1016/j.immuni.2009.12.004](https://doi.org/10.1016/j.immuni.2009.12.004)
  29. Coomes SM, Pelly VS, Kannan Y et al (2015) IFN $\gamma$  and IL-12 Restrict Th2 Responses during Helminth/Plasmodium Co-Infection and Promote IFN $\gamma$  from Th2 Cells. *PLoS Pathog* 11(7):e1004994. doi:[10.1371/journal.ppat.1004994](https://doi.org/10.1371/journal.ppat.1004994)
  30. Kim BS, Kim IK, Park YJ et al (2010) Conversion of Th2 memory cells into Foxp3+ regulatory T cells suppressing Th2-mediated allergic asthma. *Proc Natl Acad Sci U S A* 107(19):8742–8747. doi:[10.1073/pnas.0911756107](https://doi.org/10.1073/pnas.0911756107)
  31. Conti HR, Shen F, Nayyar N et al (2009) Th17 cells and IL-17 receptor signaling are essential for mucosal host defense against oral candidiasis. *J Exp Med* 206(2):299–311. doi:[10.1084/jem.20081463](https://doi.org/10.1084/jem.20081463), [jem.20081463](https://doi.org/10.1084/jem.20081463) [pii]
  32. Huang W, Na L, Fidel PL, Schwarzenberger P (2004) Requirement of interleukin-17A for systemic anti-*Candida albicans* host defense in mice. *J Infect Dis* 190(3):624–631

33. Ye P, Garvey PB, Zhang P et al (2001) Interleukin-17 and lung host defense against *Klebsiella pneumoniae* infection. *Am J Respir Cell Mol Biol* 25(3):335–340
34. Iwakura Y, Nakae S, Saijo S, Ishigame H (2008) The roles of IL-17A in inflammatory immune responses and host defense against pathogens. *Immunol Rev* 226:57–79. doi:[10.1111/j.1600-065X.2008.00699.x](https://doi.org/10.1111/j.1600-065X.2008.00699.x), IMR699 [pii]
35. Ishigame H, Kakuta S, Nagai T et al (2009) Differential roles of interleukin-17A and -17F in host defense against mucocutaneous bacterial infection and allergic responses. *Immunity* 30(1):108–119. doi:[10.1016/j.immuni.2008.11.009](https://doi.org/10.1016/j.immuni.2008.11.009), S1074-7613(08)00554-2 [pii]
36. Atarashi K, Tanoue T, Ando M et al (2015) Th17 cell induction by adhesion of microbes to intestinal epithelial cells. *Cell* 163(2):367–380. doi:[10.1016/j.cell.2015.08.058](https://doi.org/10.1016/j.cell.2015.08.058)
37. Ling Y, Cypowij S, Aytakin C et al (2015) Inherited IL-17RC deficiency in patients with chronic mucocutaneous candidiasis. *J Exp Med* 212(5):619–631. doi:[10.1084/jem.20141065](https://doi.org/10.1084/jem.20141065)
38. Zhou L, Ivanov II, Spolski R et al (2007) IL-6 programs T(H)-17 cell differentiation by promoting sequential engagement of the IL-21 and IL-23 pathways. *Nat Immunol* 8(9):967–974
39. Nurieva R, Yang XO, Martinez G et al (2007) Essential autocrine regulation by IL-21 in the generation of inflammatory T cells. *Nature* 448(7152):480–483
40. Yang XO, Panopoulos AD, Nurieva R et al (2007) STAT3 regulates cytokine-mediated generation of inflammatory helper T cells. *J Biol Chem* 282(13):9358–9363
41. Bettelli E, Carrier Y, Gao W et al (2006) Reciprocal developmental pathways for the generation of pathogenic effector TH17 and regulatory T cells. *Nature* 441(7090):235–238
42. Veldhoen M, Hocking RJ, Atkins CJ, Locksley RM, Stockinger B (2006) TGFbeta in the context of an inflammatory cytokine milieu supports de novo differentiation of IL-17-producing T cells. *Immunity* 24(2):179–189
43. Ivanov II, McKenzie BS, Zhou L et al (2006) The orphan nuclear receptor RORgammat directs the differentiation program of pro-inflammatory IL-17+ T helper cells. *Cell* 126(6):1121–1133
44. Mangan PR, Harrington LE, O'Quinn DB et al (2006) Transforming growth factor-beta induces development of the T(H)17 lineage. *Nature* 441(7090):231–234
45. McGeachy MJ, Chen Y, Tato CM et al (2009) The interleukin 23 receptor is essential for the terminal differentiation of interleukin 17-producing effector T helper cells in vivo. *Nat Immunol* 10(3):314–324. doi:[10.1038/ni.1698](https://doi.org/10.1038/ni.1698), ni.1698 [pii]
46. Ahern PP, Schiering C, Buonocore S et al (2010) Interleukin-23 drives intestinal inflammation through direct activity on T cells. *Immunity* 33(2):279–288. doi:[10.1016/j.immuni.2010.08.010](https://doi.org/10.1016/j.immuni.2010.08.010), S1074-7613(10)00293-1 [pii]
47. Sano T, Huang W, Hall JA et al (2015) An IL-23R/IL-22 circuit regulates epithelial serum amyloid A to promote local effector Th17 responses. *Cell* 163(2):381–393. doi:[10.1016/j.cell.2015.08.061](https://doi.org/10.1016/j.cell.2015.08.061)
48. Zielinski CE, Mele F, Aschenbrenner D, Jarrossay D, Ronchi F, Gattorno M, Monticelli S, Lanzavecchia A, Sallusto F (2012) Pathogen-induced human TH17 cells produce IFN- $\gamma$  or IL-10 and are regulated by IL-1beta. *Nature* 484(7395):514–8. doi:[10.1038/nature10957](https://doi.org/10.1038/nature10957)
49. Shaw MH, Kamada N, Kim YG, Nunez G (2012) Microbiota-induced IL-1beta, but not IL-6, is critical for the development of steady-state TH17 cells in the intestine. *J Exp Med* 209(2):251–258. doi:[10.1084/jem.20111703](https://doi.org/10.1084/jem.20111703), jem.20111703 [pii]
50. Ciofani M, Madar A, Galan C et al (2012) A validated regulatory network for Th17 cell specification. *Cell* 151(2):289–303. doi:[10.1016/j.cell.2012.09.016](https://doi.org/10.1016/j.cell.2012.09.016)
51. Yosef N, Shalek AK, Gaublotte JT et al (2013) Dynamic regulatory network controlling TH17 cell differentiation. *Nature* 496(7446):461–468. doi:[10.1038/nature11981](https://doi.org/10.1038/nature11981)
52. Wang C, Yosef N, Gaublotte J et al (2015) CD5L/AIM regulates lipid biosynthesis and restrains Th17 cell pathogenicity. *Cell* 163(6):1413–1427. doi:[10.1016/j.cell.2015.10.068](https://doi.org/10.1016/j.cell.2015.10.068)
53. Gaublotte JT, Yosef N, Lee Y et al (2015) Single-cell genomics unveils critical regulators of Th17 cell pathogenicity. *Cell* 163(6):1400–1412. doi:[10.1016/j.cell.2015.11.009](https://doi.org/10.1016/j.cell.2015.11.009)
54. Yu X, Rollins D, Ruhn KA et al (2013) TH17 cell differentiation is regulated by the circadian clock. *Science* 342(6159):727–730. doi:[10.1126/science.1243884](https://doi.org/10.1126/science.1243884)
55. Farez MF, Mascanfroni ID, Mendez-Huergo SP et al (2015) Melatonin contributes to the seasonality of multiple sclerosis relapses. *Cell* 162(6):1338–1352. doi:[10.1016/j.cell.2015.08.025](https://doi.org/10.1016/j.cell.2015.08.025)
56. Ghoreschi K, Laurence A, Yang XP et al (2010) Generation of pathogenic T(H)17

- cells in the absence of TGF-beta signalling. *Nature* 467(7318):967–971. doi:[10.1038/nature09447](https://doi.org/10.1038/nature09447), nature09447 [pii]
57. McGeachy MJ, Bak-Jensen KS, Chen Y et al (2007) TGF-beta and IL-6 drive the production of IL-17 and IL-10 by T cells and restrain T(H)-17 cell-mediated pathology. *Nat Immunol* 8(12):1390–1397. doi:[10.1038/ni1539](https://doi.org/10.1038/ni1539), ni1539 [pii]
  58. Gagliani N, Vesely MC, Iseppon A et al (2015) Th17 cells transdifferentiate into regulatory T cells during resolution of inflammation. *Nature* 523(7559):221–225. doi:[10.1038/nature14452](https://doi.org/10.1038/nature14452)
  59. Hirota K, Duarte JH, Veldhoen M et al (2011) Fate mapping of IL-17-producing T cells in inflammatory responses. *Nat Immunol* 12(3):255–263. doi:[10.1038/ni.1993](https://doi.org/10.1038/ni.1993)
  60. Hirota K, Turner JE, Villa M et al (2013) Plasticity of Th17 cells in Peyer's patches is responsible for the induction of T cell-dependent IgA responses. *Nat Immunol* 14(4):372–379. doi:[10.1038/ni.2552](https://doi.org/10.1038/ni.2552)
  61. Obermajer N, Popp FC, Soeder Y et al (2014) Conversion of Th17 into IL-17A(neg) regulatory T cells: a novel mechanism in prolonged allograft survival promoted by mesenchymal stem cell-supported minimized immunosuppressive therapy. *J Immunol* 193(10):4988–4999. doi:[10.4049/jimmunol.1401776](https://doi.org/10.4049/jimmunol.1401776)
  62. Harbour SN, Maynard CL, Zindl CL, Schoeb TR, Weaver CT (2015) Th17 cells give rise to Th1 cells that are required for the pathogenesis of colitis. *Proc Natl Acad Sci U S A* 112(22):7061–7066. doi:[10.1073/pnas.1415675112](https://doi.org/10.1073/pnas.1415675112)
  63. Sakaguchi S, Sakaguchi N, Asano M, Itoh M, Toda M (1995) Immunologic self-tolerance maintained by activated T cells expressing IL-2 receptor alpha-chains (CD25). Breakdown of a single mechanism of self-tolerance causes various autoimmune diseases. *J Immunol* 155(3):1151–1164
  64. Fontenot JD, Gavin MA, Rudensky AY (2003) Foxp3 programs the development and function of CD4+CD25+ regulatory T cells. *Nat Immunol* 4(4):330–336
  65. Hori S, Nomura T, Sakaguchi S (2003) Control of regulatory T cell development by the transcription factor Foxp3. *Science* 299(5609):1057–1061
  66. Wan YY, Flavell RA (2007) Regulatory T-cell functions are subverted and converted owing to attenuated Foxp3 expression. *Nature* 445(7129):766–770
  67. Passerini L, Santoni de Sio FR, Roncarolo MG, Bacchetta R (2014) Forkhead box P3: the peacekeeper of the immune system. *Int Rev Immunol* 33(2):129–145. doi:[10.3109/08830185.2013.863303](https://doi.org/10.3109/08830185.2013.863303)
  68. Josefowicz SZ, Lu LF, Rudensky AY (2012) Regulatory T cells: mechanisms of differentiation and function. *Annu Rev Immunol* 30:531–564. doi:[10.1146/annurev.immunol.25.022106.141623](https://doi.org/10.1146/annurev.immunol.25.022106.141623)
  69. Huber S, Schramm C, Lehr HA et al (2004) Cutting edge: TGF-beta signaling is required for the in vivo expansion and immunosuppressive capacity of regulatory CD4+CD25+ T cells. *J Immunol* 173(11):6526–6531
  70. Schramm C, Huber S, Protschka M et al (2004) TGFbeta regulates the CD4+CD25+ T-cell pool and the expression of Foxp3 in vivo. *Int Immunol* 16(9):1241–1249. doi:[10.1093/intimm/dxh126](https://doi.org/10.1093/intimm/dxh126), dxh126 [pii]
  71. Fantini MC, Becker C, Monteleone G et al (2004) Cutting edge: TGF-beta induces a regulatory phenotype in CD4+CD25- T cells through Foxp3 induction and down-regulation of Smad7. *J Immunol* 172(9):5149–5153
  72. Chen W, Jin W, Hardegen N et al (2003) Conversion of peripheral CD4+CD25- naive T cells to CD4+CD25+ regulatory T cells by TGF-beta induction of transcription factor Foxp3. *J Exp Med* 198(12):1875–1886
  73. Kretschmer K, Apostolou I, Hawiger D et al (2005) Inducing and expanding regulatory T cell populations by foreign antigen. *Nat Immunol* 6(12):1219–1227
  74. Marie JC, Letterio JJ, Gavin M, Rudensky AY (2005) TGF-beta1 maintains suppressor function and Foxp3 expression in CD4+CD25+ regulatory T cells. *J Exp Med* 201(7):1061–1067
  75. Bennett CL, Christie J, Ramsdell F et al (2001) The immune dysregulation, polyendocrinopathy, enteropathy, X-linked syndrome (IPEX) is caused by mutations of FOXP3. *Nat Genet* 27(1):20–21
  76. Brunkow ME, Jeffery EW, Hjerrild KA et al (2001) Disruption of a new forkhead/winged-helix protein, scurfy, results in the fatal lymphoproliferative disorder of the scurfy mouse. *Nat Genet* 27(1):68–73
  77. Huber S, Gagliani N, Esplugues E et al (2011) Th17 cells express interleukin-10 receptor and are controlled by Foxp3- and Foxp3+ regulatory CD4+ T cells in an interleukin-10-dependent manner. *Immunity* 34(4):554–565. doi:[10.1016/j.immuni.2011.01.020](https://doi.org/10.1016/j.immuni.2011.01.020), S1074-7613(11)00129-4 [pii]
  78. Fahlen L, Read S, Gorelik L et al (2005) T cells that cannot respond to TGF-beta

- escape control by CD4+CD25+ regulatory T cells. *J Exp Med* 201(5):737–746
79. Annunziato F, Cosmi L, Liotta F et al (2002) Phenotype, localization, and mechanism of suppression of CD4(+)CD25(+) human thymocytes. *J Exp Med* 196(3):379–387
80. Bopp T, Becker C, Klein M et al (2007) Cyclic adenosine monophosphate is a key component of regulatory T cell-mediated suppression. *J Exp Med* 204(6):1303–1310
81. Hori S (2014) Lineage stability and phenotypic plasticity of Foxp3(+) regulatory T cells. *Immunol Rev* 259(1):159–172. doi:10.1111/imr.12175
82. Haringer B, Lozza L, Steckel B, Geginat J (2009) Identification and characterization of IL-10/IFN-gamma-producing effector-like T cells with regulatory function in human blood. *J Exp Med* 206(5):1009–1017. doi:10.1084/jem.20082238, jem.20082238 [pii]
83. Roncarolo MG, Gregori S, Battaglia M et al (2006) Interleukin-10-secreting type 1 regulatory T cells in rodents and humans. *Immunol Rev* 212:28–50. doi:10.1111/j.0105-2896.2006.00420.x, IMR420 [pii]
84. Cobbold SP, Nolan KF, Graca L et al (2003) Regulatory T cells and dendritic cells in transplantation tolerance: molecular markers and mechanisms. *Immunol Rev* 196:109–124, doi: 078 [pii]
85. Gagliani N, Jofra T, Stabilini A et al (2010) Antigen-specific dependence of Tr1-cell therapy in preclinical models of islet transplant. *Diabetes* 59(2):433–439. doi:10.2337/db09-1168, db09-1168 [pii]
86. Pestka S, Krause CD, Sarkar D et al (2004) Interleukin-10 and related cytokines and receptors. *Annu Rev Immunol* 22:929–979. doi:10.1146/annurev.immunol.22.012703.104622
87. Cavani A, Nasorri F, Prezzi C et al (2000) Human CD4+ T lymphocytes with remarkable regulatory functions on dendritic cells and nickel-specific Th1 immune responses. *J Invest Dermatol* 114(2):295–302. doi:10.1046/j.1523-1747.2000.00881.x, jid881 [pii]
88. Strobl H, Emshoff R, Rothler G (1999) Conservative treatment of unilateral condylar fractures in children: a long-term clinical and radiologic follow-up of 55 patients. *Int J Oral Maxillofac Surg* 28(2):95–98
89. Cerwenka A, Swain SL (1999) TGF-beta1: immunosuppressant and viability factor for T lymphocytes. *Microbes Infect* 1(15):1291–1296, doi:S1286-4579(99)00255-5 [pii]
90. Groux H, O'Garra A, Bigler M et al (1997) A CD4+ T-cell subset inhibits antigen-specific T-cell responses and prevents colitis. *Nature* 389(6652):737–742
91. Levings MK, Gregori S, Tresoldi E et al (2005) Differentiation of Tr1 cells by immature dendritic cells requires IL-10 but not CD25+CD4+ Tr cells. *Blood* 105(3):1162–1169. doi:10.1182/blood-2004-03-1211, 2004-03-1211 [pii]
92. Gregori S, Tomasoni D, Pacciani V et al (2010) Differentiation of type 1 T regulatory cells (Tr1) by tolerogenic DC-10 requires the IL-10-dependent ILT4/HLA-G pathway. *Blood* 116(6):935–944. doi:10.1182/blood-2009-07-234872, blood-2009-07-234872 [pii]
93. Grossman WJ, Verbsky JW, Tollefsen BL et al (2004) Differential expression of granzymes A and B in human cytotoxic lymphocyte subsets and T regulatory cells. *Blood* 104(9):2840–2848. doi:10.1182/blood-2004-03-0859, 2004-03-0859 [pii]
94. Grossman WJ, Verbsky JW, Barchet W et al (2004) Human T regulatory cells can use the perforin pathway to cause autologous target cell death. *Immunity* 21(4):589–601
95. Magnani CF, Alberigo G, Bacchetta R et al (2011) Killing of myeloid APCs via HLA class I, CD2 and CD226 defines a novel mechanism of suppression by human Tr1 cells. *Eur J Immunol* 41(6):1652–1662. doi:10.1002/eji.201041120
96. Gagliani N, Magnani CF, Huber S et al (2013) Coexpression of CD49b and LAG-3 identifies human and mouse T regulatory type 1 cells. *Nat Med* 19(6):739–746. doi:10.1038/nm.3179
97. Heinemann C, Heink S, Petermann F et al (2014) IL-27 and IL-12 oppose pro-inflammatory IL-23 in CD4+ T cells by inducing Blimp1. *Nat Commun* 5:3770. doi:10.1038/ncomms4770
98. Bacchetta R, Lucarelli B, Sartirana C et al (2014) Immunological outcome in haploidentical-HSC transplanted patients treated with IL-10-energized donor T cells. *Front Immunol* 5:16. doi:10.3389/fimmu.2014.00016
99. Mascanfroni ID, Takenaka MC, Yeste A et al (2015) Metabolic control of type 1 regulatory T cell differentiation by AHR and HIF1-alpha. *Nat Med* 21(6):638–646. doi:10.1038/nm.3868
100. Okamura T, Fujio K, Shibuya M et al (2009) CD4+CD25-LAG3+ regulatory T cells controlled by the transcription factor Egr-2. *Proc Natl Acad Sci U S A* 106(33):13974–

13979. doi:[10.1073/pnas.0906872106](https://doi.org/10.1073/pnas.0906872106), 0906872106 [pii]
101. Facciotti F, Gagliani N, Haringer B et al (2015) IL-10-producing forkhead box protein 3-negative regulatory T cells inhibit B-cell responses and are involved in systemic lupus erythematosus. *J Allergy Clin Immunol* 137(1): 318–321. doi:[10.1016/j.jaci.2015.06.044](https://doi.org/10.1016/j.jaci.2015.06.044)
102. Burton BR, Britton GJ, Fang H et al (2014) Sequential transcriptional changes dictate safe and effective antigen-specific immunotherapy. *Nat Commun* 5:4741. doi:[10.1038/ncomms5741](https://doi.org/10.1038/ncomms5741)
103. Apetoh L, Quintana FJ, Pot C et al (2010) The aryl hydrocarbon receptor interacts with c-Maf to promote the differentiation of type 1 regulatory T cells induced by IL-27. *Nat Immunol* 11(9):854–861. doi:[10.1038/ni.1912](https://doi.org/10.1038/ni.1912), ni.1912 [pii]
104. Vieira PL, Christensen JR, Minaee S et al (2004) IL-10-secreting regulatory T cells do not express Foxp3 but have comparable regulatory function to naturally occurring CD4+CD25+ regulatory T cells. *J Immunol* 172(10):5986–5993
105. Maynard CL, Harrington LE, Janowski KM et al (2007) Regulatory T cells expressing interleukin 10 develop from Foxp3+ and Foxp3- precursor cells in the absence of interleukin 10. *Nat Immunol* 8(9):931–941. doi:[10.1038/ni1504](https://doi.org/10.1038/ni1504), ni1504 [pii]
106. Passerini L, Di Nunzio S, Gregori S et al (2011) Functional type 1 regulatory T cells develop regardless of FOXP3 mutations in patients with IPEX syndrome. *Eur J Immunol* 41(4): 1120–1131. doi:[10.1002/eji.201040909](https://doi.org/10.1002/eji.201040909)
107. Iwasaki Y, Fujio K, Okamura T et al (2013) Egr-2 transcription factor is required for Blimp-1-mediated IL-10 production in IL-27-stimulated CD4+ T cells. *Eur J Immunol* 43(4): 1063–1073. doi:[10.1002/eji.201242942](https://doi.org/10.1002/eji.201242942)
108. Pot C, Apetoh L, Awasthi A, Kuchroo VK (2010) Molecular pathways in the induction of interleukin-27-driven regulatory type 1 cells. *J Interferon Cytokine Res* 30(6):381–388. doi:[10.1089/jir.2010.0047](https://doi.org/10.1089/jir.2010.0047)

## FACS Analysis of Memory T Lymphocytes

Enrico Lugli, Veronica Zanon, Domenico Mavilio, and Alessandra Roberto

### Abstract

Flow cytometry is a powerful and robust technology for detecting and monitoring multiple markers at the level of single cells. Since its early development, flow cytometry has been used to assess heterogeneity in a cell suspension. Over the years, the increasing number of parameters that could be included in a single assay combined with physical separation by fluorescence-activated cell sorting (FACS) revealed that the T cell compartment is extremely heterogeneous in terms of phenotypic diversity, functional capacity, and transcriptional regulation. While naïve T cells are fairly homogenous, diversity becomes extreme in the antigen-experienced memory compartment. The precise identification of memory subsets by the simultaneous analysis of multiple markers by flow cytometry is key not only to basic science but also for the correct immunomonitoring of patients undergoing immunotherapy or for T cell-based therapeutic approaches. In this chapter, we provide guidelines to optimize complex flow cytometry panels, to achieve correct fluorescence compensation and determine positivity for a given antigen. Correct selection of reagents and their validation is essential to the success of the assay. Despite having been developed for the identification of human naïve and memory T cell subsets, the concepts illustrated here can be applied to any experiment aiming to investigate  $n$  parameters by flow cytometry.

**Key words** Polychromatic flow cytometry, Naïve T cells, Memory T cells, FACS, Antibody, Cell sorting, Compensation, Reagent titration, T cell differentiation

---

### 1 Introduction

Following positive and negative selection in the thymus, CD4<sup>+</sup> and CD8<sup>+</sup> T cells are released in the periphery as mature T cells and harbor a given specificity for their cognate antigen that is encoded at the level of the T cell receptor. Before antigen encounter, T cells are defined as “naïve” (T<sub>N</sub>) and preferentially recirculate between the blood and secondary lymphoid organs [1]. Once activated, T<sub>N</sub> differentiate into effector cells which are highly cytotoxic and are capable to kill infected or tumor cells. The vast majority of these cells is short-lived and is eliminated after the antigen is cleared. Only a small population of activated cells generates memory T cells which are able to persist in the body in the long term [2]. The highly diverse memory T cell compartment can be dissected into

several subsets according to their surface and intracellular phenotypes [1]. Phenotypically defined subsets display different patterns of gene expression, have different persistent capacities *in vivo* and differently integrate environmental cues such as antigen stimulation, cytokine responsiveness, and interaction with surrounding tissues [3]. These concepts are important in the context of immune reconstitution and adoptive cell transfer approaches for cancer and viral infections, as subsets with improved functionality may influence the outcome of patients treated with cell-based immunotherapies [3].

Polychromatic flow cytometry, *i.e.*, a technology capable to measure up to 18 antigens on a single cell, played a pivotal role in defining the diversity of the peripheral and tissue-resident naïve and memory T cell pools. Polychromatic flow cytometry has become simpler over the years thanks to better hardware components, reagents, and softwares for data analysis. Nonetheless, combining up to 18 fluorescently conjugated antibodies (mAbs) in the same panel may be complex due to spillover between fluorochromes, fluorescence spread and poor signal sensitivity (separation) in a given channel [4]. Here we provide a detailed workflow to design and optimize a polychromatic flow cytometry panel for the identification of memory T cell subsets, in both CD8<sup>+</sup> and CD4<sup>+</sup> T cells [5]. This includes exclusion of dead cells to avoid false positive events (dead cells indeed bind antibodies in a nonspecific manner), careful reagent titration to optimize positive signal detection with minimal increase in background fluorescence due to unspecific staining and selection of reagent–fluorochrome combinations. Specific considerations on machine performance and optimization, quality control and hardware validation are not discussed in this chapter as a comprehensive protocol is available elsewhere [6].

Using a combination of mAbs that specifically recognize different antigens, it is now possible to investigate the expression of multiple markers on single T cells simultaneously, hence defining their heterogeneity. In addition, flow cytometry combined with fluorescently activated cell sorting, allows to isolate subsets of interest for further functional and molecular analysis. A diverse array of markers can be used to track naïve and memory T cells, although many of these are highly redundant in their expression [1]. A consensus in this regard still has to be reached. Here we propose to reduce the dimensionality of polychromatic assays to a core of four surface markers (*i.e.*, CD45RO, CCR7, CD27, and CD95) along with T cell lineage markers to identify the main subsets of naïve and memory T cells [5]. CD45RO is the low molecular weight splicing isoform of the CD45 protein and is present on most memory T cells. It is generally mutually exclusive with the long isoform CD45RA, that is characteristic of naïve. For this reason, these two markers are generally interchangeable. However, CD45RO is preferable since it allows the exclusion of the few CD45RO<sup>+</sup>/CD45RA<sup>+</sup> activated

memory cells. Moreover, ~1% of individuals do not splice CD45RA completely upon activation due a polymorphism in the CD45 gene. As a consequence, the vast majority of memory T cells are CD45RA<sup>+</sup>CD45RO<sup>+</sup>. CCR7 identifies those T cells that are capable to recirculate through secondary lymphoid tissues and distinguishes between T<sub>CM</sub> and T<sub>EM</sub> cells. CCR7 is generally co-expressed with CD62L (also known as I-selectin). However, the former is preferred as evidence reports that CD62L can be reliably detected only on fresh samples [4]. The costimulator CD27 is lost upon peripheral memory differentiation and allows to separate CD27<sup>+</sup> transitional memory (T<sub>TM</sub>) from CD27<sup>-</sup> effector memory (T<sub>EM</sub>) cells. Finally, CD95 is expressed on all memory cells while it is absent on naïve. Importantly, a small population of early differentiated T cells with a naïve-like phenotype but memory in function, i.e., the T<sub>SCM</sub>, is CD95<sup>+</sup> [7, 8]. The classification suggested here may not satisfy all applications, as different markers may be used to delineate T cell phenotypes on the basis of specific functions rather than stages of peripheral differentiation. In any case, it is important to stress that multiple markers must be detected simultaneously to pinpoint specific T cell subsets and exclude contaminants with unknown functions. When combined together, these antibodies allow to identify highly purified T<sub>N</sub> as well as multiple subsets of memory T cells, including T<sub>SCM</sub>, T central memory (T<sub>CM</sub>), T<sub>TM</sub>, T<sub>EM</sub> and T terminal effector (T<sub>TE</sub>) cells. Such a design leaves many channels open for the investigation of additional antigens, such as chemokine receptors, phosphoproteins, inhibitory receptors, activation molecules, or functional markers.

---

## 2 Materials

1. Peripheral Blood Mononuclear Cells (PBMCs).
2. Hanks' balanced salt solution without calcium and magnesium (HBSS<sup>-/-</sup>).
3. Phosphate buffered saline without calcium and magnesium (PBS<sup>-/-</sup>).
4. Fetal bovine serum (FBS).
5. FACS Buffer: PBS + 2% (vol/vol) FBS.
6. R10 complete medium: RPMI-1640, 10% (vol/vol) FBS, and 0.02% (w/vol) sodium azide.
7. Cytotfix/Cytoperm fixation and permeabilization kit (BD Biosciences): dilute 10× BD Perm/Wash buffer in distilled H<sub>2</sub>O to a final concentration of 1× prior to use.
8. FACS tubes.
9. Fluorescently conjugated mAbs to CD3, CD4, CD8, CD45RO, CCR7, CD27, and CD95.

10. Compensation beads (BD Biosciences).
11. ArC™ Amine Reactive Compensation Bead Kit (Thermo Fisher Scientific).
12. Viability dye such as Aqua Live Dead (Thermo Fisher Scientific) or Zombie Aqua (BioLegend).
13. Formalin (Tousimis): dilute to 1% working solution in PBS.
14. Multiparameter flow cytometer equipped with blue, red, violet, and yellow/green laser and capable to collect at least eight colors.
15. FlowJo analysis software (Tree Star Inc).

---

### 3 Methods

#### **3.1 Identify Priority Markers for the Study of Memory T Cells**

Current flow cytometers allow the simultaneous detection of 17–18 antigens on the surface. Nowadays, antibodies directed to a given antigen are available in multiple, although not in all cases, conjugations, and therefore, a priority in the decision of markers to be included in the staining should be outlined before starting the experiment, as such:

1. Priority markers, in this protocol CD45RO, CCR7, CD27 and CD95.
2. Lineage markers, in this protocol CD3, CD4 and CD8. Multiple conjugates are available to these antigens, thereby allowing a high degree of flexibility.
3. Additional markers, i.e., markers that can provide additional information but are potentially dispensable.

#### **3.2 Instrument Configuration and Antigen/Fluorochrome Combination**

The panel proposed here applies to a flow cytometer/cell sorter equipped with a 405 nm violet laser, a 488 nm blue laser, a 560 nm yellow/green laser, and a 640 red laser, and modified to collect up to 17 fluorescences simultaneously. Even if not used, more detectors (and the related filters and mirrors) allow a better separation of fluorochromes according to emission wavelengths. Compensation can thus be minimized. The panel may be rearranged so that it can be used on machines with a limited number of detectors, as recently described [5]. To this end, machine configuration and therefore the fluorochromes that can be detected must be taken into account.

Both the properties of each fluorochrome and the relative expression of the antigen of interest are important for the success of the panel. The general rule is to assign dimly expressed antigens to antibodies conjugated to bright fluorochromes. These include BV421, PE, and APC. Lineage molecules such as CD3, CD4, and CD8 are highly expressed on the cell surface and are easily detected with dimmer fluorochromes. Conversely, naïve and memory

markers are generally not characterized by bimodal distribution, rather they are differentially expressed according to the specific subset (a smear of fluorescence). For instance, CD95 is not expressed on naïve, while it is dim on T<sub>SCM</sub> cells and bright on all other memory T cells [5]. In general, we take advantage of anti-CD95 PE conjugates for the proper detection of T<sub>SCM</sub> cells.

### **3.3 Excluding Dead Cells**

Samples that have been cryopreserved and/or stimulated with antigens or other stimuli can include large numbers of dead cells, which can bind monoclonal antibodies nonspecifically, thus generating false positives. These artifacts are particularly critical when detecting rare cells (e.g., intracytoplasmatic cytokine staining, peptide-MHC Class I assays) [9]. Moreover, dead cells tend to have increased autofluorescence compared to live cells, also in this case appearing as positive. A number of fixable fluorescent amine reactive dyes are nowadays available commercially, and cover most of the visible spectrum. In the proposed protocol, we use Aqua dye which can be excited by a violet laser (405 nm) and has a maximum emission at 526 nm. The choice of this viable dye is driven by the little availability of fluorochrome-conjugated antibodies emitting in this particular channel. Should the user not be able to detect Aqua, additional dyes excited by the blue or the red lasers and emitting at different wavelengths are also available. To exclude dead cells, proceed as follows:

1. Isolate PBMC from circulating blood by using standard Ficoll density gradient isolation. Alternatively, digest the tissue of interest with appropriate protocols to obtain a single cell suspension containing leukocytes.
2. Wash cells with 10 mL HBSS<sup>-/-</sup> or PBS<sup>-/-</sup>. Should cells be thawed from frozen aliquots, wash cells thoroughly to remove serum proteins in order to avoid reaction with viability dyes. Centrifuge at  $515 \times g$  for 10 min and remove supernatant.
3. Prepare viability dye mix. Dilute 0.5  $\mu$ L of viability dye (LIVE/DEAD<sup>®</sup> Fixable Aqua Dead Cell Stain Kit or Zombie Aqua<sup>™</sup> Fixable dyes) in 19.5  $\mu$ L of water, mix well, then add 380  $\mu$ L of HBSS<sup>-/-</sup>. 100  $\mu$ L of mix stain up to  $10^7$  cells. The amount of dye to be used in the staining has been determined by titration experiments, according to the procedure reported in Subheading 3.4. We did not observe differences between reagent lot in the amount of dye that is optimal to detect dead cells.
4. Mix cell pellet with viability mix, vortex, and incubate for 15 min at room temperature (24 °C, RT) in the dark.
5. Wash cells with 2 mL FACS Buffer (generally, 20-fold the staining volume) and centrifuge cells at  $515 \times g$  for 5 min.

### 3.4 Optimizing the Reagents: Antibody Titration

Reagent titration and optimization is the first pivotal step to be undertaken when building flow cytometry panels. Antibody titration is necessary to validate reagents and to ensure that optimal antibody concentration is used to determine the best separation over background [10]. Generally, companies recommend a concentration (expressed in  $\mu\text{L}$ , in a final volume of 100  $\mu\text{L}$ ) at which a given mAb should be used. However, in most cases, this results in poor separation due to increased background staining, thereby causing nonoptimal detection of the antigen. This is critical when investigating those antigens that are dimly expressed. A number of parameters influence the optimal titer of a given antibody, including temperature, time of incubation and buffers (especially those containing fixatives). Titration experiments must therefore be optimized under the conditions of the assay. The vast majority of the mAbs perform well when used at RT for 20 min in a final volume of 100  $\mu\text{L}$ . However, some antigens are better detected at 37 °C (e.g., CCR7) due to recycling across the plasma membrane [11]. To titrate antibodies, proceed as follows:

1. Prepare a 2 $\times$  Ab staining mix (containing the Ab of interest) in excess to compensate for pipetting error (generally, 15% in excess). Use twofold the titer suggested by companies: if a volume of 10  $\mu\text{L}$  in 100  $\mu\text{L}$  is suggested, add 23  $\mu\text{L}$  in 92  $\mu\text{L}$  of FACS buffer. Adjust the amount of FACS buffer is a different volume if antibody is used.
2. Vortex mix, then centrifuge in a microcentrifuge at 15,000 $\times g$  (or top speed) for 3 min to pellet antibody aggregates.
3. In the meantime, prepare eight FACS tubes and add 50  $\mu\text{L}$  of FACS Buffer from tube 2 to tube 8. Add 50  $\mu\text{L}$  of the twofold mix in tube 1 and in tube 2, perform twofold serial dilution from tube 2 to tube 7. Pipet up and down to resuspend the mAb mix with the FACS buffer at each dilution step. Discard 50  $\mu\text{L}$  from tube 7. Tube 8 will serve as unstained control (*see Note 1*).
4. Remove supernatant from pelleted cells. Resuspend cells in 450  $\mu\text{L}$  of FACS buffer and pipette 50  $\mu\text{L}$  of cell suspension to tube 1–8 (*see Note 2*).
5. Vortex tubes and incubate for 20 min at RT in the dark.
6. Wash cells with 2 mL FACS buffer, centrifuge cells at 515 $\times g$  for 5 min and discard supernatant.
7. Fix cells in 100  $\mu\text{L}$  of 1% formalin (diluted in HBSS–/–) for 30 min at RT in the dark.
8. Wash cells in 2 mL HBSS–/– and centrifuge at 515 $\times g$  for 5 min.
9. Discard supernatant and resuspend cells in 200  $\mu\text{L}$  of HBSS–/–.
10. Acquire samples at the flow cytometer (*see Note 3*).

11. To determine the optimal titer, identify positive and negative populations by using a flow cytometry analysis software.
12. Determine the frequency of positive cells. This should be similar to what is expected (e.g., CD3<sup>+</sup> T cells are ~70% of circulating PBMCs) (*see Note 1*).
13. Determine the optimal mAb concentration by choosing the titer with the best separation between the positive and the negative signal and without increase in the background. This is best observed by concatenating titration files in a single file by using FlowJo and by visualizing fluorescence as a function of the titer (Fig. 1a) (*see Note 4*).
14. Calculating the signal-to-noise ratio may help in defining the optimal titer: divide the median fluorescence intensity of the positive with that of the negative population ( $\text{MFI ratio} = \text{MFI}^+ / \text{MFI}^-$ ). Choose the concentration of mAb giving the highest ratio (Fig. 1b) (*see Note 5*).

### 3.5 Multicolor Compensation

Compensation is the mathematical subtraction of the unwanted fluorescence deriving from a primary channel that is detected in a secondary channel as a consequence of spectral overlap between fluorochromes [12]. Indeed, photomultiplier tubes (PMTs) are equipped with filters capable to collect fluorescence resulting from the excitation of different fluorochromes. Fluorescence compensation is ideally necessary when working with >1 parameter in flow cytometry. However, some fluorochromes may be distant enough

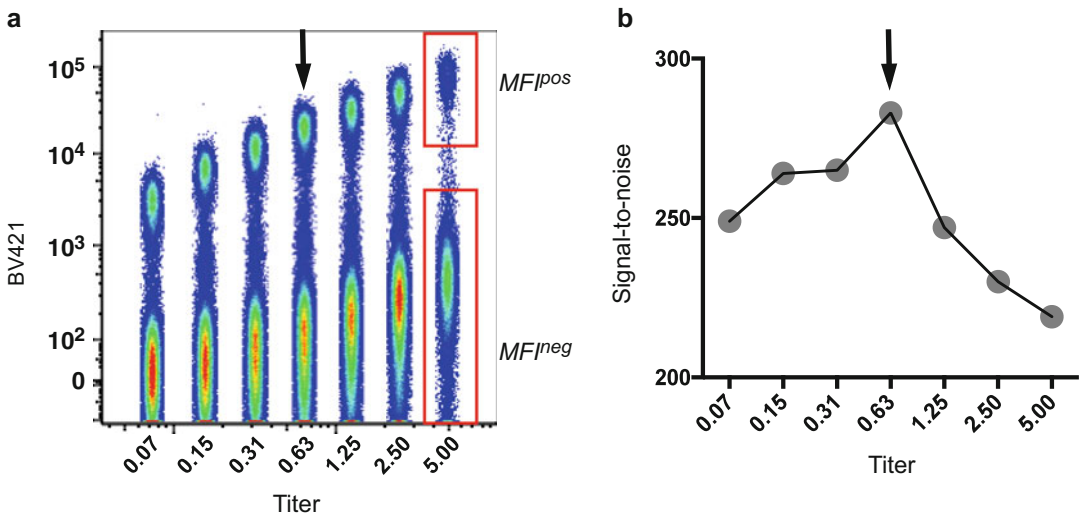


**Fig. 1** Reagent titration and validation. **(a)** PBMC were stained with a BV421-conjugated mAb at different concentrations (range 0.07–5  $\mu\text{L}$ ). Separate acquisition files were concatenated in FlowJo and fluorescence is visualized as a function of the titer. Gates identify positive and negative cells and MFIs were subsequently calculated. **(b)** Signal-to-noise ratio ( $\text{MFI}^{\text{pos}}/\text{MFI}^{\text{neg}}$ ) expressed as a function of the mAb titer. In both plots, the black arrows indicate the optimal titer

in their emission spectra (e.g., BV421 and PE-Cy7) and not require compensation. Multicolor compensation can be achieved by using controls stained with single mAbs or fluorescent probes. Both cells and antibody-capture beads may be used for compensation; however, beads provide a uniform binding capacity compared to cells, thus resulting in very bright and narrow fluorescence. In case of mAbs or probes that are not captured by the beads, cellular compensation controls must be used.

Proper compensation can be achieved by following three major rules that are independent on the fluorescent signals and the number of parameters in a given assay:

1. Use single-stained compensation controls that are at least as bright as the test sample.
2. Have paired positive and negative controls with the same autofluorescence (i.e., same unstained beads, lymphocytes, and cell line).
3. Prepare compensation controls with the same fluorochrome that is being used in the staining, if that fluorochrome is a tandem. Indeed, tandem dyes may display company- or lot-dependent variability. Should the fluorochrome not be a tandem, any antibody conjugated to the same fluorochrome can be used (*see Note 6*).

Prepare comp tubes as indicated below:

1. Prepare a compensation control for each fluorescent dye in the panel. In the proposed experiment, all antibodies included in the panel are captured by BD CompBeads™. For this reason, a single universal unstained control (unstained BD CompBeads™) can be used. Importantly, Aqua viability dye is bound by beads (the ArC™ Amine Reactive Compensation Bead Kit) that are different from those used for antibodies, thus requiring its negative control. In an eight-color assay detecting Aqua, CD3, CD4, CD8, CD45RO, CCR7, CD27, and CD95, prepare ten compensation controls.
2. Beads tend to form aggregates over time: sonicate beads for 2 min on a regular basis before use. Vortex comp beads (BD Comp Beads™ and ArC™ Amine Reactive Compensation Beads) and aliquot 30 µL to predefined tubes.
3. Add fluorochrome-conjugated antibodies to specific tubes and incubate for 15 min at RT. Beads bind antibodies with very high affinity, and therefore, the same amount of reagent used in the staining should be sufficient to obtain a very bright fluorescent signal.
4. Wash compensation controls by adding 2 mL of FACS buffer to each tube and centrifuge at  $515 \times g$  for 5 min. Resuspend cells in appropriate buffer (*see Note 7*).

5. Acquire using the same PMT voltages for both test samples and compensation controls. Unstained ArC™ Amine beads should be mixed with Aqua-stained ArC™ Amine beads before acquisition and collected in the same file.
6. Define positive and negative gates by using the machine acquisition software, the Wizard function contained in FlowJo or an equivalent algorithm.
7. Calculate compensation (define the compensation matrix).
8. Refer to next paragraph to troubleshoot compensation issues.

### **3.6 Troubleshooting Compensation**

Compensation is probably the most common source of artifacts in a flow cytometry experiment. We discourage to perform compensation manually, rather we suggest to perform automated compensation via software. Manual compensation is impractical in multicolor experiments. A given fluorescent signal may have spectral overlap in  $n$  channels, and hence,  $2n$  pairwise combinations should be considered when compensating flow cytometry data. Nevertheless, attention should be paid to automated compensation as well. Incorrect compensation may in fact result from improper controls. Tools such as the N by N viewer in FlowJo are very useful to check compensation as every fluorescent signal is rapidly visualized in relation to all others in the staining (Fig. 2a). FlowJo as well as other flow cytometry analysis software allow to change compensation in a pairwise combination, however, it should be considered that this may affect distribution in other channels, given the possible spectral overlap between multiple fluorochromes. Therefore, it is better to optimize compensation controls rather than changing compensation manually after acquisition. Listed below are examples in which compensation was improperly calculated.

Example 1. Single stained control is not as bright as the test stain. Figure 2b shows that fluorescence signal in the primary channel is undercompensated in the secondary channel. This was caused by a compensation control that was not as bright as the test staining. Importantly, the software calculates compensation in the range between a positive and a negative signal. Indeed, note that fluorescent signals are correctly compensated in this range (horizontal red line), but not above (diagonal red line; Fig. 2b). To overcome this issue, test the following approaches:

1. Increase the mAb concentration when preparing single-stained beads.
2. Use a different mAb that generates a brighter single-stained control, if that mAb is not a tandem.
3. Use single-stained cells.
4. Decrease the titer of the mAb in the test staining NOTE. This is generally possible only if the antigen has bimodal expression, and thus allows efficient separation over background even at

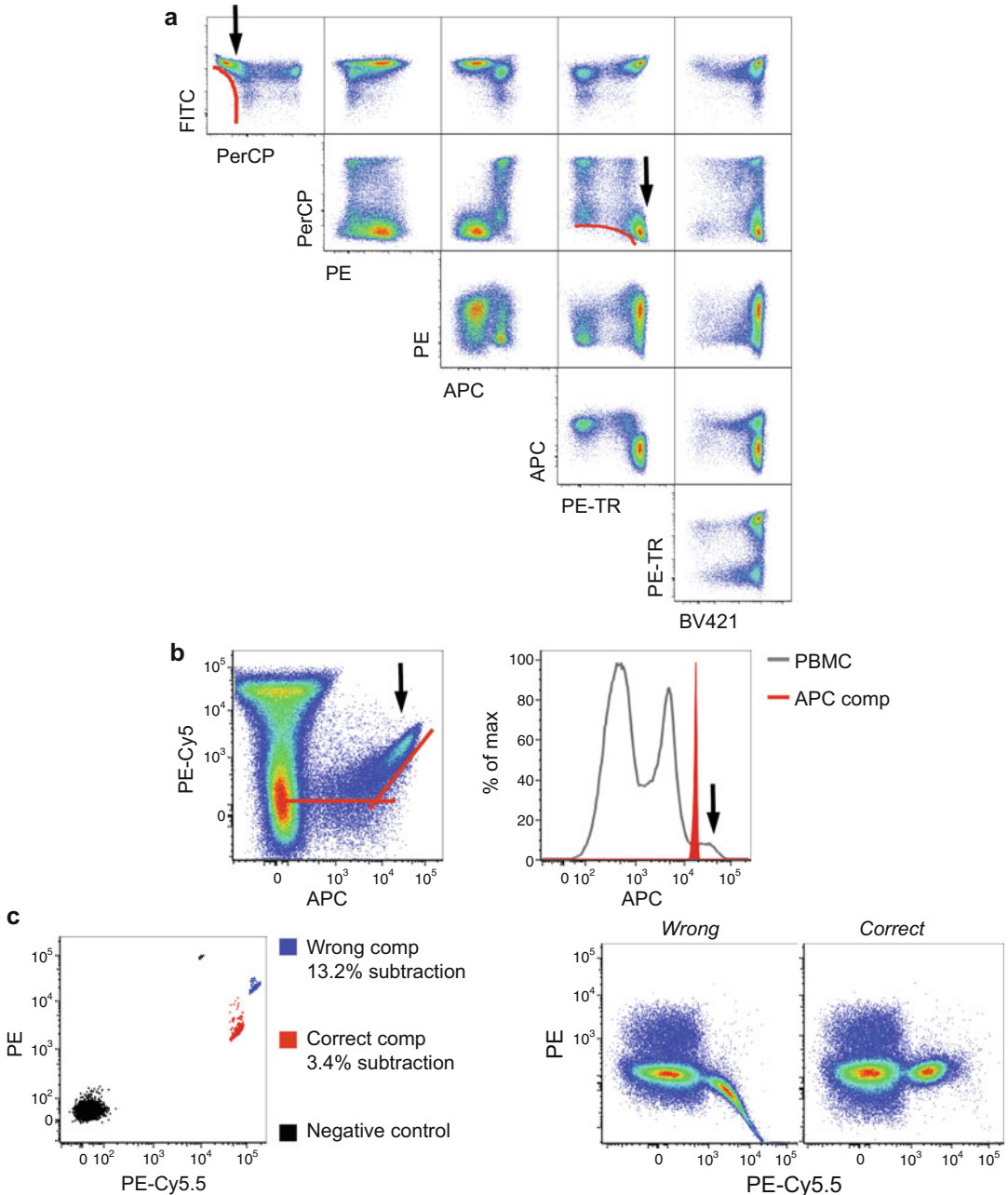


**Fig. 2** Troubleshooting compensation. **(a)** Matrix-like visualization of fluorescent parameters in a six-color assay. *Black arrows* indicate uncompensated combinations and *curve red lines* indicate uncompensated patterns. **(b)** *Left plot*: uncompensated APC and PE-Cy5 combination resulting from an APC compensation control (*red filled histogram*) that was not as bright as the staining in the PBMC sample (*grey line*). *Black arrow* in the left plot indicates the uncompensated portion of the APC data, while that in the right plot indicates those cell signals that are brighter than the comp control. **(c)** Overcompensated PE-Cy5.5 signal into PE resulting from the use of the wrong single-stained comp control

subsaturating concentrations of the mAb. However, in this particular example, staining is rather a smear, therefore lowering the mAb titer may result in poor resolution and loss of positive cells. This is exacerbated when staining a large number of cells (i.e., the absolute number of target sites is increased).

Example 2. Single stained control was performed with a reagent that is different from that used in the test staining. Figure 2c shows that reagent A and reagent B have similar fluorescent signal in the primary channel, but different spillovers in the secondary channel, hence resulting in different subtractions.

### 3.7 Coping with Spreading Error

The introduction of dyes emitting in the far red such as PE-Cy7, APC-Cy7, BV711, and similar, led to determine that a limited number of photons is collected at high wavelengths, thus causing improper measurement that results in “spread” of the data (Fig. 3a) [12]. This spreading error is directly proportional to the staining intensity and is revealed after compensation is applied. On a practical level, data spread does not impact the fluorescent signal in the primary channel but potentially decreases the sensitivity, i.e., the possibility to detect dim signals, in a secondary channel. This is true when the markers in the primary and secondary channels (in the example APC and Alexa 700) are co-expressed and the latter is not bright enough to separate from the negative cells (Fig. 3b, c). Negative cells, if not receiving data spread from a third or fourth channel, are not affected (Fig. 2b). Similarly, data spread does not affect fluorescent signals in a secondary channel if that signal is bright enough to ensure separation from negative cells (Fig. 2b). The success of the panel largely depends on the spillover spreading [13]. Should a combination of antibodies not work because of data spread, a number of alternative possibilities are available:

1. Change the combination of Abs in order to have dimmer signals in the primary channel and brighter signals in the secondary channel. Also, ensure that bright signals in the secondary channel do not affect sensitivity in other channels of interest, where dim signals are to be revealed.
2. Since data spread is proportional to signal intensity, decrease the concentration of the mAb in the primary channel. This is possible only if mAbs capable to clearly identify separate populations are used. Refer to the titration curve performed in Subheading 3.4 in order to predict the fluorescence signal in the primary channel. Also, compensating single-stained samples will allow to measure data spread in secondary channels (*see Note 8*).

### 3.8 Staining Protocol of T Cell Subsets

1. Obtain a single cell suspension as indicated in Subheading 3.3.
2. If starting from frozen aliquots from liquid nitrogen, thaw cells by submerging vial in a 37 °C water bath. Wait approximately 2 min, then transfer cells in a 15 mL conical tube con-

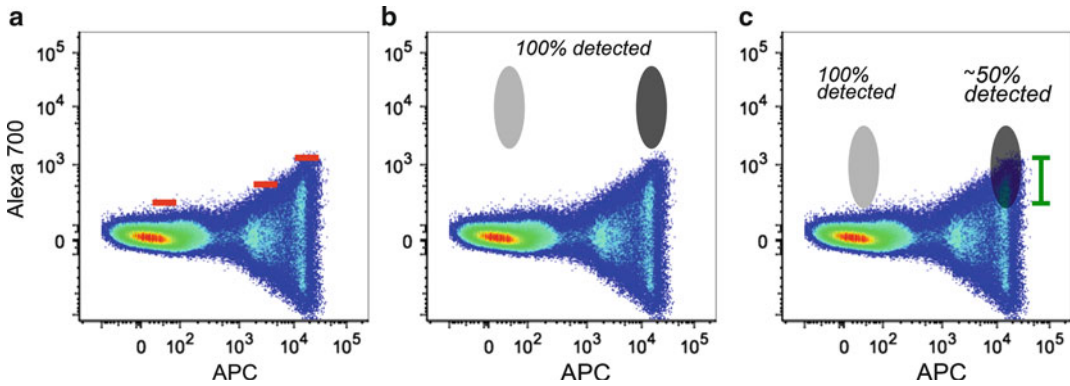


**Fig. 3** Spreading error and loss of detection sensitivity. (a) APC data spread into the Alexa 700 channel. *Red lines* indicate the threshold of positivity in the Alexa 700 channel according to APC fluorescence. (b) A given marker detected in the Alexa 700 channel is bright enough to allow 100% detection even if co-expressed with APC (*dark grey*). (c) A given marker detected in the Alexa 700 channel is not bright enough to be separated from the APC data spread (*green lines* indicate the portion of cells that are “covered”). In this case, only 50% of the cells are detected as positive (*dark grey*). In both cases, Alexa 700<sup>+</sup>APC<sup>-</sup> cells (*light grey*) are not affected

taining pre-warmed R10 medium and mix thoroughly. Centrifuge cells at  $515 \times g$  for 10 min (*see Note 9*).

3. Remove supernatant by vacuum aspiration. Repeat washing step by adding 10 mL HBSS<sup>-/-</sup> to remove residual DMSO.
4. Perform viability dye staining as described in Subheading 3.3.
5. Prepare the anti-CCR7 antibody mix by adding the optimal titer of anti-CCR7 antibody to FACS buffer. Prepare 15% excess mix to compensate for pipetting error. Vortex the mix, then centrifuge in a microcentrifuge at  $15,000 \times g$  (or top speed) for 3 min to pellet mAbs aggregates.
6. Eliminate supernatant from pelleted cells and resuspend them with 100  $\mu$ L CCR7 mix. Incubate for 20 min at 37 °C in the dark (*see Note 10*).
7. Wash cells with FACS buffer (typically, by diluting the volume 20-fold) and pellet cells at  $515 \times g$  for 5 min.
8. In the meantime prepare the surface staining antibody mix, as described in **step 5**.
9. Remove supernatant from the pelleted cells, resuspend pellet in 100  $\mu$ L mix, and incubate for 20 min at RT in the dark (*see Note 10*).
10. Wash cells as in **step 7**.
11. Fix samples as described in Subheading 3.4, **steps 7–9**, and acquire within 24 h.
12. Acquire samples at the machine. There is no need to perform compensation at the machine, unless cell subsets needs to be separated by using a FACS sorter. After acquisition (test samples and compensation controls), export all files and compen-

save data offline by using a dedicated flow cytometry software. Refer to the software manual for technical details on how to perform compensation.

### **3.9 Optimize and Validate Panels Using Appropriate Controls**

Panels should be tested in pilot experiments before proceeding with test samples. Appropriate controls facilitate flow cytometry panels optimization [14]. Consider including (or excluding) the following controls to determine positivity in a given sample.

1. Unstained cells are useless to determine background staining: indeed, this may be increased if mAbs are not appropriately titrated. Moreover, the simultaneous effect of multiple fluorochromes can lead to decreased sensitivity in a given channel due to data spread (*see* Subheading 3.7).
2. Isotype controls: these are mAbs of the same species of the mAb used in the staining and conjugated to the same fluorochrome, but with an irrelevant Fab. Isotype controls are popular in flow cytometry but should be used with caution. Indeed, the fluorochrome–protein ratio may be different between the isotype and the test staining, thus resulting in different fluorescence (improper control). Moreover, even if used at the same concentration of the mAb of interest, isotype controls may result in increased fluorescence due to increased unspecific binding that is not necessarily related to the unspecificity of the mAb of interest, but to binding to Fc receptors. Rather, reagent titration may help in defining non-specific background staining. Thorough discussions on the use of isotype controls can be found at <http://www.cyto.purdue.edu/hmarchiv>.
3. “Fluorescence Minus One” (FMO) controls: samples that are labeled with all antibodies except the one of interest [15]. This control can be used for setting the threshold of positivity and to determine whether compensation is correct.
4. Internal negative control: a population of cells that does not express the antigen of interest. This population remains relatively unlabeled in an antibody-labeled cell suspension. Differently from unstained cells, this control gives a more accurate measurement of the background fluorescence. In the example proposed here, naïve and memory T cells are identified on the basis of markers expressed on the surface. Some of these antigens are not expressed by other lymphocytes, e.g., CD45RO on B cells. Co-staining with a B cell-specific antigen such as CD19 can help to identify those cells that are negative for CD45RO (*see* Note 11).

### **3.10 Gating Strategy to Identify Memory T Cell Subsets**

The flow cytometry gating strategy to identify memory T cell subsets should be performed as follows (Fig. 4):

1. First gate on the time parameter to ensure that fluorescence (in this case of Aqua LIVE/DEAD dye) is stable during acquisition.

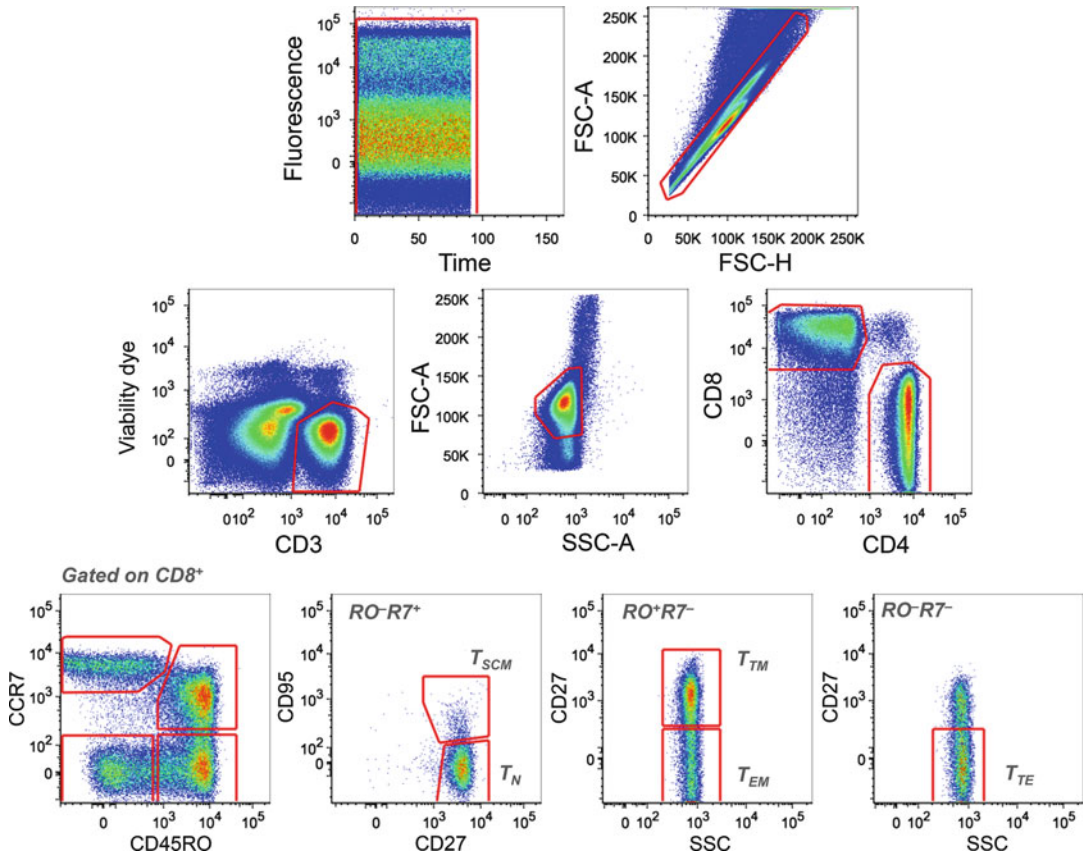


**Fig. 4** Gating strategy for the identification of T cell subsets. Time-gated cells are selected as singlets on the basis of FSC-A and SSC-A parameters. T cells are identified by CD3 positivity. Dead cells are excluded by the Aqua LIVE/DEAD probe. Lymphocytes display low FSC-A and low SSC-A physical parameters. Identification of subsets are shown for CD8<sup>+</sup> T cells, but the same gating strategy may be applied to CD4<sup>+</sup> T cells as well. T<sub>N</sub> cells are first gated as CD45RO<sup>-</sup>CCR7<sup>+</sup>, then as CD27<sup>+</sup>CD95<sup>-</sup>, to exclude CD95<sup>+</sup> cells that are T<sub>SCM</sub> cells. T<sub>CM</sub> are CD45RO<sup>+</sup>CCR7<sup>+</sup>, T<sub>TM</sub> are CD45RO<sup>+</sup>CCR7<sup>-</sup>CD27<sup>+</sup>, T<sub>EM</sub> are CD45RO<sup>+</sup>CCR7<sup>-</sup>CD27<sup>-</sup>, and T<sub>TE</sub> are CD45RO<sup>-</sup>CCR7<sup>-</sup>CD27<sup>-</sup>.

2. Exclude doublets using a forward scatter-area (FSC-A) vs. forward scatter-height (FSC-H) plot: singlets lie on the diagonal.
3. Use the viability dye and a lineage marker to exclude dead cells and identify T cells.
4. Gate on “lymphocytes” on the basis of physical parameters: FSC indicates the size, SSC is proportional to the complexity of the cell (cytoplasm components, pseudopodes, granules, etc.).
5. Identify cytotoxic or helper T cell on the basis of CD8 or CD4, respectively.
6. In both CD8<sup>+</sup> and CD4<sup>+</sup> compartments (here, CD8<sup>+</sup> T cells only are shown for simplicity), plot CCR7 vs. CD45RO to identify: naïve-like T cells (CCR7<sup>+</sup>CD45RO<sup>-</sup>), T<sub>CM</sub> cells (CCR7<sup>+</sup>CD45RO<sup>+</sup>), CCR7<sup>-</sup>CD45RO<sup>+</sup>, and CCR7<sup>-</sup>CD45RO<sup>-</sup>.

7. Pure  $T_N$  cells can be identified by gating for additional markers, in this case  $CD27^+CD95^-$ . The use of only two markers is indeed insufficient for this purpose, as memory contaminants may be included [16].
8. Gate on  $T_{SCM}$  cells by selecting  $CD27^+CD95^+$  cells in the  $CCR7^+CD45RO^-$  gate (*see* **Note 12**).  $T_{TM}$  can be separated from  $T_{EM}$  cells in the  $CCR7^-CD45RO^+$  by  $CD27$  expression, while  $T_{TE}$  cells are  $CD27^-$  in the  $CCR7^-CD45RO^-$  gate.
9. Examine the expression of other markers of interest in each subsets (e.g., Ki-67, HLA-DR, and CD57).

---

## 4 Notes

1. A ninth tube containing a positive control, i.e., cells stained with a mAb that has been previously validated, should be also included.
2. The same procedure can be applied to mAbs directed to intracellular markers (e.g., Ki-67). In this case, the antibody mix must be prepared in a cell permeabilization buffer (such as 1× CytoPerm; BD Biosciences). After **step 4**, resuspend cells in 100  $\mu$ L of cold BD Cytofix solution and incubate for 20 min at 4 °C in the dark. Wash cells with 1 mL of cold 1× CytoPerm buffer and proceed as indicated in **steps 4–10** by using 1× CytoPerm buffer instead of FACS buffer and incubating cells at 4 °C instead of RT. After **step 10** resuspend cells in 200  $\mu$ L of 1× CytoPerm buffer.
3. Fixative solution can be removed after incubation by washing cells with FACS buffer. Prolonged fixation may alter fluorochrome properties and spillover into secondary channels.
4. Antigens may show an “on/off” expression (e.g., CD3, CD4, and CD8), thus allowing a simple definition of positive and negative events, otherwise not clearly separate from the background because of their relative low expression (e.g., CCR5) or because they are expressed as a continuum (e.g., CD45RO). In the case, the best approach is to co-stain with additional antibodies in order to identify a cell population that does not express the marker of interest. For example,  $CD19^+$  B cells do not express CD45RO, and can be thus used to define background staining.
5. Two classes of antibodies are defined as revealed by staining in flow cytometry: saturating and non-saturating. In the former case, the saturation occurs when the MFI of the positive population does not increase by increasing mAb concentration. Conversely, mAbs are defined as non-saturating. In the latter case, a separating titer is chosen, i.e., a titer at which the positive

population is clearly separated from the negative. Note that mAbs that do not follow this rule may identify dim populations even at increased concentrations compared to those indicated in the data sheet.

6. Chemically-distinct fluorochromes (for example, CFSE and FITC) would have different compensation requirements even if detected in the same channel of the flow cytometer.
7. Compensation controls should be resuspended in the same buffer that is used for cells. Indeed, formalin may alter spectral properties and thus affect compensation. There is no need to resuspend compensation controls in fixation buffers if exposure to buffers is limited in time (such as fixation/permeabilization procedures).
8. Decreasing the mAb titer may lead to suboptimal staining. This can be an issue when large number of cells are to be stained, such as in cell sorting experiments.
9. Supplementing the medium with 20  $\mu\text{g}/\text{mL}$  DNase helps to dissociate cell aggregates that result from DNA release by dead cells.
10. As a general rule, 100  $\mu\text{L}$  volume is sufficient to stain up to  $10^7$  cells. If more cells are to be stained, scale up volumes accordingly.
11. This is possible only whether  $\text{CD}3^+$  T cells and  $\text{CD}19^+$  B cells in the panel have the same level of background staining due to data spread from other channels. This is dependent on the mAb combination in the panel of interest.
12. In the case of  $\text{CD}4^+$  T cells,  $\text{T}_{\text{N}}$  can be further subdivided into  $\text{CD}31^+$  recent thymic emigrants ( $\text{T}_{\text{RTE}}$ ) and  $\text{CD}31^-$  mature  $\text{T}_{\text{N}}$  cells [17]. Conversely, CD31 has no value to identify  $\text{CD}8^+$  naïve T cell subsets.

---

## Acknowledgments

The authors wish to thank the members of the Laboratory of Translational Immunology for critical discussion and Mario Roederer and Stephen Perfetto (Vaccine Research Center, NIH, Bethesda, MD) for continuous support. This work was supported by grants from the Fondazione Cariplo (Grant Ricerca Biomedica 2012/0683), the Italian Ministry of Health (Bando Giovani Ricercatori GR-2011-02347324) and the European Union Marie Curie Career Integration Grant 322093 (all to E.L.). E.L. is an International Society for the Advancement of Cytometry (ISAC) Marylou Ingram scholar. V.Z. is a student of the Ph.D. program at the University of Milan, Italy. A.R. is a recipient of the Guglielmina Lucatello e Gino Mazzega Fellowship from the Fondazione Italiana per la Ricerca sul Cancro (FIRC).

## References

1. Mahnke YD, Brodie TM, Sallusto F, Roederer M, Lugli E (2013) The who's who of T-cell differentiation: human memory T-cell subsets. *Eur J Immunol* 43(11):2797–2809. doi:[10.1002/cji.201343751](https://doi.org/10.1002/cji.201343751)
2. Kaech SM, Cui W (2012) Transcriptional control of effector and memory CD8+ T cell differentiation. *Nat Rev Immunol* 12(11):749–761. doi:[10.1038/nri3307](https://doi.org/10.1038/nri3307)
3. Gattinoni L, Klebanoff CA, Restifo NP (2012) Paths to stemness: building the ultimate antitumour T cell. *Nat Rev Cancer* 12(10):671–684. doi:[10.1038/nrc3322](https://doi.org/10.1038/nrc3322)
4. Perfetto SP, Chattopadhyay PK, Roederer M (2004) Seventeen-colour flow cytometry: unravelling the immune system. *Nat Rev Immunol* 4(8):648–655. doi:[10.1038/nri1416](https://doi.org/10.1038/nri1416), nri1416 [pii]
5. Lugli E, Gattinoni L, Roberto A et al (2013) Identification, isolation and in vitro expansion of human and nonhuman primate T stem cell memory cells. *Nat Protoc* 8(1):33–42. doi:[10.1038/nprot.2012.143](https://doi.org/10.1038/nprot.2012.143)
6. Perfetto SP, Ambrozak D, Nguyen R, Chattopadhyay PK, Roederer M (2012) Quality assurance for polychromatic flow cytometry using a suite of calibration beads. *Nat Protoc* 7(12):2067–2079. doi:[10.1038/nprot.2012.126](https://doi.org/10.1038/nprot.2012.126)
7. Gattinoni L, Lugli E, Ji Y et al (2011) A human memory T cell subset with stem cell-like properties. *Nat Med* 17(10):1290–1297. doi:[10.1038/nm.2446](https://doi.org/10.1038/nm.2446), nm.2446 [pii]
8. Lugli E, Dominguez MH, Gattinoni L et al (2013) Superior T memory stem cell persistence supports long-lived T cell memory. *J Clin Invest* 123(2):594–599. doi:[10.1172/JCI66327](https://doi.org/10.1172/JCI66327)
9. Perfetto SP, Chattopadhyay PK, Lamoreaux L et al (2010) Amine-reactive dyes for dead cell discrimination in fixed samples. *Curr Protoc Cytom* Chapter 9:Unit 9.34. doi:[10.1002/0471142956.cy0934s53](https://doi.org/10.1002/0471142956.cy0934s53)
10. Kantor A, Roederer M (1997) FACS analysis of lymphocytes. In: Herzenberg LA, Weir DM, Blackwell C (eds) *Handbook of experimental immunology*, vol 2, 5th edn. Blackwell Science, Cambridge
11. Berhanu D, Mortari F, De Rosa SC, Roederer M (2003) Optimized lymphocyte isolation methods for analysis of chemokine receptor expression. *J Immunol Methods* 279(1–2):199–207, doi:[S0022175903001868](https://doi.org/S0022175903001868) [pii]
12. Roederer M (2001) Spectral compensation for flow cytometry: visualization artifacts, limitations, and caveats. *Cytometry* 45(3):194–205. doi:[10.1002/1097-0320\(20011101\)45:3<194::AID-CYTO1163>3.0.CO;2-C](https://doi.org/10.1002/1097-0320(20011101)45:3<194::AID-CYTO1163>3.0.CO;2-C)
13. Nguyen R, Perfetto S, Mahnke YD, Chattopadhyay P, Roederer M (2013) Quantifying spillover spreading for comparing instrument performance and aiding in multi-color panel design. *Cytometry A* 83(3):306–315. doi:[10.1002/cyto.a.22251](https://doi.org/10.1002/cyto.a.22251)
14. Hulspas R, O'Gorman MR, Wood BL, Gratama JW, Sutherland DR (2009) Considerations for the control of background fluorescence in clinical flow cytometry. *Cytometry B Clin Cytom* 76(6):355–364. doi:[10.1002/cyto.b.20485](https://doi.org/10.1002/cyto.b.20485)
15. Baumgarth N, Roederer M (2000) A practical approach to multicolor flow cytometry for immunophenotyping. *J Immunol Methods* 243(1–2):77–97
16. De Rosa SC, Herzenberg LA, Roederer M (2001) 11-color, 13-parameter flow cytometry: identification of human naive T cells by phenotype, function, and T-cell receptor diversity. *Nat Med* 7(2):245–248. doi:[10.1038/84701](https://doi.org/10.1038/84701)
17. Kimmig S, Przybylski GK, Schmidt CA et al (2002) Two subsets of naive T helper cells with distinct T cell receptor excision circle content in human adult peripheral blood. *J Exp Med* 195(6):789–794

## Intravital Microscopy Analysis of Hepatic T Cell Dynamics

Alexandre Pierre Benechet, Lucia Ganzer, and Matteo Iannacone

### Abstract

T cells play critical roles in controlling hepatotropic viral infections and liver tumors. The protective capacity of these cells is mediated by antigen-experienced effector cells and depends on their ability to migrate to and traffic within the liver, recognize pathogen- or tumor-derived antigens, get activated and deploy effector functions.

While some of the rules that characterize T cell behavior in the healthy and cancerous antigen-expressing liver have been characterized at the population level, we have only limited knowledge of the precise dynamics of T cell interactions with different kinds of liver cells at the single-cell level. Here, we describe in detail an intravital microscopy technique that allows the analysis of T cell dynamic behavior in the liver of anesthetized mice at high spatial and temporal resolution. A detailed understanding of the spatiotemporal dynamics of T cells within the liver is important for the rational design of targeted immunotherapeutic approaches for chronic liver infections and tumors.

**Key words** Multiphoton intravital microscopy, In vivo imaging, Liver, CD8+ T cells, Lymphocyte motility

---

### 1 Introduction

Intravital microscopy allows for the direct visualization of lymphocyte behavior in their physiological tissue environment at cellular and subcellular resolution. This technique has been utilized in the last several years to understand the dynamic events leading to the activation, expansion and effector differentiation of naïve T cells within secondary lymphoid organs [1, 2]. By contrast, less is known on the spatiotemporal aspects that govern T cell migration and function at peripheral sites, such as the liver.

Here we detail an intravital microscopy method to study T cell dynamics within the liver at the single-cell level [3–5]. The protocol begins with T cell isolation, purification, and eventual differentiation into effector cells, T cell labeling with fluorescent dyes and subsequent intravenous injection into antigen (Ag)-expressing recipient mice. It then provides a step-by-step surgical procedure to expose the liver for intravital microscopy using an inverted

microscope setup, accompanied by protocols validated by our group to image several hepatic cells utilizing commercially available reagents. Finally, it describes the basic analyses of intravital microscopy movies to compute several motility parameters.

---

## 2 Materials

### 2.1 Preparation and Injection of T Lymphocytes to be Tracked In Vivo

1. Spleen and lymph nodes from donor wild type or TCR transgenic mice (e.g., P14 [6], OT-I [7], BC10 [3, 8]).
2. Immunomagnetic cell purification kit for CD4<sup>+</sup> or CD8<sup>+</sup> T cells (e.g., mouse CD8<sup>+</sup> T cell negative selection kit from Miltenyi Biotec).
3. RPMI 1640 medium.
4. Recombinant IL-2 or EL-4 supernatant [9].
5. 5-chloromethylfluorescein diacetate (CMFDA, CellTracker™ Green; Thermo Fisher Scientific).
6. CellTracker™ Red (CMTPX; Thermo Fisher Scientific).
7. 5-(and-6)-(((4-chloromethyl)benzoyl)amino)tetramethylrhodamine (CMTMR, CellTracker™ Orange; Thermo Fisher Scientific).
8. CellTracker™ Deep Red (Thermo Fisher Scientific).
9. 6-(((4,4-difluoro-5-(2-thienyl)-4-bora-3a,4a-diaza-s-indacene-3-yl)styryloxy)acetyl)aminohexanoic acid (BODIPY 630/650-X) (Thermo Fisher Scientific).
10. Phosphate buffered saline (PBS).
11. Complete RPMI 1640: 10% FBS, 2 mM l-glutamine, 50 μM 2-mercaptoethanol, 10 mM HEPES, 100 μM nonessential amino acids, penicillin plus streptomycin.

### 2.2 Surgical Anesthesia

1. Isoflurane (Iso-Vet, Piramal Healthcare) (*see Note 1*).
2. Anesthetic vaporizers (G.A.S. General Anesthetic Services Ltd).
3. Oxygen supply connected to the isoflurane vaporizer.

### 2.3 Surgical Preparation of the Mouse Liver for Intravital Microscopy Using an Inverted Microscope Setup (Fig. 1)

1. Custom-built stage (specifics and dimensions are provided in Fig. 1a).
2. Mouse restrainer (e.g., Tailveiner Restrainer from Braintree Scientific).
3. Small animal clipper (e.g., Pocket Pro from Wahl).
4. Medical adhesive tape (e.g., Durapore™ 3M).
5. Hair removal cream (e.g., Veet).
6. 15 cm cotton tipped applicators (e.g., Heinz Herenz).
7. Gauze sponges (e.g., Heinz Herenz).

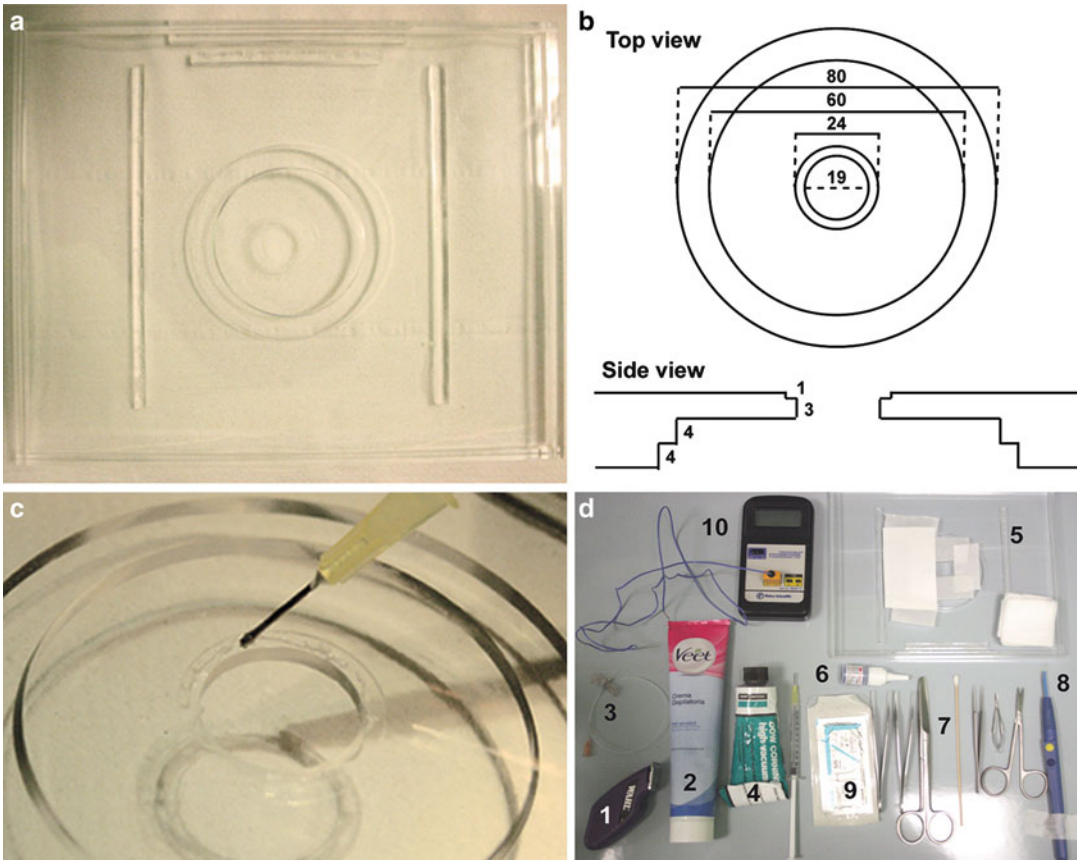


**Fig. 1** Equipment. **(a)** Custom-built microscope stage. **(b)** Schematic view of the microscope stage with exact dimensions (in cm). **(c)** Application of a thin layer of grease on the perimeter of the coverslip holder. **(d)** 1: Clipper; 2: Hair removal cream; 3: Tail vein catheter set; 4: Vacuum grease; 5: Final stage with coverslip and a rectangle ( $4 \times 10$  cm) of blotting paper; 6: Tissue glue; 7: Surgical instruments; 8: Electrocautery device; 9: Suture thread; 10: Digital thermometer with probe

8. Precision Wipes ( $11 \times 21$  cm, Kimtech Science, Kimberly-Clark Professional).
9. Spring scissors (Cohan-Vannas 6 mm blade).
10. Extra thin iris scissors (10.5 cm).
11. Dumont #2 laminectomy forceps Inox.
12. Adson forceps (12 cm).
13. Standard pattern scissors (large loops, sharp/blunt 14.5 cm).
14. Suture thread: 5-0 braided silk (suture size), C-1 (needle type), 13.1 mm (needle length), 3/8c (needle shape) (Johnson-Johnson Intl.).
15. Tissue glue (e.g., Vetbond™ from 3M).
16. Round glass coverslips (24 mm in diameter, 0.17 mm thickness, Ted Pella Inc).

17. High-viscosity vacuum grease (e.g., Dow Corning).
18. Digital thermometer (e.g., Traceable expanded-range thermometer).
19. Miniature K type thermocouples (e.g., 5SC-TT-K-40-72 from Omega).
20. Electrocautery device (Surtron).
21. Tail vein catheter (e.g., Vevo MicroMarker™ from Fujifilm VisualSonic).
22. Blotting paper.
23. Plastic wrap.
24. 0.9% saline solution.

**2.4 Multiphoton  
Intravital Microscopy  
of the Mouse Liver  
Using an Inverted  
Microscope Setup**

1. Inverted multiphoton microscope (*see* **Notes 2** and **3**) equipped with: (a) at least one (preferably two) tunable femtosecond (fs)-pulsed Ti:Sa lasers (e.g., 680–1080 nm, 120 fs pulse-width, 80 MHz repetition rate, Ultra II, Coherent); (b) an optional Optical Parametric Oscillator (e.g., 1000–1600 nm, 200 fs pulse-width, 80 MHz repetition rate, Chameleon Compact OPO, Coherent); (c) at least two (ideally four or five) non-descanned photomultiplier tubes (e.g., Hamamatsu H7422-40 GaAsP High Sensitivity PMTs and Hamamatsu H7422-50 GaAsP High Sensitivity red-extended PMT from Hamamatsu Photonics K.K.); (d) a high numerical aperture, water-immersion multiphoton objective (preferably Olympus ref: XLPLN25XWMP2, 25×, 1.05 NA, 2 mm working distance).
2. Mercury arc lamp (e.g., HG Precentered Fiber Illuminator—Intensilight from Nikon).
3. Custom-made thermostatic chamber that surrounds the entire microscope with the exclusion of the scanhead (e.g., The Box, Life Imaging Services).
4. Digital thermometer (Traceable expanded-range thermometer, Fisher Scientific).
5. Fluorescently labeled anti-F4/80 antibody (clone BM8).
6. Fluorescently labeled anti-CD49 antibody (clone HM $\alpha$ 2).
7. Hoescht 33342 (Thermo Fisher Scientific).
8. Qtracker vascular label (Thermo Fisher Scientific).
9. SYTOX dye (Thermo Fisher Scientific).

**2.5 Image  
Acquisition,  
Processing  
and Analysis**

1. Computer workstation with high graphics processing capability (e.g., Apple Inc Mac Pro computer model: Processor: 2×2.4 GHz Quad-core Intel Xeon or higher, Memory: 32GB 1066 MHz DDR3 ECC, Graphics: ATI Radeon HD 5870 1024 MB, System: MAC OS×Lion 10.7 or higher).

2. Image analysis software (e.g., Imaris; Volocity, Improvision; ImageJ, National Institute of Health).
3. Custom-made scripts (Matlab, Mathworks, or Python) for more complicated analyses.

---

## 3 Methods

### 3.1 Preparation and Injection of T Cells to Be Tracked In Vivo

1. Purify CD8<sup>+</sup> T cells from lymph nodes and spleens of wild-type or T cell receptor (TCR) transgenic mice by negative immunomagnetic selection, according to the manufacturer's instructions.
2. (Optional) To generate effector CD8<sup>+</sup> T cells [3, 10], incubate purified T cells from TCR transgenic mice with 10 µg/ml of cognate peptide at 37 °C for 1 h, washed, and cultured in complete RPMI 1640 medium. Two days later, replace with fresh medium supplemented with 20 ng/ml of recombinant IL-2 or with 2.5% (vol/vol) EL-4 supernatant. Replace medium supplemented with cytokines every 2 days. After 7–9 days of culture, test the expression of CD8, CD69, CD25, CD44, CD62L, CCR7, IFN-γ, and granzyme B by flow cytometry prior to subsequent use, as described [3].
3. Wash naïve or effector CD8<sup>+</sup> T cells on pre-warmed serum-free RPMI to remove residual FBS.
4. Incubate cells at  $1 \times 10^7$  cells/ml and stained with 2.5 µM CMFDA, 7.5 µM CMTPIX, 10 µM CMTMR, CellTracker™ Deep Red or 2.5 µM BODIPY 630/650-X for 20 min in the dark at 37 °C in plain pre-warmed RPMI 1640. Stop the reaction by adding 2 mL of FBS, which binds residual protein-binding dyes.
5. Wash cells twice with pre-warmed RPMI and resuspend in PBS at the desired concentration for injection (typically between  $5 \times 10^6$  and  $2 \times 10^7$  per cell population). As an alternative to cell staining with fluorescent organic dyes, T cells from mice expressing a fluorescent protein (e.g., green fluorescent protein or its variants) under a ubiquitous or T cell-specific promoter can be used.
6. Inject fluorescently labeled naïve or effector CD8<sup>+</sup> T cells intravenously into recipient mice through the tail vein. Alternatively, inject cells during the imaging session through a tail vein catheter (*see* later at Subheading 3.2, **step 3** for the detailed procedure). Recipient mice typically would express the relevant cognate antigen(s) in the liver because they are transgenic mice (e.g., HBV replication-competent transgenic mice [3, 11]), because they have been transduced with hepatotropic viral vectors (e.g., adenoviruses or adeno-associated viruses [3, 12]) or because they have been infected with hepatotropic viruses (e.g., LCMV [3]).

### 3.2 **Microscope Setup and Presurgery Preparations**

1. Turn the system on (set the thermal chamber at 37 °C, turn on the computer, lasers, mercury arc lamp, open the oxygen supply connected to the isoflurane vaporizer system and check the isoflurane volume).
2. Stage preparation. Apply a thin layer of vacuum grease on the perimeter of the coverslip holder and gently place the coverslip on top of it (Fig. 1c). Secure the coverslip on each side with tape (Fig. 1d). Finally place on the left side of the coverslip holder a rectangle (~4 × 10 cm) of blotting paper (Fig. 1d). This paper will ultimately be positioned underneath the mouse to absorb any fluid leakage that could interfere with imaging.
3. Mouse shaving (*see Note 4*). The abdomen, back, and both flanks of the mouse are shaved using the clipper and the hair removal cream. Thoroughly wipe off the cream using moist gauzes. The goal is to remove hair entirely as they are very autofluorescent and therefore can interfere with imaging.
4. Tail vein catheterization (Fig. 2a). Fill the polyethylene catheter with saline solution, making sure to avoid bubble formation. Place the mouse into the restrainer and dilate the tail veins either by dipping the tail in warm water (~35–40 °C) for ~30 s or by using a heat lamp. Introduce the needle with the bevel uppermost into either tail vein and check the correct placement by saline injection (there should be almost no resistance when the syringe plunger is depressed and the vein should be flushed clear of blood as the injection is made). A drop of tissue glue on and around the needle is used to secure the intravenous line. Additional tape can be applied to ensure proper stabilization.

### 3.3 **Surgical Anesthesia**

Anesthetize the mouse with 5% isoflurane through a nose cone also delivering oxygen at 1 L min<sup>-1</sup> (*see Note 1*). Adequate anesthesia is achieved if the mouse does not react to firm pinching of the footpad. Perform follow-up surgery and liver intravital imaging with lower concentrations of isoflurane (between 0.8 and 1%). Adjust anesthesia based on breathing rate (~55–65 breaths per minute).

### 3.4 **Surgical Preparation for Liver Intravital Microscopy**

1. Position the mouse on the stage by using adhesive tape to secure the nose cone and upper legs.
2. Open the skin by performing a midline incision and carefully detach peritoneal adhesences (Fig. 2b). From this moment onwards, keep the surgical area moist by applying small quantities of saline solution (0.9% NaCl).
3. Cauterize the major subcutaneous vessels prior to performing left and right subcostal incisions to expose a large peritoneal surface (Fig. 2c).
4. Perform midline and left subcostal incisions in the peritoneum through a high-temperature cautery (Fig. 2d). The left subcostal incision should be carried out along the ribcage all the way down to the spleen.

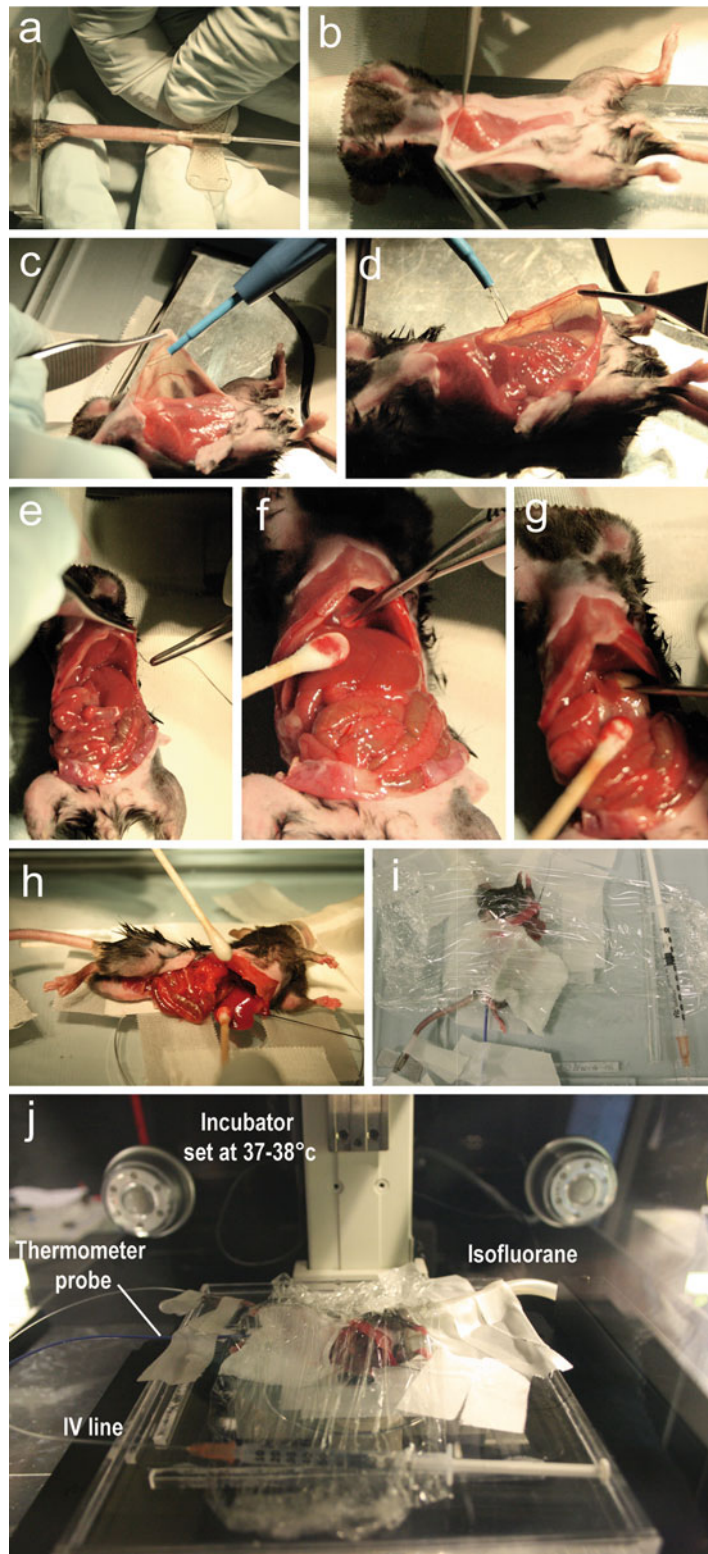


**Fig. 2** Surgical procedure. (a) Insertion of the tail vein catheter. (b) Removal of subcutaneous adhesions. (c) Cauterization of the major subcutaneous vessels prior to performing left and right subcostal incisions. (d) Left subcostal incisions in the peritoneum through a high-temperature cauter. (e) Application of a suture thread on the left side of the peritoneum. (f) Resection of the falciform ligament. (g) Resection of the hepatogastric ligament. (h) Positioning of the liver lobe on the coverslip. (i) The preparation is covered by a plastic film to minimize heat loss. (j) Final positioning in the intravital microscope

5. By gently pulling on the xiphoid process, expose and cut the falciform ligament with small spring scissors, making sure to preserve the diaphragm integrity (Fig. 2f).
6. Cut the hepatogastric ligament between the stomach and the liver (Fig. 2g).
7. Place a suture thread on the left side of the peritoneum (approximately half way between the xiphoid process and the spleen, Fig. 2e).
8. Place the mouse in a left lateral position and gently exteriorize the left liver lobe onto the coverslip by simultaneously gently pulling on the suture thread (Fig. 2h) to separate the diaphragm from the left liver lobe, thus preventing transmission of breathing movements (*see Note 5*).
9. The suture thread is secured with the adhesive tape.
10. The liver lobe is held in place and stabilized by a small piece of plastic wrap (small enough to avoid contact with the rib cage, thereby limiting the transmission of breathing movements).
11. Internal organs are gently separated from the liver and kept moist using wet gauzes previously soaked with warm PBS.
12. Lubricate the temperature probe with vacuum grease prior to inserting into the mouse rectum.
13. Seal the whole preparation with plastic wrap to avoid heat loss and dehydration (Fig. 2i).
14. Transfer the stage to the intravital microscope into the 37 °C pre-warmed thermal chamber (Fig. 2j).

### **3.5 Image Acquisition**

1. Check laser beam alignment according to the manufacturer's instructions. Adjust wavelengths of the laser beams according to the fluorescent dyes used in the experiment (two photon excitation spectra of most commonly used fluorescent probes can be found for example at <http://goo.gl/4qYhWx>). Typically, we tune the two Ti:Sa lasers at 800 nm and 900–930 nm, respectively, and the OPO at 1200 nm. This setup allows us to excite most fluorescent molecules whose emission range from ~450 to ~700 nm. Spectral separation is achieved by dichromatic mirrors and bandpass filters in front of each PMTs. Again, selection of filters should be guided by the fluorescent molecules used in the experiment. Our setup includes the following filters: 455/50 nm (to detect e.g., second harmonic, CFP, CMAC, Hoechst), 525/50 nm (to detect e.g., eGFP, CFSE, CMFDA), 590/50 nm (to detect e.g., CMTMR, dsRed), and 665/50 nm (to detect e.g., BODIPY, qDots 655).
2. As lymphocyte migration is highly temperature dependent, keep the thermostatic chamber at 37–38 °C and continuously monitor the mouse body temperature through a rectal probe to ensure that a narrow range of 37–38 °C is maintained at all time.

3. Using the ocular and the mercury lamp illumination, scan the overall preparation and choose an adequately perfused area with minimal tissue perturbation.
4. Before starting image acquisition, adjust laser power, PMT gain, offset, etc. in order to get the best possible signal-to-noise ratio. We suggest to acquire a test short time-lapse recording, in order to check stability of the preparation (with particular attention to z-drift), blood flow and cell motility.
5. Once an area of interest is found, begin actual recording. Typically, we found that stacks of 7–9 square  $x y$  sections ( $512 \times 512$  pixel) sampled with  $4 \mu\text{m}$   $z$  spacing acquired every 5–10 s for a period of ~60 min provide a sufficient amount of cell tracks for meaningful statistical analyses. Our experimental setup allows for continuous recording for at least 4–5 h.
6. Depending on the experimental question, liver sinusoids, several hepatic resident and infiltrating leukocytes and cell death can be visualized thanks to the intravenous injection of commercially available antibodies and probes (Fig. 3) (*see Note 6*). The hepatic vascular structure is directly visualized thanks to the injection of 10  $\mu\text{L}$  of fluorescently labeled non-targeted quantum dots (e.g., Qtracker 655). Kupffer cells can be visualized thanks to the injection of 1  $\mu\text{g}$  of fluorescently labeled (e.g., PE) anti-F4/80 antibody. Platelets can be visualized thanks to the injection of 3  $\mu\text{g}$  of fluorescently labeled (e.g., FITC) anti-CD49b antibody. Cell nuclei can be visualized thanks to the injection of 10  $\mu\text{L}$  of Hoechst 33342. Hepatocytes can be easily distinguished from other nonparenchymal cells or infiltrating leukocytes based on size and ploidy of the nuclei. Cell death can be visualized thanks to the injection of 4 mL of fluorescent Sytox (e.g., Sytox green).

### **3.6 Image Processing and Data Analysis**

Initially, the sequences of image stacks are transformed into volume-rendered 4D time-lapse movies with image analysis software (e.g., Imaris Bitplane or Fiji ImageJ) (Fig. 4a). The 3D positions of the cell centroids are segmented by semi-automated cell tracking algorithm from Imaris or using the TrackMate Fiji plugin.

### **3.7 Qualitative Analysis**

Examine migratory behavior of the cell population by plotting the trajectories of the tracked cell centroids over time in two dimensions. Shift the first position of each individual cell to the same starting point in space while maintaining its orientation (Fig. 4b), allowing to assess whether cells are traveling in a preferred direction. If all possible directions are equally covered, this indicates that motion is random on the timescale of the duration of the plotted tracks (plotting tracks only give qualitative information).

### **3.8 Quantitative Analysis**

Several different motility parameters can be quantified, including:

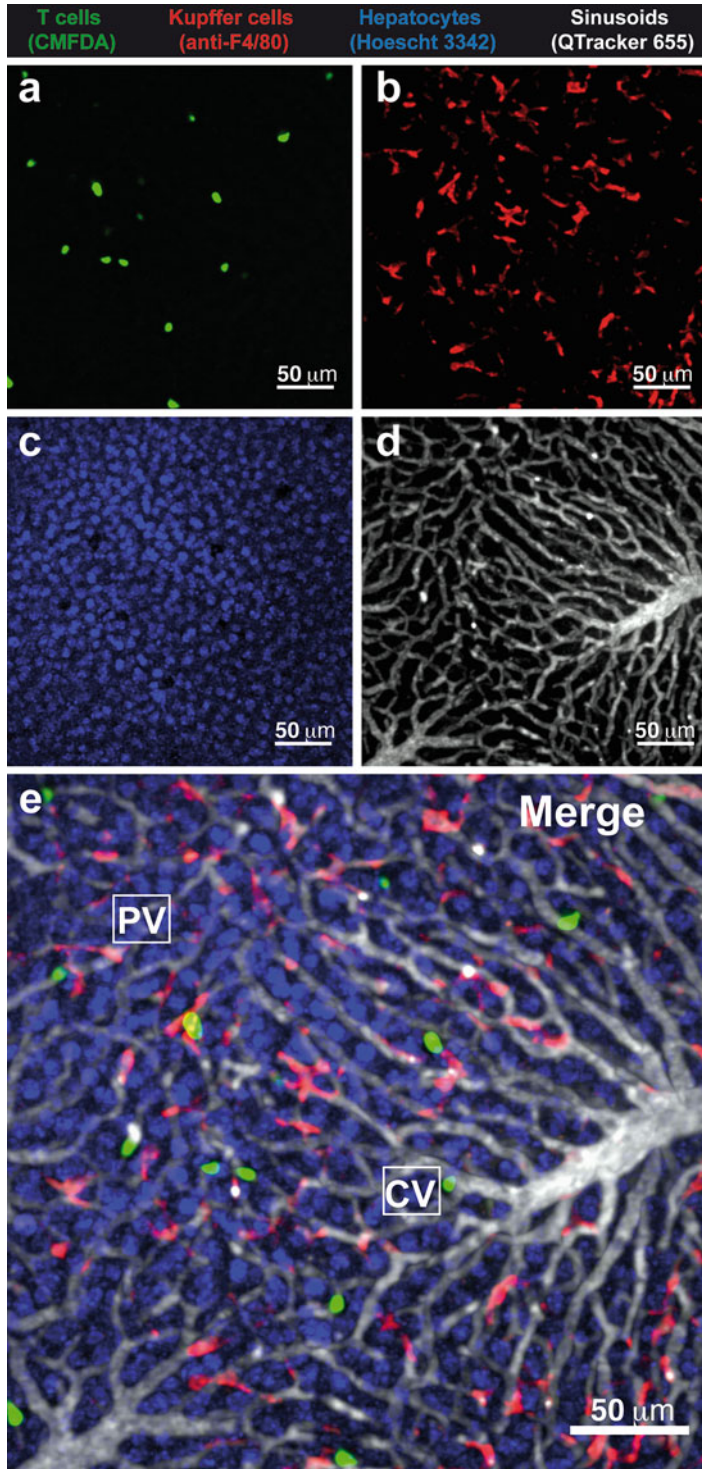


**Fig. 3** Intravital multiphoton microscopy of the mouse liver. (a–d) Intravital single-channel micrographs of the liver of a mouse injected with T cells. (a) CMFDA-labeled T cells; (b) Kupffer cells (stained by the injection of PE-labeled anti-F4/80 antibody); (c) Hepatocyte nuclei (stained by the injection of Hoechst 3342); (d) Liver blood circulation (visualized thanks to the injection of Qtracker 655). (e) Merged image. CV central vein; PV Portal vein. Scale bars represent 50 μm

1. Mean speed (Fig. 4c): mean velocity of a cell over several time steps (usually the entire imaging period, in  $\mu\text{m}/\text{min}$ ).
2. Displacement (Fig. 4d): distance between the first and the last imaging point (in  $\mu\text{m}$ ).
3. Straightness (Fig. 4e): The ratio between the displacement and the total track length. It is a measure of the straightness or confinement of cell tracks. It can vary between 0 (if the cell returns to the exact position where it started) and 1 (in case of a perfectly straight cell track).
4. Instantaneous speed (Fig. 4f): the ratio between the displacement and the interval time between frames (in  $\mu\text{m}/\text{min}$ ).
5. Contact time: the duration of physical association between two or more tracked particles (in min).

### 3.9 Morphological Analysis

It is also possible to analyze dynamically the morphological features of a cell. The images can be analyzed with software like Fiji to quantify several parameters that give information about a cell shape:

1. Perimeter: the length of the path that surrounds the cell shape.
2. Surface area: the total area encompassing the perimeter of the outer cell layer.
3. Circularity:  $(4\pi \times \text{area})/\text{perimeter}^2$ . A value of 1.0 indicates a perfect circle. As the value approaches 0, it indicates an increasingly elongated shape.
4. Shape index: ratio between the long and the short axis of the cell. It gives information about cell polarization.

Pseudopods of migrating cells can be identified with skeletonization, a technique that reduces a binary shape into a series of connected lines (the skeleton) (Fig. 4g). The temporal evolution of the skeleton highlights the dynamic nature of the cell protrusions. The software Fiji provides a plugin (AnalyzeSkeleton or Skeletonize3D) that tags all pixels in a skeleton image and calculates the total length of the skeleton and the number and length of each junction and branch (Fig. 4g) for every image in the temporal stack.

---

## 4 Notes

1. Although injectable anesthetics can be used in place of inhalational anesthetics, we favor the latter ones because they can be adjusted quickly as needed during the experiment, they allow for longer imaging sessions and for more physiological heart rate, breathing rate, and hemodynamic parameters (which are particularly critical when studying intravascular events).
2. Although we have also devised a liver intravital microscopy model suitable for an upright microscope setting [13], we favor

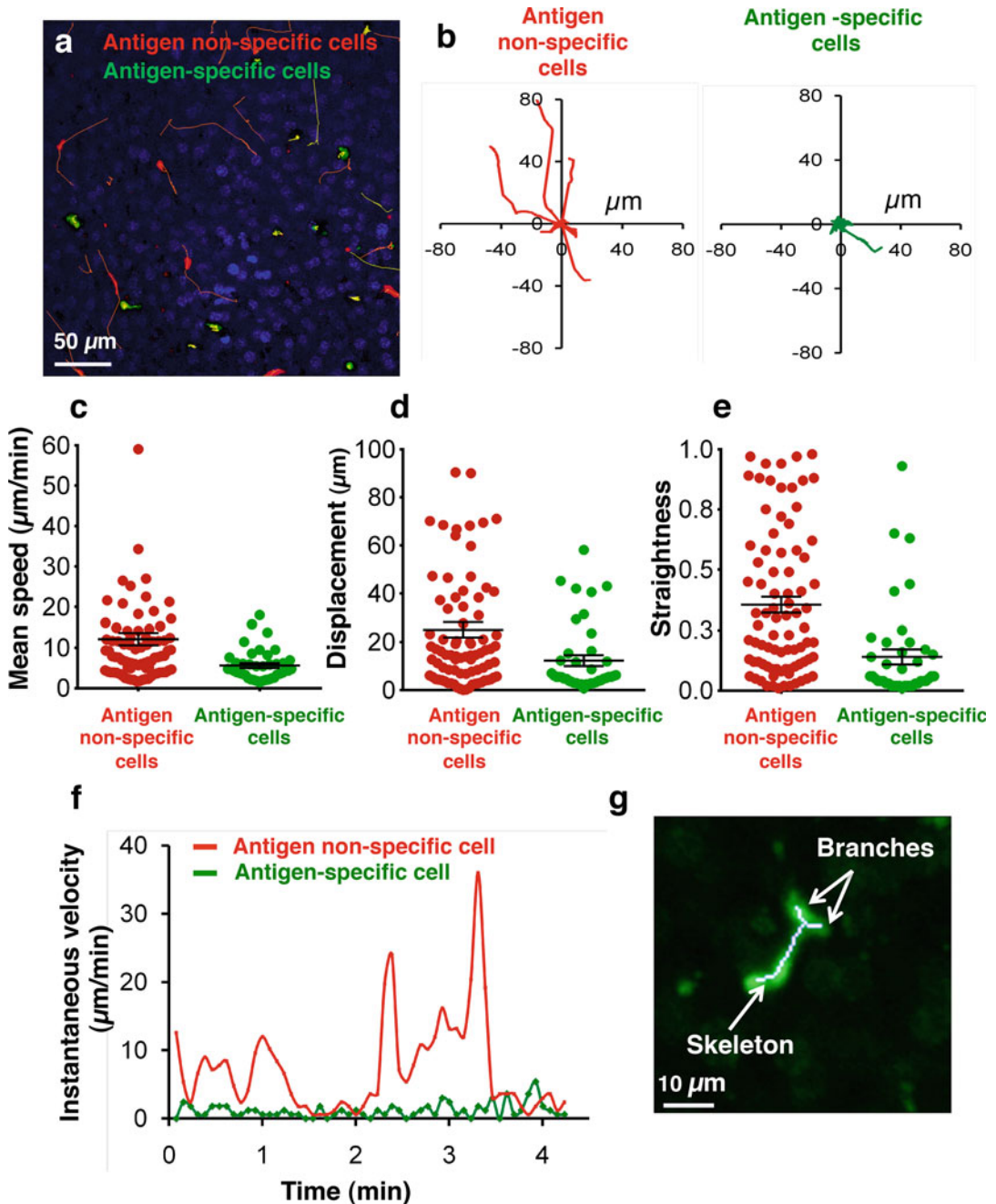


**Fig. 4** Image analyses. **(a)** Cell tracks in an intravital multiphoton microscopy movie in the liver of an hepatitis B virus (HBV) replication competent transgenic mouse transferred with antigen-specific (*green*) or antigen nonspecific (*red*) T cells. Hepatocyte nuclei are depicted in *blue*. Scale bar represents 50  $\mu\text{m}$ . **(b)** Track plots starting from the same origin of antigen non-specific (*red*, *left panel*) and antigen-specific (*green*, *right panel*) T cells. **(c–e)** Mean speed **(c)**, displacement **(d)**, and straightness **(e)** of individual antigen non-specific (*red*) and antigen-specific (*green*) T cells. **(f)** Instantaneous speed for individual antigen non-specific (*red*) and antigen-specific (*green*) T cells. **(g)** Example of the skeletonization of a T cell

the procedure detailed in this review as it is easier to perform, it generally offers a more stable preparation and it enables imaging over a greater liver surface area.

3. A spinning disk confocal system can be used in place of a multiphoton microscope.
4. As mouse shaving requires the use of isoflurane, we usually perform it a day before the imaging session (in order to limit isoflurane exposure right before the surgery). It is important to thoroughly rinse off the hair removal cream and hair fragments with PBS as they are both autofluorescent and can interfere with imaging. Moreover, long exposure to hair removal cream can induce undesirable skin inflammation.
5. Placement of the liver lobe on the center of the coverslip is a critical step that requires coordinated movements of the suture thread and the mouse body in order to ensure that the diaphragm is separated from the left liver lobe. We found that gently tilting the mouse head backwards (Fig. 2h) helps correct positioning of the left liver lobe.
6. The injection through the intravenous catheter during the imaging session has to be performed as slow as possible to avoid acute heart failure.

## References

1. Germain RN, Robey EA, Cahalan MD (2012) A decade of imaging cellular motility and interaction dynamics in the immune system. *Science* 336(6089):1676–1681. doi:[10.1126/science.1221063](https://doi.org/10.1126/science.1221063)
2. Murooka TT, Mempel TR (2012) Multiphoton intravital microscopy to study lymphocyte motility in lymph nodes. *Methods Mol Biol* 757:247–257. doi:[10.1007/978-1-61779-166-6\\_16](https://doi.org/10.1007/978-1-61779-166-6_16)
3. Guidotti LG, Inverso D, Sironi L et al (2015) Immunosurveillance of the liver by intravascular effector CD8(+) T cells. *Cell* 161(3):486–500. doi:[10.1016/j.cell.2015.03.005](https://doi.org/10.1016/j.cell.2015.03.005)
4. Iannacone M (2015) Hepatic effector CD8(+) T-cell dynamics. *Cell Mol Immunol* 12(3):269–272. doi:[10.1038/cmi.2014.78](https://doi.org/10.1038/cmi.2014.78)
5. Inverso D, Iannacone M (2015) Spatiotemporal dynamics of effector CD8+ T cell responses within the liver. *J Leukoc Biol* 99(1):51–55. doi:[10.1189/jlb.4MR0415-150R](https://doi.org/10.1189/jlb.4MR0415-150R)
6. Pircher H, Bürki K, Lang R et al (1989) Tolerance induction in double specific T-cell receptor transgenic mice varies with antigen. *Nature* 342(6249):559–561. doi:[10.1038/342559a0](https://doi.org/10.1038/342559a0)
7. Hogquist KA, Jameson SC, Heath WR et al (1994) T cell receptor antagonist peptides induce positive selection. *Cell* 76(1):17–27. doi:[10.1016/0092-8674\(94\)90169-4](https://doi.org/10.1016/0092-8674(94)90169-4)
8. Isogawa M, Chung J, Murata Y et al (2013) CD40 activation rescues antiviral CD8+ T cells from PD-1-mediated exhaustion. *PLoS Pathog* 9(7):e1003490. doi:[10.1371/journal.ppat.1003490](https://doi.org/10.1371/journal.ppat.1003490)
9. Iannacone M, Sitia G, Isogawa M et al (2005) Platelets mediate cytotoxic T lymphocyte-induced liver damage. *Nat Med* 11(11):1167–1169. doi:[10.1038/nm1317](https://doi.org/10.1038/nm1317)
10. Manjunath N, Shankar P, Wan J et al (2001) Effector differentiation is not prerequisite for generation of memory cytotoxic T lymphocytes. *J Clin Invest* 108(6):871–878. doi:[10.1172/JCI13296](https://doi.org/10.1172/JCI13296)
11. Guidotti LG, Matzke B, Schaller H, Chisari FV (1995) High-level hepatitis B virus replication in transgenic mice. *J Virol* 69(10):6158–6169
12. Iannacone M, Sitia G, Narvaiza I et al (2007) Antiplatelet drug therapy moderates immune-mediated liver disease and inhibits viral clearance in mice infected with a replication-deficient adenovirus. *Clin Vaccine Immunol* 14(11):1532–1535. doi:[10.1128/CVI.00298-07](https://doi.org/10.1128/CVI.00298-07)
13. Sitia G, Iannacone M, Aiolfi R et al (2011) Kupffer cells hasten resolution of liver immunopathology in mouse models of viral hepatitis. *PLoS Pathog* 7(6):e1002061. doi:[10.1371/journal.ppat.1002061](https://doi.org/10.1371/journal.ppat.1002061)

## Analysis of T Cell Activation by Confocal Microscopy

Paola Larghi, Antonella Viola, and Barbara Molon

### Abstract

Antigen-recognition by T cells requires the physical association with an antigen presenting cell (APC). At the interface between a T cell and an APC, the orchestrated redistribution of lipids, membrane receptors, and intracellular adaptors assembles a highly specialized junction, controlling the communication between the two cells, named the immunologic synapse (IS). The proper organization of the IS is a key step in host defense. Indeed, an appropriate T cell–APC interaction ensures the elimination of a wide range of pathogens and aberrant cells, whereas a deregulated IS formation leads to pathological situations such as infections, tumor development, or autoimmunity. Over the last decades T-cell scientists pioneered new imaging approaches to investigate IS assembly and organization. Microscopy techniques enable researchers to directly monitor, in space and time, the dynamics regulating T cell activation.

In this chapter, we describe in detail different microscopy protocols to visualize and analyze the recruitment of different molecules and organelles at the IS.

**Key words** Immunologic synapse, T cells, Antigen presenting cells, Microscopy, Calcium flux

---

### 1 Introduction

The onset and effectiveness of T-cell mediated adaptive immune responses primarily rely on the proper formation of a specialized junction, named the immunologic synapse (IS). The IS between a T cell and one or more antigen-presenting cells (APCs) is characterized by the spatiotemporal segregation of lipids and proteins, signaling compartmentalization and by the bidirectional exchange of soluble/membrane-bound transmitters. Thus, this immune junction represents a highly organized and dynamic structure where signals delivered by the T-cell receptors, adhesion molecules, as well as costimulatory and coinhibitory receptors are decoded and integrated. The canonical organization of the IS consists of concentric rings of molecules, with a central TCR–pMHC interaction cluster (pSMAC) surrounded by a ring of LFA-1–ICAM-1 adhesion (pSMAC) and a distal ring including the transmembrane tyrosine phosphatase CD45 (dSMAC) [1, 2]. Nonetheless, the aforementioned concentric organization does not appear as the

universal one. Alain Trautmann and colleagues, so far demonstrated that the IS within T and dendritic cells (DC) is more complex and intricate and it is characterized by the TCR clustering at multiple sites at T–DC cell interface [3]. Mapping the complex networks of molecules, crowding the IS upon antigen recognition, represents a crucial steps in the definition of T-cell signaling and activation. Activation thresholds, so far allow T cells to interpret the context in which the antigen is presented, recognize infectious stimuli, and finally decide between activation and tolerance [4].

Several approaches have been used to identify the precise positioning of the different molecules recruited at T cell–APC interface. However, neither conventional biochemistry nor classical cell-biology strategies can provide an integrated view of what is dynamically occurring during immune synapse formation. To overcome this limitation, over the last decades T-cell scientists pioneered new imaging approaches to investigate IS assembly and organization. Beside “classical” microscopy (Table 1), more sophisticated techniques to visualize lymphocyte signaling at the IS are emerging, defined as super-resolution microscopy techniques. These last, have the advantage to overcome the diffraction limit of light and allows the visualization of single molecules, instead of clusters of molecules. In general, super-resolution microscopy techniques can be various, and the one which better provides information on T cell signaling events is the single molecule localization microscopy (SMLM) [5, 6] (Table 1). Nonetheless, super-resolution techniques need specific platforms and often, specific fluorescent probes which are not always applicable to primary T cells [7]. Therefore, we decided to focus this methods review on the study of T cell activation and IS formation with more “classical” microscopy techniques.

In particular, we will focus on three different type of IS: the T cell–B cell synapse, the T cell–DC synapse, and the culture of T cells on CD3–CD28 coated activating surfaces which can be *bona fide* considered an IS. In the first case, we use B cells as APC and load them with a specific antigen, which can be presented in the context of MHC-II molecules and recognized by T cells. The advantage of this technique is the availability of B cells, which, in primary samples from patients and mice, can be easily purified from organs and blood. In addition, the size of T and B cells is similar, thus maximizing the possibility to form a single T–B synapse. In the second case, as previously mentioned, the organization of the IS and the resulting T cell activation might be different, as DC are professional APC and might provide stronger costimulation than B cells. In addition, DC adhere strongly on the glass slide and are bigger in size than T cells, thus providing the possibility to study T cell “scanning” of the DC surface before IS formation. In this case, it is likely that more than one T cell will form IS with the same DC.

**Table 1**  
**Looking at the immune synapse: imaging approaches**

<i>Wide field epi-illumination fluorescence microscopy</i>
In a conventional wide field optical epi-fluorescence microscope, the entire specimen is illuminated by a xenon or mercury arc-discharge lamp. This approach allows rapid acquisition of data, a large field of view and a big range of excitation wavelength. Through image deconvolution it is possible to obtain good quality images. It is very useful for imaging IS formation in living cells and to monitor fast events such as calcium signaling/dynamics.
<i>Confocal laser scanning microscopy</i>
In a confocal microscope, the light from the laser source scans across the specimen in a defined focal plane on the sample is focused as a confocal point at the detector pinhole aperture. Confocal microscopy offers several advantages over conventional wide field optical microscopy, because it allows to control the depth of the field, as well as to reduce the out-of-focus blur through the use of the pinhole and, importantly, to collect serial optical sections. This will allow the reconstruction of the immunological synapse in three dimensions.
<i>Spinning (Nipkow) disk confocal microscopy</i>
Nipkow (spinning) disk uses a disk containing multiple sets of spirally arranged pinholes which, as the disk rotates, allow to scan the specimen with approximately 1000 individual light beams that can traverse the entire image plane in less than a millisecond. Thus, while “classical” laser-scanning confocal microscopes illuminate and gather intensity information serially, spinning disk confocal microscopes enable the specimen to be sampled in parallel. This means that the effective illumination time per individual pixel is largely increased in comparison to a point scanning confocal microscope operated at a similar frame rate, resulting in a lower energy needed to illuminate the sample, thus decreasing phototoxicity and photobleaching.
<i>Two-photon and multi-photon laser scanning microscopy</i>
For the long-term imaging of live cells and in particular for in vivo imaging of tissues (such as lymph nodes), scientists use two-photon or multi-photon microscopy. Two-photon excitation involves the almost simultaneous absorption by a fluorophore of energy from two photons, each of which contributes one half of the total energy required to induce fluorescence. This technique allows deep tissue penetration (~350 $\mu\text{m}$ ) with a significant control of photobleaching and phototoxicity.
<i>SMLM (Single-molecule localization microscopy)</i>
A Super-resolution techniques requiring photoswitchable fluorescent probes and algorithmic processing. This approach is capable of bypassing the diffraction limit in optical microscopy and it is exploited to perform nanoscale observations and single-molecule localizations.
<i>TIRFM (Total Internal Reflection Fluorescence Microscope)</i>
TIRFM allows the selective visualization of the portion of the sample, which is close to the glass slide with a depth, which could be around 100–200 nm, meaning that it allows the visualization of the molecules that have been recruited and are close to, or at the plasma membrane, but not the molecules that are present in distal portions of cytoplasm.

In both T-DC and T-B synapse, most of the conjugates will be viewed “in profile”, thus restricting the observer’s visualization of the IS structure. In order to better visualize the synapse from the “top”, another option is to use coated substrates.

Coating of glass slides with CD3-CD28 antibodies is a simple technique to allow spreading of T cells on the glass surface upon TCR triggering and display some advantages compared to the “true” synapse. For instance, it allows the study of cytoskeleton remodeling dynamics, which is easier to visualize and, in addition, it allows the use of TIRFM (Table 1).

More recently, the coating of CD3-CD28 coated glass surfaces have been substituted with lipid bilayers, pioneered in McConnel laboratory in the 1980s [8] where proteins could be attached and can move freely in two dimensions. Although lipid bilayers are artificial structures, that lack cytoskeleton, lipid rafts and other characteristics of an APC, they have the advantage to maintain the movement of ligands as well as their orientation. For detailed protocols to prepare lipid bilayers, *see* ref. 9.

---

## 2 Materials

1. Human CD4<sup>+</sup> T lymphocytes and APCs purified from blood of healthy donors or patients or from surgically removed tissues.
2. Mouse lymphocytes isolated from the spleen or lymph nodes of wild-type or transgenic mice.
3. Murine DC derived from bone marrow (BM) precursors [10].
4. Human cell lines, such as Jurkat T cells (Clone E6-1) or Raji B cells, and cell lines expressing fluorescent proteins, such as Jurkat E6-1 cells stably expressing the mitochondrial targeting Red Fluorescent Protein (mtRFP) [11].
5. Slides: Thermo Scientific Menzel Gläser, 13 mm diameter (round glass slides), 76 × 26 mm (microscopy slides).
6. 0.1% poly-L-lysine solution (Sigma Aldrich): dilute 1/5 or 1/10 in distilled water.
7. Fibronectin (Sigma Aldrich): resuspend in distilled water at the concentration of 1 mg/ml (stock solution) and dilute 1/100 in distilled water.
8. PBS: weigh 8 g of NaCl, 0.2 g of KCl, 1.44 g of Na<sub>2</sub>HPO<sub>4</sub>, 0.24 g of KH<sub>2</sub>PO<sub>4</sub> and dissolve in 1 l of distilled water. Adjust to pH 7.4 and sterilize by autoclaving.
9. Complete medium: RPMI 1640 medium supplemented (or not, according to applications) with 10% heat-inactivated FCS, 20 mM glutamine, 1000 U/ml penicillin, and 1 mg/ml streptomycin and G418.
10. CellTracker™ Blue CMAC (7-amino-4-chloromethylcoumarin; Thermo Fisher): dilute in DMSO at the concentration of 10 mM (stock solution). Dilute in medium without serum.

11. Staphylococcal enterotoxin E and B (SEE and SEB) and toxic shock syndrome toxin-1 (TSST1; all from Toxin Technology): resuspend in PBS to make a stock solution of 1 mg/ml and use a working concentration of 100 ng/ml.
12. OVA peptide, amino acids 323–339 (PolyPeptide): dilute in PBS to make a stock solution of 1 mg/ml and use a working concentration of 10 µg/ml.
13. 37% formaldehyde (Sigma Aldrich): dilute 1/10 in PBS.
14. 10 mM Glycine: weigh 0.3 g in 0.5 l of PBS.
15. Anti human CD3ε antibody, clone OKT3 (eBioscience). Dilute in PBS.
16. Anti-mouse CD3ε antibody, clone 145-2C11 (BD Pharmingen). Dilute in PBS.
17. Anti-human CD28 antibody, clone CD28.2 (BioLegend).
18. Anti-mouse CD28 antibody, clone 37.51 (BD Pharmingen).
19. 5% bovine serum albumin (BSA): weigh 0.5 g BSA and dilute it in 10 ml PBS. Aliquot and freeze.
20. 5% saponin: weigh 0.5 g saponin and dilute it in 10 ml PBS. Aliquot and freeze.
21. Blocking and permeabilization buffer: PBS + 0.2% BSA + 0.05% Saponin.
22. 1 mM acetoxy-methyl-ester Fura-2 stock solution (Fura-2 AM; Invitrogen): add 50 µl of DMSO to a 50 µg vial. Use dry DMSO packed under nitrogen and it is necessary to remove the DMSO with a needle by puncturing the septum to prevent hydration of the DMSO. Keep Fura-2 AM solution in a dark dry place. Fura-2 AM in DMSO is stable at RT for 24 h and is stable at -20 °C in a dry container for several months.
23. Fura-2 AM working solution: Hank's balanced salt solution (HBSS) containing 1% FBS, pluronic F-127 (0.1%, w/v), sulfinpyrazone, and 3 µM Fura-2 AM.
24. Hoechst (Invitrogen): dilute 1 µl in 10 ml of water to have the working concentration.
25. Prolong (Invitrogen).
26. Microscopes. For fixed samples, it is possible to use a wide field upright microscope equipped for image deconvolution or a confocal microscope. Microscopes should be equipped with a 100× Plan Apo violet-corrected oil-immersion objective (numerical aperture, 1.4) and a highly sensitive cooled interlined charge-coupled device camera; in addition, a piezoelectric motor is suitable for z positioning. Alternatively, for live imaging, it is possible to use a scanning confocal microscope with Nipkow disk mounted on the microscope, equipped with an APO violet-corrected 60× oil-immersion objective with a numerical aperture of

1.40, laser illumination (405 nm and 50 mW; 491 nm and 100 mW; and 561 nm and 100 mW) and a camera. Finally, a microscope equipped with a 100× APO TIRF objective with numerical aperture of 1.45 and an electron-multiplying charge-coupled device camera can be used for TIRF microscopy of fixed and live cells (at 37 °C for live cells).

---

### 3 Methods

#### 3.1 Synapse Formation for Analysis on Fixed Samples

##### 3.1.1 T-B Synapse

1. Coat slides first. By working at room temperature, sterilize microscopy slides (glass coverslips) by washing them with 98% ethanol. Carefully plunge the slide in ethanol and leave it dry in the sterile hood until ethanol has completely evaporated (*see Note 1*).
2. Dilute poly-L-lysine to 0.02% in sterile water and drop 150 µl directly on each slide. Incubate for 30 min in the hood. Cover slides to avoid evaporation.
3. Wash out poly-L-lysine by plunging the slide in a beaker filled with sterile water and leave the slides dry in the hood until water has completely evaporated (*see Note 2*).
4. Prepare B cells by collecting B lymphocytes in a falcon tube, wash and resuspend cells in RPMI 1640 medium without serum, at the concentration of 10<sup>6</sup>/ml. Add 50 µM CellTracker™ Blue CMAC and incubate for 30 min at 37 °C.
5. Wash cells twice with complete RPMI 1640 medium, split them in two parts: add the model antigen (*see Note 3*) in one of the two, and an unrelated antigen or nothing in the other one. Incubate for 30 min at 37 °C.
6. Wash cells twice with complete RPMI 1640 medium and resuspend them at the concentration of 10<sup>6</sup>/ml. Drop 100 µl of cell suspension, corresponding to 10<sup>5</sup> cells, directly on the slide and let cells attach to the slides for minimum 30 min at 37 °C.
7. Upon incubation, carefully take out the excess of medium containing the B cells that did not adhere to poly-L-lysine and gently drop 100 µl of medium to wash once the slide (*see Note 4*).
8. Prepare T lymphocytes by collecting them in a falcon tube, wash and resuspend cells in complete RPMI 1640 medium at the concentration of 10<sup>6</sup>/ml.
9. Transfect cDNA constructs by electroporating 50 µg DNA for 10<sup>7</sup> cells using an electroporation system. Transfected cells are selected and maintained in culture in the presence of the appropriate selection antibody. Primary T cells could be transiently transfected using the nucleoporation system (Amaxa Biosystems) according to the manufacturer's guidelines [12–14].

10. Allow the formation of conjugates by dropping 100  $\mu\text{l}$  of cell suspension, corresponding to  $10^5$  cells, directly on the slide already incubated with B cells and let cells form synapses with B cells upon antigen recognition. B cells, which carry unrelated antigens or no antigen, are used as controls.
11. Let cells co-incubate at 37 °C for the required time points, which might vary according to the type of signaling event of interest (*see Note 5*).
12. At the end of the T-B cell incubation, gently remove the excess of medium and wash once with 100  $\mu\text{l}$  of PBS to take out all the T cells that did not form conjugates with B cells (*see Note 4*).
13. Gently drop 100  $\mu\text{l}$  of 3.7% formaldehyde to the slides and incubate for 10 min at room temperature.
14. At the end of the incubation, carefully remove the excess of formaldehyde and add 100  $\mu\text{l}$  of 10 mM glycine for 10 min at room temperature. This step is required to quench the aldehydic bonds that are unmasked by formaldehyde and can give rise to aspecific binding of the primary antibody (*see Note 6*).
15. At the end of the incubation, substitute glycine with PBS for subsequent immunofluorescence staining (*see Note 7*).
16. If live cell imaging is of interest, let B cells attach to the slide as in **step 6** and use attached cells to set the focus of the microscope and find a good field. Prepare T cells as described above (**step 8**). It is valuable to directly visualize molecules by expressing fluorescent proteins tagging the molecules of interest, as previously described (**step 9**) (*see Note 8*). Start recording and immediately drop T cells on the slide trying not to loose the focus and wait for one or more cells to come into focus in the field (*see Note 9*). Since signaling events are very rapid, it is important to start the movies before adding the cells.

### 3.1.2 T-DC Synapse

1. Coat slides as described in Subheading 3.1.1, but with either 0.01% poly-L-lysine or with 10  $\mu\text{g}/\text{ml}$  fibronectin (*see Note 10*).
2. Collect DC in a falcon tube, wash and resuspend cells in RPMI 1640 medium without serum, at the concentration of  $10^6/\text{ml}$ . Add 50  $\mu\text{M}$  CellTracker™ Blue CMAC and incubate for 30 min at 37 °C. Wash cells twice with complete RPMI 1640 medium, and split them in two parts: add the model antigen (*see Note 3*) in one of the two, and an unrelated antigen or nothing in the other one. Incubate for 30 min at 37 °C.
3. Wash cells twice with complete RPMI 1640 medium and resuspend them at the concentration of  $3\text{--}4 \times 10^5/\text{ml}$ .
4. Drop 100  $\mu\text{l}$  of cell suspension, corresponding to  $3\text{--}4 \times 10^4$  cells, directly on the slide and let cells attach to the slides for minimum 30 min at 37 °C.

5. Upon incubation, carefully take out the excess of medium containing the DC that did not adhere to the slide and gently drop 100  $\mu\text{l}$  of medium to wash once the slide (*see Note 4*).
6. Proceed with **steps 8–15** from Subheading **3.1.1**.
7. If live cell imaging is of interest, refer to Subheading **3.1.1**, **step 16**.

### 3.1.3 CD3-CD28 Synapse

1. Precoat microscopy slide with poly-L-lysine as described in Subheading **3.1.1**, **steps 1–3**.
2. When slides are dried, drop 80  $\mu\text{l}$  of 10  $\mu\text{g}/\text{ml}$  anti-CD3/CD28 antibodies. Incubate overnight at 4 °C (*see Note 11*).
3. Wash out anti-CD3/CD28 and immediately drop cells on the slide (*see Note 12*).
4. Prepare T cells as described in Subheading **3.1.1**, **steps 8** and **9**.
5. If signaling events on fixed samples are of interest, drop 50–100  $\mu\text{l}$  of cell suspension, corresponding to  $0.5\text{--}1 \times 10^5$  cells directly on the anti-CD3/CD28-coated slide to allow the formation of conjugates. Incubate for the required time points, which might vary according to the type of signaling event of interest (*see Note 5*). Fix slides as described in Subheading **3.1.1**, **steps 13–15**, and proceed with Subheading **3.2**.
6. For live cell imaging, gently drop 10  $\mu\text{l}$  of T cells (corresponding to  $10^4$  cells) on the slide and wait a few minutes for the T cells to come in contact with the bottom of the chamber. Use these cells to set the microscope (focus and TIRFM angle) and to choose a good field. Recording should start before dropping cells on the chamber as signaling events are very rapid (*see Notes 8* and **9**).

### 3.1.4 Immunofluorescence Staining on Fixed Samples

All steps must be performed very carefully to avoid unwanted cell detachment from the slide.

1. Drop 100  $\mu\text{l}$  of blocking and permeabilization buffer and incubate for minimum 30 min at room temperature (*see Note 13*).
2. Take out blocking and permeabilization buffer from the slides and substitute it with 100  $\mu\text{l}$  of the same buffer containing the primary antibody at the working concentration. Incubate for 2 h at room temperature (*see Note 14*).
3. Take out primary antibody from the slides and wash by dropping 100  $\mu\text{l}$  of blocking and permeabilization buffer. Repeat three times.
4. Take out blocking and permeabilization buffer from the slides and substitute it with 100  $\mu\text{l}$  of the same buffer containing the secondary antibody at the working concentration. Incubate for 45 min at room temperature.

5. Wash as in **step 3**.
6. Optional: nuclei staining. Take out blocking and permeabilization buffer from the slides and substitute it with 100  $\mu$ l of the same buffer containing Hoechst at the working concentration (*see* **Note 15**). Incubate for 45 min at room temperature.
7. Wash as in **step 3**.
8. Mount slides by putting one drop of Prolong on a microscopy slide (*see* **Note 16**). Plunge the slide in a beaker filled with sterile water and place the slide overturned on the microscopy slide, so that the surface with cells is in contact with the surface of the microscopy slide.
9. Leave the slides overnight at room temperature and keep them at 4 °C for few days, or store them at -20 °C for future use.

### 3.1.5 Acquisition

Given the small size of molecule clusters to be visualized, a conventional wide field optical epi-fluorescence microscope is not sufficient. Instead, confocal microscopy offers several advantages over conventional wide field optical microscopy, because it allows to control the depth of the field as well as to reduce the out-of-focus blur through the pinhole, and, most importantly, to collect serial optical sections that will allow the 3D reconstruction of the immunological synapse. “Classical” confocal microscopes are ideal for the acquisition and analysis of fixed samples, whereas spinning disk confocal microscope are preferred for live samples. This last uses a disk containing multiple sets of spirally arranged pinholes which allow to scan the specimen with approximately 1000 individual light beams as the disk rotates. In such a way, the entire image plane is traversed in less than a millisecond. Therefore, while “classical” laser-scanning confocal microscopes illuminate and gather intensity information serially, spinning disk confocal microscopes enable the specimen to be sampled in parallel. This means that the effective illumination time per individual pixel is largely increased in comparison to a point scanning confocal microscope operating at a similar frame rate, hence resulting in lower energy that is needed to illuminate the sample and, as a consequence, to decrease phototoxicity and photobleaching. While confocal microscopes are ideal for the study of T-B and T-DC synapses, the total internal reflection fluorescence microscope (TIRFM) is best to study the CD3/CD28 synapse. Indeed, the TIRFM allows the selective visualization of the portion of the sample most close to the glass slide with a distance between molecules and the glass slide, which could be around 100–200 nm, meaning that it allows the visualization of the molecules that have been recruited and are close to, or at the plasma membrane, but not the molecules that are present in distal portions of the cytoplasm.

Fixed samples. When analyzing an immunological synapse between a T cell and a DC or a B cell, it is better to choose

synapses in which the T cell contacts only one B or DC. Indeed, T cells are able to form more than one synapse simultaneously, thus causing different distribution of intracellular molecules. For fixed samples, it is important to reconstruct the full cell in 3D because activation molecules might be very small and they might be present only in one focal plan. Set the microscope in order to acquire as many z stacks as needed to cover the whole cell dimension and set the shortest possible distance between one stack and the other, according to the microscope characteristics and the photobleaching; typically, the distance between z stacks is 200–500 nm.

For TIRFM acquisition, it is not necessary to perform z reconstruction, as the light only illuminates the portion of the cell that is close to the slide, but does not allow to visualize the rest of the cell.

Live samples. Activation occurs as soon as the T cell recognizes the antigen or the CD3/CD28 antibodies. It is important to not lose the first signaling steps. Record with the shortest interval between frames while avoiding photobleaching.

### 3.1.6 Analysis

For the analysis of specific molecules recruitment at the immunological synapse, different methods could be adopted. We provide here some examples of analysis that can be adapted on either T-B or T-DC synapses.

1. Synapse recruitment of membrane molecules. This type of analysis can be used for molecules that are normally distributed in different portions of the plasma membrane and that can translocate specifically to the immunological synapse, once formed (Fig. 1a). The relative recruitment index (RRI) could be calculated as the mean fluorescence intensity (MFI) at synapse (a)/the average MFI of three regions—equal in dimension to the first one—outside the synapse (b, c, d) (Fig. 1b). MFI is quantified with the NIH Image J program. A minimum of 20 cells (or 20 conjugates) have to be examine quantitatively for each experiment.

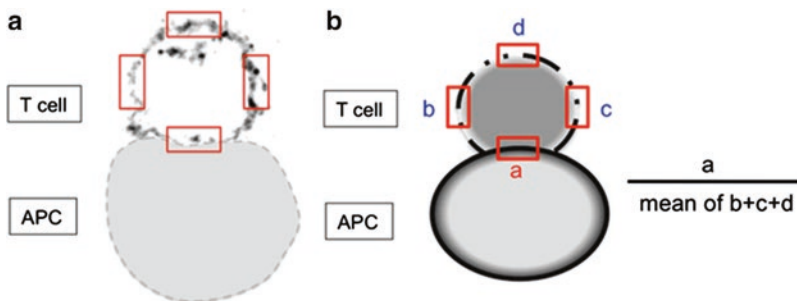


**Fig. 1** IS recruitment of membrane molecules. (a) Example of CD4<sup>+</sup> primary T cells forming a synapse with an APC; cells were co-incubated for 30 min at 37 °C, fixed, permeabilized, and stained for a T cell specific surface marker. As alternative, fluorescent proteins could be transfected in either primary T cells or T cell lines. (b) Schematic model for the calculation of the IS recruitment index of membrane molecules

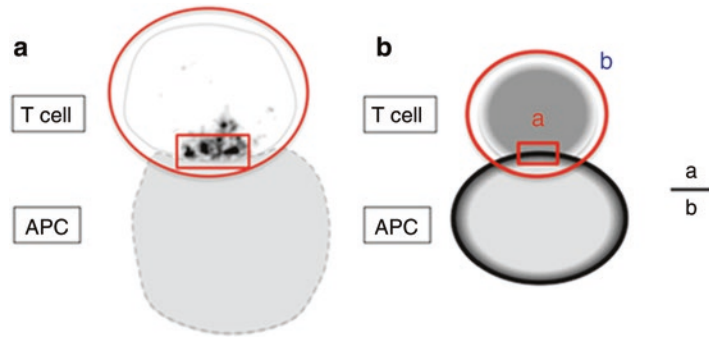


**Fig. 2** Synapse recruitment of intracellular molecules. (a) Example of CD4<sup>+</sup> primary T cells forming a synapse with an APC; cells were co-incubated for 30 min at 37 °C, fixed, permeabilized, and stained for a T cell specific intracellular marker. As alternative, fluorescent proteins could be transfected in either primary T cells or T cell lines. (b) Schematic model for the calculation of the IS recruitment index of intracellular molecules

2. Synapse recruitment of intracellular molecules. This type of analysis can be used for molecules that are present in different compartments inside the cell or free in the cytoplasm, and that can translocate to the immunological synapse, once formed (Fig. 2a). In this case, the MFI of the signal in a given region of the synapse is divided by the MFI of the total cell (including the synapse region). The calculation is made on two independent *z*-planes and the average of the two calculations is then plotted (Fig. 2b).
3. Molecules recruitment at the anti-CD3/CD28 coated slide. The interface between the cell and the anti-CD3/CD28 coated slide can be considered *bona fide* an immunological synapse. Therefore, in order to quantify the recruitment of molecules at the synapse it is necessary to count the number of molecules or clusters that are present in the bright field of the TIRF microscope (Fig. 3). In order to calculate the number of recruited molecules in a high number of cells to perform quantifications, it is possible to develop a “macro” which can be run on the imaging free software ImageJ (<http://imagej.nih.gov/ij/>). Basically, the “macro” identifies the isolated points with the highest fluorescence intensity in the cell area [6].

### 3.2 Mitochondrial Dynamics at the IS

As an alternative to conventional dyes (*see Note 17*), a suitable tool to study mitochondria dynamics in either fixed or living cells is the generation of cell lines, stably expressing mitochondria -targeting fluorescent proteins. As an example, Jurkat T cells stably expressing a mitochondrially targeted red fluorescent protein (mtRFP) can be used to study mitochondria localization at the IS [15].

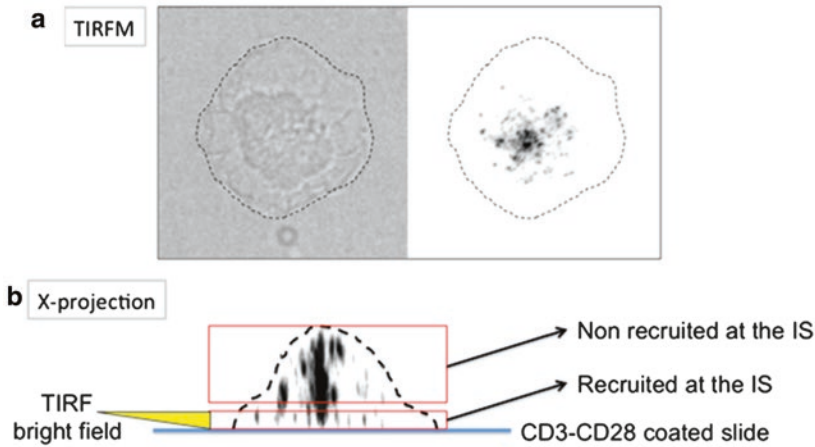


**Fig. 3** Molecules recruitment at the CD3-CD28 coated slide. **(a)** Example of primary ( $CD4^+$ ) T cells spread on CD3-CD28 coated slide for 10 min at  $37^\circ\text{C}$ . Cells were fixed, permeabilized, and stained and images were acquired upon setting up of the bright field of TIRFM. **(b)** X-projections (without TIRF settings) were performed to visualize all the molecules present on different stacks in 3D

### 3.2.1 Mitochondria Recruitment at the IS on Fixed Samples

1. First proceed with slide coating. Carry out this procedure at room temperature. Sterilize glass coverslips by washing them with 98% ethanol. Carefully plunge the slide in ethanol and leave it dry in the sterile hood until ethanol has completely evaporated.
2. Drop  $150\ \mu\text{l}$  of 0.02% poly-L-lysine directly on each slide. Incubate for 30 min in the hood. Cover slides to avoid evaporation.
3. Wash out poly-L-lysine by plunging the slide in a beaker filled with sterile water and leave the slides dry in the hood until water has completely evaporated (*see Note 2*).
4. Collect APCs in a falcon tube, wash and resuspend them in medium without serum, at the concentration of  $10^6/\text{ml}$ . For experiments with primary resting human  $CD4^+$  T cells, incubate B cells with  $1\ \mu\text{g}/\text{ml}$  of superantigens SEA, SEB, and SEE at  $37^\circ\text{C}$  for 2 h, mixing every 30 min. For experiments with Jurkat cells, APC are incubated only with  $1\ \mu\text{g}/\text{ml}$  SEE.
5. Collect T lymphocytes in a falcon tube, wash and resuspend cells in medium supplemented with 10% FCS, at the concentration of  $10^6/\text{ml}$ .
6. Transfect cDNA constructs by electroporating  $50\ \mu\text{g}$  DNA for  $10^7$  cells using an electroporation system. Transfected cells are selected and maintain in culture in the presence of the appropriate selection antibody. Primary T cells could be transiently transfected using the nucleoporation system (Amaxa Biosystems) according to the manufacturer's guidelines [15].
7. To allow the formation of conjugates, drop  $100\ \mu\text{l}$  of Jurkat cell suspension corresponding to  $10^5$  cells (double the amount

of primary resting human CD4<sup>+</sup> T cells in the same volume), directly on the slide already incubated with B cells and let cells form synapses with B cells upon antigen recognition. B cells which carry unrelated antigens or no antigen will be considered as controls. Let cells in co-incubation at 37 °C for the required time points, which might vary according to the type of signaling event of interest (*see Note 5*).

8. Fixation. At the end of the T-B cell incubation, gently take out the excess of medium and wash once with 100 µl of PBS to take out all the T cells, which did not form conjugates with B cells (*see Note 4*). Gently drop 100 µl of 3.7% formaldehyde to the slides and incubate for 10 min at room temperature. At the end of the incubation, carefully remove the excess of formaldehyde and add 100 µl of 10 mM glycine for 10 min at room temperature (*see Note 6*). At the end of the incubation, substitute glycine with PBS for subsequent immunofluorescence staining (*see Note 7*).
9. Proceed with acquisition. For fixed samples, it is important to reconstruct the full cell in three dimensions because activation molecules might be very small and they might be present in one focal plane but not in another. Set the microscope in order to acquire as many z stacks as needed to cover the whole cell dimension and set the shortest possible distance between one stack and the other, according to the microscope features and the photobleaching; typically, the distance between z stacks is 200–500 nm. For each experimental condition, take images randomly from different field of the microscope slide.
10. Analyze data as follows. For recruitment of mitochondria to the IS, draw boxes in the half part of the cell close to the IS and in the whole cell in the z-projection of the stacks. Measure fluorescence integrated density and apply the following formula: [(integrated density of fluorescence in the half part of the cell close to the IS)/(integrated density of fluorescence in the whole cell)].

Cells are scored as polarized when (1) at least 66% of the mitochondria fluorescence is localized in the half-part of the cell close to the area in contact with the APC or the slide and (2) mitochondria are localized close to the plasma membrane (representative images of T cells with mitochondria recruited or not to the IS are shown in Fig. 4 and in the video at the following link: <http://emboj.embopress.org/content/embojnl/29/23/4035/DC3/embed/inline-supplementary-material-3.mov?download=true>).

### 3.2.2 Mitochondria Recruitment at the IS on Living Cells (Real Time, Time-Lapse Microscopy)

1. Sterilize microscopy slides by washing them with 98% ethanol. Carefully plunge the slide in ethanol and leave it dry in the sterile hood (*see Note 1*) until ethanol has completely evaporated.

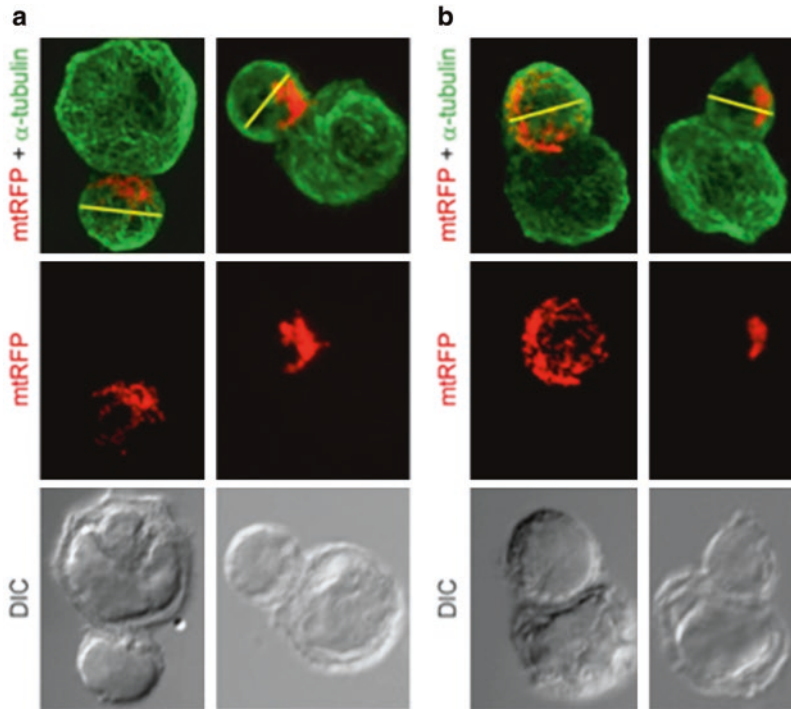


**Fig. 4** Mitochondria recruitment at the IS. Representative images of T cells with mitochondria recruited (**a**) or not (**b**) to the IS. Cells were scored polarized when (1) at least 66% of the mitochondria fluorescence was localized in the half part of the cell close to the area in contact with the APC and (2) mitochondria were localized close to the plasma membrane at the IS level. The *yellow line* is exemplificative for the division of T cell into two halves (reproduced from ref. [15] with permission from Wiley Online Library)

2. Drop 150  $\mu\text{l}$  of 5  $\mu\text{g}/\text{ml}$  fibronectin directly on each slide. Incubate for 30 min in the hood at RT. Cover slides to avoid evaporation. Wash slides three times in PBS.
3. Collect APCs (DC, B cells, EBV-B cells) in a falcon tube, wash and resuspend cells in medium without serum, at the concentration of  $10^6/\text{ml}$  with 1  $\mu\text{g}/\text{ml}$  of superantigens SEA, SEB, and SEE at 37  $^{\circ}\text{C}$  for 2 h, mixing every 30 min. For experiments with primary resting human  $\text{CD4}^+$  T cells, APCs are incubated only with 1  $\mu\text{g}/\text{ml}$  SEE.
4. To allow the formation of conjugates, plate T cells for 1 h on 24 mm diameter microscope slides coated with fibronectin and add pre-stimulated APCs. Perform real-time experiments at 37  $^{\circ}\text{C}$  in 0.1% BSA in serum-free RPMI medium.
5. Image APC–T cell conjugates on inverted microscope using the spinning disk microscope and the software associated with the microscope (Nikon software, Leica software, Metamorph, or others, according to the brand of the microscope in use). Acquisition and exposure time should be adjusted in relation to

experimental conditions. Approximately, acquire Bright field and fluorescence emission every 5 s, with exposure time of 500 ms per image. Stop the acquisition to the appropriate end-point.

6. To analyzed data, process images using NIH-Image J software. To determine recruitment of mitochondria to the IS, in the z-projection of the stacks, draw boxes in the half part of the cell close to the IS and in the whole cell. Measure Fluorescence integrated density and apply the following formula:  $[(\text{integrated density of red fluorescence in the half part of the cell close to the IS})/(\text{integrated density of red fluorescence in the whole cell})]$ .

### **3.3 Calcium Imaging at the IS**

1. Slide Coating. Sterilize glass coverslips by washing them with 98 % ethanol. Carefully plunge the slide in ethanol and leave it dry in the sterile hood (*see Note 1*) until ethanol has completely evaporated.
2. Drop 150  $\mu\text{l}$  of 5  $\mu\text{g}/\text{ml}$  fibronectin directly on each slide. Incubate for 30 min in the hood at RT. Cover slides to avoid evaporation. Wash slides three times in PBS.
3. Collect APCs (DC, B cells, EBV-B cells) in a falcon tube, wash and resuspend cells in medium without serum, at the concentration of  $10^6/\text{ml}$  with 1  $\mu\text{g}/\text{ml}$  of bacterial superantigens (SAGs) SEA, SEB, and SEE at 37 °C for 2 h, mixing every 30 min. For experiments with primary resting hCD4<sup>+</sup> T cells, APCs are incubated only with 1  $\mu\text{g}/\text{ml}$  SEE.
4. Load T cells with Fura2-AM working solution. Incubate cells for 30 min at 37 °C, wash and finally resuspend in HBSS containing 1 % FBS, and kept at RT protected form light.
5. To allow the formation of conjugates, plate T cells for 1 h on 24 mm diameter microscope slides coated with fibronectin and add pre-stimulated APCs to the slides. Perform real-time experiments at 37 °C.
6. Image APC–T cell conjugates on inverted microscope. The ratiometric Ca<sup>2+</sup> sensor fura-2 is alternatively excited at the excitation wavelengths of 340 and 380 nm using the appropriate imaging system (a confocal microscope equipped with a spinning disk or a epi-fluorescence microscope coupled with a CCD camera) and software (as ImageJ). Acquisition and exposure time should be adjusted in relation to experimental conditions. Approximately, acquire images every 3 s, with exposure time of 100 ms per image. It is recommended to reduce UV light exposure (no more than 15 s) and UV light intensity (use neutral density filter) to the minimum to prevent phototoxicity. Stop the acquisition to the appropriate end-point.
7. Process images by using the appropriate imaging software. Draw the region of interest tool (ROI) to define the areas of the image in which you want to measure calcium fluorescence

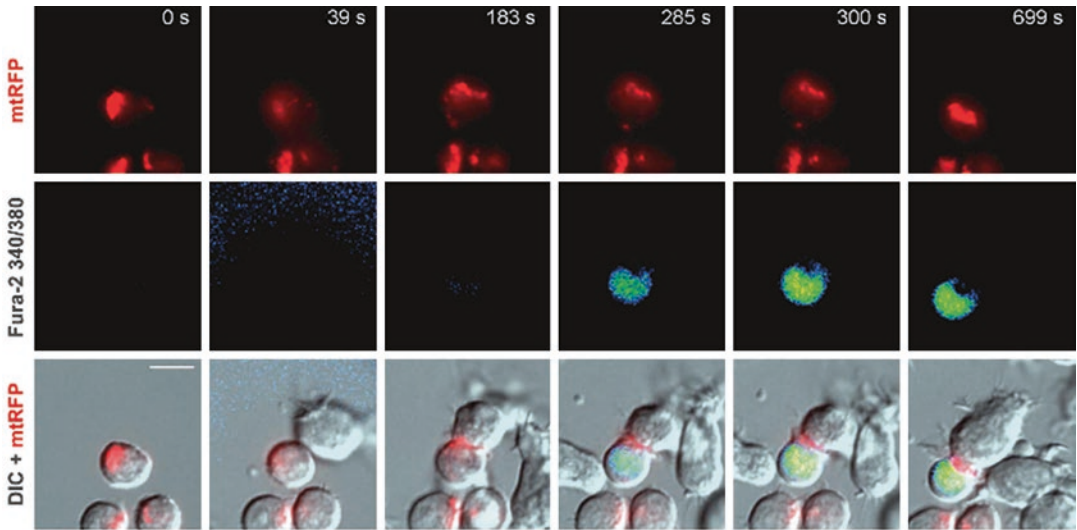


**Fig. 5** Calcium Imaging at the IS. Jurkat T cells expressing the mitochondrial marker mtRFP were plated with SEE-pulsed B cells and monitored by time-lapse microscopy for mitochondria relocation and calcium signaling. Representative images taken from the digital movies at the indicated times are shown. Bars, 10  $\mu\text{m}$ . (Reproduced from ref. [15] with permission from Wiley Online Library)

(see **Note 18**). Use software to collect time-lapse ratio measurements for each ROI in each image. Import the ratio measurements into an analysis program. Fura-2 traces are generated by averaging pixel signals within regions of interest (ROIs). Calculated offline Fura-2 pseudocolor ratiometric images as the ratio between the intensity emissions at the excitation wavelengths of 340 and 380 nm using the appropriate software, as ImageJ Software (Fig. 5).

8. Analysis of  $\text{Ca}^{2+}$  signals.  $\text{Ca}^{2+}$  signals are measured as fura-2 emission ratio changes,  $\Delta R = R(t) - R(0)$ , where  $t$  is time,  $R(t)$  is fura-2 emission intensity excited at 340 nm divided by the intensity excited at 380 nm, and  $R(0)$  indicates pre-stimulus ratio. Estimates of the cytosolic free calcium concentration ( $[\text{Ca}^{2+}]_c$ ) were obtained from ratio values using the Grynkiewicz formula:

$$[\text{Ca}^{2+}]_c(t) = K_d \cdot \left( \frac{R(t) - R_{\min}}{R_{\max} - R(t)} \right) \cdot \left( \frac{F_f}{F_b} \right)$$

9.  $R_{\min}$  and  $R_{\max}$  refer to minimum and maximum ratio values recorded in situ in the absence of  $\text{Ca}^{2+}$  and when Fura-2 is saturated, respectively.  $F_f/F_b$  is the ratio of the fluorescence values of the  $\text{Ca}^{2+}$ -free and  $\text{Ca}^{2+}$  bound forms at 380 nm and  $K_d$ , the dissociation constant of fura-2 at 22  $^{\circ}\text{C}$ , was assumed to be 280 nM.

---

## 4 Notes

1. Leave slides in a petri dish internally covered with Parafilm, so that you can close the Petri dish with its cover and put slides in incubator whenever needed in sterile conditions. Parafilm is hydrophobic, so the cell suspension will easily stay on the slide instead of spreading out in the petri dish. Normally it is not necessary to sterilize Parafilm, but sterilization may be needed for longer incubations. In this case, it can be sterilized with either radiation or hydrogen peroxide.
2. Slides can be either immediately used or dried stocked at room temperature for 2 weeks.
3. Human lymphocytes purified from blood are polyclonal and are to be activated with a mix of superantigens such as SEE, SEB and TSST1. In the case of mouse lymphocytes, it is necessary to use transgenic cells whose TCR is restricted for one model antigen, such as ovalbumin (OVA). For example, OT-II mice have OVA-specific CD4 T cells recognizing the amino-acidic sequence 323–339 of the OVA protein.
4. Cells do not adhere strongly to the slide, therefore it is very important to be very delicate in this step to avoid cell detachment. It is suitable to perform this step with a p200 pipette.
5. In some cases, the activation of signaling events upon synapse formation might be very rapid. One possibility to slow down the kinetic is to perform this step at room temperature or by putting the Petri dish containing the slides directly on ice.
6. Glycine is used to quench formaldehyde as it reacts with the excess of formaldehyde and thus stops the fixation process. This also allows to decrease the background for subsequent immunofluorescence staining.
7. At this step slides are fixed and can be stored in PBS at 4 °C. It is recommended to dunk the slides in a 24 well plate and seal it with Parafilm.
8. T cells must express a fluorescent tag on the molecule that needs to be studied. GFP and RFP are usually the most commonly used tags, although RFP is usually preferred for its lower background. Alternatively and according to the type of study, T cells can be loaded with a fluorescent dye that stains the organelle of interest.
9. It is possible that T cells in the chosen field are not on focus or do not interact with B cells or DC. To avoid changing the microscopy chamber every time, one possibility is to start dropping 30  $\mu$ l of T cell suspension (corresponding to  $3 \times 10^4$  cells) and repeat the same procedure three or four times for each microscopy chamber, choosing every time a different field.

10. Poly-L-lysine is toxic at high concentration, particularly for DC. Fibronectin is preferred.
11. Anti-CD3/CD28 can be also incubated for 3 h at 37 °C.
12. Anti-CD3/CD28-coated slides must not dry. They can be stored for one day in PBS at 4 °C.
13. BSA is used to block aspecific binding of antibodies and can be efficiently substituted by other blocking reagents, such as cold water fish gelatin. Saponin is used to permeabilize cell membranes and can be substituted with other permeabilization reagents, such as 0.1% Triton or 0.02% NP-40. If saponin is used, all antibodies incubations must be carried out in saponin containing buffers because its permeabilization effect is reversible.
14. Some antibodies can be incubated overnight at 4 °C, especially if the expression of the antigen is low. If the working antibody concentration is unknown, titrate reagents starting from a concentration of 5 µg/ml.
15. Hoechst can be substituted with 500 ng/ml DAPI diluted in water and incubated for 10 min at RT.
16. Prolong can be substituted with other mounting media, to be used according to the manufacturer's instructions.
17. Several mitochondria targeting dyes to monitor mitochondrial morphology and function are commercially available. The new generation of mitochondrial probes (as MitoTracker Green FM, Orange CMTMRos, Red CMXRos, and Deep Red FM) allow the visualization of these organelles in either living cells or after fixation and permeabilization steps.
18. It is generally useful to have at least one ROI that covers the cell body of the cell. When defining the ROIs, it is useful to play the movie of the images to verify that the cells do not move during the course of the experiment.

## References

1. Davis DM, Dustin ML (2004) What is the importance of the immunological synapse? *Trends Immunol* 25(6):323–327. doi:[10.1016/j.it.2004.03.007](https://doi.org/10.1016/j.it.2004.03.007)
2. Monks CR, Freiberg BA, Kupfer H, Sciaky N, Kupfer A (1998) Three-dimensional segregation of supramolecular activation clusters in T cells. *Nature* 395(6697):82–86. doi:[10.1038/25764](https://doi.org/10.1038/25764)
3. Brossard C, Feuillet V, Schmitt A et al (2005) Multifocal structure of the T cell—dendritic cell synapse. *Eur J Immunol* 35(6):1741–1753. doi:[10.1002/eji.200425857](https://doi.org/10.1002/eji.200425857)
4. Viola A, Contento RL, Molon B (2010) Signaling amplification at the immunological synapse. *Curr Top Microbiol Immunol* 340:109–122. doi:[10.1007/978-3-642-03858-7\\_6](https://doi.org/10.1007/978-3-642-03858-7_6)
5. Larghi P, Williamson DJ, Carpier JM et al (2013) VAMP7 controls T cell activation by regulating the recruitment and phosphorylation of vesicular Lat at TCR-activation sites. *Nat Immunol* 14(7):723–731. doi:[10.1038/ni.2609](https://doi.org/10.1038/ni.2609)
6. Williamson DJ, Owen DM, Rossy J et al (2011) Pre-existing clusters of the adaptor Lat do not participate in early T cell signaling events. *Nat Immunol* 12(7):655–662. doi:[10.1038/ni.2049](https://doi.org/10.1038/ni.2049)
7. Rossy J, Pigeon SV, Davis DM, Gaus K (2013) Super-resolution microscopy of the immunological synapse. *Curr Opin Immunol* 25(3):307–312. doi:[10.1016/j.coi.2013.04.002](https://doi.org/10.1016/j.coi.2013.04.002)

8. Hafeman DG, von Tscherner V, McConnell HM (1981) Specific antibody-dependent interactions between macrophages and lipid haptens in planar lipid monolayers. *Proc Natl Acad Sci U S A* 78(7):4552–4556
9. Zheng P, Bertolet G, Chen Y, Huang S, Liu D (2015) Super-resolution imaging of the natural killer cell immunological synapse on a glass-supported planar lipid bilayer. *J Vis Exp.* doi:[10.3791/52502](https://doi.org/10.3791/52502)
10. Granucci F, Zanoni I (2009) The dendritic cell life cycle. *Cell Cycle* 8(23):3816–3821
11. Campello S, Lacalle RA, Bettella M et al (2006) Orchestration of lymphocyte chemotaxis by mitochondrial dynamics. *J Exp Med* 203(13):2879–2886. doi:[10.1084/jem.20061877](https://doi.org/10.1084/jem.20061877)
12. Contento RL, Molon B, Boullaran C et al (2008) CXCR4-CCR5: a couple modulating T cell functions. *Proc Natl Acad Sci U S A* 105(29):10101–10106. doi:[10.1073/pnas.0804286105](https://doi.org/10.1073/pnas.0804286105)
13. Molon B, Gri G, Bettella M et al (2005) T cell costimulation by chemokine receptors. *Nat Immunol* 6(5):465–471. doi:[10.1038/ni1191](https://doi.org/10.1038/ni1191)
14. Tavano R, Contento RL, Baranda SJ et al (2006) CD28 interaction with filamin-A controls lipid raft accumulation at the T-cell immunological synapse. *Nat Cell Biol* 8(11):1270–1276. doi:[10.1038/ncb1492](https://doi.org/10.1038/ncb1492)
15. Contento RL, Campello S, Trovato AE et al (2010) Adhesion shapes T cells for prompt and sustained T-cell receptor signalling. *EMBO J* 29(23):4035–4047. doi:[10.1038/emboj.2010.258](https://doi.org/10.1038/emboj.2010.258)

## Phenotypic and Functional Analysis of Antigen-Specific T Cell Exhaustion

Kristin L. Boswell and Takuya Yamamoto

### Abstract

In some cancers and chronic infections exhausted T cells increase their expression of inhibitory receptors and demonstrate an impaired ability to produce cytokines and to proliferate. Immunological techniques such as MHC class I tetramer staining, intracellular cytokine staining, and CFSE dilution can be used to determine the memory status, inhibitory receptor expression, cytokine production, and proliferative capacity of antigen-specific CD8<sup>+</sup> T cells. Here, we describe approaches to define the inhibitory receptor expression, cytokine production, and proliferative capacity of antigen-specific CD8<sup>+</sup> T cells from HIV-infected and CMV-infected donors by using polychromatic flow cytometry.

**Key words** T cells, Exhaustion, Inhibitory receptors, HIV, CMV, MHC class I tetramer, Intracellular cytokine staining, Carboxyfluorescein succinimidyl ester, Flow cytometry

---

### 1 Introduction

In some chronic infections and cancers, T cells become “exhausted” and demonstrate a reduced ability to proliferate and produce cytokines [1, 2]. Exhausted T cells upregulate a combination of inhibitory receptors, including programmed death-1 (PD-1), CD160, 2B4, and lymphocyte activation gene 3 protein (LAG-3) [1–4]. The corresponding ligands of inhibitory receptors (including PD-L1, PD-L2, HVEM, and CD48, respectively) are expressed on antigen-presenting cells and bind to inhibitory receptors during antigen presentation [1, 2]. Ligand interactions with the inhibitory receptors result in negative signaling for T cell function. For example, PD-L1 and PD-L2, which are expressed on dendritic cells and B cells, recognize PD-1 on T cells and inhibit proliferation and cytokine production from PD-1 positive T cells [5–8]. Antibodies that block the interaction between PD-1 and its ligands, PD-L1 and PD-L2, can restore exhausted CD8<sup>+</sup> T cell function and are currently being tested in cancer and chronic infection settings [9–11].

Phenotypic and functional properties of antigen-specific T cells can be examined using multiple techniques including peptide-MHC class I staining, intracellular cytokine staining (ICS) typically for IFN- $\gamma$  or TNF, and carboxyfluorescein succinimidyl ester (CFSE) dilution to measure proliferation [12–15]. It is possible to compare the expression and impact of inhibitory receptors on antigen-specific CD8<sup>+</sup> T cells from different chronic infection settings, including human immunodeficiency virus (HIV) and human cytomegalovirus (HCMV) [3, 4, 7, 8].

MHC class I tetramers mounting peptides restricted for the given MHC and conjugated to specific fluorochromes provide a method to quantify the frequency of antigen-specific CD8<sup>+</sup> T cells in blood and tissues by flow cytometry. MHC class I tetramer staining can be combined with surface marker staining of memory markers (CD27, CD45RO, and CCR7) and inhibitory receptors (PD-1, CD160, 2B4, and LAG-3) to determine the memory status and inhibitory receptor expression on antigen-specific CD8<sup>+</sup> T cells. Furthermore, MHC class I tetramer staining may also be combined with ICS to determine the cytokine production (including but not limited to IFN- $\gamma$ , IL-2, and TNF) of antigen-specific CD8<sup>+</sup> T cells with epitope-specific peptide stimulation. In chronic HIV and HCMV infection, exhausted CD8<sup>+</sup> T cells often demonstrate a limited capacity to produce IFN- $\gamma$ , IL-2, and TNF [3, 4].

Exhausted CD8<sup>+</sup> T cells in chronic infections also show a reduced ability to proliferate. Blockade of inhibitory receptor pathways such as PD-1 has been shown to increase the proliferative capacity of exhausted CD8<sup>+</sup> T cells [3, 4]. These studies can be achieved by using functional antibodies to block inhibitory receptor signaling and CFSE dilution to measure the impact of T cell exhaustion on proliferation.

---

## 2 Materials

### 2.1 *Intracellular Cytokine Staining*

1. Peripheral blood mononuclear cells (PBMC; cryopreserved or fresh) isolated from whole blood by Ficoll gradient centrifugation from HIV-infected, HCMV-infected and uninfected donors.
2. “R10” medium: RPMI-1640, 10% heat-inactivated fetal bovine serum and 100 U/mL penicillin, 100  $\mu$ g streptomycin, 2 mM glutamine filtered through a 0.22  $\mu$ m PES filter, 0.01% DNase.
3. Dimethyl sulfoxide (DMSO).
4. Monensin (GolgiStop; BD Biosciences).
5. Brefeldin A (BFA) stock solution: 10 mg/mL BFA in DMSO.
6. HCMV pp65 Peptide Set (15-mers overlapping by 11 residues; NIH AIDS Reagent Program): resuspend peptides in DMSO and combine so that the final concentration of each peptide in the pool is 400  $\mu$ g/mL.

7. HIV-1 Consensus B Gag Peptide Set (15-mers overlapping by 11 residues; NIH AIDS Reagent Program): resuspend peptides in DMSO and combine so that the final concentration of each peptide in the pool is 400  $\mu\text{g}/\text{mL}$ .
8. Staphylococcus enterotoxin B (SEB) stock solution: 200  $\mu\text{g}/\text{mL}$  SEB in deionized  $\text{H}_2\text{O}$ .
9. Anti-CD28 (L293; BD Biosciences) (*see Note 1*).
10. Anti-CD49d (L25; BD Biosciences) (*see Note 1*).
11. Phosphate-buffered solution (PBS).
12. LIVE/DEAD fixable dead cell stain (Life Technologies): resuspend one vial of desiccated Aqua dye in 50  $\mu\text{L}$  DMSO to make the stock solution. The stock solution may be stored at  $-30^\circ\text{C}$ . For staining, the stock solution must first be diluted. Each lot should be titrated to determine the appropriate volume of diluted dye to add to the cells.
13. Antibodies for surface stain: anti-CD3 (SK7; BD Biosciences), anti-CD14 (M5E2; BD Biosciences), anti-CD19 (B43; BD Biosciences), anti-CD4 (OKT4; BioLegend), anti-CD8 (3B5; Life Technologies), anti-CD27 (O323; BioLegend), anti-CD45RO (UCHL1; Beckman Coulter), anti-CCR7 (3D12; BD Biosciences), anti-PD-1 (EH12.2H7; BioLegend), anti-CD160 (BY55; BD Biosciences), anti-2B4 (C1.7 Beckman Coulter), and anti-LAG-3 (17B4; eBioscience) (*see Note 2*).
14. Wash Buffer: PBS, 1% (vol/vol) fetal bovine serum (FBS), 0.02% (w/vol)  $\text{NaN}_3$ .
15. Cytofix-Cytoperm kit (BD Biosciences): Cytofix-Cytoperm reagent and 10 $\times$  Perm/Wash Buffer diluted to 1 $\times$  with deionized  $\text{H}_2\text{O}$ .
16. Antibodies for intracellular stain: IFN- $\gamma$  (B27; BD Biosciences), IL-2 (MQ1-17H12; BioLegend) and TNF (MAb11; BD Bioscience).
17. Fixative solution: 1% (vol/vol) paraformaldehyde (PFA) in PBS.
18. Antibody capture beads (BD Biosciences) for compensation.
19. ViViD/Aqua beads; ArC<sup>TM</sup> Amine Reactive Compensation Bead Kit (ThermoFisher).

## 2.2 MHC Class I Tetramer Staining

1. iTAg Tetramer/APC—HLA-A\*02:01 HIV gag (SLYNT VATL) (MBL International).
2. iTAg Tetramer/APC—HLA-A\*02:01 HCMV pp65 (NLVPM VATV) (MBL International).

## 2.3 Carboxyfluorescein Succinimidyl Ester Dilution (CFSE) Assay

1. CFSE stock solution: 10 mM CFSE in DMSO (*see Note 3*). For working solution, add 1  $\mu\text{L}$  of 10 mM CFSE stock solution to 1 mL of PBS to achieve 10  $\mu\text{M}$  CFSE working solution. Working solution must be used fresh.

2. Heat-inactivated fetal bovine serum (HI-FBS).
3. Purified anti-PD-L1 (MIH1; eBioscience).
4. Isotype control antibody IgG2a (eBM2a; eBioscience).

#### **2.4 General Lab Equipment**

1. 15 or 50 mL conical centrifuge tubes.
2. Tabletop centrifuge.
3. CO<sub>2</sub> tissue culture incubator.
4. 5 mL round bottom polystyrene test tube with snap cap, sterile.
5. Cell counter.
6. Polychromatic flow cytometer.

---

### **3 Methods**

#### **3.1 Intracellular Cytokine Staining (ICS)**

1. Calculate the total number of PBMCs needed for ICS ( $3 \times 10^6$  PBMCs per condition including: (1) negative control, (2) antigen-specific condition(s), and (3) positive control).
2. If PBMCs are cryopreserved, thaw the cells in a 37 °C water bath until only a small frozen pellet remains. Quickly transfer the cells into a 15 mL conical tube containing 10 mL of pre-warmed R10 medium with 0.01 % DNase I.
3. Wash the cells by centrifugation at  $500 \times g$  for 5 min at room temperature (~25 °C). Decant the supernatant and resuspend cells in 10 mL pre-warmed R10 medium containing DNase I.
4. Repeat wash step.
5. Rest the cells for at least 1 h at 37 °C and 5 % CO<sub>2</sub> (*see Note 4*).
6. Count cells to determine cell number and viability.
7. Dilute cells to  $3 \times 10^6$  PBMCs per milliliter of R10 medium and transfer 1 mL of PBMCs to a 5 mL round bottom polystyrene tube (*see Note 5*).
8. Add antigen-specific peptides to a final concentration of 2 µg/mL (5 µL/mL). For the positive control, add SEB to a final concentration of 2 µg/mL. For the negative control, add an equivalent volume of DMSO.
9. After 1 h, add protein transport inhibitors: monensin (0.7 µg/mL final concentration) and Brefeldin A (10 µg/mL final concentration) (*see Note 6*).
10. Incubate the PBMCs containing stimulation reagents and protein transport inhibitors for an additional 5 h at 37 °C and 5 % CO<sub>2</sub> so that cells are stimulated for a total of 6 h.
11. After stimulation, add 2 mL of PBS to each tube and centrifuge at  $500 \times g$  for 5 min at room temperature (*see Note 7*).
12. Resuspend the cells in 100 µL of PBS. Add diluted LIVE/DEAD fixable dye.

13. Incubate the cells for 5 min at room temperature in the dark.
14. Add the surface antibody mixture to the cells (anti-CD4, anti-CD8, anti-CD27, anti-CD45RO, anti-CCR7, anti-CD160, anti-2B4, anti-LAG-3, anti-PD-1).
15. Incubate for 20 min at room temperature in the dark.
16. Add 2 mL of wash buffer and centrifuge at  $500 \times g$  for 5 min at room temperature.
17. Decant the supernatant and resuspend the cells in 200  $\mu$ L of Cytotfix/Cytoperm reagent. Mix well.
18. Incubate for 20 min at room temperature in the dark.
19. Add 2 mL of Perm/Wash Buffer to the cells and centrifuge at  $500 \times g$  for 5 min at room temperature.
20. Decant the supernatant. Resuspend cells in residual Perm/Wash Buffer. Add antibodies for intracellular staining (anti-CD3, anti-TNF, anti-IL-2, anti-IFN- $\gamma$ ). Finger-flick to mix thoroughly. CD3 is stained intracellularly as CD3 downregulation may occur following peptide stimulation.
21. Incubate for 20 min at room temperature in the dark.
22. Add 2 mL of Perm/Wash Buffer to the cells.
23. Centrifuge at  $500 \times g$  for 5 min at room temperature.
24. Decant the supernatant. Resuspend cells in 250  $\mu$ L of fixative solution. Store cells at 4 °C in the dark until analysis by flow cytometry.
25. Analyze samples by flow cytometry (*see Note 8*).
26. For analysis, gate on lymphocytes, singlets, live cells (Aqua<sup>-</sup>), CD3<sup>+</sup>, CD4<sup>-</sup>, CD8<sup>+</sup> T cells. Naïve CD8<sup>+</sup> T cells are defined as CCR7<sup>+</sup>CD27<sup>+</sup>CD45RO<sup>-</sup>; central memory as CCR7<sup>+</sup>CD27<sup>+</sup>CD45RO<sup>+</sup>; transitional memory as CCR7<sup>-</sup>CD27<sup>+</sup>CD45RO<sup>+</sup>; effector memory as CCR7<sup>-</sup>CD27<sup>-</sup>CD45RO<sup>+</sup> and effectors as CCR7<sup>-</sup>CD27<sup>-</sup>CD45RO<sup>-</sup> (CCR7 might be optional if there is no opened channel). Naïve CD8<sup>+</sup> T cells express the lowest levels of the inhibitory receptors and can be used to set the gates for the inhibitory receptors. First determine the median fluorescent intensity (MFI) and percentage of the PD-1, CD160, 2B4, and LAG-3 expression on total CD8<sup>+</sup> T cells and CD8<sup>+</sup> T cells within each memory compartment. To determine the MFI and percentage of PD-1, CD160, 2B4, and LAG-3-positive cells in the HIV-specific or CMV-specific CD8<sup>+</sup> T cell population, first gate on the CD8<sup>+</sup>cytokine<sup>+</sup> T cells and then determine the MFI and percentage of inhibitory receptors (Fig. 1a).

### 3.2 Tetramer Staining

1. Follow the **steps** from **1** to **6** in Subheading **3.1**.
2. Resuspend the cells in 100  $\mu$ L of PBS. Add diluted LIVE/DEAD fixable amine dye.

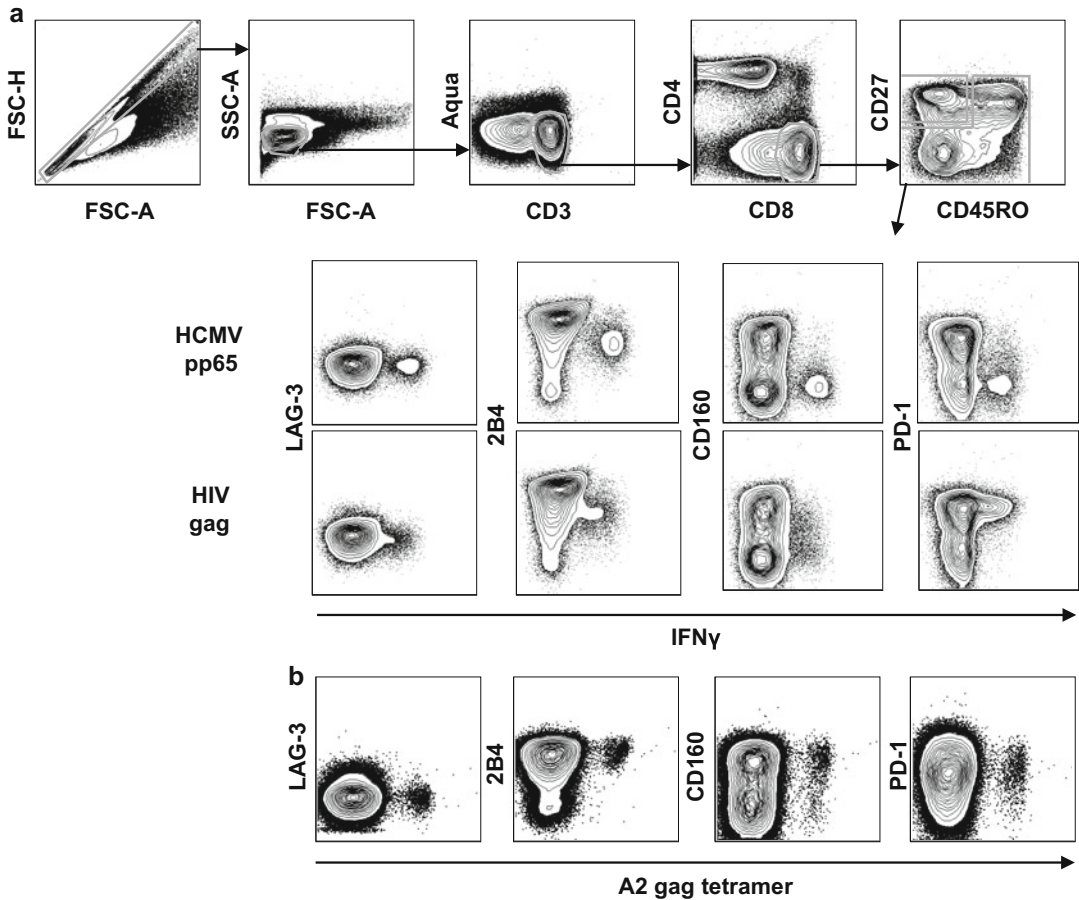


**Fig. 1** Inhibitory molecule expression on antigen-specific CD8<sup>+</sup> T cells. **(a)** Total PBMCs from an HIV<sup>+</sup> donor were stimulated with the HCMV pp65 peptide pool or HIV gag peptide pool for 6 h and stained as described in Subheading 3.1 (ICS). Cells were gated on singlets, lymphocytes, live, CD3<sup>+</sup>, CD4<sup>-</sup>, CD8<sup>+</sup>, and total memory. The expression of inhibitory receptors versus IFN $\gamma$ . **(b)** Total PBMCs from an HIV<sup>+</sup> donor were stained for tetramer as described in Subheading 3.2 (Tetramer staining). Cells were gated on singlets, lymphocytes, live, CD3<sup>+</sup>, CD4<sup>-</sup>, CD8<sup>+</sup>, and total memory. The expression of inhibitory receptors versus A2 gag tetramer was shown

3. Incubate the cells for 5 min at room temperature in the dark.
4. Add tetramers to the cells and incubate for 15 min on ice.
5. Add the surface antibody mixture to the cells (anti-CD3, anti-CD4, anti-CD8, anti-CD27, anti-CD45RO, anti-CCR7, anti-CD160, anti-2B4, anti-LAG-3, anti-PD-1).
6. Incubate for 20 min at room temperature in the dark.
7. Add 2 mL of wash buffer.
8. Centrifuge at  $500 \times g$  for 5 min at room temperature.
9. Decant the supernatant into a biohazard waste container. Resuspend cells in 250  $\mu$ L of fixative solution. Store cells at 4  $^{\circ}$ C in the dark until analysis by flow cytometry.

10. Analyze samples by flow cytometry.
11. For analysis, follow **step 26** in Subheading **3.1** (Fig. **1b**).
12. Tetramer staining can be used in conjunction with ICS. For ICS with tetramer staining, follow **step 17** in Subheading **3.1** after surface staining.

### **3.3 CFSE Dilution**

1. Calculate the total number of freshly isolated PBMCs needed for the experiment ( $3\text{--}4 \times 10^6$  PBMCs per condition).
2. Follow the **steps** from **1** to **6** in Subheading **3.1**.
3. Add CFSE working solution to cells ( $1 \times 10^6$  cells/mL) in a 50 mL conical tube. Incubate at  $37^\circ\text{C}$  for 20 min in the dark (*see Note 9*).
4. Add 1 mL of cold HI-FBS to each conical tube of CFSE-labeled cells. Bring volume total up to 50 mL with PBS. Centrifuge at  $500 \times g$  for 5 min. Repeat FBS/PBS wash step twice more.
5. After final wash, resuspend cells in R10 medium at a concentration of  $3\text{--}4 \times 10^6$  cells/mL.
6. Add 1 mL of CFSE-labeled cells to a 5 mL round bottom polystyrene tube.
7. Add anti-PD-L1 or Isotype control antibody (*see Note 10*).
8. Stimulate cells with  $0.2\ \mu\text{g}/\text{mL}$  of peptides corresponding to full-length HIV-1 Gag or HCMV pp65. Include a negative control (DMSO only) and a positive control (SEB final concentration should be  $0.1\text{--}1\ \mu\text{g}/\text{mL}$ ).
9. Incubate cells for 6 days at  $37^\circ\text{C}$  and 5%  $\text{CO}_2$ .
10. After 6 days, stain cells with LIVE/DEAD cell stain and, if needed, stain for tetramer and/or cytokines as described in **steps 10–16** of Subheading **3.1** (*see Note 11*).
11. Fix cells with 250  $\mu\text{L}$  of fixative solution. Store cells at  $4^\circ\text{C}$  in the dark until analysis by flow cytometry.
12. Analyze samples by flow cytometry (*see Note 12*).
13. For analysis, the percentage of CFSE<sup>low</sup> cells indicates the proliferative capacity of the cells. Compare the percentage of CFSE<sup>low</sup> CD8<sup>+</sup> T cells between HIV<sup>-</sup> and HCMV<sup>-</sup> specific stimulations and amongst the different antibody blocking conditions (Fig. **2**).

---

## **4 Notes**

1. Co-stimulatory antibodies may be included to boost the cytokine response. The concentration of co-stimulatory monoclonal antibodies (anti-CD28 and anti-CD49d) should be  $1\ \mu\text{g}/\text{mL}$  for each.

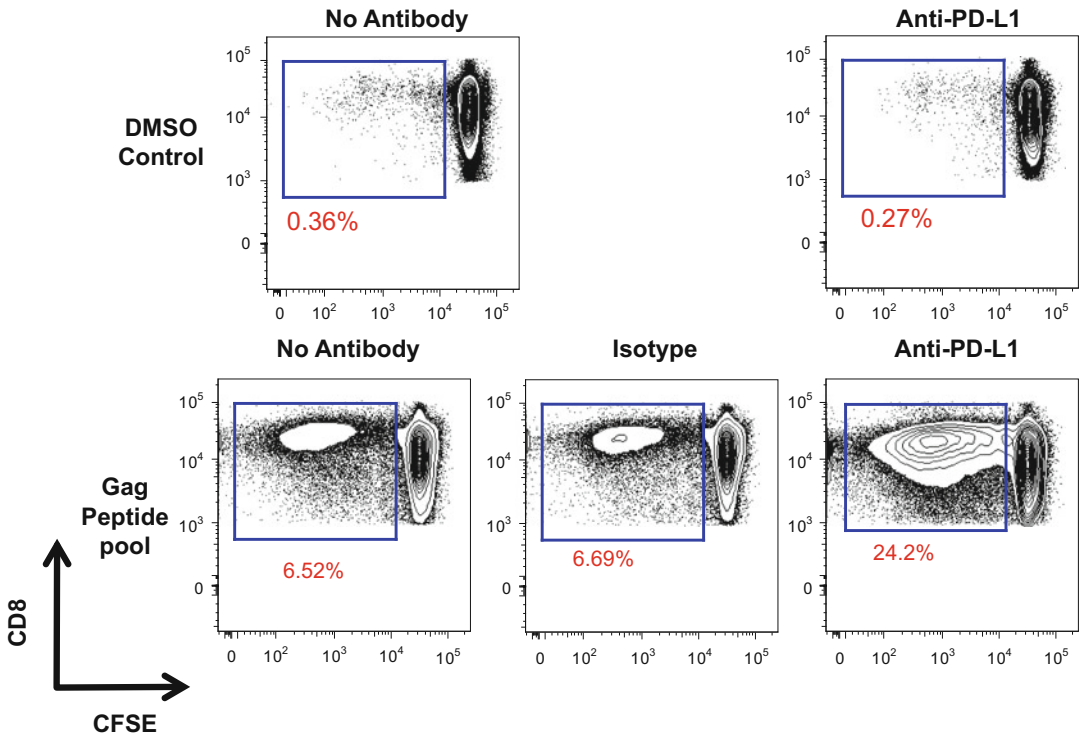


**Fig. 2** CFSE dilution in cells treated with anti-PD-L1. Total PBMCs from an HIV<sup>+</sup> donor were stained with CFSE dye and stimulated with gag peptide pools or DMSO control for 6 days as described in Subheading 3.3 (CFSE dilution). Anti-PD-L1 treatment (10  $\mu$ g/mL) boosted CD8<sup>+</sup> T cell proliferation compared to the isotype control antibody. Cells were first gated on lymphocytes, singlets, live, CD3<sup>+</sup>, CD8<sup>+</sup> T cells

2. Fluorescently labeled antibody conjugates must first be titrated.
3. CFSE is excited at 492 nm and emits at 517 nm. Other dyes may be used if a different excitation/emission spectrum is desirable.
4. Alternatively, cells may be incubated overnight at 37 °C prior to stimulation although more cell death may occur.
5. This protocol describes stimulation of cells in 1 mL of media in 5 mL round bottom polystyrene tubes. The protocol may be adjusted to 96-well microtiter plates, although more cell death may occur. In this case,  $3 \times 10^6$  PBMCs may be resuspended in 200  $\mu$ L of R10 medium and cultured in a round bottom 96-well plate.
6. Brefeldin A and monensin inhibit protein transport by interfering with membrane trafficking from the endoplasmic reticulum to the Golgi apparatus, and by neutralization of endosomes and lysosomes, respectively.
7. Check that the cell pellet is visible following centrifugation.
8. For compensation, add each antibody individually to compensation beads. Include unstained beads as a control. Also include Aqua/ViViD LIVE/DEAD compensation beads.

9. If more than  $50 \times 10^6$  cells are to be labeled, use multiple 50 mL conical tubes.
10. Blocking antibodies should be titrated to avoid nonspecific stimulation. Minimal CFSE dilution should occur with addition of blocking antibodies in the absence of peptide or SEB stimulation. In our studies, we found 10  $\mu\text{g}/\text{mL}$  induced minimal background (Fig. 2).
11. Do not use antibodies conjugated to FITC or Alexa 488 as the CFSE emission peak is 517 nm. If desirable, one may also stain for IFN- $\gamma$  and TNF. In this case, cells will need to be restimulated with the same peptides for 4 h at 37 °C (add the tetramer together with peptide stimulation if needed) and then proceed with the ICS protocol (Subheading 3.1).
12. For compensation, add each antibody individually to compensation beads. Include unstained beads as a control. To compensate CFSE, include cells stained only with CFSE and unstained cells as a control. Also include Aqua/ViViD LIVE/DEAD compensation beads.

## References

1. Wherry EJ, Kurachi M (2015) Molecular and cellular insights into T cell exhaustion. *Nat Rev Immunol* 15(8):486–499. doi:10.1038/nri3862
2. Kuchroo VK, Anderson AC, Petrovas C (2014) Coinhibitory receptors and CD8 T cell exhaustion in chronic infections. *Curr Opin HIV AIDS* 9(5):439–445. doi:10.1097/COH.0000000000000088
3. Yamamoto T, Price DA, Casazza JP et al (2011) Surface expression patterns of negative regulatory molecules identify determinants of virus-specific CD8+ T-cell exhaustion in HIV infection. *Blood* 117(18):4805–4815. doi:10.1182/blood-2010-11-317297
4. Peretz Y, He Z, Shi Y et al (2012) CD160 and PD-1 co-expression on HIV-specific CD8 T cells defines a subset with advanced dysfunction. *PLoS Pathog* 8(8):e1002840. doi:10.1371/journal.ppat.1002840
5. Freeman GJ, Long AJ, Iwai Y et al (2000) Engagement of the Pd-1 immunoinhibitory receptor by a novel B7 family member leads to negative regulation of lymphocyte activation. *J Exp Med* 192(7):1027–1034. doi:10.1084/jem.192.7.1027
6. Latchman Y, Wood CR, Chernova T et al (2001) PD-L2 is a second ligand for PD-1 and inhibits T cell activation. *Nat Immunol* 2(3):261–268
7. Trautmann L, Janbazian L, Chomont N et al (2006) Upregulation of PD-1 expression on HIV-specific CD8+ T cells leads to reversible immune dysfunction. *Nat Med* 12(10):1198–1202. [http://www.nature.com/nm/journal/v12/n10/supinfo/nm1482\\_S1.html](http://www.nature.com/nm/journal/v12/n10/supinfo/nm1482_S1.html)
8. Day CL, Kaufmann DE, Kiepiela P et al (2006) PD-1 expression on HIV-specific T cells is associated with T-cell exhaustion and disease progression. *Nature* 443(7109):350–354. [http://www.nature.com/nature/journal/v443/n7109/supinfo/nature05115\\_S1.html](http://www.nature.com/nature/journal/v443/n7109/supinfo/nature05115_S1.html)
9. Barber DL, Wherry EJ, Masopust D et al (2006) Restoring function in exhausted CD8 T cells during chronic viral infection. *Nature* 439(7077):682–687. [http://www.nature.com/nature/journal/v439/n7077/supinfo/nature04444\\_S1.html](http://www.nature.com/nature/journal/v439/n7077/supinfo/nature04444_S1.html)
10. Velu V, Titanji K, Zhu B et al (2009) Enhancing SIV-specific immunity in vivo by PD-1 blockade. *Nature* 458(7235):206–210. [http://www.nature.com/nature/journal/v458/n7235/supinfo/nature07662\\_S1.html](http://www.nature.com/nature/journal/v458/n7235/supinfo/nature07662_S1.html)
11. McDermott DF, Atkins MB (2013) PD-1 as a potential target in cancer therapy. *Cancer Med* 2(5):662–673. doi:10.1002/cam4.106
12. Lamoreaux L, Roederer M, Koup R (2006) Intracellular cytokine optimization and standard operating procedure. *Nat Protoc* 1(3):1507–1516. doi:10.1038/nprot.2006.268
13. Chattopadhyay PK, Melenhorst JJ, Ladell K et al (2008) Techniques to improve the direct ex vivo detection of low frequency antigen-specific CD8+ T cells with

- peptide-major histocompatibility complex class I tetramers. *Cytometry A* 73A(11):1001–1009. doi:[10.1002/cyto.a.20642](https://doi.org/10.1002/cyto.a.20642)
14. Lyons AB, Blake SJ, Doherty KV (2001) Flow cytometric analysis of cell division by dilution of CFSE and related dyes, *Current protocols in cytometry*. Wiley, New York. doi:[10.1002/0471142956.cy0911s64](https://doi.org/10.1002/0471142956.cy0911s64)
  15. Appay V, Rowland-Jones SL (2002) The assessment of antigen-specific CD8<sup>+</sup> T cells through the combination of MHC class I tetramer and intracellular staining. *J Immunol Methods* 268(1):9–19. doi:[10.1016/S0022-1759\(02\)00195-3](https://doi.org/10.1016/S0022-1759(02)00195-3)

## pMHC Multiplexing Strategy to Detect High Numbers of T Cell Responses in Parallel

Daisy Philips, Marlous van den Braber, Ton N. Schumacher, and Pia Kvistborg

### Abstract

The development of peptide loaded major histocompatibility complexes (MHC) conjugated to fluorochromes by Davis and colleagues 20 years ago provided a highly useful tool to identify and characterize antigen-specific T cells. In this chapter we describe a multiplexing strategy that allows detection of high numbers of T cell responses in parallel.

**Key words** pMHC complexes, Antigen-specific T cell immunity, Qdots, Flow cytometry, Multiplexing, Boolean gating

---

### 1 Introduction

T cells recognize cognate antigen in the context of MHC molecules. The technique to mimic this interaction between the T cell receptor and the peptide (p)MHC complex in a stable manner was pioneered by Davis and colleagues 20 years ago [1]. The use of the fluorescently labeled pMHC multimers has become a crucial tool for the analysis of antigen-specific T cell immunity in mouse and human settings.

The classical approach with pMHC multimer detection is to have a single fluorescent dye coupled to a specific pMHC complex. This approach limits the number of epitopes towards which T cell reactivity can be detected in for example limited patient material. To overcome this limitation, we and others developed multiplexing strategies that increases the number of T cell reactivities that can be detected in a single sample significantly [2, 3].

The multiplexing strategy we have developed is based on the generation of dual fluorochrome codes per pMHC complex of interest (illustrated in Fig. 1). The number of unique codes that can be generated when having a given number of fluorochromes available can best be calculated using factorial operations. As an example: eight different fluorochromes can result in:

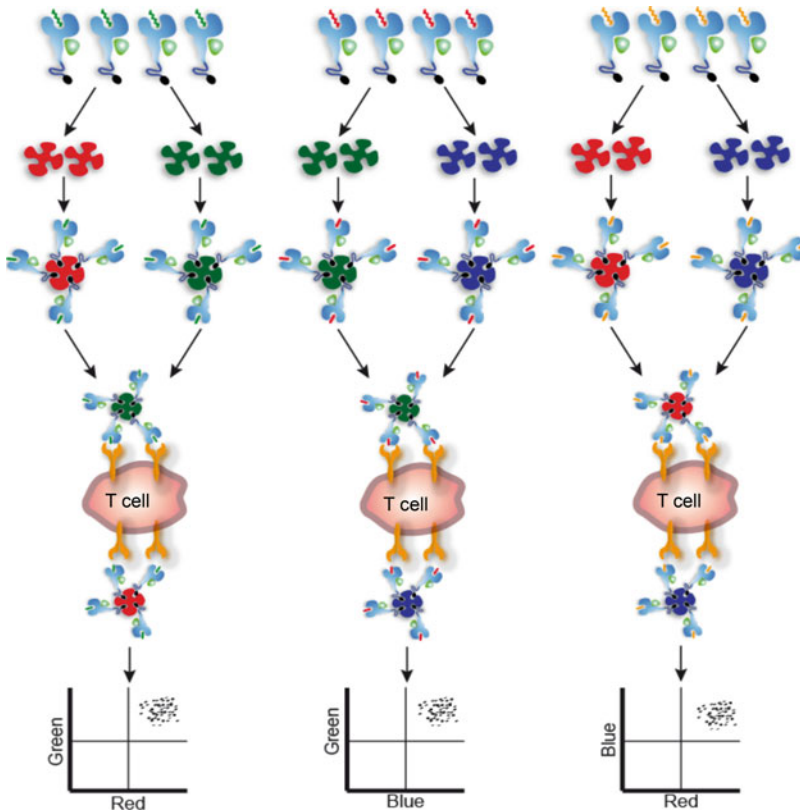


**Fig. 1** Dual color combinatorial coding principle

Dual codes:

$$(8 \times 7) / (1 \times 2) = 28 \text{ unique codes.}$$

Triple codes:

$$(8 \times 7 \times 6) / (1 \times 2 \times 3) = 56 \text{ unique codes.}$$

When just three fluorochromes are available for the pMHC multimers, the number of codes basically breaks even and is likewise three (*see* Fig. 1).

A benefit from using this dual code strategy is that it becomes possible to reduce the background signal and thereby to greatly enhance the sensitivity compared to when using single fluorescent dyes per pMHC complex. With a Boolean gating strategy, the read out can be focused on T cells that are only dual fluorochrome positive (for the fluorochromes used for generating the pMHC multimers) which will filter out any signal detected in one or more than two detectors. It was previously shown that this strategy reduces the background signal approximately tenfold—and therefore increases the sensitivity tenfold [3].

Restricting the code to two fluorochromes will require a higher number of fluorochromes available compared to making codes with all possible combinations. Therefore the choice of strategy is

a cost benefit decision where need for complexity (with few fluorochromes) and need for sensitivity are main factors to consider. However, if high end flow cytometers are available, high level of complexity can be reached with the dual code strategy. We are currently able to detect up to 47 different T cell responses in parallel.

The multiplexing strategy described in this chapter was developed to facilitate dissection of T cell reactivity against large epitope panels such as patient private mutated antigens.

---

## 2 Materials

### 2.1 UV Mediated Peptide Exchange

1. Biotinylated p\*MHC complexes refolded with conditional UV cleavable ligands (p\*) [4].
2. Peptides of interest: dissolve in dimethyl sulfoxide (DMSO) stock solution at a final concentration of 10 mg/ml (*see Note 1*).
3. 1× phosphate-buffered saline (PBS; filter sterile).
4. Polypropylene microplate 96-well V sharp (Greiner Bio-One) (*see Note 2*).
5. Microtube 1.5 ml with cap (Sarstedt) (*see Note 2*).
6. UV-lamp 366 nm CAMAG YV cabinet 3 (CAMAG) fitted with UV lamp long-wave UV, 366 nm, 2 × 8 W (CAMAG) (*see Note 3*).
7. Centrifuge with rotor for microtiter plates.

### 2.2 Multimerization of MHC Class I Molecules

1. Polypropylene microplate 96-well V sharp (Greiner Bio-One) with exchanged monomers prepared according to 3.1 UV mediated peptide exchange.
2. Fluorochromes: APC Streptavidin, R-PE Streptavidin, PE-Cy7 Streptavidin, Qdot 585 streptavidin conjugate, Qdot 605 streptavidin conjugate, Qdot 625 streptavidin conjugate, Qdot 655 streptavidin conjugate, Qdot 705 streptavidin conjugate, Qdot 805 streptavidin conjugate (all from Invitrogen).
3. Biotin/azide stock (20×): add 2.11 ml of a 5 mM D-biotin stock with 800 µl of a 10% NaN<sub>3</sub> in a 50 ml tube. Fill up to 20 ml with 1× PBS (17.1 ml). This will give a 20× stock solution of 500 µM D-biotin with 0.4% NaN<sub>3</sub>.
4. Corning® 96-well microplate aluminum sealing tape, nonsterile (Corning Costar).

### 2.3 Multimer Staining

1. Polypropylene microplate 96-well V sharp (Greiner Bio-One) with exchanged monomers prepared according to 3.2 Multimerization of MHC class I molecules.
2. Fluorochrome-conjugated monoclonal antibodies: CD8-AF700, CD4-FITC, CD14-FITC, CD16-FITC, CD19-FITC.

3. LIVE/DEAD® Fixable Near-IR Dead cell stain kit (Invitrogen).
4. Benzonase stock (100×): dilute benzonase (Novagen) 10× with plain RPMI to obtain a 100× stock solution of 2.5 U/μl.
5. Staining buffer: 1× PBS, 0.5% bovine serum albumin (BSA), 0.02% sodium azide.
6. Polypropylene microplate 96-well V sharp (Greiner Bio-One).
7. Corning® 96-well microplate aluminum sealing tape, nonsterile (Corning Costar).
8. Microtube 1.5 ml with cap (Sarstedt) (*see Note 2*).
9. Eppendorf centrifuge cooled to 4 °C.
10. BD™ LSR II Flow cytometer (BD Biosciences).

---

### 3 Methods

#### 3.1 UV Mediated Peptide Exchange

1. Thaw the biotinylated p\*MHC complexes on ice (*see Note 3*). Thaw peptides at room temperature if dissolved in DMSO, otherwise on ice.
2. Adjust the biotinylated p\*MHC complexes in PBS to 100 μg/ml in a microtube.
3. Calculate amount of peptide to use, end concentration 200 μg/ml.
4. Pipette peptide into well of either a 96- or 384-well V-bottom plate.
5. Immediately add the correct amount of monomers and carefully mix at least 5× without generating bubbles or foam.
6. After pipetting all the peptides/monomers place the 96-well plate under a UV lamp (366 nm) for 1 h at 4 °C, with a distance between the UV lamp and sample of approximately 5 cm (*see Note 4*).
7. Spin the 96-well plate at 2250×g for 10 min at 4 °C.
8. Transfer the supernatant to a new plate. Keep the plate at an angle to avoid transferring any pellet. This is to remove aggregated protein.

#### 3.2 Multimerization of MHC Class I Molecules

1. Pipette fluorochrome into wells. In Table 1 is listed the fluorochromes for which we have positive experience. The amounts listed should only be used as a guide. It is highly important to titrate all fluorochrome:MHC monomers when establishing the technology. For further *see* Subheading 3.3 and Note 5.
2. Immediately add exchanged monomers on top and mix well.

**Table 1**  
**Streptavidin-fluorochrome conjugates used for multimerization**

	/100 ng monomer
SA-PE	0.09 µg
SA-PE-Cy7	0.09 µg
SA-APC	0.06 µg
SA-Qdot605	0.15 pmol
SA-Qdot625	0.10 pmol
SA-Qdot655	0.15 pmol
SA-Qdot705	0.15 pmol
SA-Qdot800	0.10 pmol
SA-BV421	0.020 µg
SA-PE-CF594	0.014 µg
SA-PerCP-eFluor710	0.015 µg

3. After pipetting all of the fluorochrome/monomers cover plate with a microplate aluminum sealing plate and leave to conjugate for 30 min on ice in the dark.
4. Add 20× biotin/azide solution to wells to a final concentration of 25 µM D-biotin and 0.02 % NaN<sub>3</sub> and mix well (*see Note 6*).
5. Incubate for at least 30 min on ice in the dark or store in the fridge in the dark (*see Note 7*).

### 3.3 Titrations Multimerization Monomers

1. Prepare multimers in different fluorochrome/monomer ratios to determine the staining index (*see Note 8*).
2. For example, SA-PE at 0.07, 0.08, 0.09, 0.10, and 0.11 µg/1 µl monomer.
3. Stain cells with different amounts of the prepared multimers (*see Subheading 3.5*) and analyze on a flow cytometer.
4. Calculate staining index as follows:  

$$(\text{MFI positive population} - \text{MFI negative population}) / 2 \times \text{standard deviation of the negative population, defined as the scatter in MFI within the negative population.}$$
5. Select the optimal concentration based on staining index.

### 3.4 Collecting Multimers

1. Collect multimers in a polypropylene microtube. This should only be initiated right before using the p\*MHC multimer panel to stain cell samples (*see Note 9*).
2. Spin multimers 10,000 × g for 2 min at 4 °C (*see Note 10*).

### 3.5 Multimer Staining

1. Place thawed cells in a polypropylene round bottom 96-well plate and add benzonase to a final concentration of 25 U/ml.
2. Incubate for (at least) 30 min at 37 °C.
3. Spin cells at 250 × *g* for 3 min.
4. Discard supernatant.
5. Add multimer mix supernatant to the cells and fill up to 100 µl with staining buffer and mix.
6. Incubate for 15 min at 37 °C in the dark
7. Add antibody stain to the cells and mix. For 1 sample add: CD8-AlexaFluor700 (2 µl), CD4 FITC (1 µl), CD14-FITC (1 µl), CD16 FITC (1 µl), CD19-FITC (3 µl), IR dye (0.5 µl).
8. Incubate for 30 min on ice.
9. Add 100 µl FACS buffer to each well and spin plate 250 × *g* for 3 min.
10. Discard supernatant.
11. Add 200 µl FACS buffer to each well and spin plate 250 × *g* for 3 min.
12. Discard supernatant.
13. Add 200 µl FACS buffer to each well and transfer cells to FACS tube.
14. Analyze on a flow cytometer.

### 3.6 Multiplexing

1. When screening for multiple peptides, multiplexing can be used to reduce cell numbers needed for staining.
2. When using more than 2 fluorochromes making a staircase scheme for pipetting is preferable. For an example *see* Fig. 2.
3. Follow the protocol for generation of exchanged monomers, multimerization and staining.

### 3.7 Gating Strategy (Fig. 3)

1. Gate on lymphocytes in the FSC/SSC plot.
2. Gate out duplicates using for example FSC W/FSC H and SSC W/SSC W plots.
3. Gate out dead cells.
4. Gate on CD8<sup>+</sup>, CD4/CD14/CD16/CD19<sup>-</sup> negative cells.
5. Plot CD8 against each multimer fluorochrome. Determine the cutoff between positive and negative for each fluorochrome.
6. Invert all the multimer fluorochrome gates to NOT gates to have the negative gates as well for the Boolean gating.
7. Use the following Boolean gating strategy for the multimers (*see* **Note 11**): for each used multimer fluorochrome make an AND gate for the positive cells, e.g., PE AND APC; combine this with NOT gates for the not used fluorochromes for this

PE	APC	Qdot605	Qdot625	Qdot655	Qdot705	Qdot800	PE-Cy7	
	1	2	3	4	5	6	7	PE
		8	9	10	11	12	13	APC
			14	15	16	17	18	Qdot605
				19	20	21	22	Qdot625
					23	24	25	Qdot655
						26	27	Qdot705
							28	Qdot800
								PE-Cy7

PE	APC	Qdot605	Qdot625	Qdot655	Qdot705	Qdot800	PE-Cy7	
	1	2	3	4	5	6	7	PE
		8	9	10	11	12	13	APC
			14	15	16	17	18	Qdot605
				19	20	21	22	Qdot625
					23	24	25	Qdot655
						26	27	Qdot705
							28	Qdot800
								PE-Cy7

**Fig. 2** Staircase scheme for pipetting when using more than 2 fluorochromes. An example of a pipetting scheme when using eight different fluorochromes. In this case, a total of 28 combinations can be made (indicated by the numbers)

multimer, e.g., APC AND PE, NOT Qdot605, NOT Qdot625, NOT Qdot655, NOT Qdot705, NOT Qdot800, NOT BV421, NOT PE-CF594, NOT PerCP-eFluor710 gate.

### 3.8 Confirmation of Positive Responses

1. We have determined a cutoff for the assay to at least 0.005 % of the CD8<sup>+</sup> cells with at least 10 events. This can obviously be set according to what is biologically meaningful.
2. To confirm identified responses, it is highly recommendable to conduct confirmatory experiments by making new reagents where the dual fluorochrome is changed for each pMHC of interest according to Subheading 3.2.
3. Stain cells according to Subheading 3.5.

## 4 Notes

1. Ligand exchange may be less efficient when using peptides that have a poor solubility in water. It is possible to add ligands from stocks in DMSO, and ligand exchange reactions have been shown to proceed normally in the presence of up to 10 % DMSO.

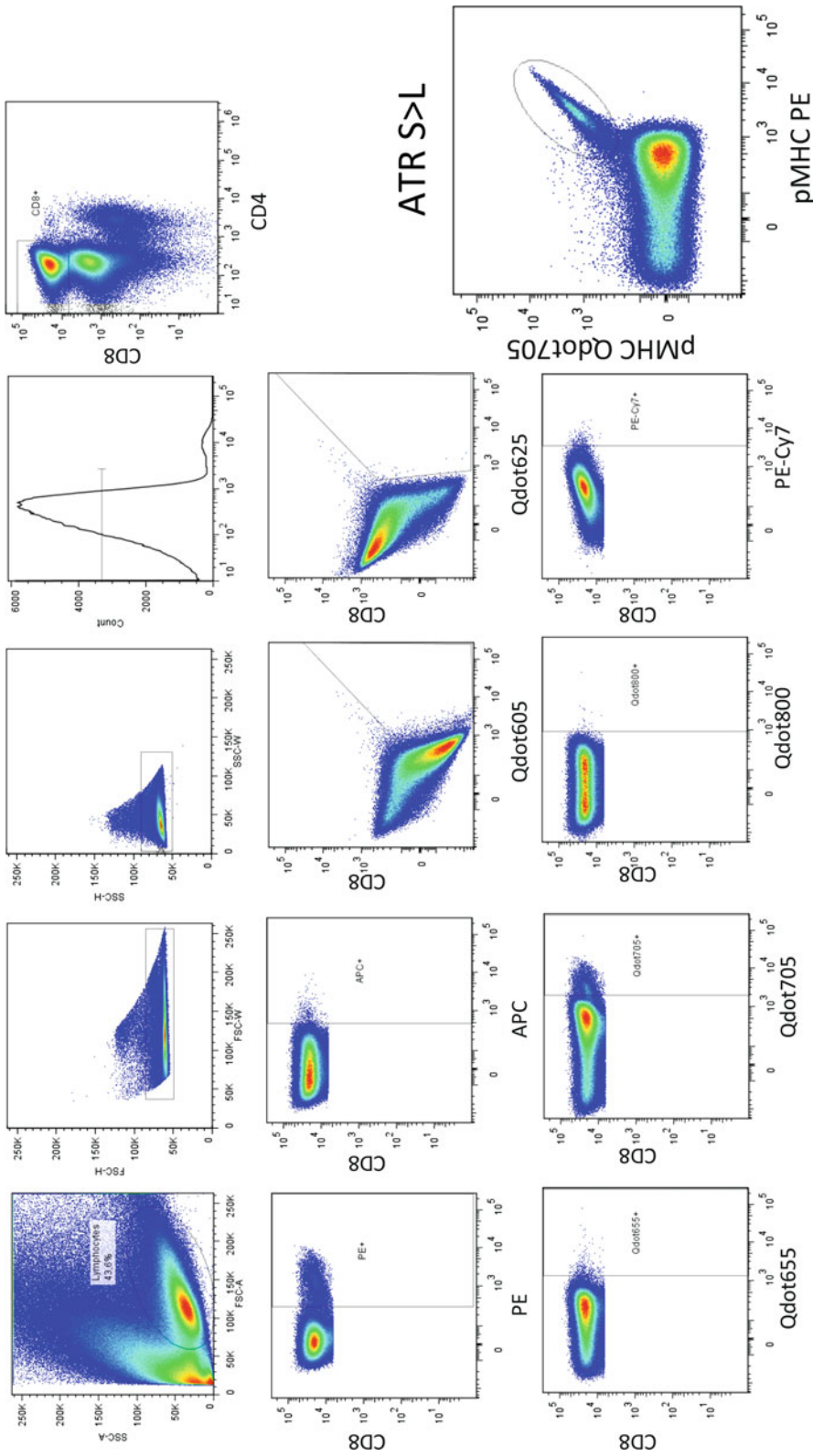


**Fig. 3** Gating strategy neo antigen screen of a representative patient. In total 8 different fluorochromes were used for multimer formation, adding up to 26 dual color codes. In this particular tube, multimer positive staining was visible in the combination of PE and Qdot705 (3.3% of CD8+ cells), corresponding to a mutated peptide of the ATR kinase

2. Use polypropylene material to avoid sticking of the peptide/protein to the plate/tubes.
3. p\*MHC complexes are light sensitive. Keep them in the dark when possible.
4. If not cooled, temperature of the solution may rise to approximately 30 °C. Leave at 4 °C to avoid overheating and vaporization.
5. Amount of fluorochrome to be used needs to be determined per center (*see* Subheading 3.3).
6. The addition of D-biotin ensures the blockage of any remaining free binding sites on the SA-conjugated fluorochromes, thereby preventing the binding of unconjugated pMHC complexes to other fluorochromes when collecting the pMHC multimer collections prior to staining.
7. p\*MHC multimers are stable up to 1 week in the dark at 4 °C.
8. For each flow instrument optimal fluorochrome/monomer ratios and staining volume need to be determined.
9. Always take 1.5× the volume to avoid staining with aggregates.
10. Spinning the multimers is crucial to avoid aggregate interference in the staining of the cells.
11. Boolean gating is necessary to limit false positive signals due to background.

## References

1. Altman JD, Moss PA, Goulder PJ et al (1996) Phenotypic analysis of antigen-specific T lymphocytes. *Science* 274(5284):94–96
2. Newell EW, Klein LO, Yu W, Davis MM (2009) Simultaneous detection of many T-cell specificities using combinatorial tetramer staining. *Nat Methods* 6(7):497–499. doi:[10.1038/nmeth.1344](https://doi.org/10.1038/nmeth.1344)
3. Hadrup SR, Bakker AH, Shu CJ et al (2009) Parallel detection of antigen-specific T-cell responses by multidimensional encoding of MHC multimers. *Nat Methods* 6(7):520–526. doi:[10.1038/nmeth.1345](https://doi.org/10.1038/nmeth.1345)
4. Toebes M, Coccors M, Bins A et al (2006) Design and use of conditional MHC class I ligands. *Nat Med* 12(2):246–251. doi:[10.1038/nm1360](https://doi.org/10.1038/nm1360)

## Differentiation of Diverse Progenies of Memory T Cells from Naïve CD8<sup>+</sup> T Cell Precursors

Veronica Zanon and Enrico Lugli

### Abstract

Following recognition of the cognate antigen, naïve T cells differentiate in a diverse progeny of memory T cells which differ at the phenotypic, gene expression and metabolic level. These molecular differences are at the basis of discrete functionality, migratory capacity and persistence in the long-term. Such a division of labor benefits adoptive T cell transfer immunotherapy approaches for cancer and viral infections, as increased persistence and effector functions in vivo result in better control of the disease. Preclinical data suggest that early-differentiated T memory stem cells are the most powerful anti-tumor T cell population following adoptive transfer, but their paucity ex vivo limits translation to the clinic. Here, we describe a simple protocol to derive large numbers of T memory stem cell and effector CD8<sup>+</sup> T cell subsets from highly-purified CD8<sup>+</sup> naïve T cell precursors. The obtained cells can be studied in vitro to understand the molecular basis of human memory T cell differentiation, or, when redirected with T cell receptor or chimeric antigen receptor, potentially used in vivo to favour T cell reconstitution or to treat established tumors or chronic infections.

**Key words** CD8<sup>+</sup> T cells, Naïve, Memory, T memory stem cells, Effector T cells, Adoptive cell transfer, Immunotherapy, Cancer, Cytokines, TCR stimulation

---

### 1 Introduction

Dozens of experiments performed with human CD8<sup>+</sup> T cells in vitro or in the mouse model in vivo in the last decade have revealed that memory T cell differentiation from naïve T cell precursors can be modulated by cell intrinsic or cell extrinsic mechanisms [1]. Several transcription factors have been demonstrated to alter the balance between effector vs. memory T cell formation. Similarly, environmental cues, such as the dose of the antigen, the type of priming (i.e., of the antigen presenting cell), or the inflammatory milieu, influence T cell clonal expansion, differentiation, and functional capacity [2]. This information has tremendous implications for adoptive T cell transfer approaches that are currently being used for treating established tumors or chronic viral infections: indeed, the type of cell product obtained

in vitro at the time of transfer has been correlated with functionality in vivo, thereby leading to a model where (products enriched with) less differentiated memory T cells are predictive of enhanced response [3]. Among memory T cells, the recently described T memory stem cells ( $T_{SCM}$ ) exhibit superior expansion, survival and functional capacity following adoptive transfer both in mice and in humans, owing to their stem cell-like properties [4–6]. Unfortunately, these  $T_{SCM}$  cells only comprise a small proportion of the total T cell compartment in the periphery, thus limiting their use in clinical protocols [7]. Here we describe a protocol to derive large numbers of early-differentiated  $T_{SCM}$  cells as well as effector T ( $T_{EFF}$ ) cells from human naïve T cell precursors by using cytokine cocktails combined with T cell receptor stimulation. Highly purified  $CD8^+ T_N$  cells are physically isolated with a FACS sorter [7] and stimulated by beads coated with antibodies directed to CD3, CD2, and CD28, or a combination of them. IL-7 and IL-15 [8] or IL-2 and IL-12 [3] are then used to generate  $T_{SCM}$  and  $T_{EFF}$  cells in 7 or 10 days, respectively. Despite focused on  $CD8^+$  T cells, the protocol can be efficiently applied to  $CD4^+$  T cells as well.

---

## 2 Materials

### 2.1 Cells

1. Peripheral blood mononuclear cells (PBMCs) from healthy individuals (50 mL of blood) or from a buffy coat (*see Note 1*).

### 2.2 Buffers, Cell Separation Components and Cell Culture Medium

1. Ficoll-Paque Plus or equivalent lymphocyte separation solution.
2. Hank's balanced salt solution (HBSS).
3. Fetal bovine serum (FBS).
4. Dimethyl sulfoxide (DMSO).
5. FACS staining buffer: HBSS, 2% (vol/vol) FBS.
6. Complete culture medium (R10): 10% (vol/vol) FBS, 1% (vol/vol) Penicillin/Streptomycin/L-Glutamine in RPMI 1640 medium with phenol red.
7. Trypan Blue solution for cell counting: dilute 0.4% stock solution to 0.04% working solution in PBS.
8. EasySep™ human  $CD8^+$  T cell enrichment kit (STEMCELL Technologies).
9. Robosep™ buffer (STEMCELL Technologies).
10. Cryogenic medium: FBS, 10% (vol/vol) DMSO.

### 2.3 Plastic Components

1. U-bottom 96-well plates.
2. Collection tubes, such as 5 mL FACS tubes (BD Biosciences) or 1.5 mL eppendorfs.
3. Neubauer chamber for cell counting or equivalent.

## 2.4 Flow Cytometry Reagents

1. Fluorescent dead cell discriminator such as Aqua LIVE/DEAD (ThermoFisher Scientific) or Zombie dye (BioLegend): resuspend powder in DMSO according to manufacturer's instructions. Store at  $-20^{\circ}\text{C}$ .
2. Fluorescently conjugated monoclonal antibodies: anti-human CCR7 PE-CF594 (BD); CD3 PE-Cy5 (BD); CD8 APC (BD); CD45RO PerCp-Cy5.5 (BioLegend); CD95 PE (BD); CD27 FITC (BD); CD45RA BV421 (BioLegend).

## 2.5 Reagents for Cell Stimulation

1. T cell activation/expansion kit, human (Miltenyi Biotec): prepare according to manufacturer's instructions (*see* **Note 2**).
2. Cytokines: recombinant human IL-2, IL-7, IL-12, and IL-15. Resuspend lyophilized cytokines in PBS added with 0.5% (vol/vol) bovine serum albumin (BSA) to a final concentration of  $100\ \mu\text{g}/\text{mL}$ .

---

## 3 Procedure

1. Isolate mononuclear cells (lymphocytes and monocytes) from peripheral blood or from buffy coat by using standard Ficoll gradient separation (*see* **Note 1**).
2. Wash cells twice in Robosep™ buffer by centrifuging at  $515\times g$  for 10 min.
3. Once PBMC are isolated, proceed immediately with  $\text{CD8}^+$  T cell enrichment or, otherwise, resuspend cells in cryogenic medium and freeze them in liquid nitrogen. At the time of the experiment, cells can be thawed according to standard procedures.
4. Resuspend  $20\ \mu\text{L}$  of cell suspension in  $80\ \mu\text{L}$  of Trypan Blue solution, mix well and load onto cell counting chamber. Prepare intermediate dilutions, should the sample be too concentrated.
5. Determine cell number by microscope count and draw cells that are needed for the experiment (*see* **Notes 2** and **3**).
6. Prepare for  $\text{CD8}^+$  T cell enrichment. Adjust cell density according to  $\text{CD8}^+$  T cell enrichment kit manufacturer's instructions.
7. Load cells onto RoboSep™ machine (STEMCELL Technologies) or proceed with manual enrichment via magnetic column (*see* **Note 4**).
8. Collect purified  $\text{CD8}^+$  T cells and determine number by cell count as indicated in **steps 4** and **5**.
9. Wash cells in PBS and spin down by centrifuging at  $515\times g$  for 10 min (*see* **Note 5**).

10. Resuspend cells in dead cell discriminator solution and incubate for 15 min at 24 °C (*see Note 6*).
11. In the meanwhile, prepare CCR7 antibody staining solution by diluting the optimal amount of CCR7 antibody (as predetermined by titration experiments) in FACS staining buffer in 1.5 mL eppendorf tube. Vortex and spin down mix on a benchtop centrifuge (15,000 for 5 min) to remove antibody aggregates.
12. Wash cells with FACS staining buffer as in **step 9**.
13. Discard supernatant by vacuum aspiration and resuspend pellet in CCR7 antibody staining solution (*see Note 6*).
14. Incubate for 20 min at 37 °C (*see Note 7*).
15. In the meanwhile, prepare antibody mix by following the same instructions as indicated in step 11. The amount of Abs to be added to the final mix should be carefully determined by titration experiments, as described in Chapter 3 of this book or according to previous publications [9]. Optimal titer is necessary to increase signal-to-noise ratio of fluorescent staining and minimize unspecific binding.
16. Wash cells as in **step 9**.
17. Discard supernatant by vacuum aspiration and resuspend pellet in surface antigen antibody staining solution. Incubate for 20 min at 24 °C.
18. Wash cells as in **step 9**.
19. Discard supernatant by vacuum aspiration and resuspend cells in FACS staining buffer at a density of  $\sim 50 \times 10^6$ /mL.
20. Proceed with FACS sorting. Identify naïve CD8<sup>+</sup> T cells by using the gating strategy depicted in Fig. 1. For details on FACS sorting procedure, refer to your facility specialist or consult our previous publication [7].
21. Collect cell numbers as determined by the FACS sorter.
22. Wash cells in R10 and centrifuge at  $515 \times g$  for 10 min.
23. Resuspend cells in R10 and adjust cell density to 50,000/100  $\mu$ L.
24. Prepare stimulation solutions in bulk. Adjust volumes according to the number of wells of a 96-well plate that are needed in the experiment. Prepare a solution containing R10 and the following stimuli (consider a final volume of 100  $\mu$ L to be added to 100  $\mu$ L of cell suspension): T<sub>SCM</sub> polarizing conditions, 0.25  $\mu$ L of CD3/CD28 antibody-coated beads (corresponding to 25,000 total beads), IL-7 and IL-15 (both at a final concentration of 10 ng/mL); T<sub>EFF</sub> polarizing conditions: 0.25  $\mu$ L of CD3/CD2/CD28 antibody-coated beads (corresponding to 25,000 total beads), IL-2 and IL-12 (both at a final concentration of 10 ng/mL). Vortex beads vigorously before adding them to stimulation solutions (*see Notes 8 and 9*).

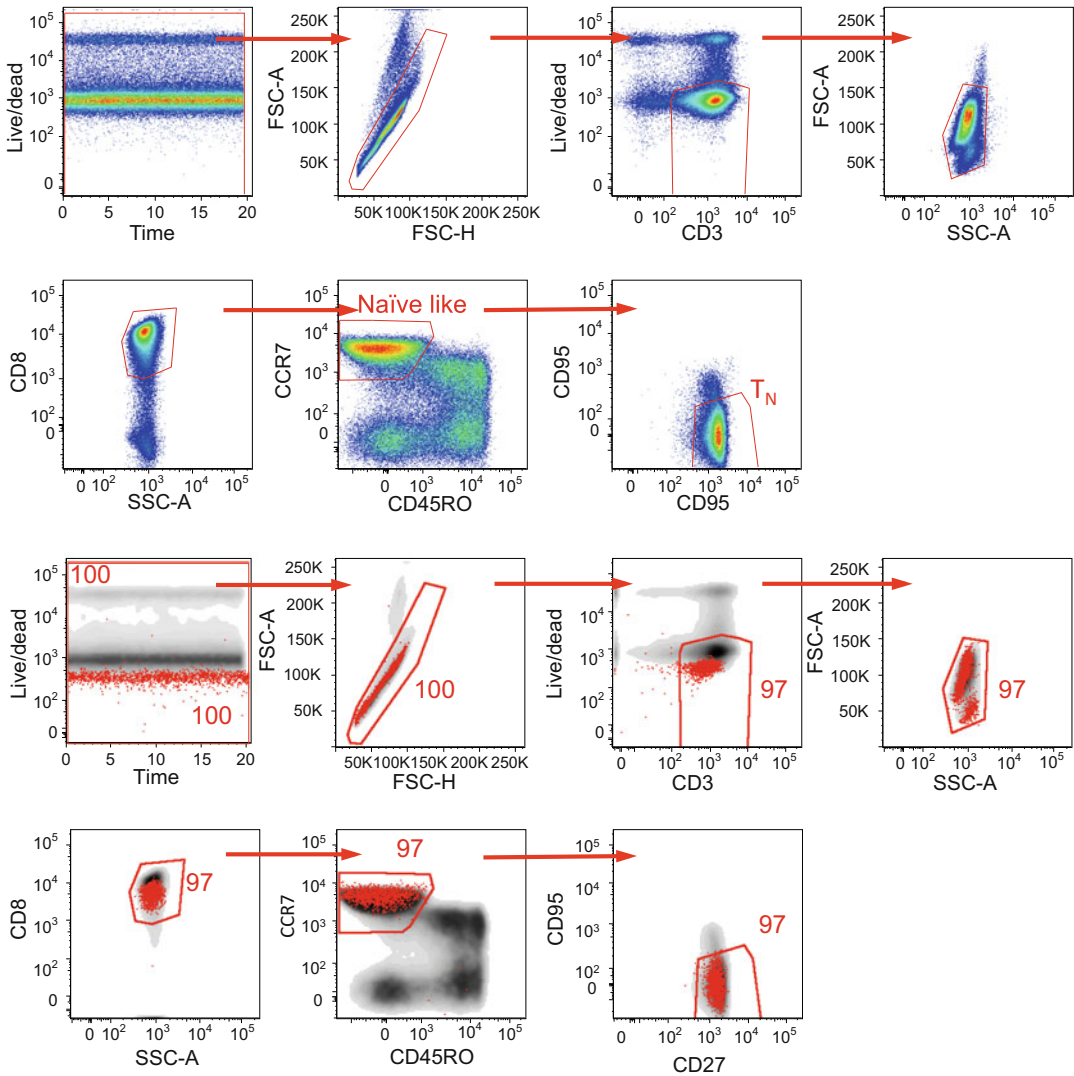


**Fig. 1** Gating strategy for the FACS sorting of highly purified  $T_N$  cells. Top: PBMCs from a healthy donor were thawed and enriched for  $CD8^+$  T cells by negative selection. Cells were subsequently stained with the AQUA dead cell discriminator dye and with mAbs directed to identify T lymphocytes. Time-gated cells are selected as singlets on the basis of FSC-A and FSC-H parameters. Live T cells are identified as  $CD3^+/AQUA^-$  and lymphocytes on the basis of FSC-A and SSC-A. Identification of naïve and memory T cell subsets in  $CD8^+$  T cells is performed by the use of 4 markers. CCR7 and CD45RO allow to discriminate naïve-like T cells (i.e.,  $CCR7^+CD45RO^-$ ) from memory cells. CD27 and CD95 markers are used to discriminate  $T_{SCM}$  (further gated as  $CD27^+CD95^+$ ) from truly naïve ( $T_N$ ;  $CD27^+CD95^-$ ) cells. Bottom: sort purity of  $CD8^+$   $T_N$  cells is shown. Following cell sorting, a small fraction of purified  $CD8^+$   $T_N$  cells was acquired to evaluate the sort purity. Sorted  $CD8^+$   $T_N$  cells (red) are overlaid on top of total PBMCs (grey). The same gating strategy described in the top panel is shown. Numbers indicated the frequency of cells in each gate as relative to the initial ungated population

25. Seed 50,000 cells/well (100  $\mu$ L) and add stimulation cocktails (100  $\mu$ L) to obtain a final volume of 200  $\mu$ L.
26. Incubate at 37  $^\circ$ C for 7–14 days (*see Note 10*).

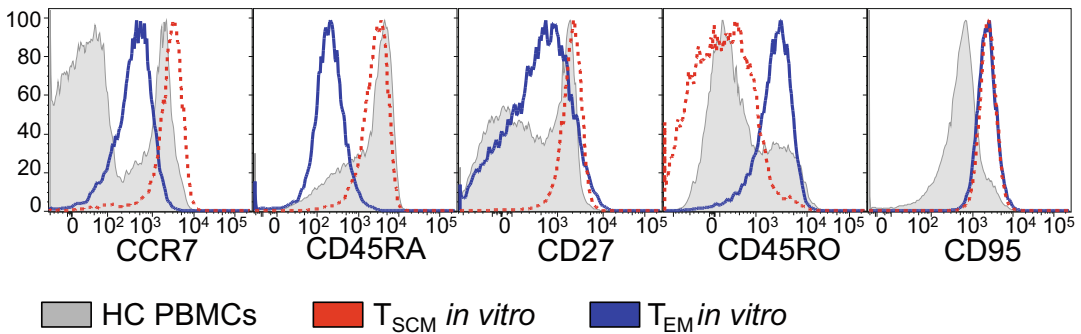


**Fig. 2** Phenotypic analysis of T<sub>N</sub>-derived T<sub>SCM</sub> and T<sub>EFF</sub> cells. The phenotype of *in vitro* generated T<sub>SCM</sub> and T<sub>EFF</sub> from sorted CD8<sup>+</sup> T<sub>N</sub> cells following 10 days of coculture is shown. As described in text, sorted CD8<sup>+</sup> T<sub>N</sub> cells were stimulated with αCD3/CD28 in the presence of IL-7 and IL-15 (T<sub>SCM</sub> conditions; red dotted line) or αCD3/CD2/CD28 in the presence of IL-2 and IL-12 (T<sub>EFF</sub> conditions; blue line). CD8<sup>+</sup> T cells gated from PBMCs of a healthy donor (filled grey histogram) are shown as a reference

27. At different time points after stimulation, collect 20 μL of cell suspension and monitor cell growth by cell counting. Split cell culture when medium turns yellow and add fresh medium containing cytokines only. Cells can be moved to 24- or 6-well plates. Keep a cell density of 50,000 cells/200 μL (see **Note 11**).
28. After the incubation period, collect cells and determine T cell phenotype as described in **steps 10–19**. As low as 50,000 cells can be used for this purpose. T<sub>N</sub> cells cultured in T<sub>SCM</sub> conditions should maintain original phenotype (CD45RO<sup>-</sup>CCR7<sup>+</sup>CD27<sup>+</sup>) but have acquired CD95 expression, while those cultured in T<sub>EFF</sub> conditions should have differentiated into a CD45RO<sup>-</sup>CCR7<sup>-</sup>CD27<sup>+/-</sup>CD95<sup>+</sup> phenotype (Fig. 2).

## 4 Notes

1. Obtain peripheral blood by venipuncture or collect buffy coats from the hospital transfusion department. Make sure you have all necessary authorizations such as internal revenue board (IRB) approvals and signed informed consent for conducting experiments with human cells. Human blood should always be considered potentially infected and therefore treated under appropriate BSL-2 safety precautions.
2. The amount of blood or PBMC to be used in the experiment should be calculated according to the frequency of CD8<sup>+</sup> T<sub>N</sub> cells that are needed. Consider that young individuals tend to harbor higher frequencies of these cells compared to old donors. Additionally, the number of CD8<sup>+</sup> T<sub>N</sub> cells to be sorted should be calculated according to the number of T<sub>SCM</sub> or T<sub>EFF</sub> cells that

are needed at the end of the culture period. Our data indicate that  $T_N$ -derived  $T_{SCM}$  grow as much as 68.5-fold (median) after a 10-day stimulation period, while  $T_{eff}$  up to 138.43.

3. Notably, fold expansion may be donor dependent. Different experiments may require different cell numbers, e.g., FACS analysis can be performed with as low as 50,000 cells, while other techniques may require much higher numbers.
4. Multiple commercially available kits can be used for  $CD8^+$  T cell enrichment such as those from Miltenyi Biotec or from STEMCELL Technologies. We suggest using negative selection kits so to obtain untouched  $CD8^+$  T cells.
5. Washing in medium without serum at this step is preferred as the serum tends to sequester the dead cell discriminator dyes.
6. As a general rule, we use 100  $\mu$ L of dead cell discriminator solution or antibody solutions to stain up to  $10^7$  cells. If more cells are needed to be stained, cells are resuspended in larger volumes bearing 2–3 times the concentration of the dye/antibody. Before proceeding with the experiment, titration experiments should always be performed in order to determine the optimal amount of reagent that is needed in solution to saturate the target molecule. For more details on such procedures, refer to the published literature [9].
7. Some antibodies, such as those detecting chemokine receptor expression, give increased fluorescence when incubated at 37 °C instead of RT. Indeed, incubation at 37 °C favors receptor recirculation through the plasma membrane, allowing more receptors to be expressed on the cell surface [10].
8. Miltenyi Biotec T cell activation/expansion kit implies the use of three different anti-human antibodies, i.e., CD3, CD2, and CD28. CD2 has to be removed to generate naïve-derived  $T_{SCM}$  cells. Add PBS<sup>-/-</sup> to compensate for the lack of anti-CD2 antibody in solution. Beads are prepared in 2 h. Plan experiments accordingly.
9. We optimized the protocol by incubating  $CD8^+$   $T_N$  cells with cytokines provided by Peprotech at a final concentration of 10 ng/mL. However, we noticed that the same cytokines from different companies may have differential activity at the same concentration. Therefore, the protocol should be optimized according to the type of cytokines that are being used in the laboratory.
10. It is not necessary to include an unstimulated control. Consider that  $CD8^+$   $T_N$  cells die rapidly in culture in the absence of external stimuli such as TCR stimulation or cytokines.
11. We noted excellent cell growth by providing cytokines only in the absence of additional bead-based TCR stimulation (E.L., personal communication). In certain cases, proliferation may not occur following stimulation. We suggest to prepare a new batch of antibody-coated beads, as they may lose activity over time.

## Acknowledgments

The authors wish to thank the members of the Laboratory of Translational Immunology for critical discussion. This work was supported by grants from the Fondazione Cariplo (Grant Ricerca Biomedica 2012/0683), the Italian Ministry of Health (Bando Giovani Ricercatori GR-2011-02347324) and the European Union Marie Curie Career Integration Grant 322093 (all to E.L.). E.L. is an International Society for the Advancement of Cytometry (ISAC) Marylou Ingram scholar. V.Z. is a student of the PhD program at the University of Milan, Italy.

## References

1. Kaech SM, Cui W (2012) Transcriptional control of effector and memory CD8+ T cell differentiation. *Nat Rev Immunol* 12(11):749–761. doi:[10.1038/nri3307](https://doi.org/10.1038/nri3307)
2. Man K, Kallies A (2015) Synchronizing transcriptional control of T cell metabolism and function. *Nat Rev Immunol* 15(9):574–584. doi:[10.1038/nri3874](https://doi.org/10.1038/nri3874)
3. Pilipow K, Roberto A, Roederer M et al (2015) IL15 and T-cell stemness in T-cell-based cancer immunotherapy. *Cancer Res.* doi:[10.1158/0008-5472.CAN-15-1498](https://doi.org/10.1158/0008-5472.CAN-15-1498)
4. Gattinoni L, Lugli E, Ji Y et al (2011) A human memory T cell subset with stem cell-like properties. *Nat Med* 17(10):1290–1297, doi:nm.2446 [pii] [10.1038/nm.2446](https://doi.org/10.1038/nm.2446)
5. Lugli E, Dominguez MH, Gattinoni L et al (2013) Superior T memory stem cell persistence supports long-lived T cell memory. *J Clin Invest* 123(2):594–599. doi:[10.1172/JCI66327](https://doi.org/10.1172/JCI66327)
6. Mahnke YD, Brodie TM, Sallusto F, Roederer M, Lugli E (2013) The who's who of T-cell differentiation: human memory T-cell subsets. *Eur J Immunol* 43(11):2797–2809. doi:[10.1002/eji.201343751](https://doi.org/10.1002/eji.201343751)
7. Lugli E, Gattinoni L, Roberto A et al (2013) Identification, isolation and in vitro expansion of human and nonhuman primate T stem cell memory cells. *Nat Protoc* 8(1):33–42. doi:[10.1038/nprot.2012.143](https://doi.org/10.1038/nprot.2012.143)
8. Cieri N, Camisa B, Cocchiarella F et al (2013) IL-7 and IL-15 instruct the generation of human memory stem T cells from naive precursors. *Blood* 121(4):573–584. doi:[10.1182/blood-2012-05-431718](https://doi.org/10.1182/blood-2012-05-431718)
9. Kantor A, Roederer M (1997) FACS analysis of lymphocytes. In: Herzenberg LA, Weir DM, Blackwell C (eds) *Handbook of experimental immunology*, vol 2, 5th edn. Blackwell Science, Cambridge
10. Berhanu D, Mortari F, De Rosa SC, Roederer M (2003) Optimized lymphocyte isolation methods for analysis of chemokine receptor expression. *J Immunol Methods* 279(1–2):199–207, doi:S0022175903001868 [pii]

## Gammaretroviral Production and T Cell Transduction to Genetically Retarget Primary T Cells Against Cancer

Gongbo Li, Kyungho Park, and Marco L. Davila

### Abstract

Adoptive T cell therapy has demonstrated tremendous outcomes against treatment-refractory leukemias and solid tumor malignancies. As opposed to industry-developed drugs that are manufactured and dispensed to hospitals and/or patients, T cells are produced in academic laboratories for clinical research and are a highly personalized therapy that represents a “living drug.” The technology behind genetic modification of primary T cells has been developed and refined by a few academic medical centers. We anticipate that the exciting results generated by these efforts will lead to further investigation by other academic and industry institutions. To facilitate this adaptation we present optimized protocols for gammaretroviral production, T cell isolation, and genetic modification to create gene-targeted T cells.

**Key words** T cell, Chimeric antigen receptor, Retroviral vector transduction, Immunotherapy, Adoptive cell therapy

---

### 1 Introduction

The past several years have generated excitement about manipulating the immune system to treat cancer. Tremendous responses have been reported in patients with chemotherapy-refractory cancer after using immunotherapies such as checkpoint-blockade inhibitors, bi-specific T cell engagers, and adoptive T cell therapy [1–4]. Checkpoint-blockade inhibitors and bi-specific T cell engagers activate and redirect tumor-specific T cells in the patient, while adoptive T cell transfer requires isolation of T cells followed by ex vivo manipulation to create a large population of activated, tumor-specific T cells for infusion back into the patient [5, 6]. Therefore, adoptively transferred T cells are a personalized and living drug created in the laboratory.

The two main forms of adoptive T cell transfer use either tumor-infiltrating lymphocytes (TILs) or chimeric antigen receptor (CAR) T cells. TILs are isolated from surgically excised tumor samples and because tumor-specificity is already encoded by their

T cell receptor (TCR) much of the *ex vivo* manipulation is directed towards expanding the small number of TILs to a sufficiently large number for infusion [5]. This process can take several weeks to a few months. In contrast to the endogenous TCR, CARs are synthetic receptors, part antibody and part TCR [7]. The antigen-binding domain of a tumor-specific antibody is joined to a transmembrane domain and signaling moieties associated with the TCR. Therefore, a CAR T cell is genetically targeted against a new tumor antigen and binding of this antigen initiates signaling through the TCR signaling moieties and mediates T cell activation and tumor killing. A bulk population of T cells genetically modified to express a CAR creates a large population of tumor-reactive T cells within a short period of time. In fact, clinical trials have reported CAR T cells can be produced in as short as 1 week [1, 8]. Most commonly the gene-transfer technology relies on robust protocols of gammaretroviral production and T cell transduction that has been continually optimized and refined [8–11]. From these efforts we present protocols for gammaretroviral production and transduction for the laboratory and/or clinical research of tumor-reactive CAR T cells. The laboratory evaluation of CAR T cells involves the adoptive transfer of mouse or human CAR T cells into, respectively, immune competent or immune deficient mice. Therefore, we describe methods for isolating T cells from mouse spleens, an easily accessed reservoir of abundant T cells, or human blood. While these protocols for T cell isolation are understandably different, the methods for transduction of T cells, whether from mouse or human origins, are largely the same. We therefore present a single protocol of T cell transduction with notes highlighting reagents that differ when using T cells of mouse or human origin. Finally, we present a useful method to estimate the gene transfer of any CAR, regardless of specificity, that is based on the binding of L protein to immunoglobulin light chains [12].

---

## 2 Materials

1. musRPMI: RPMI 1640 medium, 10% fetal bovine serum (FBS), 100 IU/mL of penicillin, 100 µg/mL of streptomycin, 1× nonessential amino acids, 1 µM sodium pyruvate, 10 mM HEPES, 2.5 µM β-mercaptoethanol, and 2 mM L-glutamine.
2. humRPMI: RPMI 1640 medium, 10% FBS, 100 IU/mL of penicillin, 100 µg/mL of streptomycin, and 2 mM L-glutamine.
3. cDMEM: DMEM, 10% FBS, 100 IU/mL of penicillin, 100 µg/mL of streptomycin, and 2 mM L-glutamine.
4. PBS–BSA: PBS, 0.5% bovine serum albumin.

5. 2× HEPES-buffered saline (HBS): 140 mM NaCl, 1.5 mM Na<sub>2</sub>HPO<sub>4</sub>, 50 mM HEPES, pH 7.05.
6. 70% ethanol: 70 mL Ethanol, 30 mL distilled and deionized water.
7. Magnet: we use the EasySep™ Magnet, but others are suitable.
8. 2 M CaCl<sub>2</sub>: 29.4 g of CaCl<sub>2</sub>, 100 mL of deionized water. Filter-sterilize and store in 1 mL aliquots at -20 °C.

---

### 3 Methods

#### 3.1 *Gammaretrovirus Production (See Note 1)*

1. Label a tube “A” adding 18 μL of 2 M CaCl<sub>2</sub>, 10 μg of DNA, and adjust volume to 150 μL with sterile H<sub>2</sub>O.
2. Label a tube “B” adding 150 μL of 2× HEPES buffered saline.
3. Using a 200 μL pipet tip, slowly add solution “A” dropwise to solution “B” while vortexing. Continue until solution “A” is depleted. This is a slow process which should be done over 1–2 min.
4. Incubate the CaPO<sub>4</sub>-DNA precipitate at room temperature for 30 min.
5. Remove the media from a plate of producers (e.g., H29, Phoenix, or RD114) that are approximately 40% confluent in a 60 mm dish.
6. Add 4 mL fresh cDMEM media (*see Note 2*).
7. Add the CaPO<sub>4</sub>-DNA precipitate dropwise to the media in the dish (*see Note 3*).
8. Incubate the cells overnight at 37 °C (5% CO<sub>2</sub>).
9. Change the media daily and collect media at 4, 5 and 6 days after transfection. Filter the viral supernatant with a 0.45 μm syringe filter and store at -80 °C until use (*see Note 4*).

#### 3.2 *T Cell Isolation (Day 1)*

##### 3.2.1 *Mouse T Cell Isolation by Antibody-Mediated Negative Selection (See Note 5)*

1. Sacrifice mice, saturate with 70% ethanol and collect spleens through a small horizontal incision directly below the left lateral rib cage. Store spleens in PBS-BSA (*see Note 6*).
2. Place the spleen onto a 40 μM cell strainer that has been rinsed with PBS-BSA and placed onto a 50 mL conical tube loaded with 10 mL PBS/BSA. Using the plunger end of a 5 mL syringe, gently push the spleen through the strainer into the 50 mL tube. Rinse the cell strainer with 30 mL of PBS-BSA to ensure all spleen cells pass through the strainer into the conical tube.
3. Spin cells at 500 × *g* for 10 min, discard supernatant, and resuspend pellet in 40 mL of PBS-BSA. Repeat centrifuge and wash once.

4. Count cells and prepare cell suspension at a concentration of  $1 \times 10^8$  cells/mL in PBS–BSA.
5. Add normal rat serum using the EasySep™ Mouse T-cell Isolation Kit (StemCell Technologies), both at 50  $\mu$ L per mL of cells of splenocytes.
6. Mix well and incubate at room temperature for 10 min.
7. Vortex EasySep™ Streptavidin RapidSpheres™ for 30 s and add to the antibody–splenocyte mixture at 75  $\mu$ L per mL of splenocytes.
8. Mix well and incubate at room temperature for 2.5 min.
9. Add PBS–BSA to the splenocyte suspension to a total volume of 2.5 mL and mix by gently pipetting up and down.
10. Place the tube into a magnet and set aside at room temperature for 2.5 min.
11. Pick up the magnet, invert, and pour off desired, unbound T cell fraction into a new tube.
12. Spin T cells at  $500 \times g$  for 10 min, discard supernatant, and resuspend pellet in PBS–BSA (*see Note 7*).

**3.2.2 Isolation of Human Peripheral Blood Mononuclear Cells (PBMC)**  
(*See Note 8*)

1. Dilute blood 1:1 with PBS in a 50 mL conical tube.
2. For each 50 mL tube, carefully overlay 20 mL Ficoll-Paque® PLUS Medium (GE Healthcare) with 20 mL of diluted blood.
3. Centrifuge at  $900 \times g$  for 30 min at room temperature in a swinging bucket rotor without brake.
4. Carefully transfer the mononuclear cell layer to a new 50 mL tube.
5. Fill the tube with PBS, mix and centrifuge at  $900 \times g$  for 15 min at room temperature.
6. Resuspend the cell pellet in 50 mL of PBS and centrifuge at  $900 \times g$  for 15 min at room temperature. Carefully remove the supernatant completely.
7. Resuspend the cell pellet in 50 mL of PBS and centrifuge at  $500 \times g$  for 10 min at room temperature. Carefully remove the supernatant completely.
8. Resuspend cell pellet in PBS and centrifuge T cells at  $500 \times g$  for 10 min at room temperature and resuspend PBMCs in PBS (*see Note 9*).

**3.3 T Cell Activation and Transduction**

**3.3.1 T Cell Activation**  
(*Day 1*)

1. Wash anti-CD3/anti-CD28 isolation and activation beads (Life Technologies, Oslo, Norway) before use by vortexing for 30 s and mixing an appropriate volume of beads (25  $\mu$ L/million T cells) with an equal volume (or at least 1 mL) of PBS–BSA.
2. Place the tube on a magnet for 1 min and discard the supernatant and resuspend the beads with PBS–BSA in original volume.

3. Count isolated cells and centrifuge for 5–10 min at  $400\times g$ . During centrifugation, mix the following components: Mus or HumRPMI (1 mL for 1–2 million T cells), IL-2 (final concentration 30 IU/mL) (*see Note 10*), pre-washed beads (25 $\mu$ L/million T cells).
4. After centrifugation remove supernatant and resuspend T cells with media, IL-2, and activation beads. Distribute the T cells in non-tissue culture treated 6-well plates at 2–5 mL/well.
5. Incubate in a tissue culture incubator at 37 °C (5% CO<sub>2</sub>).
6. Prepare non-tissue culture treated plates by adding RetroNectin™ (1  $\mu$ g/ $\mu$ L) (Takara Bio, Otsu, Japan) to enhance transduction efficiency. Add 90  $\mu$ L of RetroNectin™ with 6 mL PBS. Dispense 1 mL/well of RetroNectin/PBS into non-tissue culture treated plates. Store the plates overnight at 4 °C (*see Note 11*).

### 3.3.2 Transduction #1 (Day 2)

1. The next day, remove RetroNectin/PBS and block with PBS–BSA for 30 min at room temperature.
2. Remove blocking buffer and wash plates one time with PBS.
3. Harvest and centrifuge activated T cells at  $400\times g$  for 10 min.
4. Resuspend cells with mus or humRPMI at 3 million cells/mL and 80 IU/mL of IL-2 (*see Note 12*).
5. Distribute 1 mL of cell suspension to each well, followed by 1 mL of gammaretrovirus to each well.
6. Spin plates at  $2000\times g$  for 1 h at room temperature.
7. Incubate plates in a tissue culture incubator at 37 °C (5% CO<sub>2</sub>).

### 3.3.3 Transduction #2 (Day 3)

1. Tilt plates and carefully remove 850  $\mu$ L of media from each well (*see Note 13*).
2. Add 1 mL of virus to each well.
3. Spin plates at  $2000\times g$  for 1 h at room temperature.
4. Incubate in a tissue culture incubator at 37 °C (5% CO<sub>2</sub>).

### 3.3.4 Expansion (Day 4+)

1. Add 3 mL of mus or humRPMI with 30 IU/mL of IL-2 (*see Note 14*).
2. Incubate in a tissue culture incubator at 37 °C (5% CO<sub>2</sub>).
3. T cells can be expanded up to Day 7 without further activation, but should be expanded in larger culture volumes if media becomes yellow or concentration is more than 2 million T cells per mL (*see Note 15*).
4. Remove activation beads from T cells before analysis or experimental use by pipetting T cells in a conical tube and exposing the tube to a magnet for 2 min. Unbound T cells can be decanted from the tube exposed to the magnet.

### 3.4 Measuring Gene Transfer Efficiency (See Note 16)

Gene transfer efficiency can be measured by detection of binding of protein L to Immunoglobulin Light-chain (see Note 17)

1. Harvest transduced T cells and wash with PBS.
2. Prepare T cell suspension at a concentration of  $1 \times 10^6$  cells in PBS-BSA.
3. Add 1  $\mu\text{g}$  of reconstituted biotinylated protein L (Pierce Biotechnology, Rockford, IL, USA) per  $1 \times 10^6$  T cells and incubate at room temperature for 20 min.
4. Wash the cells with PBS and resuspend with 100  $\mu\text{L}$  PBS/BSA.
5. Add 60 ng of streptavidin PE per transduction sample and incubate at room temperature for 20 min.
6. Wash the cells with PBS and resuspend with 500  $\mu\text{L}$  of PBS/BSA and analyze transduction efficiency by flow cytometry.

---

## 4 Notes

1. This is a protocol for transient production of gammaretrovirus, which means that gammaretrovirus can be collected for only a few days. If large quantities of gammaretrovirus, with similar titers, are required then we recommend preparation of stable producers. This would involve calcium phosphate transfection of the gammaretroviral construct into a cell line that produces amphotrophic virus, such as H29. Then the collected gammaretrovirus would be used to transduce a cell line that produces ecotropic virus, such as Phoenix-E. This stable producer cell line can be cryopreserved and thawed when further virus collection is desired.
2. The producer cells must be transfected (or transduced) during log-growth phase to enhance gene-transfer. If the producer cells overgrow and stop proliferating then they should be split down and passaged through a couple of expansions before attempting transfection or transduction.
3. With the use of an inverted microscope, small, fine, and granular  $\text{CaPO}_4$ /DNA precipitates should be visible in the media. Large clumps are less effective at transfection and often times are due to a sub-optimal pH of the HBS buffer.
4. Viral titers can be estimated by transduction of a test cell line. As an example, if to assess the viral titer of a gammaretrovirus that has been prepared from an ecotropic producer that will infect only mouse cells, we use mouse NIH/3T3 cells as the test cell line. In 6-well plates we will incubate  $1 \times 10^5$  NIH/3T3 cells per well. We then prepare increasing amounts of virus with 0, 3, 10, 30, 100, and 300  $\mu\text{L}$  virus diluted to a final volume of 1 mL with cDMEM media and add 10  $\mu\text{L}$  of polybrene

(800  $\mu\text{g}/\text{mL}$ ) in each tube. Remove cultured media and add diluted virus into each well. Next day, remove supernatant and add 3 mL of cDMEM media. On the third day, remove cultured media from each well and wash cells with PBS and trypsinize cells. Centrifuge cells at  $500\times g$  for 5 min and discard supernatant. We then resuspend the cells in PBS and estimate gene-transfer by flow cytometry. The infectious units per mL (IU/mL) can be calculated as  $(1\times 10^5\times \text{percentage of CAR}^+ \text{ cells}\times 1000)/\mu\text{L}$  of virus. Adequate titer levels can vary based on the packaging cell line.

5. An alternative rapid and inexpensive system for mouse T cell enrichment is with nylon wool columns [11], which results in a T cell product that is generally less pure compared to antibody-mediated enrichment (70% vs. >95%). However, the contaminating splenocytes do not expand with CD3/CD28 bead activation and supplemental IL-2 so the purity is relatively similar at the end of the 5–7 day culture period.
6. After spleen isolation, all steps are performed on ice and under sterile-conditions unless otherwise noted.
7. For C57BL/6 mice this isolation generally results in about 12–15 million T cells per spleen.
8. All these steps for human PBMC isolation occur at room temperature.
9. Human PBMCs can be efficiently activated and transduced with gammaretrovirus without further enrichment. In contrast, mice T cell splenocyte gene-transfer efficiency is reduced if T cells are not enriched before transduction [11].
10. Human IL-2 can be used for both mouse and human T cells.
11. Retronectin coated plates can also be prepared on day of transduction, but require incubation at room temperature for 2 h, followed by blocking with PBS–BSA for 30 min, and washing one time with PBS before same-day use.
12. Counting of the cells at this timepoint and up to Day 5 of activation is unreliable because the CD3/CD28 activation beads bind the T cells tightly and result in undercounting. Therefore, activate T cells based on the previous day counts.
13. Do not disturb cells at the bottom to prevent loss with aspiration.
14. This step can also be done at day 3 after the second transduction and then cells will be ready for downstream experiments as early as day 4.
15. For expansion past 7 days T cells will need either antigen-specific or nonspecific stimulation (CD3/CD28 beads). Stimulation can be required as frequent as weekly to support

expansion. Human T cells are much easier to expand for several cycles, while mouse T cells have poor viability that limits multiple expansions with CD3/CD28 beads and IL-2.

16. CAR gene-transfer efficiency is routinely estimated by flow cytometry or RT-PCR. Using healthy-donor human T cells or mouse T cells and following these protocols should result in gene-transfer levels ranging from 30 to 70%.
17. Protein L binds to the light chain of the scFv portion of the CAR.

## References

1. Davila ML, Riviere I, Wang X et al (2014) Efficacy and toxicity management of 19-28z CAR T cell therapy in B cell acute lymphoblastic leukemia. *Sci Transl Med* 6:224ra225. doi:[10.1126/scitranslmed.3008226](https://doi.org/10.1126/scitranslmed.3008226)
2. Stevanovic S, Draper LM, Langhan MM et al (2015) Complete regression of metastatic cervical cancer after treatment with human papillomavirus-targeted tumor-infiltrating T cells. *J Clin Oncol* 33(14):1543–1550. doi:[10.1200/JCO.2014.58.9093](https://doi.org/10.1200/JCO.2014.58.9093)
3. Hodi FS, O'Day SJ, McDermott DF et al (2010) Improved survival with ipilimumab in patients with metastatic melanoma. *N Engl J Med* 363(8):711–723. doi:[10.1056/NEJMoa1003466](https://doi.org/10.1056/NEJMoa1003466)
4. Topp MS, Gokbuget N, Zugmaier G et al (2014) Phase II trial of the anti-CD19 bispecific T cell-engager blinatumomab shows hematologic and molecular remissions in patients with relapsed or refractory b-precursor acute lymphoblastic leukemia. *J Clin Oncol* 32(36):4134–4140. doi:[10.1200/JCO.2014.56.3247](https://doi.org/10.1200/JCO.2014.56.3247)
5. Restifo NP, Dudley ME, Rosenberg SA (2012) Adoptive immunotherapy for cancer: harnessing the T cell response. *Nat Rev Immunol* 12(4):269–281. doi:[10.1038/nri3191](https://doi.org/10.1038/nri3191)
6. Sadelain M, Riviere I, Brentjens R (2003) Targeting tumours with genetically enhanced T lymphocytes. *Nat Rev Cancer* 3(1):35–45. doi:[10.1038/nrc971](https://doi.org/10.1038/nrc971)
7. Davila ML, Brentjens R, Wang X et al (2012) How do CARs work?: Early insights from recent clinical studies targeting CD19. *Oncoimmunology* 1(9):1577–1583. doi:[10.4161/onci.22524](https://doi.org/10.4161/onci.22524)
8. Lee DW, Kochenderfer JN, Stetler-Stevenson M et al (2014) T cells expressing CD19 chimeric antigen receptors for acute lymphoblastic leukaemia in children and young adults: a phase 1 dose-escalation trial. *Lancet*. doi:[10.1016/S0140-6736\(14\)61403-3](https://doi.org/10.1016/S0140-6736(14)61403-3)
9. Hollyman D, Stefanski J, Przybylowski M et al (2009) Manufacturing validation of biologically functional T cells targeted to CD19 antigen for autologous adoptive cell therapy. *J Immunother* 32(2):169–180. doi:[10.1097/CJI.0b013e318194a6e8](https://doi.org/10.1097/CJI.0b013e318194a6e8)
10. Kochenderfer JN, Feldman SA, Zhao Y et al (2009) Construction and preclinical evaluation of an anti-CD19 chimeric antigen receptor. *J Immunother* 32(7):689–702. doi:[10.1097/CJI.0b013e3181ac6138](https://doi.org/10.1097/CJI.0b013e3181ac6138)
11. Lee J, Sadelain M, Brentjens R (2009) Retroviral transduction of murine primary T lymphocytes. *Methods Mol Biol* 506:83–96. doi:[10.1007/978-1-59745-409-4\\_7](https://doi.org/10.1007/978-1-59745-409-4_7)
12. Zheng Z, Chinnasamy N, Morgan RA (2012) Protein L: a novel reagent for the detection of chimeric antigen receptor (CAR) expression by flow cytometry. *J Transl Med* 10:29. doi:[10.1186/1479-5876-10-29](https://doi.org/10.1186/1479-5876-10-29)

## Measuring Telomerase Activity in Senescent Human T Cells Upon Genetic Modification

Alessio Lanna

### Abstract

Telomerase, a RNA-dependent DNA polymerase that adds telomeric DNA at the 3' ends of eukaryotic chromosomes, is essential for the lifelong preservation of the proliferative potential of antigen specific T lymphocytes. However, senescent T cells that have low telomerase activity, short telomeres and lack of replicative capacity accumulate in old humans, patients with chronic viral infections and cancer. The mechanisms inhibiting telomerase in these cells are poorly understood. Here I describe a strategy that was successfully applied to identify pathways causing telomerase dysfunction in primary human senescent T lymphocytes. Such strategy couples lentiviral vector-based gene manipulations to functional and signaling readouts directly *ex vivo*, in humans.

**Key words** T cells, Telomerase, Senescence, Intra-sensory signaling, AMP-responsive-protein kinase

---

### 1 Introduction

The ends of the eukaryotic chromosomes are characterized by repeated hexameric sequences of GT-rich nucleotides known as telomeres that provide genomic protection and stability [1]. Functional telomeres require minimal telomere length (above 4-kilo bases (kb)), an intact G-rich 3' DNA overhang and the interaction with specific telomere-binding proteins, the shelterin [2]. When telomeres become critically short after repeated cell divisions, senescent cells spontaneously activate DNA damage response (DDR) cascades and the replicative capacity ceases [3]. This can be delayed by the upregulation of the enzyme telomerase, a RNA-dependent DNA polymerase firstly identified in 1985 in the protozoan *Tetrahymena thermophila* [4]. The holoenzyme, which consists of a catalytic core (hTERT) and a RNA template (hTR or hTERC), acts by physically binding to and extending the G-rich 3' DNA overhang of the telomere (Fig. 1), to replenish the loss of genetic material that is due to the semiconservative mechanism of DNA replication [5]. Hayflick was the first to identify the

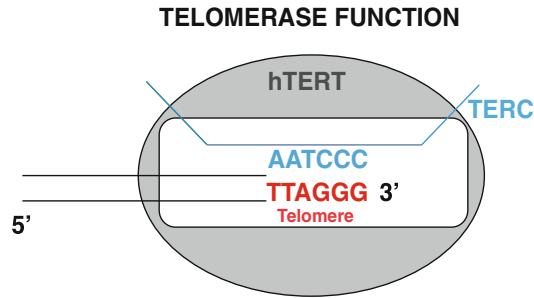


**Fig. 1** Telomerase function. The telomere–telomerase complex is shown. Telomerase is a RNA dependent DNA polymerase that extends telomeric DNA at each cell division, preventing telomere shortening. Telomerase function requires both a catalytic subunit (hTERT) and a RNA component (TERC) that directly binds to the single strand 3′ overhangs at the end of eukaryotic chromosomes. Details of telomerase function are provided in the text

existence of a limit, imposed by mechanisms of telomere erosion, to the extent at which mammalian cells can proliferate (Hayflick limit) [6]. This dictates that adult somatic cells in which telomerase activity is generally very low or undetectable, reach replicative senescence after about 50 cell passages in vitro [6]. Unlike most adult somatic cells, human T lymphocytes are able to reactivate telomerase upon antigenic challenges and this is essential for the lifelong preservation of their proliferative potential in vivo [7]. However after repeated episodes of activation, T cells progressively differentiate and lose the capacity to upregulate the enzyme telomerase, which leads to telomere erosion, loss of proliferative capacity, and ultimately telomere-dependent senescence. Conversely, elevated telomerase activity in cancer cells confers virtually unlimited proliferative potential [8]. Fine-molecular tuning of telomerase is therefore needed to control mammalian cell proliferation and ensure a balance between the delaying of cellular senescence and the risk of developing malignancy. Below, I briefly discuss the current understanding of the main mechanisms controlling telomerase expression, nuclear import, and activation.

The biological importance of telomerase is highlighted by the complexity of both transcriptional and posttranslational mechanisms tuning the expression of its catalytic subunit, hTERT [9]. The hTERT promoter is well characterized and comprises binding sites for both inhibitory and activatory transcription factors [10]. For instance, the transcription factor c-MYC binds to the hTERT promoter at regulatory sites known as “E-boxes,” hence inducing hTERT transcription [11]. This has been well documented in studies where elevated hTERT expression was directly induced by increased c-MYC activity, in cancer cells [10]. Between the E-boxes, the hTERT promoter possesses at least five distinct GC-rich DNA sequences (CpG islands) that are important for Sp1-mediated

hTERT upregulation. Similarly, the p65 subunit of the transcription factor NF- $\kappa$ B has been reported to upregulate hTERT expression [12]; however, the precise binding regulatory site has not been identified. Conversely, E2F1 is an inhibitor of hTERT transcription (four related binding sites have been identified) in which its action is coordinated by the histone deacetylase HDAC [13]. It is also well recognized that the tumor suppressor p53 inhibits hTERT expression, possibly preventing the binding of Sp1 to the hTERT promoter [14].

Although the transcriptional regulation of hTERT has been initially considered the sole regulatory mechanism, it has recently arisen that posttranslational mechanisms are also involved in telomerase regulation. In accordance with this, Liu and colleagues firstly reported the existence of notable differences between the levels of hTERT transcripts and telomerase activity in human lymphocytes [15]. In an extension of this work, the kinase AKT has been shown to phosphorylate hTERT (at 220-GARRRGGAS-229 and 817-AVRIRGKSYV-826 sites), a process required for its nuclear import and activity [16]. Indeed, defective AKT signaling is a molecular feature of human highly differentiated T cells that have low telomerase activity [17, 18]. In addition to AKT, hTERT also binds to mTOR; this interaction can be disrupted by PP2A activity, a tumor suppressor phosphatase that dephosphorylates AKT and possibly also hTERT [19]. More recently, reports on the existence of AKT-independent mechanisms in controlling telomerase activity in human highly differentiated T cells that in part involve spontaneous activation of p38 MAP kinase through an unknown mechanism [20, 21]. Intervention at the point of telomerase regulating pathways may be important to restore immune cell function during aging. We discovered that low nutrient and senescence signals converge to inhibit telomerase activity in T cells, a process triggered by the metabolic master regulator AMPK, mediated by the scaffold molecule TAB1 and exerted by the MAP kinase p38 (“Intra-sensory” pathway) [22]. Figure 2 depicts mechanisms of telomerase regulation in mammals. Below, I describe methodology successfully used to identify signaling pathways causing telomerase dysfunction in primary human senescent T cells. Thus, I herein illuminate the genetic manipulations and telomeric-repeat amplification protocols required to modulate replicative senescence in lymphocytes, with the potential to reverse it.

---

## 2 Materials

1. 1× Dulbecco’s Phosphate Buffered Saline solution (D-PBS).
2. Lymphoprep™ (Axis-Shield).
3. Magnetic Activated Cell Sorting buffer (MACS buffer, filtered and ready to use, Miltenyi Biotec).

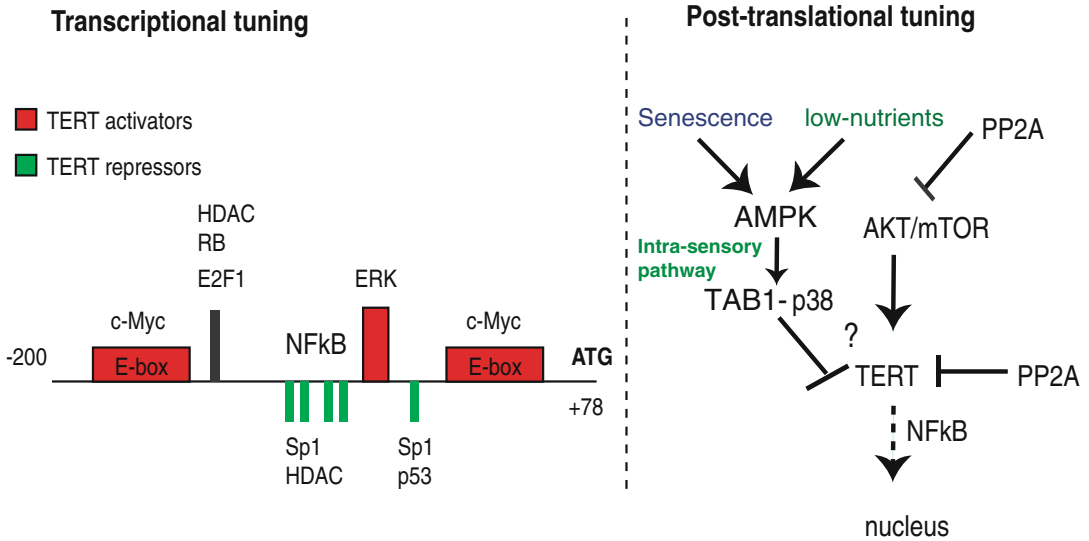


**Fig. 2** Molecular tuning of telomerase. An overview of both transcriptional (*left*) and posttranslational mechanisms (*right*) regulating the catalytic subunit of telomerase hTERT is shown. An extract (sites comprised between  $-200$  and  $+78$ ) of the telomerase catalytic subunit hTERT gene is reproduced, depicting the main transcriptional activators (c-MYC, Sp1, NFkB, and ERK) and repressors of hTERT expression (p53, E2F1, phosphorylated Rb and HDAC). Various regulatory elements have been identified within the hTERT promoter that directly or indirectly interacts with transcriptional regulators; the role of both E-box sites binding to c-MYC and Sp1-binding sites between the E-boxes is described in the text. NFkB promotes hTERT transcription but the precise binding on the hTERT promoter has not been identified. ATG in *bold* indicates gene hTERT start. The posttranslational tuning of telomerase is less well characterized; AKT can directly phosphorylate hTERT promoting its nuclear import; mTOR binds to hTERT and promotes its activity through an unknown mechanism; NFkB promotes hTERT nuclear import; PP2A inhibits telomerase activity by de-phosphorylating both AKT and hTERT. AMPK inhibits telomerase via TAB1-dependent p38 signaling, a process defined by the convergence of senescence and low nutrient deprivation signals in T cells (“Intra-Sensory” Pathway). The downstream signals regulating this pathway have not been identified

4. CD4<sup>+</sup> T cell Isolation kit (Miltenyi Biotec).
5. LS-magnetic separation columns (Miltenyi Biotec).
6. Anti-CD27 Microbeads (Miltenyi Biotec).
7. Anti-CD28 Microbead kit (Miltenyi Biotec).
8. Complete medium: RPMI 1640, 10% heat-inactivated FCS, 100 U/ml penicillin, 100 mg/ml streptomycin, 50  $\mu$ g/ml gentamicin, and 2 mM l-glutamine.
9. Anti-CD3 antibody ( $\alpha$ CD3, purified OKT3 clone; Sigma-Aldrich).
10. rh-IL2 (R&D Systems).
11. Fugene 6 (Promega).
12. shRNA-expressing lentiviral systems (either commercial or designed in-house).

13. TeloTAGGG Telomerase PCR ELISA (Roche).
14. CHAPS buffer: 10 mM Tris-HCl pH 7.5, 1 mM EGTA, 150 mM NaCl, 1 mM MgCl<sub>2</sub>, 0.25 mM sodium deoxycholate, 10% (v/v) glycerol, 5 mM β-mercaptoethanol, 1% (v/v) Nonidet P-40 (NP-40), 0.5% (w/v) 3-(3-chol-amidopropyl)-dimethylammonio-1-propanesulfonate (CHAPS), 0.1 mM [4-(2-aminoethyl)-benzene sulfonyl fluoride hydrochloride] (AEBSF).

---

### 3 Methods

1. Isolate Peripheral Blood Mononuclear Cells (PBMC) from the blood of healthy volunteers by using standard Ficoll gradient separation (*see Note 1*).
2. Isolate human CD4<sup>+</sup> (or CD8<sup>+</sup>) T cells from the PBMC preparation using “negative” selection kits and by following manufacturer’s instructions (Miltenyi Biotec; *see also Note 2*).
3. Isolate the CD27/CD28 related subsets of human CD4<sup>+</sup> (or CD8<sup>+</sup>) T cells by immune-magnetic separation (“positive” selection; Miltenyi Biotec). Importantly, the separation order will vary if working with either CD4<sup>+</sup> or CD8<sup>+</sup> T cells (*see Note 3*). This will result in the isolation of three separate populations of primary human T cells. Senescent T cells are CD27<sup>-</sup> CD28<sup>-</sup> lymphocytes within both the CD4<sup>+</sup> and CD8<sup>+</sup> memory pools (*see Note 4*).
4. Activate primary senescent human T cells by 0.5 μg/ml anti-CD3 antibody plus 10 ng/ml rh-IL2 (*see Note 5*) for 48 h in complete RPMI at 37 °C in a humidified 5% CO<sub>2</sub> incubator.
5. Transduce primary senescent human T cells using either commercial or in house-generated lentiviral particles [23]. For optimal transduction efficiency, a multiplicity of infection (MOI) of 10 should be used. The genetic manipulation should target those enzymatic activities which are endogenously deregulated in senescent T cells, as assessed by either phospho-flow or immunoblotting analysis.
6. Replace fresh complete medium with rh-IL2 every 2–3 days. For long term studies, transduced cells should be reactivated every 10 days as in **step 4**.
7. At 1 week after activation (96 h post-transduction), prepare lysates from 2 × 10<sup>5</sup> cells in 200 μl of CHAPS buffer.
8. Incubate extracts 30’ on ice, followed by ultracentrifugation at 13,000 rpm (26,451 × g) for 20’ at 4 °C. Cleared supernatants are then either stored at –80 °C (for non immediate use) or immediately used as described below.

**Table 1**  
**PCR settings used in TRAP assay (nonradioactive)**

	Time	Temperature	Cycles
Primer elongation	10–30'	25 °C	1
Telomerase inactivation	5'	94 °C	1
Amplification:	30"	94 °C	30
Denaturation	30"	50 °C 72 °C	
Annealing	90"		
Polymerization			

9. Measure telomerase activity using the nonradioactive TeloTAGGG telomerase ELISA kit (Roche), using  $2 \times 10^3$  cells. Mix the cell extracts in 25  $\mu\text{l}$  of ready-to use PCR Reaction mixture (provided with the kit), then add sterile water up to 50  $\mu\text{l}$  final volume.
10. Transfer tubes to a thermal cycler to perform combined primer elongation/amplification PCR reactions by the following protocol (Table 1):
11. Add 5  $\mu\text{l}$  of the amplification product to 20  $\mu\text{l}$  of kit-provided denaturation reagent, then incubate for 10' at 20 °C.
12. Hybridize the so-denatured biotinylated telomere-amplicons to digoxigenin (DIG)-labeled, telomeric repeat-specific detection probes by adding 225  $\mu\text{l}$  of Hybridization Buffer the transfer 100  $\mu\text{l}$  of this reaction mixture to streptavidin coated micro-plates (both provided with the kit).
13. Allow biotin-streptavidin binding for 2 h on a micro-plate shaker at 37 °C.
14. Wash micro-plates three times by adding 250  $\mu\text{l}$  of 1 $\times$ -washing solution (provided with the kit) per well. Remove washing solution.
15. Detect abundance of DIG-labeled telomere-amplicons bound to micro-plates by adding 100  $\mu\text{l}$  of anti digoxigenin-antibody conjugated to peroxidase, followed by micro-plate shaking for 30' at 20 °C.
16. Rinse plates by washing five times with 250  $\mu\text{l}$  of 1 $\times$ -washing solution.
17. Allow colored-substrate development by adding 100  $\mu\text{l}$  of TMB substrate (provided with the kit) per well and incubating for 10–20'.
18. Terminate the reactions by adding 100  $\mu\text{l}$  stop solution (provided with the kit) per well and read on an ELISA reader as absorbance emission at 450 nM.

---

## 4 Notes

1. Senescent T cells accumulate during aging or in disease (cancer, chronic viral infections, or autoimmune disorders) but are also present in peripheral blood of healthy, young volunteers (between 1 and 20% of the total T cell compartment). We obtained similar results when studying senescent T cells isolated from either young or old donors.
2. For endogenous signaling studies directly *ex vivo*, cells should not be resuspended in full-medium at any time to avoid unspecific stimulation caused by the serum or other compounds.
3. CD4<sup>+</sup> T cells first lose expression of CD27 followed by that of CD28 receptors, unlike CD8<sup>+</sup> T cells in which the opposite is true. This has to be considered when isolating subsets of senescent human T cells in either cell compartment. The reason for this opposite differentiation program is not known.
4. Interrogate endogenous signaling pathways directly *ex vivo*, without activation. Senescent human T cells exhibit a plethora of signaling abnormalities *in vivo* which can be manifested by studying signal transduction directly *ex vivo* by either Western Blotting or phospho-flow analysis.
5. Upon transduction, fresh medium with new rh-IL2 should be replaced every 2 days.

---

## Acknowledgments

I thank Profs Arne Akbar and Mala Maini for mentorship. I serve as Sir Henry Wellcome Trust Fellow under the sponsorship of Prof. Michael L Dustin (University of Oxford).

## References

1. Blackburn EH (2000) The end of the (DNA) line. *Nat Struct Biol* 7(10):847–850. doi:[10.1038/79594](https://doi.org/10.1038/79594)
2. Blasco MA (2005) Telomeres and human disease: ageing, cancer and beyond. *Nat Rev Genet* 6(8):611–622. doi:[10.1038/nrg1656](https://doi.org/10.1038/nrg1656)
3. Campisi J, d’Adda di Fagagna F (2007) Cellular senescence: when bad things happen to good cells. *Nat Rev Mol Cell Biol* 8(9):729–740. doi:[10.1038/nrm2233](https://doi.org/10.1038/nrm2233)
4. Greider CW, Blackburn EH (1985) Identification of a specific telomere terminal transferase activity in *Tetrahymena* extracts. *Cell* 43(2 Pt 1):405–413
5. Verdun RE, Karlseder J (2007) Replication and protection of telomeres. *Nature* 447(7147):924–931. doi:[10.1038/nature05976](https://doi.org/10.1038/nature05976)
6. Hayflick L, Moorhead PS (1961) The serial cultivation of human diploid cell strains. *Exp Cell Res* 25:585–621
7. Hodes RJ, Hathcock KS, Weng NP (2002) Telomeres in T and B cells. *Nat Rev Immunol* 2(9):699–706. doi:[10.1038/nri890](https://doi.org/10.1038/nri890)
8. Cong YS, Wright WE, Shay JW (2002) Human telomerase and its regulation. *Microbiol Mol Biol Rev* 66(3):407–425
9. Tesmer VM, Ford LP, Holt SE et al (1999) Two inactive fragments of the integral RNA

- cooperate to assemble active telomerase with the human protein catalytic subunit (hTERT) in vitro. *Mol Cell Biol* 19(9):6207–6216
10. Kyo S, Takakura M, Fujiwara T, Inoue M (2008) Understanding and exploiting hTERT promoter regulation for diagnosis and treatment of human cancers. *Cancer Sci* 99(8):1528–1538. doi:[10.1111/j.1349-7006.2008.00878.x](https://doi.org/10.1111/j.1349-7006.2008.00878.x)
  11. DePinho RA, Schreiber-Agus N, Alt FW (1991) myc family oncogenes in the development of normal and neoplastic cells. *Adv Cancer Res* 57:1–46
  12. Akiyama M, Hideshima T, Hayashi T et al (2003) Nuclear factor-kappaB p65 mediates tumor necrosis factor alpha-induced nuclear translocation of telomerase reverse transcriptase protein. *Cancer Res* 63(1):18–21
  13. Crowe DL, Nguyen DC, Tsang KJ, Kyo S (2001) E2F-1 represses transcription of the human telomerase reverse transcriptase gene. *Nucleic Acids Res* 29(13):2789–2794
  14. Xu D, Wang Q, Gruber A et al (2000) Downregulation of telomerase reverse transcriptase mRNA expression by wild type p53 in human tumor cells. *Oncogene* 19(45):5123–5133. doi:[10.1038/sj.onc.1203890](https://doi.org/10.1038/sj.onc.1203890)
  15. Liu K, Hodes RJ, Weng N (2001) Cutting edge: telomerase activation in human T lymphocytes does not require increase in telomerase reverse transcriptase (hTERT) protein but is associated with hTERT phosphorylation and nuclear translocation. *J Immunol* 166(8):4826–4830
  16. Kang SS, Kwon T, Kwon DY, Do SI (1999) Akt protein kinase enhances human telomerase activity through phosphorylation of telomerase reverse transcriptase subunit. *J Biol Chem* 274(19):13085–13090
  17. Henson SM, Franzese O, Macaulay R et al (2009) KLRG1 signaling induces defective Akt (ser473) phosphorylation and proliferative dysfunction of highly differentiated CD8+ T cells. *Blood* 113(26):6619–6628. doi:[10.1182/blood-2009-01-199588](https://doi.org/10.1182/blood-2009-01-199588)
  18. Plunkett FJ, Franzese O, Finney HM et al (2007) The loss of telomerase activity in highly differentiated CD8+CD28-CD27- T cells is associated with decreased Akt (Ser473) phosphorylation. *J Immunol* 178(12):7710–7719
  19. Li H, Zhao LL, Funder JW, Liu JP (1997) Protein phosphatase 2A inhibits nuclear telomerase activity in human breast cancer cells. *J Biol Chem* 272(27):16729–16732
  20. Di Mitri D, Azevedo RI, Henson SM et al (2011) Reversible senescence in human CD4+CD45RA+CD27- memory T cells. *J Immunol* 187(5):2093–2100. doi:[10.4049/jimmunol.1100978](https://doi.org/10.4049/jimmunol.1100978)
  21. Lanna A, Coutavas E, Levati L et al (2013) IFN-alpha inhibits telomerase in human CD8(+) T cells by both hTERT downregulation and induction of p38 MAPK signaling. *J Immunol* 191(7):3744–3752. doi:[10.4049/jimmunol.1301409](https://doi.org/10.4049/jimmunol.1301409)
  22. Lanna A, Henson SM, Escors D, Akbar AN (2014) The kinase p38 activated by the metabolic regulator AMPK and scaffold TAB1 drives the senescence of human T cells. *Nat Immunol* 15(10):965–972. doi:[10.1038/ni.2981](https://doi.org/10.1038/ni.2981)
  23. Escors D, Lopes L, Lin R et al (2008) Targeting dendritic cell signaling to regulate the response to immunization. *Blood* 111(6):3050–3061. doi:[10.1182/blood-2007-11-122408](https://doi.org/10.1182/blood-2007-11-122408)

# Chapter 11

## Strategies for T Helper Cell Subset Differentiation from Naïve Precursors

Francesco Annunziato and Laura Maggi

### Abstract

In vitro strategies to obtain different T helper cell subsets from naïve precursors are usually characterized by anti-CD3 plus anti-CD28 monoclonal antibody stimulation of naïve CD4<sup>+</sup> T cells (derived from both peripheral blood or umbilical cord blood) in the presence of specific polarizing cytokines. In this chapter, we describe detailed protocols to obtain in vitro differentiation of human naïve CD4<sup>+</sup> T cells into Th1, Th2, or Th17 cells.

**Key words** CD4<sup>+</sup> naïve T cells, CD4<sup>+</sup>CD161<sup>+</sup> T cells, Th1, Th2, Th17

---

### 1 Introduction

Effector CD4<sup>+</sup> T cells can be divided into functionally distinct subsets on the basis of their cytokines production, their specific transcription factors expression and their role in the protection against exogenous offending agents. In detail, T helper type 1 (Th1) secrete interferon (IFN)- $\gamma$ , express the transcription factor T-box expressed in T cells (T-bet), and protect the host against intracellular infections; Th2 cells secrete interleukin (IL)-4, IL-5, and IL-13, express the transcription factor GATA-3, and mediate host defense against helminths; Th17 cells that selectively produce IL-17A, express the transcription factor retinoic acid orphan receptor (ROR) $\gamma$ C2, and are critical for the host defense against extracellular pathogens [1–4]. Moreover, a subset of human IL-17A-producing CD4<sup>+</sup> T cells was found to produce also IFN- $\gamma$  (Th17/Th1) and both Th17 and Th17/Th1 cells exhibited plasticity towards the Th1 profile when cultured in presence of IL-12 [4]. In vivo the differentiation of naïve CD4<sup>+</sup> T cells in different subsets of T helper effector cells is determined by their interaction with dendritic cells (DCs) in lymphoid organs, which induces naïve T cells activation via MHC/TCR stimulation and co-stimulation

molecules, and by cytokines which play a major role during early stages of the differentiation. In vitro strategies to obtain different T helper cell subsets from naïve precursors aim to recapitulate in vivo settings. In particular, naïve T cells are usually activated by anti-CD3 plus anti-CD28 monoclonal antibodies (mAbs) in the presence of cytokines that were shown to induce polarization of T cells towards the different effectors Th phenotypes.

As regards to in vitro differentiation of Th1 and Th2 cells from naïve CD4<sup>+</sup> T cells (derived either from peripheral blood (PB) or umbilical cord blood (UCB)), there is a great agreement in the scientific literature that the main cytokines involved are IL-12 [5, 6] and IL-4 [7, 8], respectively.

This is not the case for Th17 in vitro differentiation where the debate is still open: various experimental protocols exist, that differ either for the source of naïve CD4<sup>+</sup> T cells or for the cocktail of polarizing cytokines. These differences among different studies in humans were attributed to the difficulty to ensure a truly naïve T-cell population (in fact the CD4<sup>+</sup> T cell fraction define as “naïve” could contain low frequency of memory T cells producing effector cytokines [9, 10]) and to the culture media used, which in some cases contains Th cell-polarizing factors [11, 12]. In particular, the main experimental protocol that has been defined for the in vitro differentiation of PB naïve CD4<sup>+</sup> T cells into Th17 cells is based on anti-CD3 plus anti-CD28 mAbs stimulation in the presence of the polarizing cytokines IL-1 $\beta$ , IL-6, IL-23, and TGF- $\beta$ . In this case IL-17 producing cells observed after 1–2 weeks of in vitro culture could derive from proliferation/stimulation of “memory” or pre-committed CD4<sup>+</sup> T cells that are present in the initial cell population. Accordingly, experimental protocols involving highly pure naïve CD4<sup>+</sup> T cells failed to induce Th17 cell differentiation in vitro [13, 14]. Recently, Kastirr et al. [14] described a new in vitro experimental protocol, based on low-density culture of cells and prolonged (12 days) TCR stimulation in presence of polarizing cytokines, to obtain Th17 cells starting from highly purified PB naïve CD4<sup>+</sup> T cells.

In addition, it has been demonstrated that human memory Th17 cells are contained within the CD161<sup>+</sup> fraction of both circulating and tissue-infiltrating CD4<sup>+</sup> T cells, and originate from naïve CD4<sup>+</sup>CD161<sup>+</sup> precursors present in UCB and newborn thymus [13]. The UCB CD4<sup>+</sup>CD161<sup>+</sup> T cell fraction contain Th17 precursors that already express RORC2, IL-1R1, and IL23R, but are not able to produce IL-17 [13]. Moreover, it has been recently demonstrated that not all UCB CD4<sup>+</sup>CD161<sup>+</sup> cells are positive for RORC2 transcription factor, for this reason it is important to underline that Th17 cells derive from a subset of UCB CD4<sup>+</sup>CD161<sup>+</sup> cells but not from UCB CD4<sup>+</sup>CD161<sup>-</sup> fraction [15]. The in vitro differentiation of CD4<sup>+</sup>CD161<sup>+</sup> precursors into Th17 cells require their stimulation with anti-CD3 plus

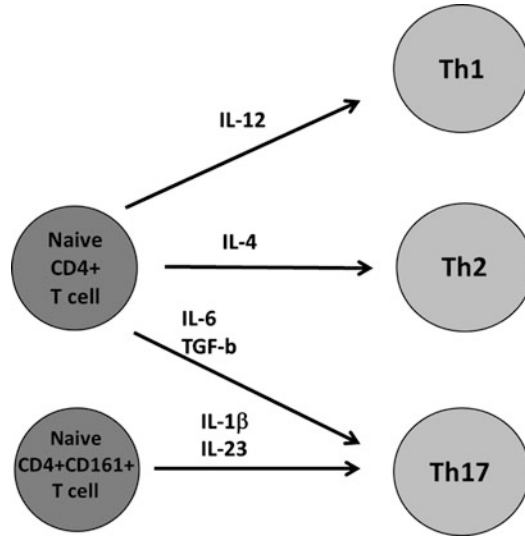


**Fig. 1** CD4+ T cell differentiation. Schematic representation of naive CD4+ T cells differentiation towards the main Th phenotype (Th1, Th2 and Th17) in presence of polarizing cytokines

anti-CD28 mAbs in the presence of the polarizing cytokines IL-1 $\beta$  and IL-23 [13]. In this model, TGF- $\beta$  is not required to induce Th17 differentiation, although it has been shown that TGF- $\beta$  increases the final frequency of IL-17 producing cells through the inhibition of the IFN- $\gamma$ -producing cells that usually arise in vitro from the UCB CD4+CD161+ precursor in presence of IL-1 $\beta$  plus IL-23 [16].

In this chapter we report detailed protocols to obtain the in vitro polarization of naïve CD4+ T cells into Th1, Th2, or Th17 cells. Since at the moment it is not possible to define an univocal in vitro protocol for Th17 polarization, we will report one protocol for the differentiation of PB naive CD4+ T cells and one for UCB naive CD4+CD161+ Th17 precursors (Fig. 1).

---

## 2 Materials

Use all materials and reagents as well as cell samples under sterile conditions.

1. Peripheral blood (PB) from healthy individuals or umbilical cord blood (UCB).
2.  $5 \times 10^{-3}$  M  $\beta$ -mercaptoethanol: add 35  $\mu$ l in 100 ml of sterile deionized H<sub>2</sub>O and store at +4 °C.
3. 0.5 M EDTA: 93 g of EDTA in 500 ml of sterile deionized H<sub>2</sub>O. Warm if necessary. Mix well and adjust pH 8 with NaOH

- (*see Note 1*). Filter with a 0.22  $\mu\text{m}$  filter system and store at +4  $^{\circ}\text{C}$ .
4. Complete RPMI 1640 medium: RPMI 1640, 2 mM L-glutamine, 1% nonessential amino acids, 1% sodium pyruvate,  $5 \times 10^{-5}$  M  $\beta$ -mercaptoethanol (*see Note 2*). Filter with a 0.22  $\mu\text{m}$  filter system, then store at +4  $^{\circ}\text{C}$  under sterile conditions.
  5. Fetal calf serum (FCS): store at  $-20^{\circ}\text{C}$ ; defrost and then heat inactivate 30 min at +56  $^{\circ}\text{C}$ , then store at +4  $^{\circ}\text{C}$  under sterile conditions.
  6. Culture medium: complete RPMI 1640, 10% FCS. Filter with a 0.22  $\mu\text{m}$  filter system, then store at +4  $^{\circ}\text{C}$  under sterile conditions.
  7. Ficoll-Hypaque.
  8. Sterile PBS.
  9. Immunomagnetic cells sorting buffer: PBS, 0.5% FCS, 2 mM EDTA. Filter with a 0.22  $\mu\text{m}$  filter system, then store at +4  $^{\circ}\text{C}$  under sterile conditions.
  10. Recombinant human cytokines: IL-12, IL-4, IL-1 $\beta$ , IL-6, IL-23, TGF- $\beta$ , IL-2 (*see Note 3*).
  11. Monoclonal antibodies (mAbs): anti-human CD3, anti-human CD28, and neutralizing anti-human IFN- $\gamma$  and anti-human IL-4. Store at +4  $^{\circ}\text{C}$  under sterile conditions or as suggested by the company (*see Note 3*).
  12. Human CD4 isolation kit (Miltenyi).
  13. Anti-human CD45RA microbeads (Miltenyi).
  14. Anti-FITC, -PE, or -APC antibody-conjugated microbeads (Miltenyi).
  15. Phorbol 12-myristate 13-acetate (PMA): 10  $\mu\text{g}/\text{ml}$  stock solution in DMSO stored at  $-20^{\circ}\text{C}$ . Dilute 1:1000 in the final volume of stimulation to use at final concentration of 10  $\text{ng}/\text{ml}$ .
  16. Ionomycin (I): 1 mM stock solution in DMSO stored at  $-20^{\circ}\text{C}$ . Dilute 1:1000 in the final volume of stimulation to use at final concentration of 1  $\mu\text{M}$ .
  17. Brefeldin A (BFA): 5  $\text{mg}/\text{ml}$  stock solution in ethanol stored at  $-20^{\circ}\text{C}$ . Dilute 1:1000 in the final volume of stimulation to use at final concentration of 5  $\mu\text{g}/\text{ml}$ .
  18. Fixing solution: 2% formaldehyde in PBS.
  19. Permeabilization solution: 0.5% bovine serum albumin (BSA), 0.5% saponin in PBS.

### 3 Methods

#### 3.1 Obtaining Naïve CD4<sup>+</sup> T Cells

1. Obtain mononuclear cell (MNC) suspensions from UCB or PB by centrifugation on Ficoll-Hypaque gradient. In detail, add 9 ml of Ficoll-Hypaque in a 30 ml tube and stratify 12 ml of whole blood on top of it so that the Ficoll–blood ratio is 2:3. Be careful to not break the Ficoll–blood interface.
2. Centrifuge at  $2500 \times g$  for 20 min. Remove the plasma (sitting on top), recover the ring of MNCs at the interface between the plasma and the Ficoll and transfer to a second tube.
3. Wash twice in PBS.
4. Resuspend in PBS + 0.5% FCS.
5. Count cells on optical microscope using a counting chamber (i.e., Neubauer Chamber), performing the appropriate dilution.
6. Obtain CD4<sup>+</sup> T cells using the CD4 isolation kit following the manufacturer's instructions (Miltenyi Biotec) (*see Note 4*). In detail, incubate MNCs with biotin–antibody cocktail (containing cocktail of biotin-conjugated monoclonal anti-human antibodies against CD8, CD14, CD15, CD16, CD19, CD36, CD56, CD123, TCR $\gamma/\delta$ , CD235a) followed by incubation with microbead Cocktail (containing both anti-biotin monoclonal antibodies and anti-human CD61 monoclonal antibody conjugated to microbeads) (*see Note 5*). The untouched CD4<sup>+</sup> T cells will be recovered in the negative fraction after the passage of MNCs through the appropriate column. Count the recovered cells and evaluate the CD4<sup>+</sup> T cells purity by flow cytometry analysis.
7. Further sort CD4<sup>+</sup> T cells into naïve T cells through CD45RA immunomagnetic separation, following the manufacture instructions (Miltenyi Biotec) (*see Note 6*). In detail, incubate CD4<sup>+</sup> T cells with anti-human CD45RA mAb conjugated to microbeads and recover CD4<sup>+</sup> naïve T cells that remain as positive fraction in the column. Count the recovered cells and evaluate the CD4<sup>+</sup> naïve T cells purity by flow cytometry analysis.

#### 3.2 Th1 and Th2 Polarization

Stimulate PB or UCB naïve CD4<sup>+</sup> T cells for 1 week with 5  $\mu\text{g}/\text{ml}$  anti-CD3 plus 5  $\mu\text{g}/\text{ml}$  anti-CD28 mAbs (*see Note 7*) in presence of 2 ng/ml IL-12 and 5  $\mu\text{g}/\text{ml}$  anti-IL-4 mAb (Th1 differentiation) or 2.5 ng/ml IL-4 and 5  $\mu\text{g}/\text{ml}$  anti-IFN- $\gamma$  mAb (Th2 differentiation). Perform cell culture in 24-well plate in a total volume of 2 ml/well of culture medium.

1. Resuspend naïve CD4<sup>+</sup> T cells at the concentration of  $1 \times 10^6/\text{ml}$  in culture medium containing soluble anti-CD3 plus anti-CD28 at  $2 \times$  concentration (10  $\mu\text{g}/\text{ml}$  each) and seed

- $1 \times 10^6$  in 24-well plates, considering at least one well for each polarizing culture condition (*see Note 8*).
2. Add 1 ml of culture medium containing the appropriate cytokines and anti-cytokines mAbs (depending on culture condition) to each well. These should be at  $2\times$  concentration (i.e., 4 ng/ml IL-12, 5 ng/ml IL-4, 10  $\mu\text{g}/\text{ml}$  anti-IL-4, and 10  $\mu\text{g}/\text{ml}$  anti-IFN- $\gamma$ ). The final volume in each well will be 2 ml.
  3. Culture cells for 7 days at 37 °C, in an atmosphere of 5 % CO<sub>2</sub>, without changing medium.
  4. After 3 days of culture, observe T cells at the inverted microscope on a daily basis to evaluate the growth rate and T cell activation (cell clumps should be present). At day 6–7 recover CD4+ T cells from each culture condition (*see Note 9*) and determine cell count. Evaluate T cell polarization as described in Subheadings 3.4, 3.5 and 3.6 (Figs. 2 and 3), taking into

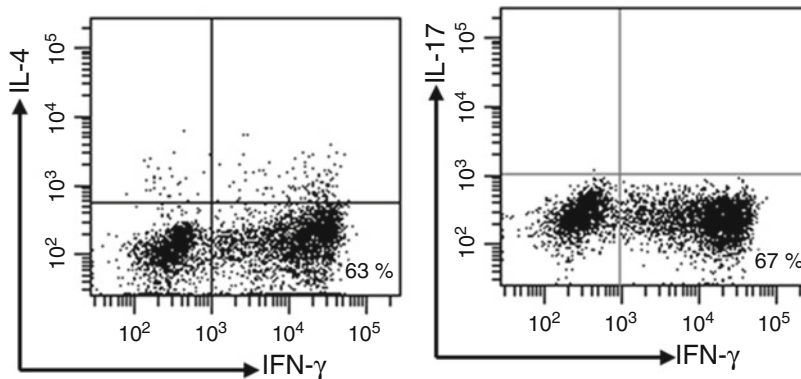


**Fig. 2** Cytokine profile of Th1 cells from UCB. UCB naive CD4+ T cells were in vitro cultured in the presence of anti-CD3 plus anti-CD28 mAbs and of IL-12 and anti-IL-4 mAbs for Th1 differentiation. After 1 week, CD4+ T cells polarization was evaluated by flow cytometry analysis of intracellular cytokines after polyclonal stimulation

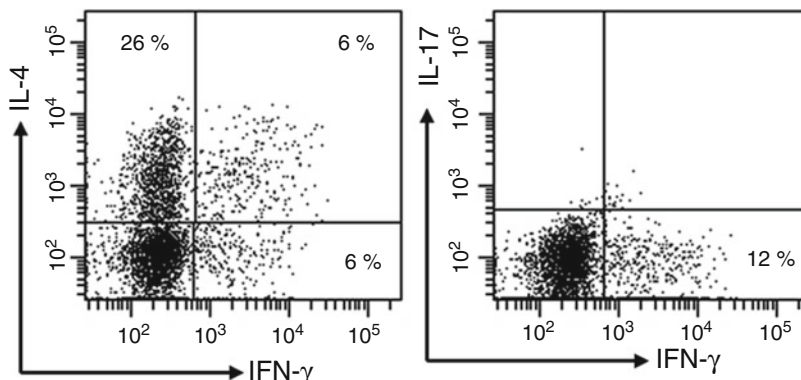


**Fig. 3** Cytokine profile of Th2 cells from UCB. UCB naive CD4+ T cells were in vitro cultured in presence of anti-CD3 plus anti-CD28 mAbs and of IL-4 and anti-IFN- $\gamma$  mAbs for Th2 differentiation. After 1 week, CD4+ T cells polarization was evaluated by flow cytometry analysis of intracellular cytokines after polyclonal stimulation

account that different strategies can be adopted, including flow cytometry analysis of intracellular cytokines after polyclonal stimulation, ELISA analysis of cytokine levels in cell culture supernatants and mRNA analysis of specific transcription factors and cytokines. In any case, the main cytokines/transcription factors to analyze to confirm Th polarization are the following: IFN- $\gamma$ /T-bet, IL-4/GATA-3, and IL-17A/RORC2 for Th1, Th2, and Th17 cells respectively.

### 3.3 Th17 Differentiation

#### 3.3.1 Th17 Differentiation from PB

Stimulate  $1 \times 10^6$  PB naïve CD4<sup>+</sup> T cells for 1 week with 5  $\mu$ g/ml anti-CD3 plus 5  $\mu$ g/ml anti-CD28 mAbs (*see Note 7*) in presence of 10 ng/ml IL-1 $\beta$ , 10 ng/ml IL-6, 20 ng/ml IL-23, 5 ng/ml TGF- $\beta$  and anti-IL-4 and anti-IFN- $\gamma$  neutralizing antibodies (5  $\mu$ g/ml each). Perform cell culture in 24-well plate in a total volume of 2 ml/well of culture medium.

1. Resuspend and seed naïve CD4<sup>+</sup> T cells as in Subheading 3.2, step 1.
2. Add 1 ml of culture medium containing the appropriate cytokines and anti-cytokines mAbs to each well at 2 $\times$  concentration, in this case 20 ng/ml IL-1 $\beta$ , 20 ng/ml IL-6, 40 ng/ml IL-2, 10 ng/ml TGF- $\beta$ , 10  $\mu$ g/ml both anti-IL-4 and anti-IFN- $\gamma$ . The final volume in each well will be 2 ml.
3. Culture cells for 7 days at 37 °C, in an atmosphere of 5% CO<sub>2</sub>, without changing medium.
4. Monitor cell growth as in Subheading 3.2, step 4. Evaluate T cell polarization as described in Subheadings 3.4, 3.5 and 3.6.

#### 3.3.2 Th17 Differentiation from UCB

Purified UCB CD4<sup>+</sup> T cells are further divided into CD161<sup>+</sup> and CD161<sup>-</sup> cell fractions by an anti-CD161 FITC, PE, or APC mAbs, followed by an anti-FITC, -PE, or -APC antibody-conjugated microbeads.

1. Wash and centrifuge UCB CD4<sup>+</sup> T cells with PBS pH 7.2+0.5% FCS, then incubate with the anti-CD161 fluorochrome-conjugated mAb for 15 min on ice after blocking Fc receptor with sterile human Ig (*see Note 10*).
2. Wash the cells with PBS pH 7.2+0.5% FCS, remove supernatant and incubate with anti-fluorochrome antibody-conjugated microbeads according to the manufacturer's instructions. The CD4<sup>+</sup>CD161<sup>-</sup> T cells are recovered in the negative fraction after the passage of UCB CD4<sup>+</sup> T cells through the appropriate column, whereas the CD4<sup>+</sup>CD161<sup>+</sup> T cells remain as positive fraction in the column and are recovered following the manufacture instructions. Count both cell fractions and evaluate their purity directly by flow cytometry analysis, without performing any additional procedure (these cells are already stained with the fluorochrome conjugated anti-CD161 mAb).

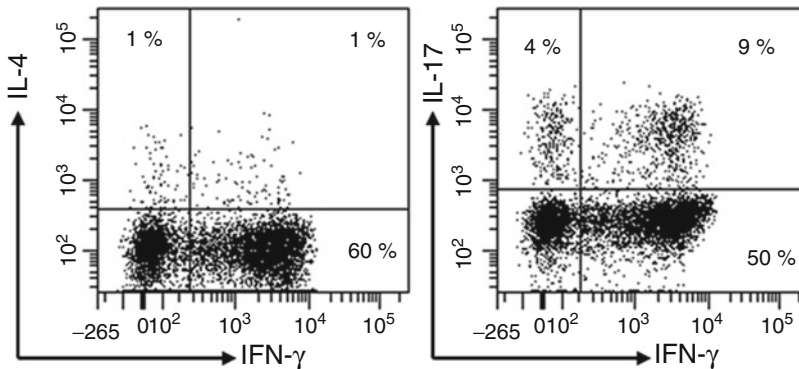


**Fig. 4** Cytokine profile of Th17 cells from UCB. UCB naïve CD4<sup>+</sup> CD161<sup>+</sup> T cells were in vitro cultured in presence of anti-CD3 plus anti-CD28 mAbs and of IL-1 $\beta$  and IL-23 for Th17 differentiation. After 1 week, CD4<sup>+</sup> T cells polarization was evaluated by flow cytometry analysis of intracellular cytokines after polyclonal stimulation

3. Stimulate UCB naïve CD4<sup>+</sup> CD161<sup>+</sup> T cells for 1 week with 5  $\mu$ g/ml anti-CD3 plus 5  $\mu$ g/ml anti-CD28 mAbs (*see Note 7*) in presence of 10 ng/ml IL-1 $\beta$  and 20 ng/ml IL-23 for Th17 differentiation (*see Note 11*). In detail, prepare naïve CD4<sup>+</sup> CD161<sup>+</sup> T cells as indicated in Subheading 3.2, **step 1**.
4. Add 1 ml of culture medium containing the appropriate cytokines at 2 $\times$  concentration (i.e., 20 ng/ml IL-1 $\beta$  and 40 ng/ml IL-23) to each well. The final volume in each well will be 2 ml.
5. Culture cells for 7 days at 37  $^{\circ}$ C, in an atmosphere of 5% CO<sub>2</sub>, without changing medium.
6. Monitor cell growth as in Subheading 3.2, **step 4**. Evaluate T cell polarization as described in Subheadings 3.4, 3.5 and 3.6 (Fig. 4).

### **3.4 Evaluation of CD4<sup>+</sup> T Cells Differentiation by Intracellular Cytokine Staining**

1. Stimulate at least  $5 \times 10^5$  cells with 10 ng/ml PMA plus 1 mM ionomycin for 6 h, the last four in the presence of 5  $\mu$ g/ml of brefeldin A, in a final volume of 0.5 ml of culture medium.
2. After stimulation, wash cells twice with PBS and resuspend in fixing solution. Incubate for 15 min at room temperature.
3. Wash cells twice with FACS washing solution.
4. Resuspend cell pellet in permeabilization solution.
5. Incubate for 15 min at room temperature in the presence of the cytokine-specific mAbs suitable for flow cytometry.
6. Wash cells twice and analyze on flow cytometer (acquire a total of  $10^4$  events for each sample). The area of positivity is determined by using an isotype-matched mAb.

**3.5 Evaluation of CD4+ T Cells Differentiation by ELISA of Cytokines in the Supernatant**

Collect culture supernatants at the end of culture, i.e., at day 6–7 before recovering expanded T cells. Alternatively, collect supernatants after restimulation of T cells with anti-CD3 anti-CD28 mAbs (5 µg/ml each one) (*see Note 7*) for 72 h in culture medium. Culture supernatants can be aliquoted and stored at –30 °C, then analyzed for the concentration of the cytokines of interest by commercially available ELISA kits.

**3.6 Evaluation of CD4+ T Cells Differentiation by Transcription Factor Profiling**

1. Stimulate at least  $2 \times 10^5$  T cells with anti-CD3 anti-CD28 mAbs (5 µg/ml each one) (*see Note 7*) or leave unstimulated in culture medium.
2. Collect T cells in RNase-free tubes.
3. Wash twice in PBS.
4. Remove supernatant completely and store pellet at –80 °C. Extract mRNA and determine transcription factor levels by using commercially available kits.

**3.7 Maintaining Cell Culture and/or Second Stimulation of Cells**

CD4+ T helper subsets obtained in vitro after naïve T cell differentiation can be maintained in culture by seeding  $1 \times 10^6$  cells/2 ml in a well of 24-well plate in the presence of 50 U/ml of IL-2 in culture medium (*see Note 8*). Monitor cell growth as in Subheading 3.2, step 4. When cells cover the surface of the well completely and form clusters (indicative of activation), split cells in two wells and add the same volume of culture medium containing IL-2 at 2× concentration (100 U/ml) to each well. Otherwise, the same CD4+ T helper subsets can be stimulated again in the same culture condition of primary stimulation. In this case repeat protocols 3.2 and 3.3 (*see Note 12*).

---

## 4 Notes

1. Exact value of pH is important to avoid further crystallization of solution over time.
2. L-glutamine 200 mM is stored at –20 °C: defrost the 100 ml stock solution and prepare 20 tube of 5 ml aliquots to store at –20 °C. Each time it is necessary to prepare a new bottle of culture medium, defrost only one 5 ml aliquot.
3. Reconstitute as indicated in the datasheet, taking into account the buffer and the concentration suggested by the company. To avoid repeated freeze–thaw cycles, aliquot the total volumes of each reconstituted reagents in small fractions (around 20–50 µl) and store at –20 to –70 °C under sterile conditions.
4. CD4+ T cells from PB or UCB MNCs could be also obtained with strategies or separation kits that are different from the Miltenyi CD4 Isolation kit. In any case, it is important to obtain highly pure, untouched CD4+ T cells.

5. In case of MNCs from UCB, it could be necessary to add additional anti-glycophorin (CD235a) microbeads during the cell depletion step to completely remove red cells. These cells, as well as erythroblasts, are particularly abundant in UCB samples, and are not completely removed by Ficoll-Hypaque gradient centrifugation and by standard quantity of anti-CD235a mAb present in the kit.
6. CD4<sup>+</sup> naïve T cells from PB can be also obtained with strategies or separation kits that are different from Miltenyi CD45RA mAb conjugated to microbeads. Cell sorting by FACS is an alternative strategy to isolate CD4<sup>+</sup> naïve T cells that were previously stained with fluorochrome-conjugated mAbs to CD45RA, CD45RO, and CD31. Naive T cells are identified as CD4<sup>+</sup>CD45RA<sup>+</sup>CD31<sup>+</sup>CD45RO<sup>-</sup>.
7. CD4<sup>+</sup> T cells activation via anti-CD3/CD28 stimulation can be performed with different methods, such as by plate-bound anti-CD3 and soluble CD28 (instead of both soluble) or by the human T Cell Activation/Expansion Kit, by following the manufacture instructions (Miltenyi). The latter is based on MACSiBead™ particles loaded with anti-CD2, -CD3, and -CD28 antibodies.
8. In case less than  $1 \times 10^6$  of CD4<sup>+</sup> naïve T cells are available for each culture condition, it is possible to scale down to 48-well plates (adding  $5 \times 10^5$  cells/0.5 ml/well), or to 96-well round bottom plates (adding  $1 \times 10^5$  cells/0.1 ml/well).
9. To efficiently recover all cells at the end of the culture, resuspend vigorously each well with the appropriate tip and wash again each well with sterile PBS. If replicate wells under the same stimulatory conditions are present, cells from these wells can be pooled and evaluated thereafter.
10. The total number of CD4<sup>+</sup> T cells recovered from UCB can be considerably high. In such a case, it is important to perform an adequate titration of the fluorochrome-conjugated mAbs to adequately stain large numbers of cells. Moreover, it is important to use sterile fluorochrome-conjugated mAb in this procedure and not those that are usually used for standard flow cytometry analysis (the latter are generally not sterile).
11. TGF- $\beta$  is not essential to induce Th17 differentiation from UCB CD4<sup>+</sup>CD161<sup>+</sup> T cells but could improve the protocol in terms of the final frequency of pure IL-17 producing cells. Indeed, TGF- $\beta$  at the concentration of 5 ng/ml inhibits the development of IFN- $\gamma$  producing cells [7].
12. It is better to perform secondary stimulation after 2–3 days of “wash-out” from TCR stimulation. So in this case the time schedule of the protocol could be the following: culture CD4<sup>+</sup> naïve T cells with primary stimulation for 6–7 days without

changing medium, then recover the cells and transfer in a new well containing culture medium and 50 U/ml IL-2 (it is not necessary to add polarizing cytokines and anti-CD3 anti-CD28 mAbs at this time). After 2–3 days, collect cells and perform a second stimulation as described for the primary one.

## References

1. Mosmann TR, Coffman RL (1989) TH1 and TH2 cells: different patterns of lymphokine secretion lead to different functional properties. *Annu Rev Immunol* 7:145–173
2. Romagnani S (1994) Lymphokine production by human T cells in disease states. *Annu Rev Immunol* 12:227–257
3. Harrington LE, Hatton RD, Mangan PR et al (2005) Interleukin 17-producing CD4+ effector T cells develop via a lineage distinct from the T helper type 1 and 2 lineages. *Nat Immunol* 6(11):1123–1132
4. Annunziato F, Cosmi L, Santarlasci V et al (2007) Phenotypic and functional features of human Th17 cells. *J Exp Med* 204(8):1849–1861
5. Hsieh CS, Macatonia SE, Tripp CS et al (1993) Development of TH1 CD4+ T cells through IL-12 produced by Listeria-induced macrophages. *Science* 260(5107):547–549
6. Szabo SJ, Sullivan BM, Peng SL et al (2003) Molecular mechanisms regulating Th1 immune responses. *Annu Rev Immunol* 21:713–758
7. Le Gros G, Ben-Sasson SZ, Seder R et al (1990) Generation of interleukin 4 (IL-4)-producing cells in vivo and in vitro: IL-2 and IL-4 are required for in vitro generation of IL-4-producing cells. *J Exp Med* 172(3):921–929
8. Swain SL, Weinberg AD, English M et al (1990) IL-4 directs the development of Th2-like helper effectors. *J Immunol* 145(11):3796–3806
9. Mercer F, Khaitan A, Kozhaya L et al (2014) Differentiation of IL-17-producing effector and regulatory human T cells from lineage-committed naive precursors. *J Immunol* 193(3):1047–1054. doi:10.4049/jimmunol.1302936
10. Takeshita M, Suzuki K, Kassai Y et al (2015) Polarization diversity of human CD4+ stem cell memory T cells. *Clin Immunol* 159(1):107–117. doi:10.1016/j.clim.2015.04.010
11. Manel N, Unutmaz D, Littman DR (2008) The differentiation of human T(H)-17 cells requires transforming growth factor-beta and induction of the nuclear receptor RORgamma. *Nat Immunol* 9(6):641–649. doi:10.1038/ni.1610
12. Veldhoen M, Hirota K, Christensen J et al (2008) Natural agonists for aryl hydrocarbon receptor in culture medium are essential for optimal differentiation of Th17 T cells. *J Exp Med* 206(1):43–49. doi:10.1084/jem.20081438
13. Cosmi L, De Palma R, Santarlasci V et al (2008) Human interleukin 17-producing cells originate from a CD161+ CD4+ T cell precursor. *J Exp Med* 205(8):1903–1916. doi:10.1084/jem.20080397
14. Kastirr I, Crosti M, Maglie S et al (2015) Signal strength and metabolic requirements control cytokine-induced Th17 differentiation of uncommitted human T cells. *J Immunol* 195(8):3617–3627. doi:10.4049/jimmunol.1501016
15. Mazzoni A, Santarlasci V, Maggi L et al (2015) Demethylation of the RORC2 and IL17A in human CD4+ T lymphocytes defines Th17 origin of nonclassical Th1 cells. *J Immunol* 194(7):3116–3126. doi:10.4049/jimmunol.1401303
16. Santarlasci V, Maggi L, Capone M et al (2009) TGF-beta indirectly favors the development of human Th17 cells by inhibiting Th1 cells. *Eur J Immunol* 39(1):207–215. doi:10.1002/eji.200838748

## Phenotypic and Functional Analysis of the Suppressive Function of Human Regulatory T Cells

Eleonora Timperi, Vincenzo Barnaba, and Silvia Piconese

### Abstract

Regulatory T cells (Tregs) are defined as immunosuppressive cells playing crucial roles in the establishment and maintenance of immune homeostasis. During the course of immune responses, Tregs control the balance between host defense from pathogens and the prevention of excessive immunity. Here, we describe the phenotypic analysis of Tregs, evaluated in peripheral blood mononuclear cells of healthy adults, by multiparameter flow cytometry, which allows examining the expression of peculiar markers of Treg subpopulations with different features, and provides efficient discrimination of multiple characteristics at the single-cell level. The same technique may be applied to characterize mononuclear cells extracted from different specimens, including whole blood, biological fluids or solid tissues. The immunoregulatory identity of a certain Treg subpopulation may be functionally verified by performing an *in vitro* suppression assay described here, testing the capability of Tregs to suppress the activation of responder cells.

**Key words** Tregs, Phenotype, Flow cytometry, *In vitro* assay, Suppression

---

### 1 Introduction

Regulatory T cells (Tregs) are a CD4<sup>+</sup> T cell subset representing 5–10% of total circulating CD4<sup>+</sup> T lymphocytes, in humans and mice. Tregs ensure the maintenance of immunological self-tolerance and immune homeostasis by preventing autoimmune responses against self-antigens [1]. Both human and murine Tregs constitutively express high levels of CD25, the interleukin-2 receptor chain  $\alpha$  (IL-2R $\alpha$ ), a component of high affinity IL-2R that is required for Treg development and survival through IL-2 responsiveness [2]. Tregs also constitutively express FOXP3, a forkhead transcription factor encoded by a gene located on the X chromosome, playing a critical role in Treg development and function. Mutations in the human *FOXP3* gene result in impaired development or dysfunctions of Tregs accompanying severe autoimmune diseases, inflammatory bowel disease, and allergy [3]. Importantly, FOXP3 expression is necessary to confer a suppressive program to

Tregs. Many data indicate that human Tregs actually represent a pool of heterogeneous subpopulations with distinct phenotypes and functional profiles.

Flow cytometry is a technique that measures optical and fluorescent characteristics on single cells. Internal composition or graininess of immune cells (represented by side scatter) and a physical property, i.e., size (represented by forward scatter), can identify specific subpopulations. Antibodies conjugated to fluorescent dyes can bind specific proteins on cell surface or within cells (cytoplasm or nucleus), and also fluorescent dyes can bind or intercalate several intracellular elements (nucleic acids, cytoplasmic molecules, etc.). Within the flow cytometer, the appropriately stained cell suspension passes through a laser beam that excites fluorescently-labeled cell components. The emitted light signals are directed to a series of filters mounted on photomultiplier tubes capable to select different wavelengths. Fluorescent signals are then digitized for computer analysis. Thanks to this technique, the use of multiple fluorochromes with different emission wavelength allows to detect several molecules, expressed on single cells, simultaneously.

Here, we have developed a multiparametric flow cytometry panel to dissect the complexity of human FOXP3<sup>+</sup> cells, and a protocol to characterize the suppressive function of CD25<sup>high</sup> Tregs *in vitro*. To the first aim, we have included in our analysis the following surface markers: CD127, that is poorly expressed in Tregs [4]; OX40, a Treg activation/survival marker [5]; CD39, a mediator of Treg suppressive function [6]; CD45RA, distinguishing resting from activated Tregs [7]. We have also added intracellular markers such as the transcription factors Helios, marking stable committed Tregs [5, 8], and FOXP3. To the second aim, i.e., the analysis of Treg suppressive capability, we describe a functional assay *in vitro*, designed to detect the proliferation of responder T cells (conventional T cells or Tconvs) when cocultured with Tregs at different ratios. This method has the limit to reproduce only certain Treg-specific suppression mechanisms, and does not recapitulate the complexity of Treg functions *in vivo*; however, it may be helpful to confirm Treg identification performed by other techniques, such as immunophenotyping. To track proliferation, cells are labeled with fluorescent dyes that covalently bind intracellular molecules: therefore, the progressive halving of their fluorescence within daughter cells allows to follow cell division by flow cytometry. By alternatively labeling Tconvs and Tregs with two different dyes, i.e., carboxyfluorescein succinimidyl ester (CFSE) or eFluor670<sup>®</sup>, it is possible to track proliferation versus suppression in each of the two cell subsets.

The described protocols may be easily translated to the characterization of tissue-infiltrating Tregs, extracted through suitable procedures [5]. Indeed, more and more data demonstrate that different tissues contain specialized subpopulations of Tregs

responding to local microenvironmental signals [9]. Therefore, it is clear that the phenotypic and the functional characterization of tissue-derived, compared to circulating, Tregs may more faithfully recapitulate the actual suppressive activity exerted by these cells *in vivo* in specific contexts. One example of such divergence is the pattern of OX40 expression in Tregs: while being poorly represented in circulating Tregs, it is highly upregulated in tumor-infiltrating Tregs [5].

---

## 2 Materials

Prepare all solutions and store them at 4 °C until use. Prepare all solutions using sterile water (Sigma; w3500). We usually do not add sodium azide to the solutions. Staining, fixation, and permeabilization steps are performed in FACS tubes.

1. FACS buffer solution: 2% of fetal bovine serum (FBS) in phosphate-buffered saline (PBS).
2. Fixation/Permeabilization Solution (Fix/Perm): mix 1 part of Concentrate buffer (eBioscience) with 3 parts of Diluent (eBioscience).
3. Permeabilization Solution: dilute the Permeabilization (Perm) Buffer 10× (eBioscience) 1:10 in H<sub>2</sub>O.
4. Fixable Viability Dye eFluor780® (eBioscience) solution: prepare 1 mL of diluted 1:1000 (1 μL in 1 mL) in PBS.
5. RPMI 1640 (Invitrogen) complete medium: 10% FBS, 2 mM L-glutamine, 2 mM penicillin–streptomycin, 1 mM nonessential amino acids, 50 μM sodium pyruvate, and 50 μM 2-mercaptoethanol.
6. Lympholyte-H (Cedarlane).
7. MACS buffer: PBS, 0.5% of bovine serum albumin (BSA), 2 mM of ethylenediaminetetraacetic acid (EDTA).
8. Ammonium-Chloride-Potassium (ACK) Lysing Buffer (Gibco).
9. CFSE: dilute lyophilized powder of CFSE in Dimethyl Sulfoxide (DMSO) at concentration of 5 mM.
10. Centrifuge.
11. FACS tubes (Falcon 12×75 mm round-bottom polystyrene tubes).
12. Sterile biosafety cabinet.
13. Pipettes (including a multichannel pipette).
14. CD4<sup>+</sup>CD25<sup>+</sup> regulatory T cell isolation kit, human (Miltenyi Biotec).

15. Columns (types LD and MS) and magnetic separators (Miltenyi Biotec).
16. 50 mL reagent reservoirs, sterile.
17. U-bottomed 96-well plate.

### 3 Methods

#### 3.1 Flow Cytometry

The following procedure refers to a single staining of  $0.5 \times 10^6$  PBMCs. Adjust amounts such to include appropriate controls and/or multiple samples. To obtain PBMCs from whole blood, please refer to Subheading 3.2.1.

1. Add  $0.5 \times 10^6$  PBMCs to a FACS tube, wash the cell suspension adding 1 mL of FACS buffer, centrifuge at  $750 \times g$  for 5 min at room temperature (RT). Discard the supernatant (*see Note 1*).
2. Resuspend the cells in 100  $\mu$ L of Fixable Viability Dye eFluor780<sup>®</sup> solution, incubate in the dark 30 min at RT.
3. Wash the cells adding 1 mL of FACS buffer and centrifuge at  $750 \times g$  for 5 min at RT. Discard the supernatant.
4. Repeat the washing step by adding 1 mL of FACS buffer and centrifuging at  $750 \times g$  for 5 min at RT. Discard the supernatant.
5. Prepare a mix of Abs to surface markers in 100  $\mu$ L of FACS buffer solution (*see Table 1*).

**Table 1**  
Antibodies to be used in Treg cell phenotyping

1st step viability dye staining 30' RT	2nd step surface staining 20' 4 °C	3rd step fix/perm 30' 4 °C	4th step intracellular staining 30' RT	Dilution of the Abs
	OX40 PE			1:50
			FOXP3 PerCPCy5.5	1:30
	CD127 PECy7			1:50
			Helios APC	1:40
Fixable viability dye eF780	CD14 APCeF780 CD56 APCeF780 CD16 APCeF780 CD19 APCeF780			1:100
	CD39 Bv421			1:50
	CD4 Bv510			1:50
	CD45RA eF605			1:50

Bv brilliant violet; eF eFluor<sup>®</sup>

6. Resuspend the cells in 100  $\mu\text{L}$  of Ab mix solution and incubate in the dark for 20 min at 4  $^{\circ}\text{C}$ .
7. Wash by adding 1 mL of FACS buffer and centrifuging at  $750\times g$  for 5 min at RT. Discard the supernatant.
8. Repeat the washing step adding 1 mL of FACS buffer and centrifuging at  $750\times g$  for 5 min at RT. Discard the supernatant.
9. Resuspend the cells in 100  $\mu\text{L}$  of Fix/Perm solution and incubate for 30 min at 4  $^{\circ}\text{C}$  in the dark.
10. Prepare a mix of Abs to intracellular markers in 100  $\mu\text{L}$  of Perm solution (*see* Table 1 and Notes 2–4).
11. Resuspend the cells in 100  $\mu\text{L}$  of intracellular Ab mix solution and incubate in the dark for 30 min at RT.
12. Wash by adding 1 mL of Perm buffer and centrifuge at  $750\times g$  for 5 min at RT. Discard the supernatant (*see* Note 5).
13. Repeat the washing step by adding 1 mL of Perm buffer and centrifuging at  $750\times g$  for 5 min at RT. Discard the supernatant.
14. Resuspend the cell pellet in 300  $\mu\text{L}$  of FACS buffer and acquire on a compatible flow cytometer. For a representative example of the gating strategy and analysis procedure, *see* Fig. 1.

### 3.2 *In Vitro* Suppression Assay

The following methods describe how to isolate  $\text{CD4}^+\text{CD25}^{\text{high}}$  Tregs and  $\text{CD4}^+\text{CD25}^-$  Tconvs and to analyze their proliferation. The assay described here is designed to obtain around  $0.2\times 10^6$  total Tregs (counting an excess of cells necessary for three replicates).

Unless otherwise specified, every procedure should be performed in sterile conditions, in a biosafety cabinet (*see* Notes 6 and 7).

#### 3.2.1 Separation of PBMCs from Whole Blood

1. Warm up the Lympholyte to RT before use.
2. Warm up RPMI complete medium to RT before use.
3. Transfer 50 mL of whole blood from a buffy coat bag into 2 distinct 50 mL tubes (25 mL per tube). Usually, 50 mL of whole blood should provide enough cells for the required amounts of Tregs and Tconvs.
4. Dilute the whole blood 1:2 with  $1\times$  PBS (for 25 mL of whole blood, add 25 mL of  $1\times$  PBS in each 50 mL tube).
5. Into four new 50 mL tubes, aliquot 12.5 mL of Lympholyte per tube.
6. Transfer, as slowly as possible, 25 mL of the blood–PBS mix over the Lympholyte layer. To avoid mixing of the two layers, let the blood flow onto the part of the wall of the tube comprised between the surface of the Lympholyte and the rim. The resulting ratio between blood–PBS and Lympholyte will be 2:1. You should have four gradient tubes overall.

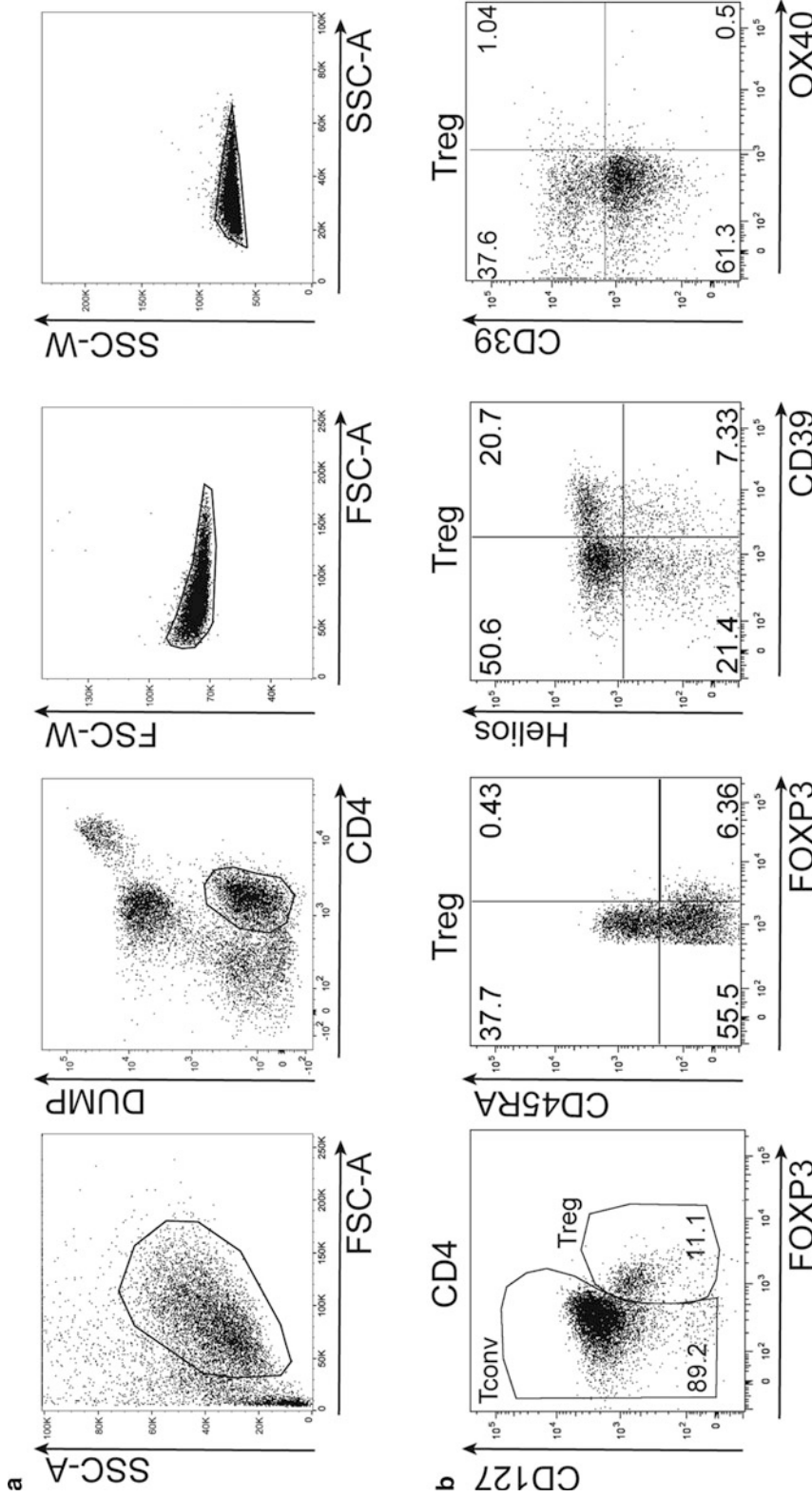


**Fig. 1** Phenotypic analysis of Tregs from PBMCs of a healthy donor. **(a)** Gating strategy to identify Tregs in PBMCs. Forward and side scatter areas (FSC-A/SSC-A) have been used to identify lymphocytes among total PBMCs. Then, CD4<sup>+</sup> cells have been delineated after exclusion of dead cells and unwanted contaminant cells. To this aim, we have used a pool of CD14, CD16, CD56, and CD19 mAbs (allowing the exclusion of NK cells, monocytes, and B cells) coupled to the same fluorescence, and emitting in the same channel of the viability dye. This approach has allowed combining all the exclusion markers into the same “dump” channel. We have excluded cell doublets in FSC-A/FSC-W and SSC-A/SSC-W panels. **(b)** Representative analysis of Treg heterogeneity. Within CD4<sup>+</sup> cells, Tregs and Tconvs have been gated as CD127<sup>low</sup>FOXP3<sup>+</sup> and FOXP3<sup>-</sup> cells, respectively. In the Treg gate, FOXP3/CD45RA panel allow distinguishing resting (CD45RA<sup>+</sup>FOXP3<sup>low</sup>) from activated (CD45RA<sup>low</sup>FOXP3<sup>high</sup>) Tregs. Helios/CD39 and CD39/OX40 panels allow visualizing that the majority of circulating Tregs express high levels of Helios, while CD39 is expressed by a variable proportions of Tregs in individual donors, depending on genetic variation in the respective gene [11]; OX40 is poorly represented in circulating Tregs of healthy donors, but can be significantly upregulated in Tregs infiltrating different tissues including cancer [5]

7. Carefully transfer the tubes to the centrifuge, as to not disturb the stratified layers, and centrifuge at  $950 \times g$  for 30 min at RT (with brake disabled or set at the minimum).
8. Carefully take out the tubes from the centrifuge. The tubes contain four distinct phases (from the bottom to the top):
  - Dark red blood cell pellet;
  - Turbid colorless phase;
  - White opaque interface, containing PBMCs;
  - Yellow transparent supernatant, containing serum and platelets.
9. Collect the white opaque interface using the pipette and transfer it into a new 50 mL tube. You should have four collection tubes overall. The collection volume should be about 10–20 mL per tube.
10. Fill up the collection tube containing the collected interface (containing PBMCs) with PBS 1 $\times$ . Centrifuge at  $600 \times g$  for 10 min at RT. Discard the supernatant.
11. Resuspend the PBMCs in 12 mL of PBS 1 $\times$  per each tube, and pool the four aliquots into a single 50 mL tube. Centrifuge at  $600 \times g$  10 min at RT. Discard the supernatant.
12. Repeat the washing step by filling up the tube with PBS 1 $\times$  and centrifuging at  $600 \times g$  for 10 min at RT. Discard the supernatant.
13. Resuspend the pellet into 1 mL of ACK solution, incubate for 5 min at 4 °C. This step is required to lyse residual erythrocytes in the PBMC preparation.
14. Fill up the tube PBS 1 $\times$  and centrifuge at  $600 \times g$  for 10 min at RT. Discard the supernatant.
15. Resuspend the cell pellet in the appropriate volume of RPMI complete medium and count the PBMCs at the microscope using a dye for dead cell exclusion (such as trypan blue). The expected yield from 50 mL of whole blood may vary significantly between different donors, but it should be at least  $100 \times 10^6$ .

### 3.2.2 Preparation of Irradiated Autologous PBMCs, Tconvs, and Tregs

1. Transfer an aliquot of the PBMC preparation to a new 50 mL tube to obtain autologous irradiated PBMCs. Calculate that a number of autologous irradiated PBMCs that is fourfold the number of Tconvs will be needed: for  $0.025 \times 10^6$  Tconvs/well, use  $0.1 \times 10^6$ /well of irradiated PBMCs (at least  $2.4 \times 10^6$  autologous irradiated PBMCs will be needed for 24 wells).
2. Irradiate the PBMCs at 3000 rads, twice.
3. Wash the irradiated PBMCs filling up with RPMI complete medium. Centrifuge at  $600 \times g$  for 10 min. Discard the supernatant.

4. Resuspend the irradiated PBMCs at a final concentration of  $2 \times 10^6$ /mL in RPMI complete medium. Store at 4 °C until use.
5. To isolate the portion of CD4<sup>+</sup>CD25<sup>high</sup> Tregs and CD4<sup>+</sup>CD25<sup>-</sup> Tconvs from PBMCs, use human CD4<sup>+</sup>CD25<sup>+</sup> Regulatory T cell isolation Kit. The separation is performed by a two-step procedure (for all details consult the web site <http://www.miltenyibiotec.com/en/>) (*see Note 8*). To obtain about  $0.2 \times 10^6$  Tregs, it is necessary to start from at least  $100 \times 10^6$  of total PBMCs.
6. After isolation, count Tregs and Tconvs.
7. Resuspend up to  $10^6$  Tconvs in 1 mL of RPMI complete medium in a 15 mL tube.
8. Resuspend up to  $10^6$  of Tregs in 1 mL of RPMI complete medium in a 15 mL tube.
9. Working in the dark, thaw an aliquot of CFSE 5 mM stock and transfer 2  $\mu$ L into the Tconv 1 mL suspension, such to obtain a 10  $\mu$ M final concentration (*see Note 9*).
10. Working in the dark, thaw an aliquot of eFluor670<sup>®</sup> 5 mM stock and transfer 2  $\mu$ L into the Treg 1 mL suspension, such to obtain a 10  $\mu$ M final concentration.
11. Incubate Tregs and Tconvs at 37 °C for 15 min.
12. Add an equal volume of FBS (1 mL) to block the reaction. Wash by filling up the tubes with RPMI complete medium and centrifuge at  $600 \times g$  for 10 min at RT. Discard the supernatant.
13. Resuspend Tregs and Tconvs at concentration of  $0.5 \times 10^6$ /mL in RPMI complete medium. Store at 4 °C in the dark until use.

### 3.2.3 Setting Up the Proliferation Assay

1. Prepare a solution of anti-CD3 Ab (clone OKT3, eBioscience) at 120 ng/mL, by transferring 0.36  $\mu$ L of the stock solution (at 1 mg/mL) in 3 mL of RPMI complete medium. The concentration of 120 ng/mL is calculated as fourfold the working concentration (30 ng/mL), as 50  $\mu$ L of such intermediate solution will be diluted in a final volume of 200  $\mu$ L in each well. Store at 4 °C until use.
2. Before seeding the cells, warm up at RT all the solutions:
  - RPMI complete medium;
  - Irradiated PBMCs ( $2 \times 10^6$ /mL);
  - eFluor670<sup>®</sup>-labeled Tregs ( $0.5 \times 10^6$ /mL);
  - CFSE-labeled Tconvs ( $0.5 \times 10^6$ /mL);
  - Anti-CD3 (120 ng/mL).
3. Seed cells and solutions according to the scheme depicted in Table 2. The experiment is performed in triplicates, for a total

**Table 2**  
**Cell culture scheme of Treg cell suppression assay**

	<b>Treg:Tconv ratio</b>	<b>1st replicate</b>	<b>2nd replicate</b>	<b>3rd replicate</b>
A	0:1	25000 Tconvs	25000 Tconvs	25000 Tconvs
B	1:0	25000 Tregs	25000 Tregs	25000 Tregs
C	1:1	25000 Tconvs 25000 Tregs	25000 Tconvs 25000 Tregs	25000 Tconvs 25000 Tregs
D	1:2	25000 Tconvs 12500 Tregs	25000 Tconvs 12500 Tregs	25000 Tconvs 12500 Tregs
E	1:4	25000 Tconvs 6250 Tregs	25000 Tconvs 6250 Tregs	25000 Tconvs 6250 Tregs
F	1:8	25000 Tconvs 3125 Tregs	25000 Tconvs 3125 Tregs	25000 Tconvs 3125 Tregs
G	1:16	25000 Tconvs 1562.5 Tregs	25000 Tconvs 1562.5 Tregs	25000 Tconvs 1562.5 Tregs
H	1:32	25000 Tconvs 781.25 Tregs	25000 Tconvs 781.25 Tregs	25000 Tconvs 781.25 Tregs

of 24 wells (*see Note 10*). Each well from the U-bottom 96-well plate should contain a final volume of 200  $\mu\text{L}$ , combined as follows:

- Irradiated PBMCs:  $0.1 \times 10^6$  in 50  $\mu\text{L}$ ;
  - eFluor670<sup>®</sup>-labeled Tregs: scaled amounts in 50  $\mu\text{L}$ ;
  - CFSE-labeled Tconvs:  $0.025 \times 10^6$  in 50  $\mu\text{L}$ ;
  - Anti-CD3: 120 ng/mL in 50  $\mu\text{L}$ .
4. First, by taking advantage of a reagent reservoir and by using a suitable multichannel pipette, add 50  $\mu\text{L}$  of RPMI complete medium in all wells of lines A, C, D, E, F, G, H (not in the B line).
  5. Transfer 100  $\mu\text{L}$  of eFluor670<sup>®</sup>-labeled Tregs in wells of line B, in triplicates ( $0.05 \times 10^6$ /well).
  6. Using a multi-channel pipette, transfer 50  $\mu\text{L}$  of Tregs from line B to lines C, D, E, F, G, and H. Discard the last residual 50  $\mu\text{L}$  of cells. At each passage, carefully mix the cells with the medium. In this way,  $0.025 \times 10^6$  Tregs will remain in line B, while being halved at each subsequent passage. At this point, all wells will contain a 50  $\mu\text{L}$  volume.
  7. Dispense 50  $\mu\text{L}$  of CFSE-labeled Tconvs ( $0.025 \times 10^6$ /well) in lines A, C, D, E, F, G, H (not in the B line).
  8. Dispense 50  $\mu\text{L}$  of RPMI complete medium in wells of line B to fill up to 200  $\mu\text{L}$  of final volume. At this point, all wells will contain a 100  $\mu\text{L}$  volume.

9. Dispense 50  $\mu\text{L}$  of irradiated autologous PBMCs in all wells.
10. Dispense 50  $\mu\text{L}$  of anti-CD3 (120 ng/mL) in all wells. In the final volume of 200  $\mu\text{L}$ , anti-CD3 will result to be diluted fourfold to the final working concentration of 30 ng/mL.
11. Incubate the plate in the dark for 5–6 days at 37 °C in the incubator with 5% carbon dioxide ( $\text{CO}_2$ ).

### 3.2.4 Analysis of Proliferation

At day 5–6, the frequency of proliferating Tconvs and Tregs will be measured by flow cytometry. Please refer to Subheadings 2, **item 1** and 3.1 for flow cytometry materials and solutions, and to Table 3 for the staining scheme (*see Note 11*). The staining may be directly performed in the same 96-well plate where cells were cultured, after extensive washing with PBS 1 $\times$ . In this setting, staining solutions may be used at a volume of 100  $\mu\text{L}$ /well. After each washing step, discard the supernatant and briefly vortex the plate. At the end of the procedure, transfer the cells into FACS tubes, using a multichannel pipette. Acquire on a flow cytometer. For a representative example of the gating strategy and analysis procedure, *see* Fig. 2.

**Table 3**  
**Antibodies and dyes to be used in cell proliferation assay**

Proliferation dyes	1st step viability dye staining 30' RT	2nd step surface staining 20' 4 °C	3rd step fix/perm 30' 4 °C	4th step intracellular staining 30' RT	Dilution of the Abs
CFSE				FOXP3 PerCPCy5.5	1:30
eF670	Fixable viability dye eF780	CD14 APCeF780 CD56 APCeF780 CD16 APCeF780 CD19 APCeF780			1:100
		CD4 Bv510			1:50

Bv brilliant violet, eF eFluor®

**Fig. 2** (continued) The eF670/CFSE plot has allowed identifying the populations labeled with one of two dyes, and in each subset FOXP3 staining has helped defining Tregs and Tconvs clearly. **(b)** Representative analysis of Treg and Tconv proliferation. *Upper dot plots* depict eF670/CFSE fluorescence in overlaid Tconvs (*grey*) and Tregs (*black*) under different Treg:Tconv ratios (0:1, 1:0, 1:1, 1:2, or 1:4). *Lower plots* represent eF670 or CFSE histograms respectively in gated Tconvs (*grey*) and Tregs (*black*) under the same ratios. *Bars* indicate the proportion (as percentages) of cells diluting the dye; mean fluorescence intensity (MFI) of each dye is also indicated in every panel. **(c)** Cumulative analysis of Treg and Tconv proliferation at different ratios, estimated as the MFI of each dye in the respective populations. With this approach, the higher the MFI, the lower is the proliferation rate. This analysis shows that Tregs alone (Treg:Tconv ratio of 1:0) are poorly proliferative (or anergic), but expand proportionally when cocultured with Tconvs (*right graph*). Conversely, Tconvs alone (Treg:Tconv ratio of 0:1) proliferate extensively, but are proportionally suppressed by Tregs at increasing ratios (*left graph*)

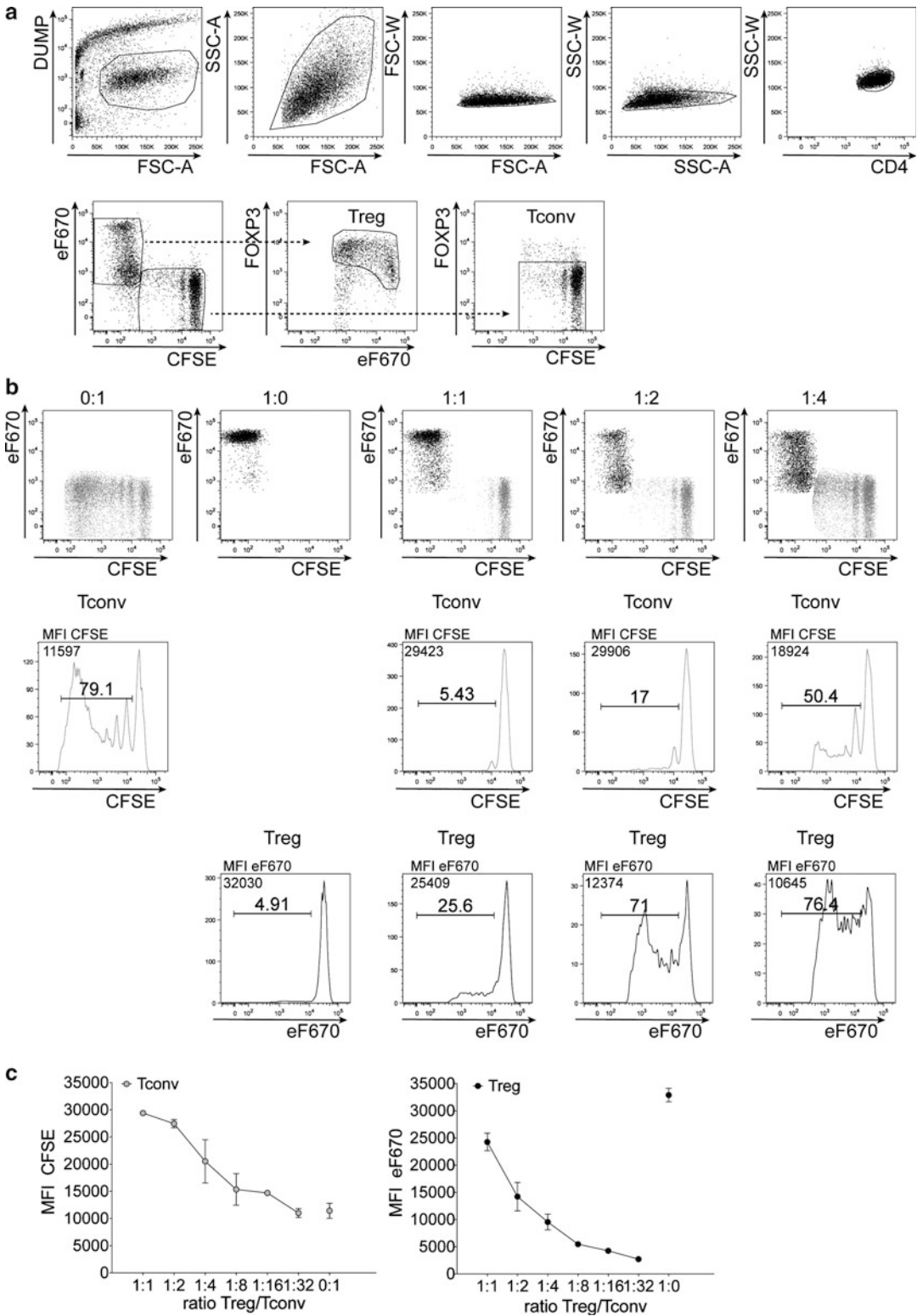


**Fig. 2** Analysis of the Treg suppression assay in vitro. **(a)** Gating strategy to identify Tregs and Tconvs after 5–6 days of culture. We have excluded dead/unwanted cells in the FSC-A/dump plot, and then sequentially identified lymphocytes (FSC-A/SSC-A), singlets (FSC-A/FSC-W and SSC-A/SSC-W) and CD4<sup>+</sup> cells (CD4/SSC-W).

---

## 4 Notes

1. Each flow cytometry procedure should be performed in the dark to preserve fluorochromes from incidental excitation.
2. A reliable analysis of Tregs requires FOXP3 detection. The staining of FOXP3 is sensitive to the fixation method. Cell fixation with paraformaldehyde is not recommended for FOXP3 detection.
3. There are several commercial anti human FOXP3 Abs that may give slightly different results [10]. In our opinion, the PCH101 clone (eBioscience) gives the most reliable results in combination with CD127.
4. It is important to check whether the staining of intracellular markers other than FOXP3 (such as Helios) is compatible with the Fix/Perm protocol required for FOXP3 detection.
5. Please note that, after fixation/permeabilization, the cell pellet will become small and faint, thus possibly less visible.
6. During cell preparation and seeding for the in vitro suppression assay, pay attention to sterility. Each solution should be prepared in sterile conditions. PBMC separation, as well as Treg/Tconv isolation, labeling, and seeding, should be performed in a sterile biosafety cabinet.
7. Use RPMI medium with phenol red, a pH indicator, such to monitor cell viability and proliferation over time.
8. By immunomagnetic separation, the purity of Tregs ranges between 80 and 90% in our hands. By staining cultured cells with a FOXP3 mAb, we have been able to exclude unwanted contaminant cells from the selected Treg or Tconv gates. However, Tregs and Tconvs may also be obtained from PBMCs through FACS-based sorting. This procedure is expected to give higher purity but lower yield in terms of cell recovery.
9. We usually avoid repeated freeze-thaw of eFluor670® and CFSE 5 mM stock solutions.
10. In the suppression assay in vitro, each condition should be tested at least in triplicates, to take into account any experimental variation.
11. To better detect at day 6 the proliferation of eFluor670®-labeled Tregs and CFSE-labeled Tconvs, the staining with a viability dye is necessary to exclude not only dead Tconvs or Tregs but also irradiated autologous PBMCs.

## References

1. Levings MK, Allan S, d’Hennezel E et al (2006) Functional dynamics of naturally occurring regulatory T cells in health and autoimmunity. *Adv Immunol* 92:119–92:155. doi:[10.1016/S0065-2776\(06\)92003-3](https://doi.org/10.1016/S0065-2776(06)92003-3)
2. Sakaguchi S, Vignali DA, Rudensky AY et al (2013) The plasticity and stability of regulatory T cells. *Nat Rev Immunol* 13(6):461–467. doi:[10.1038/nri3464](https://doi.org/10.1038/nri3464)
3. Bennett CL, Christie J, Ramsdell F et al (2001) The immune dysregulation, polyendocrinopathy, enteropathy, X-linked syndrome (IPEX) is caused by mutations of FOXP3. *Nat Genet* 27(1):20–21. doi:[10.1038/83713](https://doi.org/10.1038/83713)
4. Liu W, Putnam AL, Xu-Yu Z et al (2006) CD127 expression inversely correlates with FoxP3 and suppressive function of human CD4+ T reg cells. *J Exp Med* 203(7):1701–1711. doi:[10.1084/jem.20060772](https://doi.org/10.1084/jem.20060772)
5. Piconese S, Timperi E, Pacella I et al (2014) Human OX40 tunes the function of regulatory T cells in tumor and nontumor areas of hepatitis C virus-infected liver tissue. *Hepatology* 60(5):1494–1507. doi:[10.1002/hep.27188](https://doi.org/10.1002/hep.27188)
6. Borsellino G, Kleinewietfeld M, Di Mitri D et al (2007) Expression of ectonucleotidase CD39 by Foxp3+ Treg cells: hydrolysis of extracellular ATP and immune suppression. *Blood* 110(4):1225–1232. doi:[10.1182/blood-2006-12-064527](https://doi.org/10.1182/blood-2006-12-064527)
7. Miyara M, Yoshioka Y, Kitoh A et al (2009) Functional delineation and differentiation dynamics of human CD4+ T cells expressing the FoxP3 transcription factor. *Immunity* 30(6):899–911. doi:[10.1016/j.immuni.2009.03.019](https://doi.org/10.1016/j.immuni.2009.03.019)
8. Kim HJ, Barnitz RA, Kreslavsky T et al (2015) Stable inhibitory activity of regulatory T cells requires the transcription factor Helios. *Science* 350(6258):334–339. doi:[10.1126/science.aad0616](https://doi.org/10.1126/science.aad0616)
9. Pesenacker AM, Broady R, Levings MK (2015) Control of tissue-localized immune responses by human regulatory T cells. *Eur J Immunol* 45(2):333–343. doi:[10.1002/eji.201344205](https://doi.org/10.1002/eji.201344205)
10. Law JP, Hirschhorn DF, Owen RE et al (2009) The importance of Foxp3 antibody and fixation/permeabilization buffer combinations in identifying CD4+ CD25+ Foxp3+ regulatory T cells. *Cytometry A* 75(12):1040–1050. doi:[10.1002/cyto.a.20815](https://doi.org/10.1002/cyto.a.20815)
11. Rissiek A, Baumann I, Cuapio A et al (2015) The expression of CD39 on regulatory T cells is genetically driven and further upregulated at sites of inflammation. *J Autoimmun* 58:12–58:20. doi: [10.1016/j.jaut.2014.12.007](https://doi.org/10.1016/j.jaut.2014.12.007)

## Approaches to Detect microRNA Expression in T Cell Subsets and T Cell Differentiation

Silvia Monticelli, Tarmo Äijö, and Sara Trifari

### Abstract

MicroRNAs (miRNAs) are crucial components of the molecular networks regulating differentiation and responses of T lymphocytes in health and disease. It is therefore essential to rely on robust methods of qualitative and quantitative investigation of miRNA expression in T cell subsets, and during T cell activation and differentiation. Here, we focus on different methods for miRNA analysis, including Northern blots, quantitative RT-PCR, and next-generation sequencing, and we discuss advantages and disadvantages of each method. While we mainly focus on the study of miRNA expression in human T lymphocytes, these methods can also be applied to other species and/or cell types.

**Key words** T lymphocytes, CD4, CD8, MicroRNAs, RNA extraction, Northern blot, Next-generation sequencing, Quantitative RT-PCR

---

### 1 Introduction

Adaptive immune responses are crucial for the effective eradication of invading pathogens, but they also must be carefully regulated to avoid host tissue damage and initiation of immune pathologies. MicroRNAs (miRNAs) are short noncoding RNA species able to suppress gene expression posttranscriptionally, and mammalian cells express hundreds of different miRNAs. The final outcome of miRNA action is the inhibition of mRNA translation with or without concomitant mRNA degradation, resulting in reduced protein output. It is estimated that 30–90% of human genes are miRNA targets [1]. Over the past years, miRNAs have become recognized as central regulators of a variety of biological processes, and more specifically of gene-transcription networks at the basis of immune responses. Analysis of miRNA expression, regulation, and biogenesis is essential to understand their role in health and disease [2, 3].

During miRNA biogenesis, nascent primary miRNA transcripts (pri-miRNAs) are sequentially processed by the Microprocessor complex (DGCR8/Drosha) in the nucleus, and by the

endoribonuclease Dicer in the cytosol, to give rise first to a pre-miRNA stem-loop intermediate, and then to a mature miRNA duplex. One strand of the mature miRNA duplex is preferentially incorporated into the effector RNA Induced Silencing Complex (RISC), leading to mRNA target recognition through imperfect base-pairing (*see* ref. [4] for a recent review). Basic requirements for proper processing by Dicer include a two nucleotide (nt)-long 3' overhang generated by Drosha, as well as a 5' phosphorylated end [4], a feature that can be exploited for some applications aimed at studying miRNA expression [5].

Following antigenic stimulation, naïve CD4<sup>+</sup> T helper (T<sub>H</sub>) cells proliferate and differentiate to a number of different memory and effector subsets, with responses tailored to the specific pathogen. Such effector subsets are primarily defined by the expression of distinct cytokine profiles and chemokine receptors. T<sub>H</sub>1 cells are characterized by the ability to produce high levels of IFN $\gamma$  and are key in the response to viruses and intracellular bacteria, while T<sub>H</sub>2 cells are instrumental for the eradication of extracellular pathogens. T<sub>H</sub>17 cells, which are characterized by IL-17 production, are involved in both the elimination of extracellular bacterial and fungal pathogens, as well as of some intracellular bacteria. Another crucial function of T<sub>H</sub>1 cells is to provide help to CD8<sup>+</sup> cytotoxic T lymphocytes (CTLs), which can kill infected or tumor cells by releasing the content of cytotoxic granules to target cells, as well as via engagement of death receptors. T<sub>H</sub> cells and CTLs have a central role in orchestrating immune responses to an invading pathogen but their activity has to be tightly controlled to avoid excessive host tissue damage.

Some miRNAs have been shown to act as negative regulators of T cell function by inhibiting the expression of cytokines and effector molecules. In contrast, others may potentiate T cell functionality by repressing specific inhibitors of the immune response. Altogether, miRNAs can either reduce or augment immune signaling networks by fine-tuning the expression of negative or positive signaling molecules. For example, miR-181a was shown to regulate activation and proliferation of human T<sub>H</sub>17 cells in response to specific pathogens, such as *Candida albicans*, most likely by influencing the signal strength upon engagement of the T cell receptor [6]. In CTLs, miR-139 and miR-150 were identified as components of a miRNA network controlling perforin, eomesodermin, and IL-2R $\alpha$  expression in response to IL-2, inflammation, and antigenic stimulation [7]. In general, given the fact that each miRNA can potentially target the expression of hundreds of genes, it becomes crucial to understand how miRNAs are expressed and modulated during T cell differentiation and activation and analyze their expression in relation to their potential mRNA targets.

Different methods can be used to measure miRNA levels in cell extracts. We first describe how to obtain high quality RNA

from CD4<sup>+</sup> and CD8<sup>+</sup> T lymphocytes, focusing on human subsets obtained from peripheral blood, and subsequently we describe three different methods to investigate the expression of individual miRNAs (Northern blot and quantitative RT-PCR [qRT-PCR]), as well as of how to analyze whole genome miRNA levels (next-generation sequencing [NGS]). The choice of the method to use to analyze miRNA expression depends on quality and quantity of information that the user wishes to achieve. Northern Blot allows the analysis of the miRNA precursor and mature miRNA at the same time, provides information about the size of the mature miRNA product, and it does not require sophisticated equipment. In the recent years; however, real-time PCR has become the method of choice for the analysis of gene expression, as well as miRNAs, because of its medium-throughout capacity, the availability of premade miRNA-specific primers and its overall rapidity and technical simplicity (turnover time from RNA to results ~1 day). Both Northern Blot and PCR are somehow limited by a preconceived notion of what miRNA are known to be expressed, or supposed to be expressed, in a given cell type or tissue. Conversely, NGS-based methods are unbiased, as they do not require any a priori knowledge of the miRNA expression profile; in fact the output of a deep sequencing run contains information about all the small RNA species detectable in the samples of interest. Therefore, not only NGS allows the parallel quantification of all known miRNA species, but, with the aid of more sophisticated bioinformatics tools, it also permits identification of novel putative miRNAs. Below, we provide technical information regarding these three methods of analysis, and a more detailed comparison of their specific applications.

---

## 2 Materials

### **2.1 Isolation and Culture of CD4<sup>+</sup> and CD8<sup>+</sup> Human T Cells**

1. Sterile polypropylene tubes (50 and 15 mL).
2. Ficoll-Paque Plus.
3. Wash buffer: RPMI 1640 medium, 25 mM HEPES, 1 % FCS.
4. Trypan blue.
5. Pre-separation filters, 30 μm (Miltenyi Biotec).
6. CD4<sup>+</sup> microbeads, human (Miltenyi Biotec).
7. CD8<sup>+</sup> microbeads, human (Miltenyi Biotec).
8. MACS LS columns, with magnet and magnet holder (Miltenyi Biotec).
9. Fluorescently labeled antibodies for sorting (variable, depending on the subpopulations one is interested in).
10. MACS buffer: use autoMACS running buffer (Miltenyi Biotec) or PBS, 0.5 % human serum, and 2 mM EDTA.

11. For stimulation with plate-bound Ab: Anti-CD3 (clone TR66 or OKT3).
12. For stimulation with plate-bound Ab: Anti-CD28 (clone CD28.2).
13. Tissue-culture treated plates of appropriate size (96-well, 48-well, 24-well, 12-well or 6 wells).
14. Complete medium: RPMI-1640, 2 mM glutamine, 1% (v/v) nonessential amino acids, 1% (v/v) sodium pyruvate, 50 U/mL penicillin, 50 µg/mL kanamycin and streptomycin, 5% (v/v) human serum.
15. Recombinant human IL-2: dilute to 100 U/mL in complete medium.
16. For stimulation with Ab-coated beads: Dynabeads Human T-activator CD3/CD28 (Thermofisher).
17. Dynamag Magnet (Invitrogen).

## **2.2 Total and Small RNA Extraction**

There are now several commercially available kits and reagents to extract high-quality RNA, suitable for downstream application such as Northern blot, RT-PCR, and NGS, although not all of them efficiently retain small RNA species. Valuable alternatives to extract RNA containing miRNA species include the miRNeasy kit (Qiagen) and the mirVana kit (Ambion). Variations of the protocol reported in the manufacturer's handbooks can be used to further separate the small RNA species from the total RNA, or potentially to obtain protein from the same samples (Paris mirVana kit, Ambion).

1. RNase-free tubes (1.7 mL).
2. Nuclease-free water.
3. TRIzol.
4. 2-propanol.
5. Ethanol.
6. Glycogen (GlycoBlue, Ambion).
7. 3 M sodium acetate.

## **2.3 miRNA Northern Blot**

All solutions should be prepared with clean, nuclease-free or DEPC-treated water (*see item 6* below). All materials and work spaces should be clean and, if possible, dedicated to RNA work only.

1. Acrylamide–bis-acrylamide solution 19:1 (Bio-Rad).
2. Formamide dye loading buffer, containing xylene cyanol, and bromophenol blue such as Gel Loading Buffer II (Denaturing PAGE; Ambion).

3. Running and transfer buffer: 0.5× TBE, 50 mM Tris, 45 mM boric acid, 0.5 mM EDTA. It can be prepared as a 10× or 5× stock.
4. Urea (*see Note 1*).
5. 10% (w/v) ammonium persulfate (APS) and *N,N,N',N'*-tetramethylethane-1,2-diamine (TEMED).
6. RNase-free water: we use nuclease-free water from Ambion for small volumes, such as for resuspending RNA samples; larger volumes of water can be treated with diethylpyrocarbonate (DEPC), for example to prepare buffers. DEPC-treated water is prepared by dissolving 1 mL of DEPC in 1 L of Milli-Q water over night at RT, and subsequently autoclaved to inactivate the DEPC. Treat the water with DEPC and inactivate it before making any solution: DEPC cannot be used in combination with other chemicals such as Tris or sodium dodecyl sulfate (SDS).
7. Vertical gel electrophoresis apparatus and transfer chamber and sponges.
8. SYBR safe gel stain, provided as a 10,000× stock solution (Invitrogen).
9. 20× SSC stock solution: 3 M NaCl, 0.3 M sodium citrate; adjust to pH 7.0 with HCl. Wash buffers can be prepared by diluting the stock solution as follows: low-stringency wash, 2× SSC, 0.1% SDS; high-stringency wash, 0.1× SSC, 0.1% SDS.
10. 20× SSPE stock solution: 3 M NaCl, 0.2 M NaH<sub>2</sub>PO<sub>4</sub>, 0.02 M EDTA. Dissolve 175.3 g of NaCl, 27.6 g of NaH<sub>2</sub>PO<sub>4</sub>, and 7.4 g of EDTA in 800 mL of H<sub>2</sub>O. Adjust to pH 7.4 with NaOH and adjust the volume to 1 L.
11. 10 mg/mL salmon sperm sheared DNA solution (Invitrogen).
12. Denhardt's solution (50×): 1% (w/v) bovine serum albumin (Fraction V), 1% (w/v) Ficoll 400, 1% (w/v) Polyvinylpyrrolidone (PVP). Dissolve in water, filter and store aliquots at -20 °C.
13. Prehybridization buffer: 5× Denhardt's solution, 6× SSPE, 0.5% SDS and 100 µg/mL denatured salmon sperm DNA.
14. Hybridization buffer: 5× Denhardt's solution, 6× SSPE, 0.5% SDS, with addition of the radiolabeled probe.
15. Single-strand DNA or locked nucleic acid (LNA, Exiqon) specific oligo probes, fully complementary to the miRNA to be detected.
16. T4 polynucleotide kinase and buffer (New England Biolabs).
17. [ $\gamma$ -<sup>32</sup>P]ATP.
18. MicroSpin G-25 Sephadex columns (GE Healthcare).
19. Hybridization glass bottles and oven.

20. Amersham Hybond-N<sup>+</sup> nylon membrane.
21. Whatman 3MM chromatography paper.
22. Autoradiography films and cassettes and/or Phosphor-imaging cassettes and equipment.

#### **2.4 cDNA Reverse Transcription**

1. TaqMan<sup>®</sup> MicroRNA Reverse Transcription Kit (ThermoFisher Scientific).

#### **2.5 qRT-PCR (Taqman<sup>®</sup>)**

1. TaqMan Universal PCR Master Mix, No AmpErase UNG.
2. TaqMan MicroRNA assay for miRNA of interest and TaqMan MicroRNA assay for reference miRNA (all from Applied Biosystems).

#### **2.6 qRT-PCR (SYBR<sup>®</sup> Green)**

1. FastStart Universal SYBR Green Master (Rox) (Roche).
2. Stem-loop reverse transcription primer.
3. qPCR primers.

#### **2.7 Next-Generation Sequencing (NGS)**

(See **Note 2**).

1. TruSeq Small RNA Library Preparation Kit (see **Note 3**).
2. T4 RNA Ligase 2, truncated (New England Biolabs).
3. Agilent RNA 6000 Nano Kit.
4. Agilent High Sensitivity DNA Kit.
5. 6% Novex TBE gels, 10 well.
6. 5× Novex TBE Running buffer.
7. 10 mg/mL ethidium bromide stock solution.

---

## **3 Methods**

### **3.1 Isolation of Human T Lymphocytes from Blood Samples**

All blood separations and cell cultures should be performed under a biosafety cabinet and utilizing sterile, tissue-culture grade disposable plastic. Polypropylene plastic tubes should be preferred to polystyrene, as the latter favor the adhesion and activation of cells (monocytes in particular). All centrifuge steps are performed at 300 × *g* for 10 min at RT, unless otherwise noted.

1. For separation of mononuclear cells from peripheral blood, dilute blood with PBS 1:1, then pipette 15 mL of Ficoll-Paque Plus in a 50 mL Falcon tube and gently overlay it with 30–35 mL of diluted blood.
2. Centrifuge at 805 × *g* for 30 min at RT, with no brake and low acceleration. Erythrocytes and polymorphonuclear leucocytes will settle to the bottom of the tube, a white ring of mononuclear leucocytes will form above the Ficoll, while the clear plasma will remain on top.

3. Carefully retrieve the mononuclear leukocyte ring with a 5 mL pipette and transfer it in a new 50 mL tube. Make sure to avoid aspirating any Ficoll. Dilute the cells with up to 45 mL wash buffer.
4. Centrifuge at  $300 \times g$  for 10 min RT; discard the supernatant and repeat the washing twice.
5. To avoid clogging the column in the following steps, filter the cells on a 30  $\mu\text{m}$  pre-separation filter. This can be used on a 15-mL Falcon tube after the last wash, or directly on the column, if using a Miltenyi-based magnetic column to enrich the T cells of interest.
6. Count cells by making dilutions in trypan blue (usually 1:20 or 1:40), making sure to avoid counting small platelets or red blood cells, which can be very numerous depending on the quality of the initial blood product.
7. CD4 and CD8<sup>+</sup> T cell separation: commercial kits based on the principle of magnetic separation, or antibody-mediated immunorosette formation, are available to separate CD4<sup>+</sup> or CD8<sup>+</sup> T cells from PBMC or whole blood. All of them ensure recovery of high quality RNA from live cells, given that the manufacturer's instructions are properly followed and the blood sample is properly stored prior to cell separation. For an outline of advantages and disadvantages of the principal separation methods, *see Note 4* (more detailed protocols on T cell separation methods can also be found in other Chapters of this Volume).

### **3.2 T cell Stimulation with Plate-Bound Abs**

1. Pre-coat a tissue-culture treated 96-well plates with 5  $\mu\text{g}/\text{mL}$  anti-CD3 antibody and 1  $\mu\text{g}/\text{mL}$  anti-CD28 antibody for 2 h at 37 °C or overnight at 4 °C (antibody concentrations may be optimized depending on the specific application).
2. Rinse the wells with PBS, and block by adding complete medium and incubating the plate for 10 min at RT.
3. Add  $1\text{--}2 \times 10^5$  T cells/well in complete medium. Detach the cells by gentle pipetting after 48 h and transfer them in new plates at an approximate concentration of  $0.5 \times 10^6$  cells/ml, adding fresh medium with 40–100 U/mL rhIL-2. Split the cells as needed, every 2–3 days.

### **3.3 T Cell Stimulation with Anti-CD3/ Anti-CD28 Antibodies- Coated Beads**

1. Wash the desired number of beads twice with PBS 2% FBS (or complete medium) as recommended by the manufacturer's instructions.
2. Resuspend T cells in medium (concentration can vary from 0.4 to  $1 \times 10^6$  T cells/mL) and add the desired amount of beads per well. The ratio of beads–T cells can vary depending on the specific application; we recommend to start from 1:1 and titrate down the bead: T cell ratio.

3. On day 2 pipette up and down the cell suspension and incubate on a Dynal Magnet; while keeping the tube on the magnet recover the T cells by transferring them onto a new plate.
4. Add fresh medium with rhIL-2 (40–100 U/mL) and diluting the cells to  $0.4 \times 10^6$ /mL.
5. Split every 2–3 days as needed, by adding fresh medium with IL-2.

### 3.4 RNA Extraction

All methods to detect miRNAs will be successful only if intact, high-quality RNA is extracted efficiently from the cell subset of choice. Depending on the scientific question to be addressed and the final application, total RNA or the small RNA fraction may be preferred. For example, extraction of total RNA is recommended in cases in which expression of both miRNAs and target mRNAs is to be investigated. For applications in which total RNA is not needed and may simply interfere with the detection of small RNAs, then a method that enriches for small RNA species may be preferable.

Total and/or small RNAs are extracted following manufacturer's instructions exactly. The choice of method has to take into account not only the desired final RNA fraction but also the amount or quality of starting material. For example, selective inefficient recover of low GC-containing miRNAs has been reported extracting RNA from low number of cells using TRIzol [8]. Methods have also been developed to specifically and reliably detect miRNA expression levels from as little as 50 cells [9].

RNA concentration and presence of unwanted contaminations can be assessed with a spectrophotometer by measuring the absorbance at 230, 260, and 280 nm. Pure RNA will yield an optical density (OD) ratio 260/280 of 1.8–2, while the OD 260/230 ratio should be around 2.0 or higher to exclude contaminations by salts and organic compounds.

### 3.5 Northern Blots

The general procedure involves the separation of denatured RNA of various sizes by gel electrophoresis, followed by transfer on a suitable membrane and detection utilizing a specific radiolabeled oligo-probe [10]. For advantages and disadvantages of Northern blots compared to other miRNA detection methods *see* **Note 5**.

1. Prepare the acrylamide gel as follows: 8 M urea, 0.5× TBE, 12–15% acrylamide–bis-acrylamide 19:1. Add APS and TEMED, required for acrylamide–bis-acrylamide polymerization and the formation of a gel matrix, immediately before pouring the gel, as it will start polymerizing very quickly. The gel volume will depend on the size of your apparatus. We use gels that are 1 mm or 1.5 mm thick.
2. Use a syringe and running buffer (0.5× TBE) to remove any residue of urea, acrylamide or bubbles from the wells of the

fully polymerized gel: residues and air bubbles will interfere with the run.

3. Pre-run the gel (with no samples) in  $0.5\times$  TBE (the required voltage will depend on the apparatus you use) for 45 min at RT. Pre-running slightly warms up the gel leading to better resolution.
4. Prepare your samples by dissolving 20–30  $\mu\text{g}$  total RNA (or  $\sim 5\ \mu\text{g}$  small RNA) in 15  $\mu\text{L}$  RNase-free water and add the same volume of  $2\times$  dye loading buffer. Denature the samples before loading by heating them at  $95\ ^\circ\text{C}$  for 5–10 min; immediately place them on ice. This ensures effective denaturation of secondary structures that may interfere with the gel separation. Wash once more the wells of the pre-run gel and load the samples.
5. Run the gel for  $\sim 2$  h at RT, until the xylene cyanol in the loading buffer is more or less in the middle of the gel and the bromophenol blue is at the very bottom.
6. Carefully remove the gel and stain it for 5–10 min with SYBR safe appropriately diluted in  $0.5\times$  TBE to visualize the major RNA bands (5S and 5.8S rRNAs at  $\sim 120$ – $160$  nt respectively, and tRNA at  $\sim 75$ – $95$  nt) (Fig. 1). This simple step confirms overall RNA quality and gross assessment of correct sample loading and separation (*see Note 6*).
7. Cut the nylon membrane and six pieces of Whatman paper big enough to cover the gel completely, and mark the membrane with a pencil so to keep track of its orientation (and also which

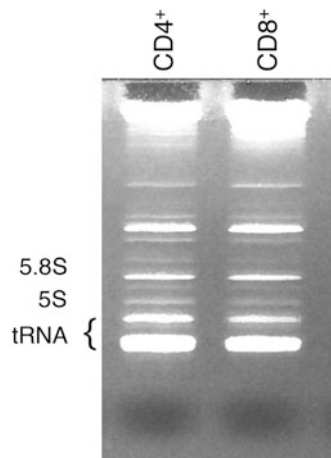


**Fig. 1** Visualization of total RNA quality and quantity by staining. Total RNA was extracted from  $\text{CD4}^+$  and  $\text{CD8}^+$  T lymphocytes and separated on a 12% acrylamide gel. For better resolution, only 1.5  $\mu\text{g}$  of total RNA was loaded on this particular gel. Bands were stained for 10 min in a solution of ethidium bromide in  $0.5\times$  TBE and visualized by UV light

side will have the bound RNA on). Soak paper and membrane in  $0.5\times$  TBE.

8. Assemble the sandwich for transfer as follows: three paper sheets, membrane, gel (face down), three paper sheets. Make sure you insert the transfer cassette in such a way that the RNA will transfer with the current from the negative to the positive pole, from the gel to the membrane. Avoid air bubbles.
9. Transfer is performed in  $0.5\times$  TBE at  $4\text{ }^{\circ}\text{C}$  for about 4 h: chose a voltage that is high enough to ensure complete transfer, but that does not overheat the chamber.
10. Disassemble the apparatus and covalently crosslink the RNA to the membrane either by UV crosslinking using a Stratalinker and following manufacturer's instructions, or by baking the membrane for 2 h at  $80\text{ }^{\circ}\text{C}$  in an oven.
11. Insert the membrane in a glass hybridization bottle; avoid overlaps as much as possible.
12. Denature the salmon sperm DNA for 10 min at  $95\text{ }^{\circ}\text{C}$  and place it immediately on ice. Add it to the pre-warmed pre-hybridization solution and pour everything into the hybridization bottle containing the membrane. Salmon sperm DNA is used as a blocking agent to reduce nonspecific probe binding and therefore background. Rotate at  $\sim 37\text{--}42\text{ }^{\circ}\text{C}$  for at least 2 h. We found that this hybridization temperature works for a wide range of probes; however, one should check the melting temperature ( $T_m$ ) of the chosen oligo probe, especially considering that for example LNA probes will have significantly higher  $T_m$  compared to ssDNA oligonucleotides. Higher hybridization temperatures will increase specificity (thereby reducing background), but reduce signal intensity and vice versa.
13. Radioactively label the oligo probe at the 5'-end using the T4 polynucleotide kinase enzyme (PNK). Set up a  $20\text{ }\mu\text{L}$  reaction containing  $2\text{ }\mu\text{L}$   $10\times$  PNK buffer,  $20\text{ pmol}$  probe,  $20\text{ }\mu\text{Ci}$  [ $\gamma\text{-}^{32}\text{P}$ ]ATP, and  $10\text{ U}$  of T4 PNK. Incubate for 1 h at  $37\text{ }^{\circ}\text{C}$  and heat-inactivate the enzyme at  $68\text{ }^{\circ}\text{C}$  for 10 min. Add  $30\text{ }\mu\text{L}$  of nuclease-free water to the reaction and remove the unincorporated radioactive nucleotides using a G-25 microspin column according to the manufacturer's instructions.
14. Substitute the pre-hybridization solution with the hybridization solution containing the radiolabeled probe. Boil the probe for 5 min to denature it immediately before adding it to the hybridization solution. Hybridize over night at  $\sim 37\text{--}42\text{ }^{\circ}\text{C}$ .
15. Remove the hybridization solution and wash the membrane as follows to eliminate any unbound probe: three  $3\times 10\text{ min}$  washes with  $2\times$  SSC,  $0.1\%$  SDS at  $35\text{ }^{\circ}\text{C}$ ;  $1\times 5\text{ min}$  wash with  $0.1\times$  SSC,  $0.1\%$  SDS at  $35\text{ }^{\circ}\text{C}$ .

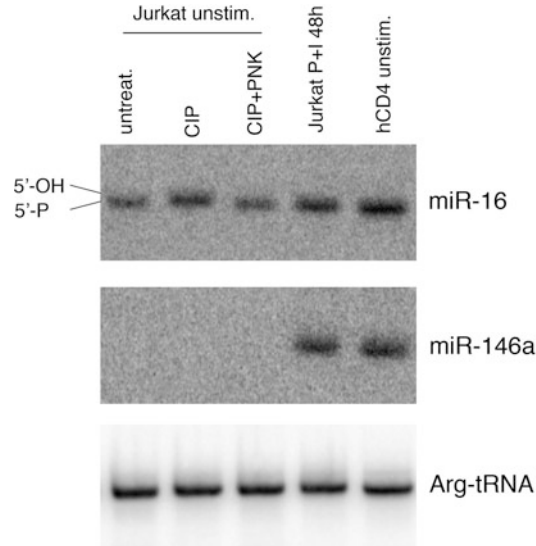


**Fig. 2** Northern blot to assess miRNA expression and 5'-end chemical modifications in human T cells. Total RNA was extracted using TRIzol from Jurkat T cells (resting or stimulated with 20 nM PMA plus 2  $\mu$ M ionomycin for 48 h) and primary human total CD4<sup>+</sup> T cells. 30  $\mu$ g of total RNA was treated with alkaline phosphatase (CIP), which removes 5'-phosphate groups), alone or followed by a sequential treatment with T4 PNK, which adds a single 5'-phosphate [20, 21]. Both enzymes were from New England Biolabs. After treatment, RNA was repurified by TRIzol extraction and loaded onto a 15% acrylamide gel. After transfer, the same membrane was sequentially reprobbed with miR-16 (showing expression in all samples and presence of a single phosphate group in the 5'-end), miR-146a (showing expression in resting primary human T cells, but not in unstimulated Jurkat cells) and an arginine tRNA as loading control

16. Expose the membrane for autoradiography or Phosphor-Imager analysis (For an example of miRNA detection in human T cell line and primary T cells by Northern blot *see* Fig. 2).
17. For reuse, blots can be stripped of the old probe by boiling in 0.1 $\times$  SSC, 0.1% SDS twice for 10 min, and then reprobbed.

### 3.6 qRT-PCR

A number of commercial qRT-PCR technologies to measure miRNA expression have been described in great detail (see for example refs. [9, 11]), and one is advised to follow the detailed instructions provided by the manufacturer for each method. Here we provide just a general outline of the work flow, and we discuss peculiarities of the miRNA PCR approaches in the indicated Subheading 4.

1. Extract RNA from fresh or cultured T cell samples.
2. Quantify RNA using NanoDrop, using water or TE as blank (*see* Note 7).

3. Perform reverse transcription using a miRNA-specific RT primer and the TaqMan<sup>®</sup> MicroRNA Reverse Transcription Kit according to the manufacturer's instructions (*see* **Note 8**).
4. Proceed to real-time PCR set up using the Taqman<sup>®</sup> microRNA assay; to choose an appropriate endogenous control, *see* **Note 9**.

### 3.7 Next-Generation Sequencing (NGS)

NGS or high-throughput sequencing is a method of massive parallel sequencing where millions of DNA fragments are sequenced in a single sample in a relatively short time, generating million of reads that are then mapped back to the reference genome, allowing precise quantification of the starting material. Different NGS platforms exist, each one with its own proprietary chemistry and detection methods, including Solexa (Illumina), SOLiD (Applied Biosystems), 454 Genome Sequencer (Roche), Ion PGM (Ion Torrent), and others. Here we will focus on Illumina platform and reagents to construct small RNA libraries, and analyze sequencing data. Methods to construct small RNA libraries for next-generation sequencing have been extensively described (*see* for example ref. [5]). We refer the reader to the Illumina TruSeq Small RNA Library Prep Guide (<https://support.illumina.com/downloads/truseq-small-rna-library-prep-guide-15004197.html>). Here we will briefly outline the RNA purification method and library preparation according to the Illumina Manual, highlighting steps that require particular care for the success of the procedure.

1. For sorted or cultured cells: pellet cells by centrifugation at  $300 \times g$ , 10 min;
2. Eliminate the supernatants using particular care not to disturb the cell pellet;
3. Wash the sample once with cold PBS (*see* **Note 10**).
4. Extract RNA using the mirVana miRNA kit, according to the manufacturer's instructions.
5. Store the extract RNA at  $-80\text{ }^{\circ}\text{C}$ ; minimize freeze-thawing to avoid degradation.
6. Assess RNA quality and integrity prior to proceed to library construction (*see* **Note 11** and Fig. 3).
7. Store the RNA at  $-80\text{ }^{\circ}\text{C}$ ; minimize freeze-thawing.
8. When ready to start the library preparation, transfer the desired amount of RNA to a new RNase-free tube or plate (*see* **Note 12**);
9. Ligate the 3'-adapter;
10. Ligate the 5'-adapter;
11. Perform reverse transcription;
12. Perform PCR amplification (*see* **Note 13**);
13. Run an aliquot of the amplified DNA sample on an Agilent DNA high sensitivity Chip (for an example of Bioanalyzer profile, *see* Fig. 3).

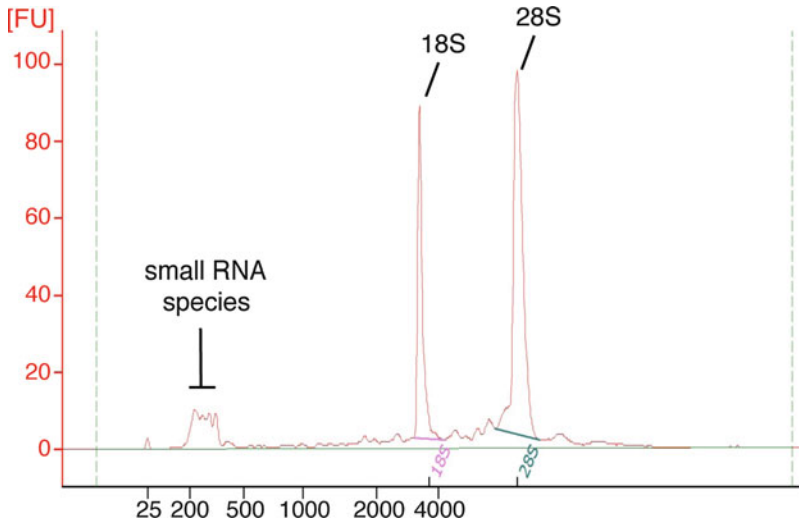


**Fig. 3** Bioanalyzer profile of a total RNA sample extract from T cells. Total RNA was extracted from cultured CD8<sup>+</sup> T cells using the miRvana isolation kit (Ambion). 1  $\mu$ L of the RNA sample was loaded on an Agilent RNA 6000 Nano Chip, and analyzed on an Agilent 2100 Bioanalyzer. The small RNA species, as well as the 18S and 28S rRNA are indicated

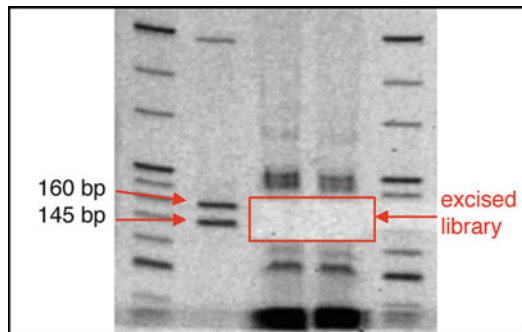


**Fig. 4** Post-excision picture of miRNA libraries run on a 6% TBE gel. Two miRNA Illumina libraries were run on a 6% TBE gel, which was stained with ethidium bromide (as per manufacturer's instructions) and visualized on a Dark Reader Gel Imaging system. The gel portion corresponding to molecular weight 145–160 base pair was excised, corresponding to the size of mature miRNAs plus ligated adapters

14. Run amplified libraries on a 6% TBE Novex Gel (*see Note 14*).
15. Before positioning the gel for cutting, wipe the area with ethanol; use a single-use razor to excise each band.
16. Excise gel area between the molecular weight marker 145 and 160 (for an example of a gel *after* library excision *see* Fig. 4).
17. Recover the DNA by using a Gel Breaker tube as recommended.
18. (Optional) Concentrate DNA by Ethanol precipitation.

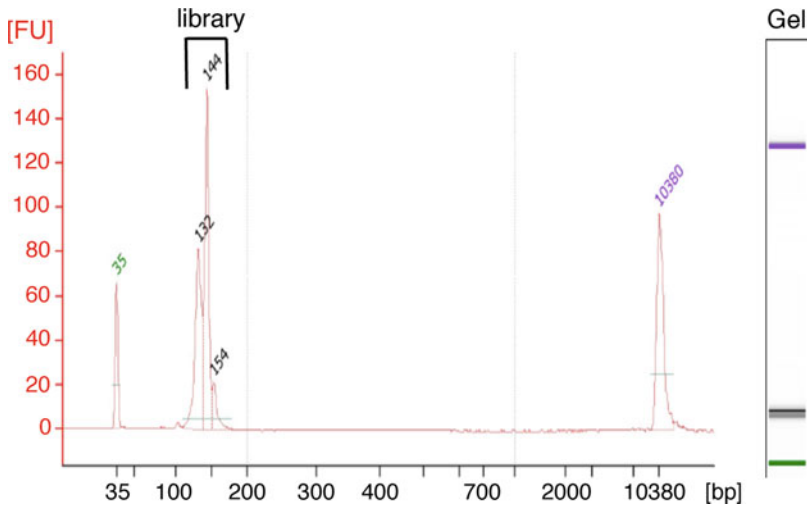


**Fig. 5** Bioanalyzer profile of an amplified miRNA library after size-selection. 1  $\mu$ L of a small RNA library was run on a DNA High Sensitivity Chip and visualized on an Agilent 2100 Bioanalyzer. The peaks corresponding to the amplified libraries are indicated

19. Validate the library by running an aliquot on an Agilent High Sensitivity DNA Chip (a representative example of a successfully sequenced library is shown in Fig. 5).
20. Use the Bioanalyzer tracks to calculate the molarity of the libraries; if the preparation has been carried out by keeping each library separate, pool individual libraries at this point following the manufacturer's recommendation (*see Note 15*).

### 3.8 Analysis of NGS Data

Given the diffusion and relatively affordability of NGS techniques, bioinformatics analysis remains in general the biggest bottleneck in several NGS application. However, analysis of standard RNA-seq, as it is described here, requires a relatively easy informatic pipeline. A more detailed explanation of RNA-seq data analysis is provided elsewhere in this Volume. Here we briefly summarize the main steps of data analysis and provide an example of reads distribution obtained from miRNA sequencing generated from T cells.

1. Combine, convert, and demultiplex per-cycle BCL base call files containing base calls and quality scores into FASTQ files using `bcl2fastq` ([http://support.illumina.com/sequencing/sequencing\\_software/bcl2fastq-conversion-software.html](http://support.illumina.com/sequencing/sequencing_software/bcl2fastq-conversion-software.html)).
2. Remove the sequencing adapter and barcodes sequences from the sequencing reads, e.g., using `cutadapt` (*Martin, Marcel. "Cutadapt removes adapter sequences from high-throughput sequencing reads." EMBnet. journal 17.1 (2011): pp-10*). If

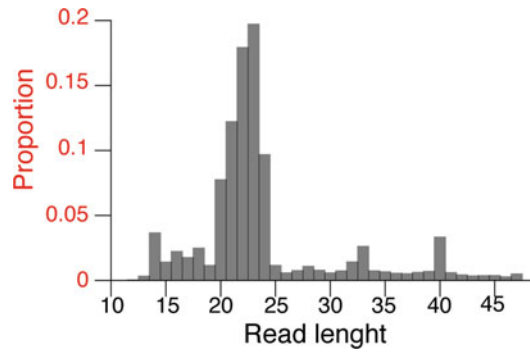


**Fig. 6** Fragment size distribution of a typical miRNA library. After adapter removal and pooled library deconvolution, fragment sizes (read lengths) of an individual library are plotted, showing that the majority of reads have the size of mature microRNA (22–25 nucleotides)

the adapter sequences are not known, then first identify the adapter sequences by detecting overrepresented sequences using FastQC (<http://www.bioinformatics.babraham.ac.uk/projects/fastqc>).

3. Check the read length distributions of sequencing libraries after trimming sequencing adapters and barcodes using FastQC for quality control.
4. If the goal is to quantify the levels of known miRNAs in the samples, then align the adapter-free sequencing reads against the miRNA hairpin sequences derived from the miRBase annotations [12]. To identify novel short RNAs and quantify levels of various short RNAs, align the adapter-free sequencing reads against the organism's reference genome. Allow multiple alignments; if there are multiple equally good alignments for a given read, then choose one of the alignments randomly.
5. Visualize the read length distributions of aligned reads and proportion of different noncoding RNA (ncRNA) families using a tool such as DARIO [13], for quality control (an example of reads distribution is shown in Fig. 6).
6. Count the number of aligned reads per mature miRNA annotated in miRBase using BEDTools [14].
7. Normalize the counts to the included spike-in control (recommended if the total amount of miRNA varies significantly between samples) [15] or to library sizes [16].
8. Identify differentially expressed miRNAs by using statistical tools, such as DESeq [17] and edgeR [18], or by prioritizing candidates by fold-changes (if there are no replicates available) for further study and validation.

---

## 4 Notes

1. Single-stranded nucleic acids form more intramolecular interactions compared to double-stranded molecules, which may result in changes in their electrophoretic mobility. Denaturing agents like urea are therefore used to disrupt any secondary RNA structure. The migration in a gel of single-stranded RNA molecules will however remain dependent on both molecular weight and charge [19]. Also, depending on the 5'-end modifications of the RNA molecule and the acrylamide–bis-acrylamide ratio utilized, the migration of RNA on a gel can be affected [20, 21] (Fig. 2).
2. The provided list contains only the essential items that have to be supplied by the user. All the Illumina NGS kits and protocols are constantly updated and/or modified: please refer to the latest manual for the specific procedure and the list of Materials that have to be supplied by the user.
3. Illumina offers kits with different Index primers; Index primers have different, known sequences, and are introduced during the PCR amplification step to allow library barcoding and pooling.
4. *Positive selection* refers to the use of antibodies directed against the antigen of interest, in this case CD4 or CD8, or CD3 (in mouse, CD90 can also be used to isolate total T cells). The advantages of positive selection reside mainly in the greater purity of the target population, and in the possibility to further process the negative fraction, which is free of antibodies. The main disadvantage is that the purified populations will carry antibody-bound beads on the surface, which may be a concern especially for functional follow up studies (for example if T cells are going to be stimulated in vitro). However, some commercial kits give the possibility to detach the magnetic beads from the enriched population.

*Negative selection* refers to methods where the population of interest is enriched, while remaining untouched and free of bound antibodies/beads. The main advantage of this method is that the cells of interest are not perturbed. The main disadvantage is that the use of such kits is based on a preconceived notion of what other cell types are present in the starting material. The commercial kits are tailored to peripheral blood or lymphoid tissues, but they are not designed to eliminate other nonimmune cells. This makes them unsuited if the starting sample is a different tissue, such as a tumor (recovery of tumor-infiltrating lymphocytes), liver, lungs, or central nervous system. In those cases, a positive selection system is recommended. Alternatively, a homemade antibody cocktail can be optimized

by introducing antibodies with the desired specificity. It is good practice to always check what antibodies are contained in the negative selection kit of your choice.

5. While Northern blots are certainly inefficient compared to qRT-PCR methods for routine analysis of miRNA expression, due to the high amount of total RNA required (20–30  $\mu\text{g}/\text{lane}$  vs. 10 ng that can be used with TaqMan-based qRT-PCR), they can be reused to quantify several different miRNAs in the same samples, by stripping and reprobing, and they remain a crucial method of choice for studies aimed at understanding putative chemical modifications of miRNAs, as well as to assess miRNA size [20, 21]. Indeed, both pre-miRNAs and mature miRNAs can undergo posttranscriptional modifications such as RNA tailing (3' terminal untemplated nucleotidyl addition), with uridylation being one of the most extensively studied (reviewed in [4, 22]). Such modifications would clearly be missed by qRT-PCR-based approaches.
6. If necessary, it is also possible to add a radiolabeled RNA molecular weight markers ranging from 10 to 150 nt (Ambion's Decade Markers System). The marker is radioactively labeled following manufacturer's instruction. While having such a marker is ideal for any preliminary experiment, and certainly for all experiments in which a precise evaluation of the band size is required, it should be noted that having to run and transfer a radiolabeled marker makes the whole procedure more cumbersome. Moreover, the amount of marker to load on the gel should be carefully balanced to the signal intensity deriving from the sample, as adding too much marker too close to the experimental samples may obliterate any weak signals coming from the samples themselves.
7. NanoDrop sensitivity and specificity is limited: the reader should be advised that the inferior detection limit of the NanDdrop is 2–5 ng nucleic acid/ $\mu\text{L}$ ; in addition, NanoDrop measurement does not provide information about RNA integrity.
8. The main difference between "standard" mRNA RT-PCR and miRNA RT-PCR is that, given the small size of the mature miRNAs, RT reactions are conducted using a so-called "stem loop primer" which will adopt a "hairpin" structure during the reverse transcription (RT) reaction. Once the cDNA is generated, under denaturing conditions used for the PCR reaction the stem loop primer provides a scaffold for the Reverse primer, while the Forward PCR primer is miRNA-specific. Therefore each miRNA has to be retrotranscribed using a specific RT primer, and then the cDNA amplified using a common Reverse primer and a miRNA-specific Forward primer. In the last several years, RT-PCR protocols have been developed and

optimized to detect hundreds of miRNAs in the same sample. The so-called Megaplex approach [23] allows detection of up to 450 miRNAs and endogenous control using one single RT reaction with multiplexed RT primers. However, given the recent diffusion and increased affordability of NGS techniques, which allow the detection of virtually all existing miRNA species in a given sample, without any prior knowledge of the expressed miRNA species, NGS is now widely used to analyze genome-wide miRNA expression.

9. The choice of an appropriate endogenous control is of paramount importance for the detection of changes in miRNA expression levels. An appropriate control should have high expression, which is not influenced by the experimental conditions and treatments. Classically, the small nucleolar RNA (snRNA) U6 has been used as normalizer; however, other snRNAs may constitute a better choice (see also [http://www3.appliedbiosystems.com/cms/groups/mcb\\_marketing/documents/generaldocuments/cms\\_044972.pdf](http://www3.appliedbiosystems.com/cms/groups/mcb_marketing/documents/generaldocuments/cms_044972.pdf)). Another viable alternative is to choose a miRNA with high expression that does not change across the samples. We suggest the use of miR-191 for T cells [7, 24]. However, we advise the reader to test at least two or three different reference small RNAs.
10. If RNA is being extracted from few T cells, in the order of  $2 \times 10^5$  total cells or less, it is advisable to always have some serum during the washing step (0.2% serum will suffice), since cells will pellet poorly in plain PBS. This may lead to significant loss of material when less than 1 million cells are pelleted in one tube. If sorted, cells may be collected directly into the RNA lysis buffer and the lysates frozen until ready to be used (sort directly in lysis buffer only if the expected number of sorted cells is  $1 \times 10^5$  or lower, to avoid excessive dilution of the lysis buffer).
11. RNA integrity is crucial to obtain reliable and reproducible miRNA expression data. RNA integrity can be measured by measuring the ratio of 28S to 18S rRNA levels (theoretical ratio 2.7:1; however, 2:1 is acceptable), based on the assumption that rRNA quality and quantity reflect those of the whole RNA sample. rRNA relative levels can be quantified by running an aliquot of the RNA sample on agarose or polyacrylamide gels. If available, we recommend the use of the 2100 Agilent Bioanalyzer, which consists in an on-chip gel assessment of RNA integrity and requires minimal amount of material. The Bioanalyzer software analyzes the RNA profile and assigns an RNA Integrity Number (RIN) to each sample, based not only on the rRNA ratio but on the whole RNA profile (see <http://www.genomics.agilent.com/article.jsp?pageId=2181>). For a detailed procedure we refer the reader to the manufacturer's

instructions. Two different kits are available (Agilent RNA 6000 Nano kit and Agilent RNA 6000 Pico Kit), depending on the concentration of the RNA samples.

12. Illumina advises to start from either the total RNA (1 µg) or from enriched small RNA fraction (10–50 ng). In general, we have found that a pre-enrichment of small RNA is not necessary to prepare miRNA libraries from T cells.
13. PCR amplification is a crucial step of any NGS library preparation; DNA is amplified for a limited number of cycles to minimize amplification bias and the production of PCR duplicates.
14. At this point it is possible to pool the libraries, if indexed, prior to running on the gel. This saves time and reduces handling. However, libraries have to be quantified using a Bioanalyzer and pooled in equimolar ratios; this is important to ensure equally representation of each library during sequencing. We usually prefer to load the libraries individually on the gel and pool them after individual quantification.
15. Quantification of individual libraries can be performed using the Bioanalyzer tracks. After pooling, libraries concentration can be reassessed using one of the commercially available Kapa PCR kits. If using a PCR-based quantification method, be aware that the average size of the DNA fragments has to be taken into consideration when calculating the library molarity.

---

## Acknowledgments

Work in the SM lab on this topic is supported by the Swiss National Science Foundation (grant 31003A\_156875) and the Swiss Multiple Sclerosis Society. ST has been supported by the Cancer Research Institute (CRI).

## References

1. Lewis BP, Burge CB, Bartel DP (2005) Conserved seed pairing, often flanked by adenosines, indicates that thousands of human genes are microRNA targets. *Cell* 120(1):15–20. doi:[10.1016/j.cell.2004.12.035](https://doi.org/10.1016/j.cell.2004.12.035)
2. Monticelli S (2013) MicroRNAs in T helper cell differentiation and plasticity. *Semin Immunol* 25(4):291–298. doi:[10.1016/j.smim.2013.10.015](https://doi.org/10.1016/j.smim.2013.10.015)
3. Baumjohann D, Ansel KM (2013) MicroRNA-mediated regulation of T helper cell differentiation and plasticity. *Nat Rev Immunol* 13(9):666–678. doi:[10.1038/nri3494](https://doi.org/10.1038/nri3494)
4. Ha M, Kim VN (2014) Regulation of microRNA biogenesis. *Nat Rev Mol Cell Biol* 15(8):509–524. doi:[10.1038/nrm3838](https://doi.org/10.1038/nrm3838)
5. Thomas MF, Ansel KM (2010) Construction of small RNA cDNA libraries for deep sequencing. *Methods Mol Biol* 667:93–111. doi:[10.1007/978-1-60761-811-9\\_7](https://doi.org/10.1007/978-1-60761-811-9_7)
6. Mele F, Basso C, Leoni C et al (2015) ERK phosphorylation and miR-181a expression modulate activation of human memory TH17 cells. *Nat Commun* 6:6431. doi:[10.1038/ncomms7431](https://doi.org/10.1038/ncomms7431)

7. Trifari S, Pipkin ME, Bandukwala HS et al (2013) MicroRNA-directed program of cytotoxic CD8<sup>+</sup> T-cell differentiation. *Proc Natl Acad Sci U S A* 110(46):18608–18613. doi:[10.1073/pnas.1317191110](https://doi.org/10.1073/pnas.1317191110)
8. Kim YK, Yeo J, Kim B, Ha M, Kim VN (2012) Short structured RNAs with low GC content are selectively lost during extraction from a small number of cells. *Mol Cell* 46(6):893–895. doi:[10.1016/j.molcel.2012.05.036](https://doi.org/10.1016/j.molcel.2012.05.036)
9. Hoefig KP, Heissmeyer V (2010) Measuring microRNA expression in size-limited FACS-sorted and microdissected samples. *Methods Mol Biol* 667:47–63. doi:[10.1007/978-1-60761-811-9\\_4](https://doi.org/10.1007/978-1-60761-811-9_4)
10. Monticelli S, Ansel KM, Xiao C et al (2005) MicroRNA profiling of the murine hematopoietic system. *Genome Biol* 6(8):R71. doi:[10.1186/gb-2005-6-8-r71](https://doi.org/10.1186/gb-2005-6-8-r71)
11. Latham GJ (2010) Normalization of microRNA quantitative RT-PCR data in reduced scale experimental designs. *Methods Mol Biol* 667:19–31. doi:[10.1007/978-1-60761-811-9\\_2](https://doi.org/10.1007/978-1-60761-811-9_2)
12. Griffiths-Jones S (2006) miRBase: the microRNA sequence database. *Methods Mol Biol* 342:129–138. doi:[10.1385/1-59745-123-1:129](https://doi.org/10.1385/1-59745-123-1:129)
13. Fasold M, Langenberger D, Binder H, Stadler PF, Hoffmann S (2011) DARIO: a ncRNA detection and analysis tool for next-generation sequencing experiments. *Nucleic Acids Res* 39(Web Server issue):W112–W117. doi:[10.1093/nar/gkr357](https://doi.org/10.1093/nar/gkr357)
14. Quinlan AR, Hall IM (2010) BEDTools: a flexible suite of utilities for comparing genomic features. *Bioinformatics* 26(6):841–842. doi:[10.1093/bioinformatics/btq033](https://doi.org/10.1093/bioinformatics/btq033)
15. Locati MD, Terpstra I, de Leeuw WC et al (2015) Improving small RNA-seq by using a synthetic spike-in set for size-range quality control together with a set for data normalization. *Nucleic Acids Res* 43(14), e89. doi:[10.1093/nar/gkv303](https://doi.org/10.1093/nar/gkv303)
16. Zhou X, Oshlack A, Robinson MD (2013) miRNA-Seq normalization comparisons need improvement. *RNA* 19(6):733–734. doi:[10.1261/rna.037895.112](https://doi.org/10.1261/rna.037895.112)
17. Anders S, Huber W (2010) Differential expression analysis for sequence count data. *Genome Biol* 11(10):R106. doi:[10.1186/gb-2010-11-10-r106](https://doi.org/10.1186/gb-2010-11-10-r106)
18. Robinson MD, McCarthy DJ, Smyth GK (2010) edgeR: a Bioconductor package for differential expression analysis of digital gene expression data. *Bioinformatics* 26(1):139–140. doi:[10.1093/bioinformatics/btp616](https://doi.org/10.1093/bioinformatics/btp616)
19. Nykanen A, Haley B, Zamore PD (2001) ATP requirements and small interfering RNA structure in the RNA interference pathway. *Cell* 107(3):309–321
20. Pak J, Fire A (2007) Distinct populations of primary and secondary effectors during RNAi in *C. elegans*. *Science* 315(5809):241–244. doi:[10.1126/science.1132839](https://doi.org/10.1126/science.1132839)
21. Sijen T, Steiner FA, Thijssen KL, Plasterk RH (2007) Secondary siRNAs result from unprimed RNA synthesis and form a distinct class. *Science* 315(5809):244–247. doi:[10.1126/science.1136699](https://doi.org/10.1126/science.1136699)
22. Lee M, Kim B, Kim VN (2014) Emerging roles of RNA modification: m(6)A and U-tail. *Cell* 158(5):980–987. doi:[10.1016/j.cell.2014.08.005](https://doi.org/10.1016/j.cell.2014.08.005)
23. Mestdagh P, Feys T, Bernard N et al (2008) High-throughput stem-loop RT-qPCR miRNA expression profiling using minute amounts of input RNA. *Nucleic Acids Res* 36(21), e143. doi:[10.1093/nar/gkn725](https://doi.org/10.1093/nar/gkn725)
24. Seumois G, Vijayanand P, Easley CJ et al (2012) An integrated nano-scale approach to profile miRNAs in limited clinical samples. *Am J Clin Exp Immunol* 1(2):70–89

# Chapter 14

## Next-Generation Sequencing Analysis of Long Noncoding RNAs in CD4+ T Cell Differentiation

Valeria Ranzani, Alberto Arrigoni, Grazisa Rossetti, Ilaria Panzeri, Sergio Abrignani, Raoul J.P. Bonnal, and Massimiliano Pagani

### Abstract

Next-generation sequencing approaches, in particular RNA-seq, provide a genome-wide expression profiling allowing the identification of novel and rare transcripts such as long noncoding RNAs (lncRNA). Many RNA-seq studies have now been performed aimed at the characterization of lncRNAs and their possible involvement in cell development and differentiation in different organisms, cell types, and tissues. The adaptive immune system is an extraordinary context for the study of the role of lncRNAs in differentiation. Indeed lncRNAs seem to be key drivers in governing flexibility and plasticity of both CD8<sup>+</sup> and CD4<sup>+</sup> T cell, together with lineage-specific transcription factors and cytokines, acting as fine-tuners of fate choices in T cell differentiation.

We describe here a pipeline for the identification of lncRNAs starting from RNA-Seq raw data.

**Key words** NGS, RNA-seq, lncRNAs, Bioinformatics, CD4<sup>+</sup> T cells, Immune system

---

### 1 Introduction

Recent genome-wide studies have revealed that the vast majority of the human genome is dynamically transcribed to produce a large fraction of lncRNAs [1]. Recent advances in transcriptome reconstruction technologies made it possible to identify and characterize thousands of novel and specific lncRNAs from short reads RNA-seq data [2–4]. The classification of lncRNA loci with respect to protein coding genes as well as the definition of their transcript abundance, exon composition and splicing efficiency can be achieved only through the analysis of RNA-seq data [5]. Nonetheless other NGS strategies provide important complementary information to define novel transcriptional units: full-length cDNA sequencing, chromatin state maps (H3K4me3 for transcription start site (TSS) information, H3K36me3 for genebody), and RNA polymerase II occupancy (Fig. 1). The class of long noncoding RNAs encompasses a

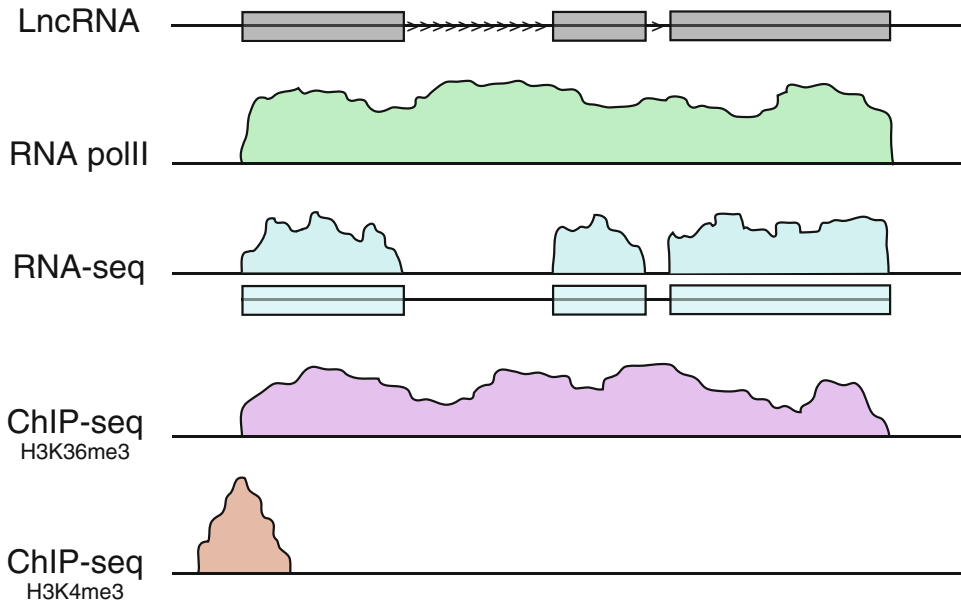


**Fig. 1** NGS methods for lncRNA prediction. RNApolII and H3K36me3 ChIP-seq indicate the transcribed portion of the genome and cover the genebodies, H3K4me3 ChIP-seq reports indication about TSS and finally RNA-seq specifies exons contribution

different set of functional transcripts characterized by a length over 200 nucleotides with no potential to encode for functional proteins. They are commonly classified in association with annotated protein-coding mRNAs and comprise: sense or antisense lncRNA, if they overlap coding mRNAs on the same or in the opposite strand and share a portion of sequence with the latter, bidirectional lncRNAs when their expression and the expression of a neighboring coding transcript is initiated in close proximity, intronic lncRNAs if they are produced starting from the intron of a protein coding gene and, finally, intergenic lncRNAs (lincRNAs) if they lie within a sequence between two genes [6, 7] (Fig. 2). Despite lncRNAs are present in all vertebrate and cover a large fraction of the genome [8], they do not show the same pattern of evolutionary conservation compared to protein-coding genes and other noncoding RNA classes [9, 10]. For this reason, a new paradigm is necessary to describe the evolutionary linkage among lncRNAs in different species. This includes different levels of evolutionary conservation: sequence, structure, function, and finally syntenic transcription [8]. The functional aspect of lncRNAs is widely investigated: they have regulatory roles at almost every stage of gene expression, from targeting epigenetic modifications in the nucleus to modulating mRNA stability and translation in the cytoplasm [1].

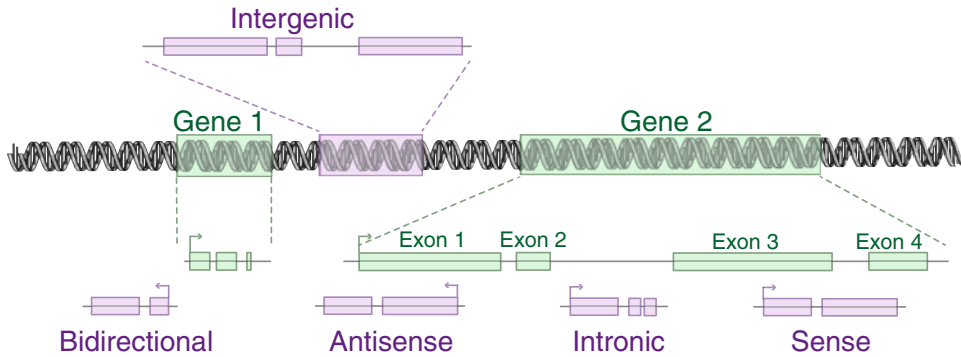


**Fig. 2** Long noncoding RNAs classification. The genomic and transcriptional contexts are commonly used for the definition of long noncoding RNAs. The figure shows five possible classes of lncRNAs (*violet*) related to coding regions (*green*)

Furthermore, these RNAs can exert their function both as *cis*- and *trans*-acting lncRNAs. The first class is involved in the control of the expression of genes located in the proximity of their transcription sites and sometimes their action can spread to long distances on the same chromosome [11]. *Trans*-acting lncRNAs can both activate or repress the expression of genes located in independent loci [12–14]. The most important feature of lncRNAs is their developmental stage-, tissue-, or cell-specific expression [15]: initially this aspect was one of the major impediments to the discovery of a possible regulatory role of these molecules, but recently with growing number of lncRNA and functional studies, this expression specificity is recognized as a key characteristic. LncRNA specificity can be exploited for the definition of novel biomarkers in different pathological contexts and for the identification of potential novel therapeutic targets [15]. For this reason, a *de novo* approach for the identification of new specifically expressed lncRNAs in RNA-seq analysis is a key step to investigate the regulation of different cellular processes, as well as differentiation or developmental stages by lncRNAs [16].

Here, we present a step-by-step protocol for the identification and characterization of lncRNA based on RNA-seq Poly-A<sup>+</sup> fractions data using paired-end Illumina reads. This pipeline includes all the software, command lines and suggestions for a complete NGS analysis of lncRNAs, starting from quality control and reads mapping to differential expression analysis or identification of lncRNA signature. It was originally developed for the identification of lncRNAs expressed in human lymphocytes populations [3] and can be applied to any available RNA-seq dataset.

---

## 2 Materials

### 2.1 Description of Standard Bioinformatics Architecture for NGS Data Analysis and Software Requirements

1. To perform all the analysis described in Subheading 3 we recommend any UNIX-based operating system (Linux, BSD, Solaris, Mac OSX) even if the majority of tools for NGS analyses have been developed with Linux as first choice. The methodologies described in the following sections have been tested on Ubuntu 12.04.5 LTS.
2. Experimental settings: the pipeline for data analysis described in Subheading 3 was tested for paired-end, poli-A<sup>+</sup> RNA Illumina libraries considering a reads length  $\geq 100$  pb.
3. One of the steps of the analysis workflow requires the use of the STAR mapper that needs a lot of memory during running time. For this reason we recommend the use of a workstation with at least 30 GB of RAM.

### 2.2 Annotation Sources

1. Reference annotation .gtf files and genomic sequence .fasta files (hg38/mm10) can be obtained at <http://www.ensembl.org/info/data/ftp/index.html> (Ensembl FTP data repository) or <ftp://hgdownload.cse.ucsc.edu/goldenPath/> (UCSC FTP data repository).
2. Integration of reference annotation with other transcripts catalogs not included in UCSC/Ensembl database can be performed by using Cufflinks' utility Cuffcompare [8], thus excluding duplicates transcripts.

### 2.3 Software Versions Used for This Protocol

1. Cufflinks/2.2.1, fastqc/0.11.3, samtools/1.2, STAR/2.4.1c, trimmomatic/0.33, cutadapt/1.8, R/3.2.0 (DESeq2), HTSeq/0.6.1, CPAT v1.2, iSeeRNA/1.2.2.

---

## 3 Methods

### 3.1 Data Preprocessing

1. *Quality control* (pre-trimming): Raw paired-end FASTQ files resulting from a sequencing experiment are analyzed in order to evaluate the overall quality. FastQC tool (<http://www.bioinformatics.babraham.ac.uk/projects/fastqc/>) carries out this type of analysis, providing a detailed overview on different aspects of sequencing data. This is an important step to verify whether any problems occurred during library preparation or sequencing running before doing any further analysis. FastQC must be performed both on “forward” and “reverse” strand reads. [`fastqc` `--outdir.<sample_path>/R1(R2).fastq.gz`] (Fig. 3) (*see* **Notes 1** and **2**).
2. *Adapter removal*: Adapters sequences that are added during library preparation must be removed using cutadapt (

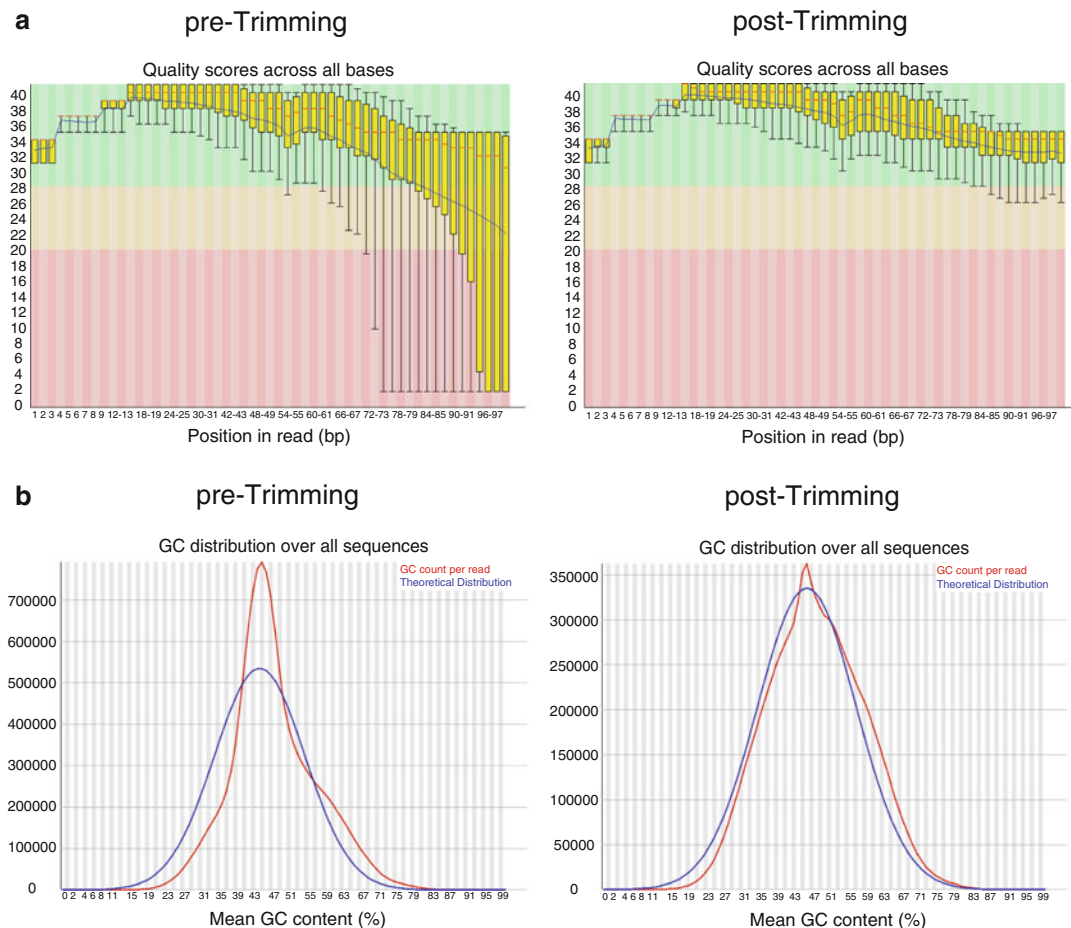


**Fig. 3** Quality control assessments. **(a)** Quality score (PHRED) of the average distribution for each base over all reads across all samples before and after trimming. **(b)** GC content distribution before and after trimming

[cutadapt.readthedocs.org/en/latest/index.html](http://cutadapt.readthedocs.org/en/latest/index.html)). This is usually necessary to avoid problems during mapping step. It is also suggested when the read length of the sequencing machine is longer than the molecule that is sequenced (for example when sequencing microRNAs). Cutadapt tool is run both for R1 and R2 indicating adapters' sequences: [cutadapt --anywhere < adapter1 > --anywhere < adapter2 > --overlap 10 --times 2 --mask-adapter --output < sample > \_R1(R2)\_cut.fastq.gz < sample\_path > /R1(R2).fastq.gz] (see Note 3).

3. *Trimming*: Trimmomatic [17] is a read trimming tool for Illumina NGS data. This software removes the sequenced bases associated with low quality score using a sliding window approach. The most important parameters to set up are: MINLEN that is the minimum length accepted for trimmed reads (50 bases in this pipeline), ILLUMINACLIP that specifies the illumina-specific sequences or adapter that must be

removed, the number of bases that could be cut in the beginning or in the end of a reads (LEADING:3 TRAILING:3), and finally the SLIDINGWINDOW parameter that scans the whole read.

4. *Quality control* (post-trimming): The “clean” FASTQ output of Trimmomatic is used as input to FastQC in order to check the results of the preprocessing steps (Fig. 3).

### 3.2 Reads Alignment to a Reference Genome

1. *Generating genome indexes*: this step should be performed before running the alignment with STAR software [18]. Starting from chromosome sequences (FASTA files) and annotation file (GTF file) available for the reference genome (see Annotation sources section), STAR builds reference indexes, that includes binary genome sequence, suffix arrays, text chromosome names and lengths information, that are necessary for reads mapping. [STAR --runMode genomeGenerate --genomeDir </path/to/GenomeDir> --genomeFastaFiles </path/to/genome/fasta1 ></path/to/genome/fasta2 > --sjdbGTFfile </path/to/annotations.gtf> --runThreadN <n>] (see Note 4).
2. *Reads Mapping*: STAR aligns the paired-end reads to the reference genome and writes several output files such as alignment files (SAM format), maps summary statistics unmapped reads, etc. The basic option to run a mapping [STAR --genomeDir </path/to/GenomeDir> --readFilesIn </path/to/read1 ></path/to/read2 > --runThreadN <n > -- <inputParameterName > --readFilesCommand zcat] (see Note 5). STAR can output alignment file in binary BAM format through --outSAMtype option, that provides also unsorted or sorted by coordinate output possibilities (see Note 6). The BAM alignment file is then indexed for further analyses (e.g., mapping visualization) using samtools utilities (<https://github.com/samtools>) [samtools index <aln.sorted.bam>] (see Note 7).

### 3.3 Data Investigation

1. *Alignment file sorting*: the BAM files should be sorted by gene identifiers in order to perform the next steps, using [samtools sort -T /tmp/aln.sorted -n -o <aln.sorted.bam ><aln.bam >] (<http://samtools.sourceforge.net/>).
2. *Read counts*: the user supplied an alignment file (BAM file) and a list of genomic features (GTF file) to count how many reads map to each feature. Genes are typically considered as feature by the user for the counting. HTSeq package [19] computes raw reads count for all samples using this command line [htseq-count [options] <alignment\_file ><gtf\_file >] (see Note 8).
3. *Principal Component Analyses (PCA)*: The raw counts produces by HTSeq are then normalized by DESeq2 [20]. The “rlog” function transforms the original samples count data to

the log scale and the final output is “variance stabilized” values. The count files are combined with a “samplesheet” to associate the different samples to the correct labels. The normalized counts are then used by DESeq2 to calculate and plot PCA analysis (using DESeq2’s “plotPCA” function)(<http://www.bioconductor.org/packages/release/bioc/vignettes/DESeq2/inst/doc/DESeq2.pdf>) (Fig. 4a).

4. *Heatmap of the sample-to-sample distances*: the transformed count data can be also used for sample clustering to obtain an overview over similarities and dissimilarities between samples. For this purpose DESeq2’s functions “hclust” and “heatmap.2” are adopted (Fig. 4b).

**3.4 De Novo Identification of Transcripts**

1. *Alignment file sorting*: the BAM files should be sorted by coordinate in order to perform de novo discovery of transcripts by Cufflinks [21] using samtools [samtools sort -T /tmp/aln.sorted -o aln.sorted.bam aln.bam].
2. *De novo Cufflinks discovery*: the identification of new transcripts (not annotated in public database) is performed by Cufflinks suite with “RABT” assembler. If a GTF file is supplied with -g option, Cufflinks identifies novel transcripts for each sample

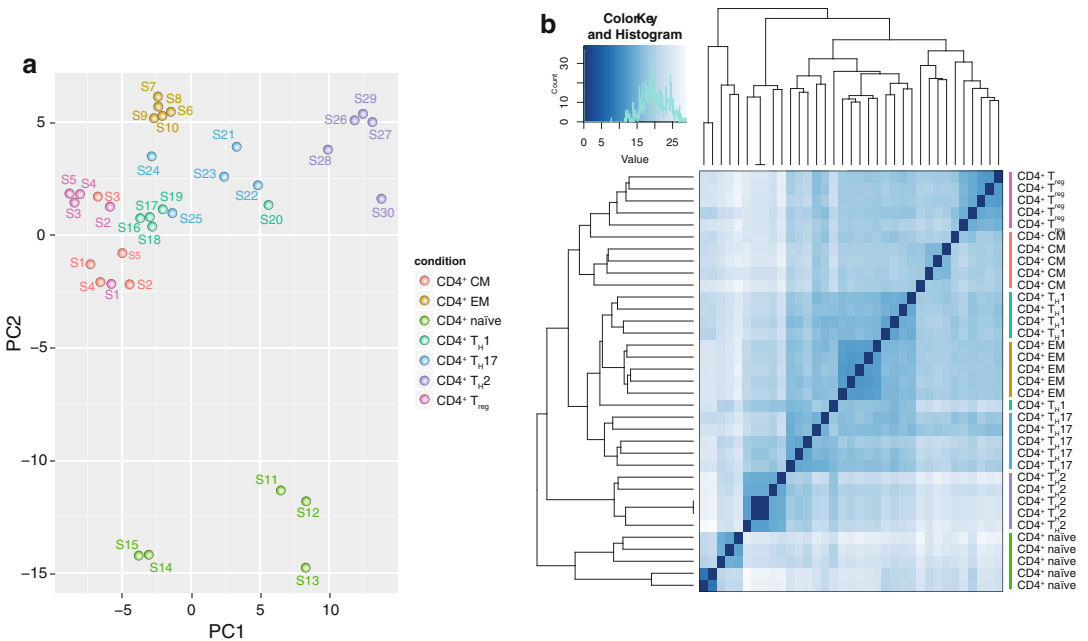


**Fig. 4** Data investigation: principal component analysis and hierarchical clustering. (a) Principal component analysis (PCA) performed using DESeq2 rlog-normalized RNA-seq data on different CD4<sup>+</sup> T cell subsets. (b) Hierarchical clustering analyses performed on the same normalized RNA-seq data. The distance metric values used for clustering are represented by a color code from *white* (low correlation) to *dark blue* (maximum correlation)

upon known reference annotation. In the output folder, the “transcripts.gtf” file contains all assembled transcripts: the annotated ones will have the correct reference gene name, the novel ones are identified instead with “XLOC” and “TCONS” prefixes, assigned respectively to genes and transcripts (*see* **Notes 9–11**).

3. *Merging assemblies with cuffmerge*: the previous step produced a catalog of predicted transcripts for each samples. It is then necessary to merge this new information with “cuffmerge” tool of Cufflinks suite. If a GTF reference file is supplied by the user, novel transcripts are integrated in the original reference annotation. The final GTF integrated file is then used as input for downstream analysis [cuffmerge <gtfs\_list> -g <ref.gtf> -s <ref\_fasta> -p <cpu\_number>].

### 3.5 De Novo Identification of lncRNAs

1. *Size selection*: For the identification of new long non coding RNAs, it is necessary to apply a size cutoff filter of 200 bp on novel identified de novo transcripts. The information about new sequences’ lengths can be recovered from “transcripts.gtf” file as a sum of exons’ lengths. The lengths of resulting transcripts could be checked on the results of “gtf\_to\_fasta” tool (included in the Cufflinks suite).
2. *Coding potential evaluation*: The novel long transcripts are translated in all six possible frames for the generation of a multi FASTA file that is the input for this analysis. The transcripts for which a PFAM match [22] is reported by HMMER’s utility “hmmscan” are filtered out. Then, CPAT [23] is used to calculate the coding potential of remaining novel long transcripts. The threshold score for the discrimination between coding/non coding is 0.364 (calculated for the human transcriptome by the authors of CPAT). The transcripts with an assigned score below this cutoff are considered putative “noncoding” RNAs (**Notes 12, 18, and 19**).

### 3.6 Differential Expression Analysis

1. *Cuffdiff*: This package (included in Cufflinks suite) allows the identification of genes that show significant changes in expression (also splicing and promoter use) between different conditions. The input of this analysis are the annotation file created with Cuffmerge and the samples BAM files. These files should be grouped in the command line (1.bam,2.bam 3.bam,4.bam) in order to defined the biological classes/populations for the comparison (class separator is the blank space). [cuffdiff [options]\* < transcripts.gtf > <sample1.bam>,<sample2.bam> <sample3.bam>,<sample4.bam>] (**Notes 13 and 14**).
2. *DEG (Differentially Expressed Genes) selection*: different output files are available for the differential expression analysis with Cuffdiff, but the “exp.diff” files (isoform\_exp.diff, gene\_exp.

diff, tss\_exp.diff, and cds\_exp.diff) contain the results of DE testing between classes/populations. The selection of DEG is carried out by extracting  $p$  or  $q$  value statistics and log<sub>2</sub>-fold change ratios across biological conditions. The “exp.diff” files also provide a column relative to the statistical significance of the test for each gene, which can be either “yes” or “no,” depending on whether  $p$  is greater than the False Discovery Rate (FDR) after Benjamini–Hochberg correction. This information as well could be used for the DEG selection. Moreover, these files can be loaded into Excel/R and used for further inspection (*see Note 15*).

3. *Intra-classes/population consistency filter*: the “read\_group\_tracking” output files of Cuffdiff could be used to assess the gene expression consistency among replicates belonging to the same class/population (*see Note 16*).

### 3.7 Downstream Analyses and Visualization

1. *Downstream analyses* are performed on normalized gene expression values obtained from “fpkm\_tracking” files of Cuffdiff output. These data can be loaded into external visualization software such as Mev (<http://www.tm4.org/mev.html>), Excel, or R.
2. *lncRNAs signatures definition*: For the identification of lncRNAs that are specifically expressed in a single class/population cluster analysis using K-means algorithm is adopted. This analysis could be integrated with the JS (Jensen-Shannon) measure to further investigate the specificity of lncRNA expression. This score is calculated on the vector of normalized values (“fpkm\_tracking” files of Cuffdiff output) using an appropriate model distribution [2, 3, 21] (*see Note 17*).

---

## 4 Notes

1. The RNA-seq raw data available in GEO database are usually in SRA format (Sequence Read Archive). It is necessary to convert these files in other formats (FASTQ, SAM, etc.) at the beginning of the analyses with SRAToolkit (<https://github.com/ncbi/sra-tools>). In particular, fastq-dump tool allows to convert the SRA format in compressed FASTQ files, running: [fastq-dump --outdir<path\_to\_outputdir> --gzip <path/input\_file>].
2. We recommend using compressed .fastq files in order to limit disk occupancy. These compressed files are accepted and directly parsed by software used in subsequent steps (FastQC and Trimmomatic for quality control and STAR for mapping step).
3. The Illumina adapter removal could be performed also by Trimmomatic tool through ILLUMINACLIP option.

4. The STAR genome indexes are saved to disk and generated only once for each genome/annotation combination.
5. During reads mapping step, we recommend adding "--genomeLoad LoadAndKeep" option to the STAR command line if several samples must be consequently analyzed. In this way STAR loads the genome index just once into shared memory and that index can be used for the next sample.
6. The compression of the SAM files could be also performed by samtools utilities, using the command line: [samtools view -bS <input\_aln.sam>><output\_aln.bam>]. Samtools also allows to sort the alignment file by chromosomal coordinates or read names running: [samtools sort -T </tmp/aln.sorted> -o <output\_aln.sorted.bam> <input\_aln.bam>].
7. Information about mapping results: several baseline statistics are retrieved also by samtools flagstat tool: [samtools flagstat <output\_aln.bam>].
8. STAR mapper performs the counting of number of reads per gene, similar to htseq-count, running the --quantMode GeneCounts option.
9. There are two alternative computational strategies for transcriptome reconstruction: mapping-first approaches and Assembly-first (de novo) methods. The Cufflinks-based approach described here belongs to the first class of methods: it first aligns all the reads to a reference genome, then merges sequences with overlapping alignment, spanning splice junctions with reads and paired-ends. In this way, computational complexity of calculations is reduced. We suggest combining this approach with Assembly-first (de novo) methods such as Trinity [24], SOAPdenovo [25], or Oases [26] in order to obtain a higher number of novel transcripts. These softwares use the reads to assemble transcripts directly, which can be mapped subsequently to a reference genome, if available. To balance specificity and sensitivity of detection for the transcriptome reconstruction of human data, it is advisable to start from more than 50 million paired-end reads (This estimate is based on the Trinity publication [24], where 52.6 million 76 bp read pairs were used).
10. If the user adopts multiple de novo strategies for the identification of novel, non-annotated, transcripts (e.g., Cufflinks, Scripture [27], Trinity), it is necessary to merge the different catalogs into single coherent and nonredundant annotation using "cuffmerge" utility from the Cufflinks suite.
11. If different biological replicates are available for a class/population in analysis, we recommend to pull all the samples in a single Cufflinks run in order to increase detection sensitivity. For the detection of alternative splicing events, data should be kept separate

12. Also iSeeRNA, a support vector machine (SVM)-based classifier, has been recently suggested for high throughput screening of lincRNAs [28]. It is possible to crosscheck CPAT results with the iSeeRNA webserver (<http://137.189.133.71/iSeeRNA/webserver.html>).
13. Cuffdiff has three different normalization methods: “classic-fpkm,” “geometric,” and “quartile.” The default for differential expression analysis is “geometric” where FPKMs and fragment counts are scaled via the median of the geometric means of fragment counts across all libraries, as described in Anders and Huber [29]. This is recommended if the user compares the obtained expression values with DESeq2 approach. The “quartile” method scales the FPKMs and fragment counts via the ratio of the 75 quartile fragment counts to the average 75 quartile value across all libraries. It can be used to improve robustness of differential expression calls for less abundant genes and transcripts.
14. Differential expression analysis by Cuffdiff is a time-consuming step, especially when the number of samples is large. For this reason, if the execution time is important for the user, we suggest to replace Cuffdiff with DESeq2 that performs gene-level DE analysis or DEXSeq (Anders and Rayers) for isoform expression characterization (based on exons occupancy evaluation). Alternative approaches, also present in Bioconductor, are “edgeR” (<http://bioconductor.org/packages/release/bioc/html/edgeR.html>) and “bayseq” (<http://www.bioconductor.org/packages/release/bioc/html/baySeq.html>).
15. The normalized FPKM values from Cuffdiff approach can be alternatively replaced with normalized counts data (rlogs) produced by DESeq2 during the previous “data investigation” step. The regularized-logarithm transformation (rlogs transformation) crosses the problem of “the variance grows with the mean” for raw count data. This normalization is similar to the ordinary log<sub>2</sub> transformation of normalized counts for high counts genes, for the lower counts the values are shrunken towards the genes’ averages across all samples [20].
16. The consistency among replicates of the same population/class is an important filter for novel identified genes because it ensures that the expression level of a specific gene is not a technical or biological artifact. This issue is more relevant when working with biological (and not technical) replicates, where a discrepancy may indicate biological differences that are peculiar to the set of donors who are chosen for the experiment.
17. The K-means clustering is employed in lncRNAs signatures definition step for the identification of specifically expressed lncRNAs. In order to define the ideal number of cluster (K)

that better described the data, a “silhouette” measure can be used (available in the R package “cluster”). Alternatively, a plot of the within groups sum of squares by number of clusters extracted can be used (<http://www.statmethods.net/advstats/cluster.html>).

18. The de novo discovery of transcripts by Cufflinks-Cuffmerge approach generates a catalog of nonredundant sets of lncRNAs named with a standard code followed by progressive integer “id” (XLOC\_id and TCONS\_id). We suggest to rename these codes by following the guidelines in **Note 18** to avoid overlap with existing external annotations.
19. At the time of writing, a “gold standard” annotation for lncRNAs is not available because the discovery of these transcripts is clearly not yet complete. Several international consortia and platforms as well as HUGO Gene Nomenclature Committee (HGNC), that provided the first guidelines for lncRNA annotation, are attempting to develop a more unified system for lncRNA annotation. We advise the readers to follow the suggestions proposed in a recent review by Mattick and Rinn [30].

## References

1. Mercer TR, Mattick JS (2013) Structure and function of long noncoding RNAs in epigenetic regulation. *Nat Struct Mol Biol* 20(3):300–307. doi:10.1038/nsmb.2480
2. Cabili MN, Trapnell C, Goff L et al (2011) Integrative annotation of human large intergenic noncoding RNAs reveals global properties and specific subclasses. *Genes Dev* 25(18):1915–1927. doi:10.1101/gad.17446611
3. Ranzani V, Rossetti G, Panzeri I et al (2015) The long intergenic noncoding RNA landscape of human lymphocytes highlights the regulation of T cell differentiation by linc-MAF-4. *Nat Immunol* 16(3):318–325. doi:10.1038/ni.3093
4. Iyer MK, Niknafs YS, Malik R et al (2015) The landscape of long noncoding RNAs in the human transcriptome. *Nat Genet* 47(3):199–208. doi:10.1038/ng.3192
5. Ilott NE, Ponting CP (2013) Predicting long non-coding RNAs using RNA sequencing. *Methods* 63(1):50–59. doi:10.1016/j.ymeth.2013.03.019
6. Pagani M, Rossetti G, Panzeri I et al (2013) Role of microRNAs and long-non-coding RNAs in CD4(+) T-cell differentiation. *Immunol Rev* 253(1):82–96. doi:10.1111/imr.12055
7. Panzeri I, Rossetti G, Abrignani S, Pagani M (2015) Long intergenic non-coding RNAs: novel drivers of human lymphocyte differentiation. *Front Immunol* 6:175. doi:10.3389/fimmu.2015.00175
8. Diederichs S (2014) The four dimensions of non-coding RNA conservation. *Trends Genet* 30(4):121–123. doi:10.1016/j.tig.2014.01.004
9. Bentwich I, Avniel A, Karov Y et al (2005) Identification of hundreds of conserved and nonconserved human microRNAs. *Nat Genet* 37(7):766–770. doi:10.1038/ng1590
10. Johnsson P, Lipovich L, Grander D, Morris KV (2014) Evolutionary conservation of long non-coding RNAs; sequence, structure, function. *Biochim Biophys Acta* 1840(3):1063–1071. doi:10.1016/j.bbagen.2013.10.035
11. Fatica A, Bozzoni I (2014) Long non-coding RNAs: new players in cell differentiation and development. *Nat Rev Genet* 15(1):7–21. doi:10.1038/nrg3606
12. Rinn JL, Kertesz M, Wang JK et al (2007) Functional demarcation of active and silent chromatin domains in human HOX loci by noncoding RNAs. *Cell* 129(7):1311–1323. doi:10.1016/j.cell.2007.05.022
13. Batista PJ, Chang HY (2013) Long noncoding RNAs: cellular address codes in development

- and disease. *Cell* 152(6):1298–1307. doi:[10.1016/j.cell.2013.02.012](https://doi.org/10.1016/j.cell.2013.02.012)
14. Guttman M, Rinn JL (2012) Modular regulatory principles of large non-coding RNAs. *Nature* 482(7385):339–346. doi:[10.1038/nature10887](https://doi.org/10.1038/nature10887)
  15. Gloss BS, Dinger ME (2015) The specificity of long noncoding RNA expression. *Biochim Biophys Acta*. doi:[10.1016/j.bbagr.2015.08.005](https://doi.org/10.1016/j.bbagr.2015.08.005)
  16. Bonnal RJ, Ranzani V, Arrigoni A, Curti S, Panzeri I, Gruarin P et al (2015) De novo transcriptome profiling of highly purified human lymphocytes primary cells. *Sci Data* 2:150051. doi:[10.1038/sdata.2015.51](https://doi.org/10.1038/sdata.2015.51)
  17. Bolger AM, Lohse M, Usadel B (2014) Trimmomatic: a flexible trimmer for Illumina sequence data. *Bioinformatics* 30(15):2114–2120. doi:[10.1093/bioinformatics/btu170](https://doi.org/10.1093/bioinformatics/btu170)
  18. Dobin A, Davis CA, Schlesinger F et al (2013) STAR: ultrafast universal RNA-seq aligner. *Bioinformatics* 29(1):15–21. doi:[10.1093/bioinformatics/bts635](https://doi.org/10.1093/bioinformatics/bts635)
  19. Anders S, Pyl PT, Huber W (2015) HTSeq—a Python framework to work with high-throughput sequencing data. *Bioinformatics* 31(2):166–169. doi:[10.1093/bioinformatics/btu638](https://doi.org/10.1093/bioinformatics/btu638)
  20. Love MI, Huber W, Anders S (2014) Moderated estimation of fold change and dispersion for RNA-seq data with DESeq2. *Genome Biol* 15(12):550. doi:[10.1186/s13059-014-0550-8](https://doi.org/10.1186/s13059-014-0550-8)
  21. Trapnell C, Williams BA, Pertea G et al (2010) Transcript assembly and quantification by RNA-Seq reveals unannotated transcripts and isoform switching during cell differentiation. *Nat Biotechnol* 28(5):511–515. doi:[10.1038/nbt.1621](https://doi.org/10.1038/nbt.1621)
  22. Bateman A, Coin L, Durbin R et al (2004) The Pfam protein families database. *Nucleic Acids Res* 32(Database issue):D138–D141. doi:[10.1093/nar/gkh121](https://doi.org/10.1093/nar/gkh121)
  23. Wang L, Park HJ, Dasari S et al (2013) CPAT: coding-potential assessment tool using an alignment-free logistic regression model. *Nucleic Acids Res* 41(6), e74. doi:[10.1093/nar/gkt006](https://doi.org/10.1093/nar/gkt006)
  24. Haas BJ, Papanicolaou A, Yassour M et al (2013) De novo transcript sequence reconstruction from RNA-seq using the Trinity platform for reference generation and analysis. *Nat Protoc* 8(8):1494–1512. doi:[10.1038/nprot.2013.084](https://doi.org/10.1038/nprot.2013.084)
  25. Xie Y, Wu G, Tang J et al (2014) SOAPdenovo-trans: de novo transcriptome assembly with short RNA-Seq reads. *Bioinformatics* 30(12):1660–1666. doi:[10.1093/bioinformatics/btu077](https://doi.org/10.1093/bioinformatics/btu077)
  26. Schulz MH, Zerbino DR, Vingron M, Birney E (2012) Oases: robust de novo RNA-seq assembly across the dynamic range of expression levels. *Bioinformatics* 28(8):1086–1092
  27. Guttman M, Garber M, Levin JZ et al (2010) Ab initio reconstruction of cell type-specific transcriptomes in mouse reveals the conserved multi-exonic structure of lincRNAs. *Nat Biotechnol* 28(5):503–510. doi:[10.1038/nbt.1633](https://doi.org/10.1038/nbt.1633)
  28. Sun K, Chen X, Jiang P et al (2013) iSeeRNA: identification of long intergenic non-coding RNA transcripts from transcriptome sequencing data. *BMC Genomics* 14(Suppl 2):S7. doi:[10.1186/1471-2164-14-S2-S7](https://doi.org/10.1186/1471-2164-14-S2-S7)
  29. Anders S, Huber W (2010) Differential expression analysis for sequence count data. *Genome Biol* 11(10):R106. doi:[10.1186/gb-2010-11-10-r106](https://doi.org/10.1186/gb-2010-11-10-r106)
  30. Mattick JS, Rinn JL (2015) Discovery and annotation of long noncoding RNAs. *Nat Struct Mol Biol* 22(1):5–7. doi:[10.1038/nsmb.2942](https://doi.org/10.1038/nsmb.2942)

# Chapter 15

## Highly Multiplexed, Single Cell Transcriptomic Analysis of T-Cells by Microfluidic PCR

Maria Dominguez, Mario Roederer, and Pratip K. Chattopadhyay

### Abstract

Recently, technologies have been developed to measure expression of 96 (or more) mRNA transcripts at once from a single cell. Here we describe methods and important considerations for use of Fluidigm's BioMark platform for multiplexed single cell gene expression. We describe how to qualify primer/probes, select genes to examine in 96-parameter panels, perform the reverse transcription/cDNA synthesis step, and operate the instrument. In addition, we describe data analysis considerations. This technology has enormous value for characterizing the heterogeneity of T-cells, thereby providing a useful tool for immune monitoring.

**Key words** Single cell analysis, Quantitative competitive real-time PCR, Microfluidic, T-cell, Transcriptome

---

### 1 Introduction

A vast array of molecules govern the maturity, homing, and function of T-cells. When measured together, combinations of these markers define a wide variety of T-cell subsets, each with a particular role in immunity [1]. As the heterogeneity of T-cells has become clear, it has also become apparent that complete characterization of an immune response requires highly multiplexed technologies. Moreover, these technologies must provide data at the single cell level, since bulk (population-based) analysis cannot resolve cell-by-cell differences in expression [2]. Finally, many markers of interest are expressed at low levels, so sensitivity is an important feature of any technology used to interrogate T-cells.

Quantitative, real-time PCR offers a particularly sensitive method for measuring T-cell markers. With the Fluidigm BioMark system, this technology has been adapted to microfluidic chips. The BioMark

---

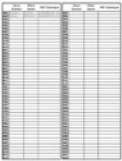
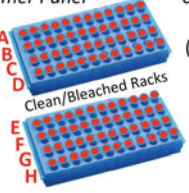
Maria Dominguez and Pratip K. Chattopadhyay contributed equally to this work.

**Electronic supplementary material:** The online version of this chapter (doi:[10.1007/978-1-4939-6548-9\\_15](https://doi.org/10.1007/978-1-4939-6548-9_15)) contains supplementary material, which is available to authorized users.

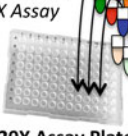
**Day 01: Fluidigm Benchtop Guide**

Use powder-free gloves  
Change often 

**Morning**

<p><b>1</b></p> <p>Select 96 TaqMan P&amp;P and create <i>TaqMan Primer Panel.xls</i></p> 	<p><b>2</b></p> <p>Remove P&amp;P aliquots from -30°C freezer</p> 	<p><b>3</b></p> <p>Thaw P&amp;P at room temp or 4°C in non-sterile plastic racks or boxes</p> 	<p><b>4</b></p> <p>Vortex all tubes thoroughly</p> 	<p><b>5</b></p> <p>Spin down tubes at 10K RPM for 30 sec</p> 	<p><b>6</b></p> <p>Sterilize tubes by wiping down exteriors with:</p> <ul style="list-style-type: none"> <li>• Wrung-out Clorox Wipe</li> <li>• Mini Hype Wipe</li> <li>• Kimwipe &amp; 10% Bleach</li> </ul> 	<p><b>7</b></p> <p>Arrange P&amp;P in 2 sterile (bleached) dry racks in same order as <i>TaqMan Primer Panel</i></p> 	<p><b>8</b></p> <p>Allow tubes to dry completely at 4°C (minimum 45 min)</p>
---	---	---	--	--	---	---	--

**Afternoon**

<p> Change before entering hood</p>	<p><b>9</b></p> <p>Dispense P&amp;Ps individually into assigned well in <i>20X Assay Plate</i></p> 	<p><b>10</b></p> <p>Combine P&amp;Ps in one tube to create <i>0.2X Assay Mix</i></p> 	<p><b>11</b></p> <p>Add DNA Suspension Buffer to <i>0.2X Assay Mix</i> to reach [0.2X]</p>	<p><b>12</b></p> <p>Heat Seal <i>20X Assay Plate</i></p> 	<p><b>13</b></p> <p>Return P&amp;Ps to -30°C freezer. Store <i>20X Assay Plate</i> &amp; <i>0.2X Assay Mix</i> at -30°C or 4°C</p> 
--	--	--	--	--	--

**Fig. 1** Illustrated guide to protocol steps for day 1

system can report expression of 96 different genes from a single cell, with a limit of detection at the level of a single mRNA molecule. Cells can be isolated for BioMark analysis using proprietary cell capture systems (like Fluidigm’s C1) or fluorescence-activated cell sorting (FACS). The latter allows very efficient capture of single T-cells (>99%, compared to 60–80% on the C1), and FACS-purified cells can be selected based on the expression profile of surface proteins.

The protocol presented here focuses on cell capture by FACS, and subsequent processing and analysis steps in the BioMark workflow. Figures 1 and 2 summarize the steps involved, and can be kept at the lab bench for easy reference. Methods and considerations are presented for designing BioMark panels, primer/probe qualification, cell preparation, reverse transcription/cDNA amplification, microfluidic chip setup, and data analysis.

**2 Materials**

**2.1 Instrument, Primer/Probes, Materials Necessary for Qualification**

1. BioMark HD (Fluidigm).
2. IFC Controller (Fluidigm).
3. TaqMan Gene Expression Assays (ThermoFisher).
4. Phorbol 12-myristate 13-acetate (PMA).

## Day 02: Fluidigm Benchtop Guide

Use powder-free gloves  
Change often

## Morning

**1** 30-45 min prior: Remove *Cells Direct 2X Rxn Mix* from mini freezer

**2** <5 min prior: Remove 0.2X *Assay Mix* from freezer

**3** Remove *SuperscriptIII Platinum Taq & SupersaseIN* from mini freezer

**4** Vortex all tubes thoroughly

**5** Spin down tubes at 10K RPM for 30 sec

**6** Sterilize tubes by wiping down exteriors with:

- Wring-out Clorox Wipe
- Mini Hype Wipe
- Kimwipe & 10% Bleach

**7** Change before entering hood

Prepare volume of RT-PreAmp rxn mix calculated from 04 – FACS RT-PreAmp Reaction Mix.xls

FACS RT-PreAmp Rxn Mix

## Afternoon

**8** Use sterile reservoir & multichannel pipette to dispense 10ul of *FACS RT-PreAmp Rxn Mix* into every well in 96-well plate

**9** Seal Plate with plastic pressure seal, spin down at 1200 RPM for 5 sec and chill on ice until

**10** FACS sort into plate, Use chilled plate-holder

**11** Seal plate with heated sealer, cooling plate btwn seals

**12** Cool top and bottom of plate, vortex plate and spin down (1200 RPM; 5 sec)

**13** Place plate on thermocycler and run the RT-PreAmp Protocol: 'Maria'

**14** Dilute cDNA 1:5 in DNA suspension buffer.

Fig. 2 Illustrated guide to protocol steps for day 2

5. Ionomycin at 20 ng/mL, ionomycin at 1 µg/mL.
6. RNAeasy Plus Universal Kit (Qiagen).
7. Chlorox Wipe (Clorox), Mini-Hype Wipe (Fisher Scientific), or a Kimwipes (Kimtech Science).
8. JMP software (SAS Institute).

## 2.2 Assay Mix, Assay Plate, Heat Sealer

1. DNA Suspension Buffer.
2. 96-Well PCR Plate.
3. Thermo Easy Pierce Heat Sealing Foil.
4. ALPS 25 Manual Heat Sealer (ThermoFisher).

## 2.3 Pre-Amp Reaction Mix and FACS Media

1. DPEC-treated water.
2. CellsDirect One-Step qRT PCR kit (ThermoFisher).
3. Superase In RNAase Inhibitor (ThermoFisher).
4. FACS Staining Media: RPMI1640 without biotin or phenol red (available as a custom order from ThermoFisher). Alternatively, PBS or PBS with 10% fetal or newborn calf serum may be substituted.

## **2.4 IFC and Chip Materials**

1. Assay Loading Reagent (Fluidigm).
2. GE Sample Loading Reagent (Fluidigm).
3. Control Line Fluid (Fluidigm).
4. 96.96 Dynamic Array Chip for Gene Expression (Fluidigm).

---

## **3 Methods**

### **3.1 Primer/Probe Selection, Qualification, and Storage**

1. TaqMan Gene Expression Assays (the primers and probes used in the BioMark system, “Assays”) are available for a large number of human and mouse mRNA targets. We selected transcripts to study based on their relevance in T-cell immunity, including T-cell homing markers, cytokines, cytolytic enzymes, apoptosis genes, signal transduction molecules, and transcription factors. Assays were then chosen from the catalog of “inventoried” or “made-to-order” TaqMan Assays qualified for standard qPCR. Notably, this did not guarantee that an Assay would work in the BioMark system; therefore, we developed the Assay qualification procedure described below (and in [3]).
2. Where multiple Assays were available for the same transcript, base your initial selection as such: (a) exon boundaries, to ensure that mRNA is amplified, (b) size of amplicon (140 bp or less), and (c) the number of reference sequences. These criteria cannot always be met, nor do they guarantee a primer would qualify.
3. Qualify each Assay in the BioMark panels by assessing the following [3]: (a) Is amplification efficient; does signal double with each PCR cycle? (b) Is amplification linear; is final signal proportional to input RNA?, and (c) Do primers compete when multiplexed; are efficiency and linearity preserved when a primer is added to an existing set?
4. The number of copies of a transcript can differ dramatically between genes and across cell types. Therefore, for Assay qualification, use a bulk mixture of RNA obtained from resting and PMA-ionomycin stimulated PBMC. Perform Assay qualifications on 12-point, twofold dilution series of this RNA mixture, and replicate them eight times across the PCR plate. Perform reverse transcription, cDNA amplification, and Biomark analysis under the same conditions as experimental samples, as described later in this protocol.
5. Analyze the Assay qualification data using an iterative, piecewise approach [3]. First, plot Et values (40-Ct) for each replicate dilution series against log RNA concentration. Within a dilution series, evaluate overlapping segments of six data points for linear and efficient amplification. (For example, for each of the eight replicate dilution series, the linearity and efficiency of the CCR7 Assay was evaluated for dilution points 1–6, 2–7,

3–8, 4–9, 5–10, 6–11, and 7–12.) An Assay qualifies if a single “piece” of five consecutive dilutions from any of the dilution segments (across any of the dilution series) gives linear and efficient amplification (*see Note 1*).

6. A procedure for testing Assay competition is presented in [3]. In short, we did not find Assay competition problems in our testing of the BioMark workflow, and no longer include this step in our Assay qualifications (*see Note 2*).
7. Supplemental File 1 (Assay Database.xls) summarizes all TaqMan Gene Expression Assays we have tested to date. The database can be used as a starting point for designing BioMark panels, sparing the time and expense associated with the qualification process.
8. We store TaqMan Gene Expression Assays in 50  $\mu$ L aliquots (at  $-30^{\circ}\text{C}$ ) to prevent repeated freeze-thaw cycles. Aliquots are discarded after the fifth use, or if in storage for more than 2 years. When the same assay is used on consecutive days, it may be stored at  $4^{\circ}\text{C}$ .

### 3.2 Panel Design

1. When designing Assay panels for large studies, marker correlation should be considered. Pairs of markers that are highly correlated provide no unique information, so it is worth considering replacement of one member of the pair.
2. To test correlation between markers, perform preliminary experiments in which 25–100 cells are sorted from cell populations of interest. Follow the BioMark workflow (described in detail later in the protocol), and test the pairwise correlation between the Assays. These correlations are clustered, to more easily identify Assays that are highly correlated (Fig. 3) (*see Note 3*).

### 3.3 Assembling BioMark Panels

The steps in this section should be performed 2 days before the experiment.

#### 3.3.1 Thawing Assays

1. We have developed a worksheet that tracks the Assays used in a particular panel and can be used in our data analysis workflow. Open Supplemental File 2 (AssayPanelWorksheet.xls), and fill in the appropriate information for the Assays that will be run.
2. We have developed a spreadsheet that automatically calculates the volume of each Assay to add for the reverse transcription/cDNA synthesis step (using the FACS 0.2 $\times$  Assay Mix, *see Subheading 2*) and for the BioMark on-chip amplification (using the 20 $\times$  Assay Plate, *see Subheading 2*). Open Supplemental File 3 (FACS 0.2 $\times$  Assay Mix and 20 $\times$  Assay Plate.xls) and enter into the green boxes the total number of plates that will be run in the experiment and the number of Assays (usually 96) that will be used in the experiment. This spreadsheet can also be used to plan reagent needs for large studies.

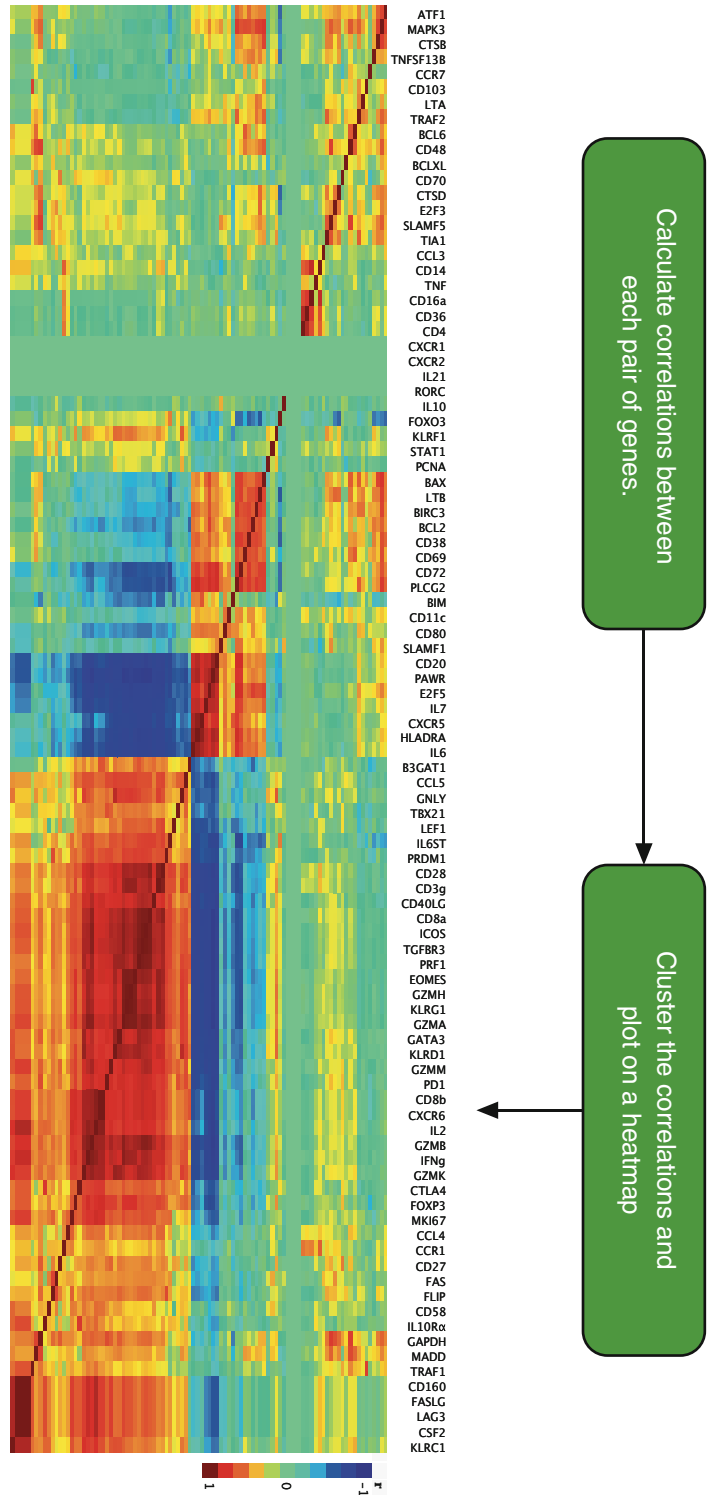


**Fig. 3** Cluster analysis of gene expression. Example demonstrating how correlations between assays can be clustered and plotted. Highly correlated or anti-correlated assays can be considered for replacement

3. Remove aliquots of 20× Taqman Assays from freezer and keep on dry ice while arranging in racks. Be sure to follow the same order as indicated in the Assay Panel Worksheet (*see* Subheading 3.3.1, **step 2**; Supplemental File 2). Work quickly and only remove a few boxes of Assays from -30 °C storage at a time.
4. Transfer these racks (containing the Assay aliquots) to a 4 °C refrigerator to thaw overnight.

### 3.3.2 Building 0.2× Assay Mix and 20× Assay Plate

1. The morning after the Assay aliquots have thawed, vortex, and spin at  $56 \times g$  for 30 s in a microcentrifuge.
2. While transferring vials from microcentrifuge, sterilize Assay aliquots by wiping down exterior of tube with Chlorox Wipe (that has been rung out to release excess fluid), Mini-Hype Wipe, or a Kimwipes that has been sprayed with 10% bleach.
3. Carefully place each sterilized assay aliquot into a rack treated with bleach (and dried), ensuring that the order of assays is the same as that listed in the Assay Panel Worksheet (Supplemental File 2).
4. Place racked Assay aliquots into 4 °C for at least 1 h to allow tubes to dry completely. This prevents drops of bleach from entering the uncapped tube and disassociating the probe from the primer.
5. In the afternoon, pull the first rack of Assays to build the 0.2× Assay Mix and 20× Assay Plate. Leave any other racks at 4 °C until they are ready to be dispensed.
6. Open Supplemental File 3 (FACS 0.2× Assay Mix and 20× Assay Plate.xls) and dispense the indicated volume of each Assay, first into the FACS 0.2× Assay Mix and then into the 20× Assay Plate.
7. To the FACS 0.2× Assay Mix, add the volume of DNA Suspension Buffer (low EDTA buffer TE) indicated in Supplemental File 3 (FACS 0.2× Assay Mix and 20× Assay Plate.xls). Mix to reach a final concentration of 0.2× per Assay.
8. Store Assay aliquots and FACS 0.2× Assay Mix in -30 °C freezer (for long-term storage) or at 4 °C (for use within 1 week).

### 3.3.3 Heat Sealing the 20× Assay Plate(s)

1. If the 20× Assay Plate contains more than 50 µL/well, split across multiple plates to limit freeze-thaws. This occurs typically when making 20× Assay plates that cover more than 10 or more FACS plates.
2. Prepare metal plate holders by freezing them at -30 °C (*see Note 4*).
3. Remove heat seals carefully from the package, so as to not touch the metallic underside of the seal (or any other seals in the package). Orient the package so the white matte side is facing up,

and use thumb and forefinger to pinch the topmost section of the seal to separate it from other seals in the package.

4. Place the seal on the 20× Assay Plate.
5. Push the heater past the first stop, and hold for 5 s.
6. Immediately place the plate in the frozen metal plate holder, and use a rubber roller to apply rolling pressure to the entire surface. Work from the middle to the outer edge of the seal, paying particular attention to the corners and edges of the plate.
7. Orient the plate in the opposite direction and repeat **steps 6** and **7**.
8. Repeat in various orientations until a concave seal is observed for each well; replace the frozen metal plate holder with another, if needed.
9. Store 20× Assay Plates in  $-30\text{ }^{\circ}\text{C}$  freezer until use.

### **3.4 Cell Sorting, Reverse Transcription, and cDNA Amplification**

#### **3.4.1 Preparation**

This protocol is written for analysis of a single cell per well; however, it can be adapted to study multiple cells per well (*see Note 5*).

1. Open Supplemental File 4 (04-FACS RT-PreAmp Reaction Mix.xls) to calculate the volume of reverse transcription/cDNA amplification reaction mix (“RT-preAmp mix”) needed for the experiment.
2. One hour before cell sorting, stain cells for 15 min with the fluorescently tagged antibodies that will be used to define the cell populations of interest. Wash cells twice and resuspend in FACS Staining Media (*see* Subheading **2**).
3. Remove Cells Direct 2× Rxn Mix from freezer and thaw at room temperature for 30–45 min before cell sorting.
4. Five minutes before sorting, remove FACS 0.2× Assay Mix from freezer. Thaw at room temperature.
5. Remove Superscript III Platinum Taq and Superase IN from freezer, place in cold ( $4\text{ }^{\circ}\text{C}$ ) block.
6. Vortex all reagents thoroughly. Spin in microcentrifuge at  $5590\times g$  for 30 s. Wipe down exterior of tubes, as in **step 2** of Subheading **3.3.2**. Take care not to soak tubes, wipe off excess bleach solution. Put all reagents on ice.
7. Change gloves, and enter a PCR hood. Prepare the RT-PreAmp Mix by dispensing the appropriate volume of each reagent as calculated in Supplemental File 4 (**step 1** of this section). Prepare this mix in a sterile (autoclaved) tube. Vortex.
8. Open a sterile multichannel pipette reservoir inside the PCR hood. Pour RT-PreAmp mix into reservoir, and use a multichannel pipette to dispense  $10\text{ }\mu\text{L}$  into every well of a sterile 96-well PCR plate.
9. Seal plate with plastic pressure seal (without heat), and spin in centrifuge at  $500\times g$  for 5 s. Place on ice while transporting to FACS instrument.

### 3.4.2 FACS, Reverse Transcription, and cDNA Amplification

1. Follow manufacturer's instructions for instrument setup, ensuring in particular that sorter is properly aligned with 96-well PCR plate.
2. Place the unsealed 96-well PCR plate in a frozen/chilled metal plate holder. Sort cells of interest directly into plate.
3. Record relevant sample information into Supplemental File 5 (Sample Map.jump) or Supplemental File 6 (Sample Map.xls). Supplemental File 5 is compatible with our workflow for mapping and labeling samples and Assays.
4. Immediately after sorting, heat seal plate as described in Subheading 3.3.3. If multiple applications of the heat sealer are needed, ensure the top of the plate has cooled before applying more heat.
5. Once sealed, vortex plate and centrifuge at  $500\times g$  for five seconds.
6. Place the plate in a thermocycler set for the following protocol: (a)  $50\text{ }^{\circ}\text{C}$  for 15 min (reverse transcription), (b)  $95\text{ }^{\circ}\text{C}$  for two minutes (Reverse Transcriptase inactivation), and (c)  $95\text{ }^{\circ}\text{C}$  for 15 s +  $60\text{ }^{\circ}\text{C}$  for 4 min for 18 cycles (cDNA amplification).
7. Once thermocycling is complete, the resultant cDNA can be stored at  $4\text{ }^{\circ}\text{C}$  overnight (if the plate will be run on the BioMark the next day), or at  $-30\text{ }^{\circ}\text{C}$  for long-term (3 months) storage.

## 3.5 Preparing the BioMark Chip

### 3.5.1 cDNA Dilution

1. Thaw cDNA plate (if necessary) on ice. Vortex, and centrifuge at  $500\times g$  for 5 s. Sterilize plate by adapting the method described in **step 2** of Subheading 3.3.2. Dry plate completely, and return to ice.
2. Peel off plate seal outside of hood.
3. Obtain a new, sterile 96-well PCR plate. Add 20  $\mu\text{L}$  of DNA Suspension Buffer into every well. Use a multichannel pipettor and sterile reservoir.
4. Pipette mix three times (going no further than the first stop on the pipettor) and transfer 5  $\mu\text{L}$  from each well in the cDNA plate into the matching well in the new 96-well plate (containing the DNA suspension buffer). When dispensing the cDNA only push the pipette trigger to the first stop. Do not pipette mix after dispensing the cDNA. This keeps cDNA quantities uniform across wells and avoid introducing bubbles.
5. Heat seal the plate, as described in Subheading 3.3.3. If the diluted cDNA will be run on the BioMark within 1 day, it may be stored at  $4\text{ }^{\circ}\text{C}$ . Otherwise store diluted cDNA at  $-3\text{ }^{\circ}\text{C}$ .

### 3.5.2 Create the $10\times$ Assay Plate

1. Thaw  $20\times$  Assay Plate, created in Subheadings 3.3.2 and 3.3.3, on ice. Vortex, and centrifuge at  $500\times g$  for 5 s. Sterilize plate by adapting the method described in **step 2** of Subheading 3.3.2. Dry plate completely, and return to ice. Thaw Assay Loading Reagent.

2. Obtain a new, sterile 96-well PCR plate. Dispense 4  $\mu\text{L}$  of Fluidigm GE Assay Loading Reagent into every well. This will become the 10 $\times$  Assay Plate.
3. Dispense a 4  $\mu\text{L}$  of 20 $\times$  Assay from the 20 $\times$  Assay Plate, into the matching well of the 10 $\times$  Assay Plate. Follow the same instructions for pipette handling as in **step 4** of Subheading 3.5.1.
4. Only prepare enough 10 $\times$  Assay Plates for the week's experiments. These plates expire in 1 week.
5. Heat seal the plate, as described in Subheading 3.3.3. Keep on ice until use, or in  $-30\text{ }^{\circ}\text{C}$  freezer. Use within 1 week.

### 3.5.3 Create the Real-Time Reaction Mix

1. Thaw TaqMan Universal PCR Master Mix (part of *ellsDirect* Kit), Fluidigm Sample Loading Reagent, and diluted cDNA plate, if necessary. Vortex, and centrifuge at  $200\times g$  for thirty seconds. Sterilize bottles and cDNA plate by adapting the method described in **step 2** of Subheading 3.3.2. Dry plate and all materials completely, and return to ice.
2. Create the Real-Time Reaction Mix for a single BioMark plate at a time. It must be used immediately. In a sterile tube, add 80  $\mu\text{L}$  of Fluidigm Sample Loading Reagent and 800  $\mu\text{L}$  of the TaqMan Universal PCR Master Mix. Vortex, and centrifuge at  $200\times g$  for 30 s.

### 3.5.4 Prime the Chip

1. The process of priming lubricates the microfluidic channels and valves in the chip. This process takes 30 min.
2. Turn on the IFC Controller. Open the cardboard package containing a new chip; do not unwrap the chip from its aluminum packaging.
3. Wearing gloves, grasp the chip on the sides (not on the top and bottom) and bring it into the PCR hood. Open the chip's aluminum wrap in the hood. Take care not to pass your hand over the chip; work with sterile technique.
4. Remove the Control Line Fluid Syringes from the packaging and use covered syringes to depress the intake valves on both sides of the chip.
5. Working with one syringe at a time, remove the plastic black cap, point the needle down, and allow 1–2 drops of fluid to fall inside the hood before starting.
6. Between drops (i.e., while the syringe is not dripping), quickly insert the syringe into the closest intake valve and depress the plunger to fully inject all the fluid in the syringe.
7. Remove syringe slowly to avoid splatter. If any liquid falls onto the center of the chip (where the microfluidic channels are) or around the intake valves, then discard the chip and start again.
8. Turn chip around so that the other intake valve is closest, repeat **steps 4–7**.

9. Remove the protective plastic from beneath the plate. Place chip inside aluminum packaging to protect it while walking to the instrument.
10. Place chip on IFC Controller with the notched side lining up to “A1” and run the “Prime” script.
11. While the chip is priming, prepare the Sample Plate (Subheading 3.5.5). Once the chip is primed, the samples and primers must be dispensed into the chip inlets within 1 h.

### 3.5.5 Create the Sample Plate

1. The plate of diluted cDNA, created in Subheading 3.5.1, should be thawed (if necessary), vortexed, centrifuged (at  $5000 \times g$  in microcentrifuge for 5 s), and sterilized (by adapting the method described in **step 2** of Subheading 3.3.2). Dry plate completely; keep on ice until use.
2. Transfer the Real-Time Reaction Mix (prepared in Subheading 3.5.3) to a sterile reservoir, and use a multichannel pipette to add 4.4  $\mu\text{L}$  to every well of a new, sterile 96-well plate (“Sample Plate”). Pipette-mix Real-time Reaction solution before dispensing into wells. When transferring into wells, dispense only to the first stop on the pipette. Do not pipette mix in the 96-well plate, in order to avoid creating air bubbles.
3. Transfer 3.6  $\mu\text{L}$  from each well of the diluted cDNA plate into the corresponding well of the Sample Plate. Pipette-mix in the diluted cDNA plate, dispense only to the first stop on the pipette, and then avoid pipette mixing in the Sample Plate (to limit formation of air bubbles).
4. Heat seal the Sample Plate, as described in Subheading 3.3.3. Keep plate on ice until use.

### 3.5.6 Dispense Reagents into BioMark Chip

1. Once the BioMark chip has been primed (Subheading 3.5.4), take the 10 $\times$  Assay Plate (Subheading 3.5.2) and thaw (if necessary). Take the thawed 10 $\times$  Assay Plate and the Sample Plate (Subheading 3.5.5) and vortex, centrifuge ( $5000 \times g$  in microcentrifuge; 5 s), and sterilize. Keep plates on ice until use.
2. Remove the last four columns of tips from three or more boxes of sterile, filtered pipette-tips.
3. Unseal the 10 $\times$  Assay Plate outside of the hood and dispense 5  $\mu\text{L}$  of 10 $\times$  Assay into the appropriate inlet on the left (notched) side of the BioMark Chip. Follow the approach depicted in Fig. 4, in which eight pipette tips (**step 2**; along with a multichannel pipettor) are used to transfer the Assays from Column 1 of the 96-well plate to alternate rows of inlets on the BioMark chip.
4. When transferring from the 10 $\times$  Assay Plate, pipette-mix in the assay plate, dispense to the first pipettor stop, and avoid air bubbles. If bubbles occur, first attempt to remove the bubble

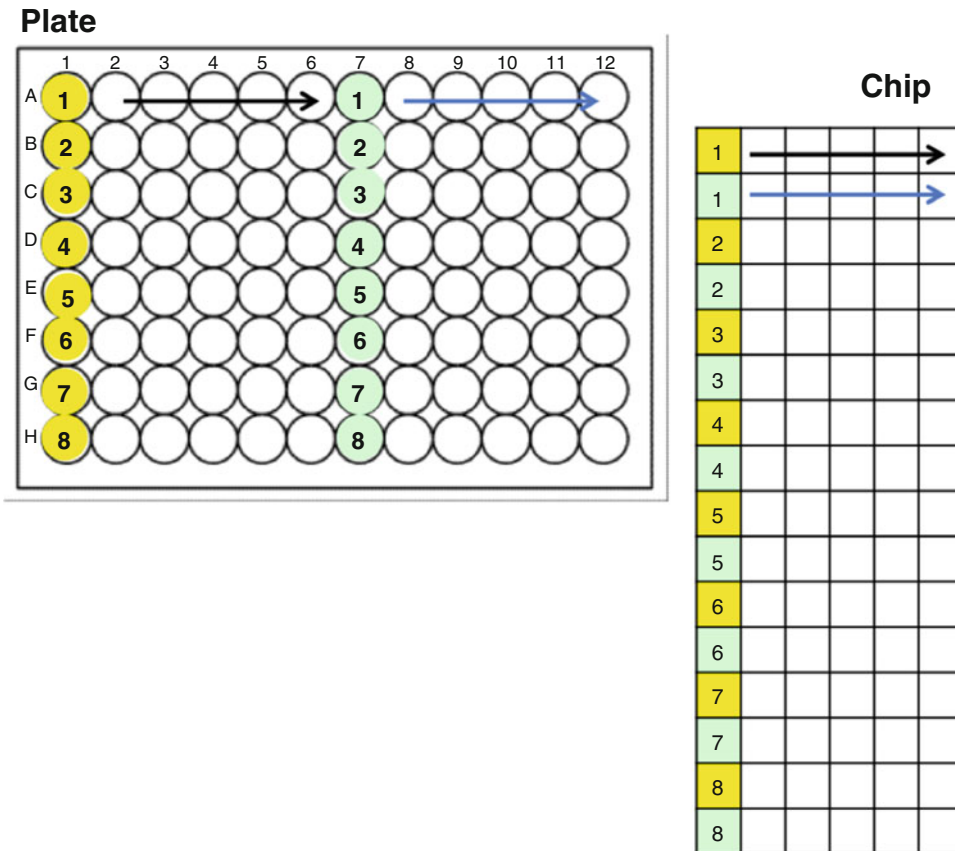


**Fig. 4** Schematic showing how 10× assays are loaded into dynamic array chip

with a sterile pipette tip (capillary action will draw the bubble towards and into the tip). If this fails, remove all material from problematic inlet (using a single channel pipettor), return to the original well, change pipette tips, and transfer attempt transfer of that single well to chip again.

5. Repeat **steps 2–4** with the Sample Plate; this time transferring to right side of chip.

### **3.6 Loading the BioMark Chip into the IFC Controller**

1. Return chip to IFC. Be sure to place the notched side of the chip at the A1 mark.
2. Run the “Load Mix” script. This will run for 1.5 h.
3. Open the BioMark software, and double-click at the prompt for warming up the lamp. The lamp will be ready in 20 min.

### **3.7 Performing Real-Time PCR on the BioMark Instrument**

1. Select “Start New Run” in the BioMark software. The tray on the instrument will open.
2. Eject tray on the IFC controller and transfer the chip to the open tray on the main instrument. Be sure to place the notched side of the chip at location A1 on the tray.

3. If no more chips will be run on the experiment day, turn off the IFC Controller (*see Note 6*).
4. Select “Load” to close the tray, select “Next” to continue.
5. Select “Browse” to choose the file location, type the file name in the “New Chip Run Name” window, and click “Next.”
6. Select the application “Gene Expression,” with the passive reference “ROX.” Under Assay, select “Single Probe” and “FAM-MGB” in the drop down menu. Select “Next” to advance to the next screen. Do not change any other default menu items.
7. Click the “Browse” button to locate the protocol file. Select the protocol “M96 Default Protocol.pcl” Select “Next” to advance to the next screen.
8. Click “Start Run.” The run will take 2 h.

### 3.8 Data Analysis

#### 3.8.1 Preliminary Analysis and Quality Control

1. Open the Fluidigm Real-Time PCR Analysis Software. Select “File” and “Open.” Select the filename of the chip that will be analyzed.
2. Click on “Detector Setup,” “New,” “Next” to choose the default setting, and then “...” under “Mapping.” Select the file “M96-Sample-SBS9.dsp.”
3. Click on “Analysis Views,” and select “Linear Derivative” as the baseline correction method. Keep the quality threshold at 0.65. Keep the Ct threshold method set to “Auto (Global).”
4. Click “Analyze.”
5. The instrument will return the data as a heatmap. Search for ‘X’-ed out cells on the heatmap. These are amplifications that the instrument has marked as failed (*see Note 7*).
6. Export the data as a .csv file (by clicking File> Export). Bring up the heat map again by selecting “Results Views” and save the image view as a .jpg file using the function under the Edit menu.

#### 3.8.2 Map the Sample Names and Probe Information

1. The data file generated in Subheading 3.8.1, step 6 should be loaded into Microsoft Excel (or a similar spreadsheet software) and edited as indicated in Supplemental File 7 (Ct Data Raw.xls). The edits consist of deleting rows and adding columns so that sample names and probe information can be automatically added (using the JMP scripts we provide in the following steps).
2. Save the table with the file name “INPUT” and load it into JMP, then save it as a JMP file.
3. Set up a directory on your drive that includes the data of the Fluidigm run and any other unique identifying information for the experiment.
4. Within that directory, copy Supplemental File 8 (FACS Mapping Script.jsl).

5. Create a subdirectory named “FACS Mapping Templates.”
6. Move the INPUT.jsp file from **step 2** above into this directory. Copy Supplemental File 9 (PROBE MAP.jsp) and Supplemental File 10 (SAMPLE MAP.jsp) into this directory.
7. Edit the SAMPLE MAP.jsp file to reflect the samples in your experiment. Save the file.
8. Open Supplemental File 2 (AssayPanelWorksheet.xls) and copy the information about the assays run in your experiment into the file “PROBE MAP.jsp.” Save the file.
9. Open “FACS Mapping Script.jsl.” Right-click inside the script window and select run. Sample and assay names will be mapped to the output file “Ct Data.jsp.” Open this file and export it as a .csv or .xls file.
10. Analyze data according to the preferred procedure (*see Notes 8–10*).

---

## 4 Notes

1. Linear amplification is defined as an  $R^2$  value greater than 0.99 for the linear-least squares correlation between [RNA] and  $2^{Et}$ . Amplification is efficient if the slope of the [RNA] vs.  $2^{Et}$  line was between 3.1 and 3.6; this represents 90–110% efficiency.
2. Once a particular Assay has been qualified, it need not be qualified again when reordering or changing lots.
3. Preliminary experiments can also reveal which transcripts are not expressed at all, particularly when the cells of interest are not the same as the cells used for qualifying the assay. Such Assays should be considered for replacement in the panel.
4. Heat sealing plates is a crucial and challenging aspect of the BioMark workflow. The process entails heating a film while it is pressed down (with substantial force) to the plate. Successful heat sealing creates a vacuum inside the well, which can be observed as an indentation in the sealing material above each well. It is advisable to practice the sealing process using empty plates, before the 20× Assay Plate is created, to ensure that sealing equipment and materials are working.
5. If less than 500 cells are sorted, the volume of the cells will not affect the reverse transcription reaction. When more than 500 cells are sorted into a well, assume that 0.5  $\mu$ L of media accompanies these cells and reduce the DEPC H<sub>2</sub>O volume in the reaction mix accordingly.
6. The IFC Controller should not be left on overnight (leaving the power on for long periods can damage the device).

7. The instrument's algorithm is quite conservative, however; these reactions may simply have unsteady baselines or late exponential phases. We do not treat these as failures until they are manually reviewed. The researcher should review each and apply the manual override if the curve appears legitimate.
8. There are three important considerations related to the analysis of these data [4]. First, is normalization against housekeeping genes necessary? Second, how can failed reactions (technical artifacts) be discriminated from lack of expression (true biology)? Third, is there a single statistical test that can consider both ways gene expression can differ across groups, namely by switching binary on/off states versus by increasing levels of expression?

Normalization of data against housekeeping genes is not necessary, for a few reasons [4]. First, the single cell is the unit of measurement in these assays; differences in the level of gene expression when one is certain that a single cell has been deposited (as is the case with FACS isolated cells) are likely to reflect true biology. Second, there is dramatic variation in transcript levels for housekeeping genes, even across clonal cells in culture [5]. To normalize against such a variable measurement is unnecessarily introducing error. Third, common housekeeping genes often show poor correlation against each other in these assays, raising the question of which should be used. Finally, normalization may mask differences in gene expression that reflect the deposition of more than one cell, or some contamination, which would otherwise be filtered out by our quality control methodology.

9. Technical artifacts can be discriminated from true biology using an approach that we developed and described elsewhere [4]. This approach had previously been implemented in an R-algorithm, stored on the GitHub repository, called "Single Cell Assay." This tool has now been replaced by MAST, available on GitHub through the RGLab repository.
10. MAST also implements a single statistical test we developed, which considers both ways gene expression can differ between groups. The Combined Likelihood Ratio (CLR) captures differences between groups that are driven either by discrete (on/off) and continuous changes in gene expression.

---

## Acknowledgments

This work is funded by the intramural research program at the National Institutes of Health. PC is an International Society for the Advancement of Cytometry Marylou Ingram Scholar.

## References

1. Chattopadhyay PK, Roederer M (2010) Good cell, bad cell: flow cytometry reveals T-cell subsets important in HIV disease. *Cytometry A* 77(7):614–622. doi:[10.1002/cyto.a.20905](https://doi.org/10.1002/cyto.a.20905)
2. Chattopadhyay PK, Gierahn TM, Roederer M, Love JC (2014) Single-cell technologies for monitoring immune systems. *Nat Immunol* 15(2):128–135. doi:[10.1038/ni.2796](https://doi.org/10.1038/ni.2796)
3. Dominguez MH, Chattopadhyay PK, Ma S et al (2013) Highly multiplexed quantitation of gene expression on single cells. *J Immunol Methods* 391(1-2):133–145. doi:[10.1016/j.jim.2013.03.002](https://doi.org/10.1016/j.jim.2013.03.002)
4. McDavid A, Finak G, Chattopadhyay PK et al (2013) Data exploration, quality control and testing in single-cell qPCR-based gene expression experiments. *Bioinformatics* 29(4):461–467. doi:[10.1093/bioinformatics/bts714](https://doi.org/10.1093/bioinformatics/bts714)
5. Livak KJ, Wills QF, Tipping AJ et al (2013) Methods for qPCR gene expression profiling applied to 1440 lymphoblastoid single cells. *Methods* 59(1):71–79. doi:[10.1016/j.ymeth.2012.10.004](https://doi.org/10.1016/j.ymeth.2012.10.004)

## Single-Cell RNA Sequencing of Human T Cells

Alexandra-Chloé Villani and Karthik Shekhar

### Abstract

Understanding how populations of human T cells leverage cellular heterogeneity, plasticity, and diversity to achieve a wide range of functional flexibility, particularly during dynamic processes such as development, differentiation, and antigenic response, is a core challenge that is well suited for single-cell analysis. Hypothesis-free evaluation of cellular states and subpopulations by transcriptional profiling of single T cells can identify relationships that may be obscured by targeted approaches such as FACS sorting on cell-surface antigens, or bulk expression analysis. While this approach is relevant to all cell types, it is of particular interest in the study of T cells for which classical phenotypic criteria are now viewed as insufficient for distinguishing different T cell subtypes and transitional states, and defining the changes associated with dysfunctional T cell states in autoimmunity and tumor-related exhaustion. This unit describes a protocol to generate single-cell transcriptomic libraries of human blood CD4<sup>+</sup> and CD8<sup>+</sup> T cells, and also introduces the basic bioinformatic steps to process the resulting sequence data for further computational analysis. We show how cellular subpopulations can be identified from transcriptional data, and derive characteristic gene expression signatures that distinguish these states. We believe single-cell RNA-seq is a powerful technique to study the cellular heterogeneity in complex tissues, a paradigm that will be of great value for the immune system.

**Key words** Single-cell RNA sequencing, T cells, CD4, CD8, Smart-Seq2, Alignment, Clustering, Gene expression, Markers

---

### 1 Introduction

T cells initiate and orchestrate adaptive immune responses against pathogenic infections and cancers, and have crucial roles in allergy, autoimmunity, and transplant rejection. Naïve T cells are activated upon recognizing antigenic peptide-MHC molecules on antigen-presenting cells during infection. This recognition is followed by transcriptional, epigenetic, and metabolic changes inside the T cells, making the cells proliferate and release signaling molecules that regulate a new immune response [1–4]. Discoveries of new states of T cell differentiation have also showed that these states are highly plastic, and rather than being “disconnected islands,” are more like neighboring territories spread out on a continuous

landscape whose borders are not clearly defined. A population of T cells associated with a particular differentiated state can acquire different properties and functions classically associated with another state during a secondary immune response, demonstrating their plasticity [5–9]. Appearance of cellular flexibility may arise from truly flexible genetic programs within individual cells or, alternatively, from heterogeneous composition of states within a population. Intrinsic plasticity of genetic programs and heterogeneity in composition can confound each other in data, making it a challenge to identify clinically relevant measurements that accurately reflect the state and capability of the human immune system. Thus, single-cell experimental and analytical approaches are needed to appropriately decipher and dissect the heterogeneity of T cell populations in order to gain further understanding of their capabilities in driving immune responses.

### **1.1 Single-Cell Profiling Methodologies**

While well-established techniques like polychromatic and imaging flow cytometry, mass cytometry, single-cell quantitative PCR (qPCR), RNA FISH (fluorescence in situ hybridization) can provide information at single-cell resolution [10, 11], such approaches can only monitor a small number of preselected candidate features at once, thus restricting the ability to examine genome-wide co-expression patterns and to interrogate cellular heterogeneity from an unbiased point of view. Furthermore, while transcriptional profiling of populations by microarrays and RNA-sequencing have proved valuable in T cell biology, it is also well-known that the average expression level of a population of cells can often be a poor representation of the states of individual cells within the population, a phenomenon known as “Simpson’s paradox” [12, 13]. Indeed, measurements using single-molecule RNA FISH indicated that levels of specific transcripts could vary by several folds between presumably equivalent cells, further illustrating the value of profiling whole transcriptomes at the single-cell level [12].

Analyses of transcriptomes through massively parallel sequencing of cDNAs, derived from cellular RNA by reverse transcription (RNA-Seq), generate millions of short fragments that can be sequenced to accurately quantify expression levels, assemble new transcripts and investigate alternative RNA processing [14]. Development of RNA-seq inspired a flurry of experimental methods that consistently lowered the required starting amounts of RNA, ideally down to single-cell quantities. One of the first groups to demonstrate single-cell RNA-sequencing [15, 16] adapted a protocol initially developed for single-cell microarray studies [17], which enabled preferential amplification of 3’ ends of mRNAs, and detection of thousands of genes expressed in single mouse oocytes and early embryonic cells [15, 16]. Since this first study, several single-cell RNA-sequencing (scRNA-seq) protocols have been reported (such as Smart-Seq, Smart-Seq2, CEL-Seq, STRT, MARS-Seq,

Drop-Seq, inDrop), enabling unbiased profiling of cellular mRNA expression [18–27] and increasing information content recovered per cell. Notably, except for the Smart-Seq and Smart-Seq2 protocols, all existing scRNA-seq methods preferentially capture reads originating from either the 3' or 5' end of transcripts, thus limiting sequencing coverage only to the ends of the molecule. One advantage of methods that capture the 3' or 5' end of the transcripts is the ability to tag each molecule during reverse transcription with a DNA barcode that serves as a unique molecular identifier (UMI) that can be used to digitally count transcript numbers without PCR amplification artifacts [23]. Table 1 highlights key features of different scRNA-seq methods that have been widely used. Recent advances based on droplet microfluidics have substantially increased the cellular throughput of scRNA-seq, making it possible to profile tens of thousands of cells in a single reaction [20, 21].

**Table 1**  
**Overview of characteristics of different single cell RNA-sequencing protocols**

	<b>Poly (A) tailing</b>	<b>Template switching</b>	<b>In vitro transcription</b>	<b>Rolling circle amplification</b>	<b>5' Selection</b>	<b>3' Selection</b>
Associated acronyms	N/A	Smart-seq, Smart-seq2	N/A	N/A	STRT	CEL-seq, MARS-seq, drop-seq, in-drop, SCRBS-Seq
Full-length transcripts	Yes	Yes	Yes	Yes	No	No
Strand-specificity	No	No	No	No	Yes	Yes
Early pooling <sup>a</sup>	No	No	No	No	Possible	Possible
Positional bias	Weakly 3'	Weakly 3'	Weakly 3'	NO	5' Only	3' Only
Unique molecular identifiers (UMIs) <sup>b</sup>	No	No	No	No	Yes	Yes
Available commercial kits	No	Yes <sup>c</sup>	No	No	No	No
Key references	[15, 16]	[24–26]	[61, 62]	[63–64]	[23, 65]	[18–22]

<sup>a</sup>Refers to the possibility to introduce a cellular barcode identifier during first-strand synthesis

<sup>b</sup>UMIs are random sequences of bases used to tag each RNA molecules prior to PCR amplification [23], thereby aiding in the identification of PCR duplicates. While losses in cDNA synthesis and bias in cDNA amplification can result into severe quantitative errors when performing scRNAseq, UMIs can help in eliminating such amplification noise by enabling counting of individual molecules

<sup>c</sup>Clontech offers multiple generations of single-cell transcriptome SMARTer analysis kits allowing performing Smart-Seq and Smart-Seq2 protocols. Furthermore, some of these SMARTer kits are compatible with the with C1 Auto Prep integrated fluidic circuits (IFCs) from Fluidigm, which enables in an integrated workflow the capture of single cells follow by RT and whole transcriptome amplification

While still an order of magnitude lower in cellular throughput compared to single-cell protein measurement techniques like flow and mass cytometry, scRNA-seq's ability to profile transcriptome-wide information in a completely unbiased manner has already enabled many novel biological discoveries. In particular, scRNA-seq approaches have revealed previously uncharacterized subsets of cells together with endogenous marker genes specific to these subsets, and shown that cell-specific splicing and allele expression patterns can differ significantly from their apparent population averages [11, 12]. Although the functional consequences of these phenomena remain to be elucidated, it must be noted that they could not have been detected in an unbiased fashion with previous single-cell methodologies like flow cytometry and qPCR.

## **1.2 Smart-Seq2 Methodology**

Here we describe introductory scRNA-sequencing and data analysis for single human T cells, whose libraries were prepared using the Smart-Seq2 (SS2) protocol ([25–27]; Fig. 1). SS2 is an improvement over the original Smart-Seq single-cell method [24], which was shown to generate quantitative and reproducible data from both single cells and small amounts of total RNA of 10 pg or more. With SS2, Picelli et al. further optimized the reverse transcription (RT), template switching, and pre-amplification steps of Smart-Seq to obtain an increased cDNA yield from single cells, as well as higher sensitivity, fewer technical biases and less variability [25, 26]. Importantly, their published protocol relies entirely on off-the-shelf reagents, making it more cost-effective than commercially available alternative kits.

Briefly, SS2 begins with reverse transcription of polyadenylated transcripts using an oligo-dT primer and a reverse transcriptase derived from the Moloney murine leukemia virus (MMLVRT) (Fig. 1). The reverse transcription is followed by a template switching reaction that relies on the terminal-transferase activity of the MMLVRT, wherein 2–5 untemplated nucleotides are added to the 3' end of the nascent cDNA by the MMLVRT upon reaching the 5' end of the mRNA [25, 26]. By the introduction of a template switch oligonucleotide primer (TSO), the MMLVRT is made to switch its template, and synthesize a complementary sequence to the TSO. As a result, every cDNA molecule derived from a full-length mRNA carries additional artificial sequences at the 5' and the 3' ends, which are identical to each other. This trick makes it possible to carry out PCR amplification of the cDNA using a single primer. The resulting cDNA is amplified to get enough material for subsequent experimental steps. This amplification is followed by an incubation step with Tn5 transposase to fragment the full-length double stranded cDNA and append adapters on each molecule, using the dual-index strategy developed by Illumina, Inc. Each single-cell library is then individually barcoded by PCR with index

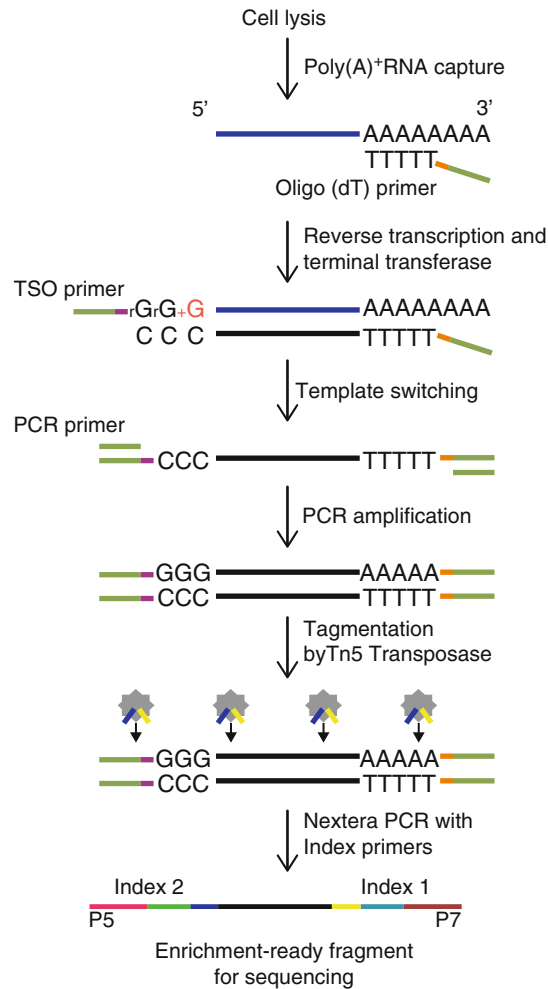


**Fig. 1** Flowchart for Smart-Seq2 single cell library preparation. The diagram, modified from Picelli et al. [26], illustrates the key experimental steps in single-cell RNA-sequencing. The library preparation is performed using the Nextera XT DNA library preparation and index kits from Illumina. Figure 1 is adapted by permission from Macmillan Publishers Ltd: [NATURE PROTOCOLS] (Picelli et al. Nat Protoc 9(1): 171–181), copyright (2014)

primers. The barcoded single cells are then pooled and sequenced on an Illumina sequencer. An important difference with other methods is that every single cell is treated independently until the very end of the protocol (including library generation). While resulting in a more expensive protocol as compared to alternatives that multiplex before cDNA amplification (Table 1), SS2 has the advantage in that if interesting patterns are observed in specific single cells upon sequencing analysis, it remains possible to go back to the cDNA of those cells and generate more in-depth sequencing

data or performing further qPCR analysis selectively. Notably, Smart-Seq and Smart-Seq2 are the only protocols that can generate full-length transcript data, which provide a number of advantages compared to 5' or 3' tagged data (Table 1). Specifically in the context of lymphocytes, full-length information can enable the simultaneous inference of TCR/BCR clonality and gene expression state [28]. Nevertheless, current limitations of Smart-Seq/Smart-Seq2 include the lack of strand specificity, UMI (unique molecular identifiers) to quantify transcript numbers, and the inability to detect non-polyadenylated RNA (Table 1).

Computational analysis of scRNA-seq data can identify groups of cells with similar expression, and characterize the key expression signatures that show variation in the data. Such information, when combined with other kinds of data (e.g., chromatin state, protein expression) can be used to derive insights into the regulatory rules that are responsible for the maintenance and plasticity of cell states. Specific goals of scRNA-seq analysis may include: (1) identifying discrete subpopulations of cells, and gene signatures that are unique to each subpopulation; (2) Identifying co-expressed gene modules and regulatory programs, and their expression levels in different subpopulations; (3) characterizing biological heterogeneity within specific discrete subpopulations, and identifying the gene modules whose variation underlie these continuous states. Notably, while there are several scRNA-sequencing protocols available [18–27], the computational workflow described below was tailored to analyze data generated from the Smart-Seq2 method.

The rest of this unit is organized as follows. We begin with a brief methodological overview of how single RNA-sequencing libraries can be prepared and sequenced using a slightly modified version of the previously published Smart-Seq2 protocol [25–27]. To illustrate the methods described in this unit, we generated single-cell libraries from 384T cells (192 CD4<sup>+</sup> and 192 CD8<sup>+</sup> T cells) FACS sorted from healthy human peripheral blood. Next, we outline the steps involved in preliminary bioinformatic analysis of single T cell RNA-sequencing data generated using the described protocol, focusing on alignment, quantification, quality control (QC), principal components analysis of expression data to determine subpopulations, differential expression analysis to determine signatures, and visualization of results. By listing these steps, which are implemented either in the Unix command line environment (i.e., alignment and expression quantification), or the R programming language (i.e., analysis of expression), we hope to introduce the reader to typical computational approaches that are widely used, and that can be applied to other datasets. We also introduce the reader to some of the commonly used software packages that are used for RNA-seq analysis, and also refer to excellent reviews that describe computational steps in more detail.

## 2 Materials

### 2.1 Generation of scRNA-Seq Libraries with Smart-Seq2

The material and equipment listed below are for generating single-cell lysate and performing the reverse transcription steps, as these are the steps that were slightly modified from the originally published method and protocols [25–27] to generate the T cell data using SS2. For the remaining reagents needed to run SS2 (including PCR amplification, quality control assessments, sequencing library generation), as well as detailed description of the SS2 protocol, please refer to Picelli et al. [26], or to Trombetta et al. [27] who describe a slightly modified version of the original protocol.

#### 2.1.1 Lysis Buffer and Single-Cell Sorting

1. Fluorescence activated cell sorting (FACS) machine.
2. Plate centrifuge.
3. Vortex.
4. Lysis buffer: 1% (vol/vol) 2-Mercaptoethanol in TCL buffer (Qiagen).
5. Cell sorting setup beads for green-yellow lasers (ThermoFisher Scientific).
6. 96-well PCR plates, skirted (Eppendorf).
7. MicroAmp clear adhesive film (ThermoFisher Scientific).
8. Peripheral blood mononuclear cells or T cell suspension.
9. 1× Phosphate Buffered Saline (PBS).
10. Human AB Serum (Corning).
11. Fluorescently conjugated antibodies to human antigens, such as TCR $\alpha\beta$ , CD3 CD4, CD8, CD62L, CD45RA, and CD45RO.
12. Dry ice.

#### 2.1.2 RNA Lysate Cleanup and First Step of Reverse Transcription Reaction

1. DynaMag-96 side-skirted magnet (ThermoFisher Scientific).
2. 8-channel and 12-channel pipettes (P20 and P200).
3. Thermal cycler.
4. RNase decontamination solution (RNaseZap, ThermoFisher Scientific).
5. Ethanol.
6. RNase-free water.
7. RNA-SPRI beads (Agencourt RNAClean XP RNA-SPRI beads, Beckman Coulter).
8. Recombinant Ribonuclease Inhibitor (Clontech).
9. 10  $\mu$ M reverse transcription DNA oligonucleotide primer (custom synthesized by Integrated DNA Technologies): AAGCAGTGGTATCAACGCAGAGTACT(30)VN.

10. dNTP mix (dATP, dCTP, dGTP, and dTTP, each at 10 mM) (ThermoFisher Scientific).
11. SuperScript II Reverse Transcriptase Kit (ThermoFisher Scientific): 5× first-strand buffer, 100 mM DTT, SuperScript II reverse transcriptase.
12. PCR 12-well tube strips and caps.
13. 50 ml conical bottom tube.
14. 1.5 ml RNase- and DNase-free microcentrifuge tubes.
15. Low retention tips (Rainin).

---

### 3 Experimental Procedure

#### 3.1 Gating Strategy and Staining of T Cell Populations

Peripheral blood mononuclear cells (PBMCs) were isolated from the blood of healthy controls individual by ficoll gradient centrifugation, followed by antibody staining, as described in Chap. 4 of this volume (“FACS analysis of memory T lymphocytes”, by Enrico Lugli and colleagues). Briefly, we used antibodies against well-established surface antigens to enrich for four phenotypic subsets in each of CD4<sup>+</sup> and CD8<sup>+</sup> T cell populations—naïve cells (CD62L<sup>+</sup> CD45RA<sup>+</sup>), central memory (CD62L<sup>+</sup> CD45RA<sup>-</sup>), effector memory (CD62L<sup>-</sup> CD45RA<sup>-</sup>), and short-lived effector cells (CD62L<sup>-</sup> CD45RA<sup>+</sup>), each at roughly 25% proportion. While these subsets are present in different abundances in circulation, our goal was to have an even representation of the four main subsets per 96-well plate. We thus opted for creating a quadrant gate of CD62L versus CD45RA (Fig. 2a) and sorted 23 cells per gated quadrant per 96-well plate (1 cell per well); one well was left empty per subset as technical control (Fig. 2b). We used this gating strategy for both CD4 (Lin<sup>-</sup> TCRαβ<sup>+</sup> CD3<sup>+</sup> CD4<sup>+</sup> CD8<sup>-</sup>) and CD8 (Lin<sup>-</sup> TCRαβ<sup>+</sup> CD3<sup>+</sup> CD4<sup>-</sup> CD8<sup>+</sup>) T cells, enabling over-sampling of rare and down-sampling of abundant cell subtypes. Figure 2b illustrates an example of plate layout. Stained cells were resuspended in 1× PBS with 2% AB human serum and kept on ice until sorted.

#### 3.2 Preparation of Single-Cell Lysate and Cell Sorting

1. Clean the working space and pipettes with 70% EtOH and RNaseZap solutions before setting up the working plates.
2. Distribute 10 μl of lysis buffer into each well of a full-skirted-side 96-well PCR plate. Cover the plate with MicroAmp clear adhesive film and keep at room temperature until ready for single-cell isolation. Centrifuge 1 min at 300×g at room temperature just before sorting to ensure the lysis buffer is at the bottom of each well of the 96-well plate.
3. In preparation to performing single-cell sorting, align sorter stream by sorting cell sorting set-up beads for green-yellow lasers. Using one of the sealed 96-well plates to be sorted in, sort 50 beads on the seal for each well of row A and H, as well

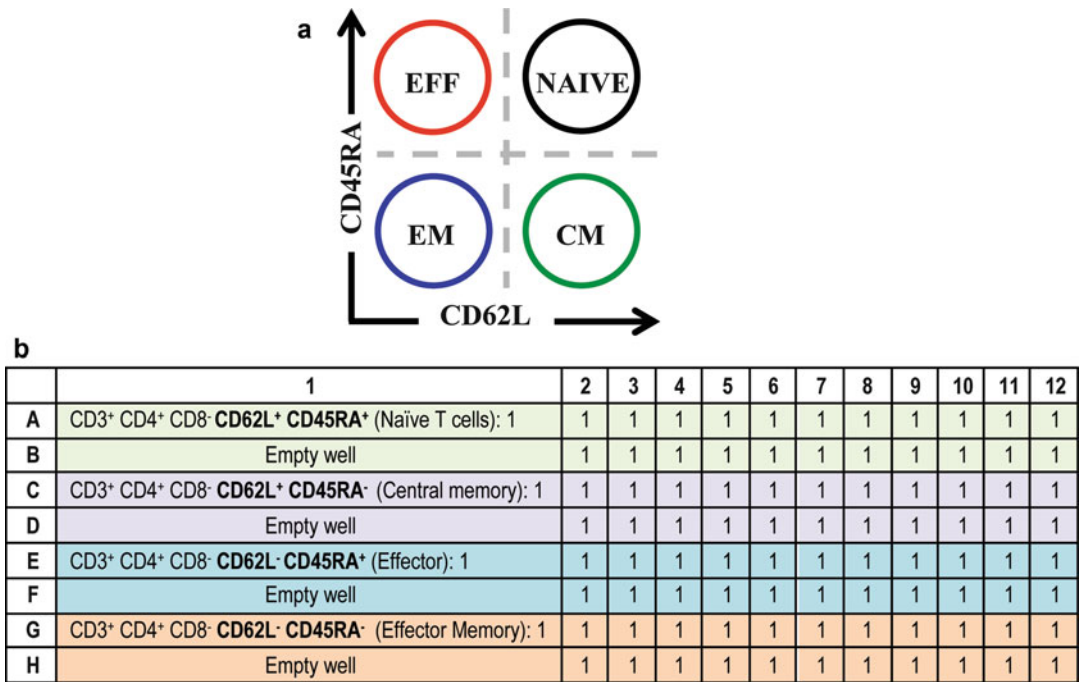


**Fig. 2** T cell sorting strategy for single-cell RNA-sequencing analysis. **(a)** Quadrant gating strategy of CD62L versus CD45RA, which together define classically established phenotypic subsets of T cells. We used this gating strategy to sort 23 cells per gate per 96-well plate for both CD4 (Lin<sup>-</sup> TCRαβ<sup>+</sup> CD3<sup>+</sup> CD4<sup>+</sup> CD8<sup>-</sup>) and CD8 (Lin<sup>-</sup> TCRαβ<sup>+</sup> CD3<sup>+</sup> CD4<sup>-</sup> CD8<sup>+</sup>) T cells. This enabled us to oversample rare subsets and down-sample abundant cell subsets. Sorted subsets included naïve cells (CD62L<sup>+</sup> CD45RA<sup>+</sup>), central memory (CM: CD62L<sup>+</sup> CD45RA<sup>-</sup>), effector memory (EM: CD62L<sup>-</sup> CD45RA<sup>-</sup>) and short-lived effector cells (EFF: CD62L<sup>-</sup> CD45RA<sup>+</sup>). Two replicate plates were sorted for each of CD4<sup>+</sup> and CD8<sup>+</sup> cells. Our dataset altogether included 396 cells, all isolated from the same healthy donor. **(b)** Layout of a 96-well plate of CD4<sup>+</sup> T cells (one plate out of two), showing two rows per subset defined in panel **a**; 1 cell was sorted into every well containing 10 μl of lysis buffer. Wells B1, D1, F1, and H1 were left emptied as technical control

as column 1 and 2, and central wells D5, D6, D7, D8, E5, E6, E7, E8. Make sure all sorted 50 beads are well centered for every well, and adjust Z-position as needed.

- Run at least 10,000 events to setup the gating strategy. To improve yield, plan to sort single cells on both the presence of a positive viability indicator (e.g., Calcein AM, Life Technologies) and the absence of a cell death marker. To limit the number of doublet cells being sorted into a single well, perform doublet exclusion by plotting of forward and sideward scatters areas, heights, and widths (FSC- and SSC-A/-H/-W). There are two common options used to gate for singlets using forward and sideward scatters. The first is to plot FSC-A vs. FSC-H. Events deviating from the diagonal are doublets. The second option is to perform a sequential gating. First FSC-H is plotted vs. FSC-W and then SSC-H vs. SSC-W. In both dotplots, events with a low signal width are to be gated in order to obtain singlets.

5. Perform single-cell sort of T cells, sorting a single cell into each well of the abovementioned 96-well plate containing lysis buffer, but leave 1 well empty as a technical control for every population to be studied. It is also possible to sort 1000–5000 cells into 1 well as a small population control. Adjust flow rate to a minimum, controlling events rate to be lower than 5000 events/s. Dilute the sample as needed to stay within these parameters.
6. Once sorting is complete, seal plate with MicroAmp clear adhesive film and centrifuge 1 min at  $300 \times g$  4 °C. Immediately upon completing centrifugation step, flash-freeze on dry ice and transfer to –80 °C freezer until ready for lysate cleanup. This is the first stopping point of the protocol.

### 3.3 Perform Lysate Cleanup and Reverse Transcription of mRNA Species

We generated our single-cell data using a slightly modified version of the Smart-Seq2 protocol [25–27]. The initial steps of the protocol including lysis of single cells, lysate cleanup, and reverse transcription of mRNA species have been slightly modified and are described below. All remaining steps of the protocol can be followed using the protocol reported by Picelli et al. [26], or to Trombetta et al. [27]. The following steps can be performed inside a biosafety cabinet or a RNA workstation (if available); otherwise, they should be carefully performed on a standard benchtop that has been thoroughly cleaned.

1. Thoroughly vortex RNA-SPRI beads to ensure a uniform suspension and aliquot volume to be used in PCR strip tubes. While bringing RNA-SPRI beads to room temperature (allow 30 min), use 70% EtOH and then RNaseZap to clean the workbench and all equipment used to process RNA.
2. Once beads are warmed up to room temperature, thaw lysate plate on ice for 1 min, and then centrifuge for 1 min at  $800 \times g$  at room temperature.

*All following steps are done at room temperature unless mentioned otherwise.*

3. Add 2.2 volume RNA-SPRI beads to each well of lysate ( $2.2 \times \sim 10 \mu\text{l}$  cell lysate = 22  $\mu\text{l}$  of beads to be added per well) and mix well by pipetting up and down ten times with P200 multichannel. Note that the PEG solution of the SPRI beads is viscous; it is recommended to use low-retention tips to limit the generation of bubbles and loss of material.
4. Incubate lysate and bead suspension for 10 min on bench (*see Note 1*).
5. Move the plate on a 96-well plate magnet (e.g., DynaMag-96 side-skirted magnet) and incubate for 5 min, while still covering the plate with a lid. After completing the incubation step, remove supernatant from each column of the plate by pipetting

up in an angle opposite to where the beads have clustered against the magnet while being careful to not aspirate the beads collected on the side of each well. If beads are aspirated, put back the supernatant in the well and wait for 2 min to enable the beads to cluster again against the magnet (*see Note 2*).

6. Wash beads by adding 100  $\mu\text{l}$  of 80% ethanol (prepared same day with nuclease-free water) to each well. It is important that all beads be submerged by the ethanol solution. Move the plate sideways back-and-forth 3 times on the magnet, allowing the beads to move across the wells, to enable further washing of the beads. Make sure to move the plate on both directions on the magnet to ensure that both beads in columns 1 and 12 are washed. Wait for 30 s to allow the beads to cluster on the magnet before aspirating ethanol using a P200 multichannel pipette. Repeat wash two additional times.
7. Aspirate final ethanol wash with a P200 multichannel pipette and then a P20 to ensure that all residual ethanol is removed. Leave the plate on the magnet and allow beads to dry for 10 min at room temperature. Keep plate loosely covered with the lid from a fresh box of pipet tips, placed slightly ajar. Beads should look cracked within 10 min if all residual ethanol was removed properly (*see Note 3*).
8. Once bead pellet has dried, elute RNA from beads by resuspending dried beads in 4  $\mu\text{l}$  of the following mix for every well (*see Note 4*):
  - 1  $\mu\text{l}$  RNase-free  $\text{H}_2\text{O}$ .
  - 1  $\mu\text{l}$  of 10  $\mu\text{M}$  of oligo-dT RT primer.
  - 1  $\mu\text{l}$  of dNTP mix (10 mM each).
  - 1  $\mu\text{l}$  RNase inhibitor dilution buffer (10% RNase-Inhib, final of 4 U/ $\mu\text{l}$ ).
9. Quickly centrifuge the plate at room temperature, letting the speed reach  $200\times g$  and then immediately stop the centrifugation step. The goal is to collect all drops on the side of the wells without getting the beads to settle too much at the bottom of the well.
10. Incubate for 3 min at 72  $^{\circ}\text{C}$  to anneal oligo-dT RT primer
11. Place plate on ice immediately following incubation. Do not let the temperature of the thermal cycler go down to 4  $^{\circ}\text{C}$  with the plate still inside.
12. Remove seal, add the RT master mix and follow the steps of the original protocol [26], starting at **step 9**.

For the remaining steps of the SS2 protocol, involving reverse transcription step (*see Note 5*), PCR amplification (*note that for the PCR amplification, 22 cycles were performed to generate the T cell data*), quality control assessments of single-cell cDNA, generation

of sequencing library, please refer to Picelli et al. [26] for the detailed description of reagents and following experimental steps, or to Trombetta et al. [27] who also describes the protocol in great detail with slight modifications. Please note, the next safe stopping point in the protocol is after having completed the PCR amplification; after that step, the cDNA can be safely stored at  $-20^{\circ}\text{C}$ .

### **3.4 Single-Cell RNA-Seq Data Analysis**

A major challenge in analyzing scRNA-seq data involves teasing out reliable biological signals from technical noise. While transcriptome-wide measurements of gene expression at single-cell resolution enables heterogeneity in cell-populations to be studied in a truly unbiased manner, one must also note that scRNA-seq ultimately relies on amplifying a very small amount of starting material. In addition to “amplification noise,” different library preparation methods involve different sources of technical biases [29, 30]. Furthermore, as in any other quantitative assay, scRNA-seq libraries can exhibit strong variation across technical replicates prepared across different days, or by different technicians (“batch effects”). Such nonbiological variation can often confound true biological signals of interest [31].

Many of the analysis steps (e.g., alignment of reads to a reference genome/transcriptome) are identical to conventional RNA-seq analysis, but some steps (e.g., determining differentially expressed genes) are uniquely designed to account for the greater technical and biological variability captured across different samples (individual cells in this regard; see [32]). It is important to carefully design experiments whenever possible so that biological heterogeneity is not confounded by technical variation [31–34]. We believe it is critical that biological and technical replicates be included in the experiments and that all the libraries be prepared using the same protocol. When this is not possible, the computational analyst must take caution to include technical sources of variation as covariates in the analysis to correct for batch effects, and interpret biological results conservatively [30–35].

In this section, we describe the canonical steps involved in the processing of scRNA-seq data and various kinds of analyses that are routinely performed to extract biological information. We note that a variety of bioinformatic tools and software packages are available for scRNA-seq analysis (Table 2), and wherever possible, we also indicate these alternatives, and refer to some excellent papers that review existing state-of-the-art methodologies. Importantly, since this is an extremely nascent field, the steps below must be regarded as guidelines intended to be as simple as possible for a starting user. Advanced users are encouraged to explore and compare alternative strategies.

#### **3.4.1 Alignment and Quantification of Sequencing Reads**

Sequencing data generated by an Illumina sequencer are conventionally stored in the FASTQ format, in the form of files carrying the .fastq or .fastq.gz extension. Successful sample demultiplexing

**Table 2**  
**Software packages for scRNA-seq analysis**

Package name (language of implementation)	Functions	References
ZIFA (Python)	Dimensionality reduction algorithm that accounts for transcript dropouts in single-cell data	[66]
Monocle (R)	Mapping transcripts on differentiation cascades, and arranging single cells along a differentiation tree (pseudotime estimation)	[67]
scLVM (Python)	Dissecting cofounding sources of variation (e.g., differentiation vs. cell-cycle) in scRNA-seq data	[68]
SCDE (R)	Testing for differential expression in scRNA-seq data where technical artifacts abound (transcript dropouts, library quality variation)	[32]
BASiCS (R)	A Bayesian framework to normalize and assess biological/technical variation in scRNA-seq data	[69]
Seurat (R)	Spatial mapping of single-cell transcriptomes based on a preexisting spatial pattern of landmark genes. R package also includes wrapper functions for analysis and visualization	[75]
Pagoda (R)	Pathway and geneset overdispersion analysis	[70]
Sincell (R)	Assessment of cell-state hierarchies	[71]
RaceID (R)	Rare cell type identification in complex populations of single cells	[72]
Scuba (Matlab)	Extracting lineage relationships from single-cell data	[73]
Scater (R)	R-based package for quality control, visualization, and preprocessing	[74]

results in a single FASTQ file (for single end sequencing), or a pair of FASTQ files (for paired end sequencing) for each sample. The two mate-pairs in paired-end reads are typically referred to as the “left read” and “right read” respectively. The first step in data analysis is to align these sequencing reads to a reference transcriptome, and obtain quantitative expression levels across various genes and transcripts for each single-cell sample (*see Note 6*).

The following workflow for alignment and quantification of single-cell RNA-seq reads uses publicly available software packages that can be run as commands on a standard Unix terminal, on a standard desktop/laptop or server. For researchers with minimal computational background, we note that these tools are also accessible on a drag-and-drop GUI interface on GenomeSpace [36], a Web-based portal that supports a wide-range of bioinformatics tools for integrative genomics and transcriptomics analysis, and data management (<http://www.genomespace.org>). Upon creating an account on the website, users can view a number of “recipes” for common bioinformatics tasks, each utilizing multiple tools. Recipes include detailed instructions and videos.

GenomeSpace is free to use, and each account is provided some cloud storage. For analysis of large datasets, the best practice use of GenomeSpace is to connect an account directly to cloud-based storage, such as Dropbox, Google Drive, or Amazon S3 buckets. We recommend the Unix-based workflow for users that have access to sufficient computing resources in their home institution.

#### Install Necessary Software Packages

1. The following programs/software should be installed locally or on a server:

##### Programs for Read Alignment and Quantification

- (a) TopHat: <https://ccb.jhu.edu/software/tophat/index.shtml>.
- (b) Bowtie2: <http://bowtie-bio.sourceforge.net/bowtie2/index.shtml>.
- (c) Kallisto: <http://pachterlab.github.io/kallisto/>.

##### Programs for Visualizing Alignment and Generating Quality Metrics

- (d) Samtools: <http://samtools.sourceforge.net/>.
- (e) Picard tools: <http://broadinstitute.github.io/picard/>.
- (f) Integrative Genomics Viewer (IGV): <https://www.broadinstitute.org/igv/>.

##### Programming Environment for Performing Statistical Analysis of Gene Expression and Clustering

- (g) R: <https://www.r-project.org/>.
- (h) RStudio: <https://www.rstudio.com/products/RStudio/>.

#### Aligning Reads to the Genome Using TopHat

2. TopHat is a fast splice junction mapper that aligns paired-end reads to a desired reference genome [37]. Commonly used spliced aligners are reviewed by Engström et al. [38].

- (a) Download pre-built genome indexes for a number of model organisms from the following link, <https://ccb.jhu.edu/software/tophat/igenomes.shtml>.

These can also be prepared by the user by following instructions on the TopHat website.

- (b) FASTQ files for the left and right read files are required for each sample in case of paired-end sequencing data. Run TopHat as follows for each sample (*see Note 7*):

```
% tophat [options] <genome_index_base> [sample
ID_leftreads.fastq] [sampleID_rightreads.fastq]
```

TopHat also allows for single-end reads as input. See <https://ccb.jhu.edu/software/tophat/manual.html> for details regarding [options].

- (c) Most alignment software output their results as SAM/BAM files, which are standard file formats within the genomics community (*see Note 8*). The output of TopHat consists of several files including `accepted_hits.bam`, which summarizes the alignment information in the BAM file format, that can be viewed in a human readable format using `samtools`:

```
% samtools view accepted_hits.bam
```

3. Most downstream programs (e.g., IGV) prefer a BAM file wherein the aligned reads are sorted according to their locations in the reference genome, and subsequently indexed for fast access. Sort BAM file using `samtools`:

```
%samtools sort accepted_hits.bam accepted_hits.sort
```

The above command will produce `accepted_hits.sort.bam`. Next, index the file for easy retrieval by downstream programs:

```
% samtools index accepted_hits.sort.bam
```

#### Performing QC and Visualizing read Alignments

4. The Picard-Tools suite provides a set of Java-based command line tools that can efficiently manipulate SAM/BAM files and also provide important QC metrics regarding the quality of the alignment (e.g., mapping rate, ribosomal RNA content, and number of genes detected). For example, the following command collects statistics on the number of reads that correctly align to the reference genome:

```
% java -jar <picard-location>/CollectAlignmentSummaryMetrics.jar [options] I=accepted_hits.sort.bam O=sampleID_align_metrics.txt
```

See <http://broadinstitute.github.io/picard/command-line-overview.html> for details on all the available command line tools, and their use-cases. Additional software packages for extracting QC metrics from BAM files are available (*see Note 9*).

5. The sequence alignment summarized in the BAM file can be graphically visualized using the Broad Institute's Integrative Genomics Viewer (IGV) program (<https://www.broadinstitute.org/igv/>). Once opened, IGV allows the user to select an appropriate reference genome and transcriptome annotation. The `accepted_hits.sort.bam` can then be loaded here and visualized as a graph of alignment counts at each location in the genome. Multiple BAM files corresponding to different samples can be loaded simultaneously and visualized as individual tracks (*see Note 10*).

## Quantifying Transcript/Gene Abundances

- Analysis of gene expression heterogeneity in single-cell RNA-seq data requires the quantification of gene or transcript abundances from the alignment of reads. A number of software packages are available for this purpose (*see Note 11*), and many review articles and protocols summarizing alternative workflows have been published [37, 38]. Here we have used Kallisto, an extremely fast and memory efficient program to quantify abundances of transcripts from RNA-seq data through “pseudoalignment” ([40]; *see Note 12*). Kallisto requires the user to build an index of the transcriptome from a FASTA file (*see Note 13*), containing the nucleotide sequences of the transcripts/gene targets that the user wishes to quantify:

```
% kallisto index -i [<index-location>/transcripts.idx]
[transcripts.fasta.gz]
```

Some transcriptome FASTA files can be downloaded from <http://bio.math.berkeley.edu/kallisto/transcriptomes/> or they can be downloaded from the UCSC table browser (<https://genome.ucsc.edu/cgi-bin/hgTables>). Once the index is built (*see Note 14*), run the following command to quantify the gene/transcript abundances for each sample:

```
% kallisto quant -i [[<index-location>/transcripts.idx] -o [sampleID]
[sampleID_leftreads.fastq] [sampleID_right reads.fastq]
```

Additional options for single-end reads, multithreading and uncertainty estimates using bootstrapping are detailed in the Kallisto website: <https://pachterlab.github.io/kallisto/manual.html>.

- kallisto quant produces a tab-separated text file `sampleID/abundance.tsv`, which summarizes the estimated numbers of RNA-Seq fragments derived from the corresponding transcripts and normalized transcript-per-million (TPM) values within the sample for each transcript/gene target listed in the transcriptome index [transcripts.idx] as separate columns (*see Note 15*). These count or TPM columns can be read into a programming language environment like R or python, and merged into a single tab-delimited expression matrix file prior to further exploration of the data (*see Note 16*).

In the following section, we explore cellular heterogeneity by analyzing the expression matrix, identify subpopulations of cells in the dataset and the gene signatures that define them. While we use the T-cell dataset as our working examples, these can be applied to other datasets. The expression data used here is available upon request to the authors by e-mail.

### 3.4.2 Exploring Single-Cell Heterogeneity and Structure Using the Expression Matrix

Single cells resident in blood or tissues are a mixture of multiple cell types (e.g., T cells vs. B cells) and cell-states (naïve vs. activated CD8<sup>+</sup> T cells). Bulk expression measurements provide an average readout over multiple diverse states, and thus conceal the underlying heterogeneity. In a number of situations, none of the underlying individual cell states might be represented in the average measurement, a phenomenon known as Simpson’s paradox [12, 41]. Single-cell RNA-seq measurements can thus provide a more accurate picture of transcriptional heterogeneity across multiple cells, and computational techniques rooted in machine learning may be fruitfully applied to explore key genes driving heterogeneity in the data (e.g., via principal components analysis), infer cell-types and cell-states in a completely unbiased manner (e.g., clustering), and find biological processes that are reflected in genes differentially expressed in one condition vs. another (e.g., pathway analysis). Here we describe some of these techniques in the context of T cells isolated from blood. These steps can serve as a template for the user to analyze data from an alternative expression matrix, although some steps might require slight modifications (e.g., based on alternative sample naming conventions).

The following steps are implemented in R (<https://www.r-project.org>), a freely available, extremely versatile and popular programming language for bioinformatics analysis. Upon installing R, we recommend that users install RStudio, a free and open source integrated development environment (IDE) for R, which provides an easy to use desktop application for writing and running R scripts, and allows users to organize their code.

It is conventional for bioinformatics research groups to create a “software package” in R to accompany the publication of a method. A number of useful packages are compiled and curated as part of the “Bioconductor” project [42], and these packages can be easily installed and loaded into RStudio. The following workflow uses a number of available packages (*see* Table 2).

Set Up the Environment, and Install Necessary Packages

1. Open RStudio, and create a working directory. Copy the kallisto inferred-read counts (rows=genes, columns=cells), and separately transcripts per million (TPM) values of gene expression as tab-delimited text files Counts.txt and TPM.txt into this directory (*see* Notes 15 and 16). The packages ggplot2, plyr, NMF, and tsne can be installed using the `install.packages()` function.

```
> install.packages("ggplot2")
> install.packages("plyr")
> install.packages("NMF");
> install.packages("tsne");
```

Install the differential expression analysis package SCDE by following instructions on the website (<http://hms-dbmi.github.io/scde/>). Once installed in the user's repository, these packages can be loaded on to the working session as:

```
library(ggplot2)
library(plyr)
library(NMF)
library(tsne)
library(scde);
```

Explore the Data

## 2. Read the counts and TPM matrix into R,

```
>Counts_mat=read.table("Counts.txt", header=TRUE, sep="\t",
row.names=1, quote="");
>TPM_mat=read.table("TPM.txt", header=TRUE, sep="\t",
row.names=1, quote="");
```

Check the first five rows and three columns of the TPM matrix to make sure the data loaded correctly,

```
> TPM_mat[1:5,1:3]
      CD4.EM_S33_S308 CD8.CM_S44_S188 CD4.CM_S38_S152
C9orf152           0.00           0.00           0.00
RPS11             533.49          1954.74          21.17
ELMO2             0.00           0.00           0.00
CREB3L1           0.00           0.00           0.00
PNMA1             0.00           0.00           0.00
```

Here the rows and columns represent genes and cells. “CD4.XX” and “CD8.XX” denote CD4<sup>+</sup> and CD8<sup>+</sup> T cells, while “CD8.EM,” “CD8.CM,” “CD8.EF,” and “CD8.NA” denote effector memory, central memory, effector, and naïve CD8<sup>+</sup> T cells (and similarly for CD4<sup>+</sup> T cells). These cells were labeled according to the quadrant gating they were sorted from (see *Gating strategy and staining of T cell populations* section). For every column, name letters preceding the first underscore symbol (“\_”) represents the cell type based on sorting, while the letters following it represents a unique identifier for that cell. For example Column 1 is an effector memory CD4<sup>+</sup> T cell with a label “S33\_S308.”

The total number of genes and cells in the dataset can be queried as the number of rows and columns in the expression matrix,

```
> dim(TPM_mat)
[1] 23686 368
```

implying 23,686 genes (rows) and 368 cells (columns). It is common practice to exclude cells that do not meet user-specified quality criteria (e.g., low mapping rates, and high 5' or 3' bias) that can be obtained from Picard Tools or other

programs. Here we only include libraries that have more than 3000 detected genes but no more than 10,000 detected genes.

```
genes.detected=apply(TPM_mat, 2, function(x) sum(x>0))
cells.use=(genes.detected>= 3e3) & (genes.detected<1e4)
TPM_mat1=TPM_mat[,cells.use]; Counts_mat1=Counts_mat[,cells.use]
```

Note that these cutoffs are data-dependent, both on the cell type/state and library quality (i.e., sequencing depth, alignment rate). Here we chose the minimum cutoff of number of genes detected per cell one standard deviation less than the mean value (~4500) of this quantity in our data. We also excluded a few outlier libraries that had more than 10,000 genes detected, as these were likely to be multiple cells sorted into a single well. The total number of cells in each of the eight samples (“CD8.EM,” “CD4.NA,” etc.) can be queried as,

```
> sample.ids=sapply(colnames(TPM_mat1), function(x) strsplit(x,"_")
[[1]][1])
> table(sample.ids)
CD4.CM CD4.EF CD4.EM CD4.NA CD8.CM CD8.EF CD8.EM CD8.NA
    45    45    46    44    43    46    45    43
```

The first command extracts the cell-type from the list of column names, which as mentioned above, have the format “CellType\_SampleID.” Thus individual samples in our dataset have 43–46 cells, totaling 357 cells.

3. It is good practice to explore the data, and make sanity checks before applying fancy computational techniques. A common approach is, for example, to make plots describing summary statistics of library quality (Fig. 3a–c) and expression patterns of key marker genes. A code to make simple barplots with error bars is provided in **Note 17**. The following command summarizes the average number of transcriptome mapped reads per cell, and the average number of genes detected per cell in each of the 8 samples (Fig. 3a, b),

```
> barplot_tcell(x=colSums(Counts_mat[,cells.use]), id=sample.ids,
name="Num. Mapped Reads per cell")
> barplot_tcell(x=genes.detected[cells.use], id=sample.ids,
name="Num. Genes per cell")
```

Figure 3c, which summarizes the mapping rate of reads to the genome, transcriptome and ribosomal RNA was created using the output of Picard-Tools CollectAlignmentSummary Metrics.jar introduced previously (could not be reproduced because of space constraints).

4. Another commonly asked question is: have libraries been sequenced to sufficient read-depth? A computational answer can be derived by randomly down-sampling the read counts within the counts matrix to varying degrees, and asking how

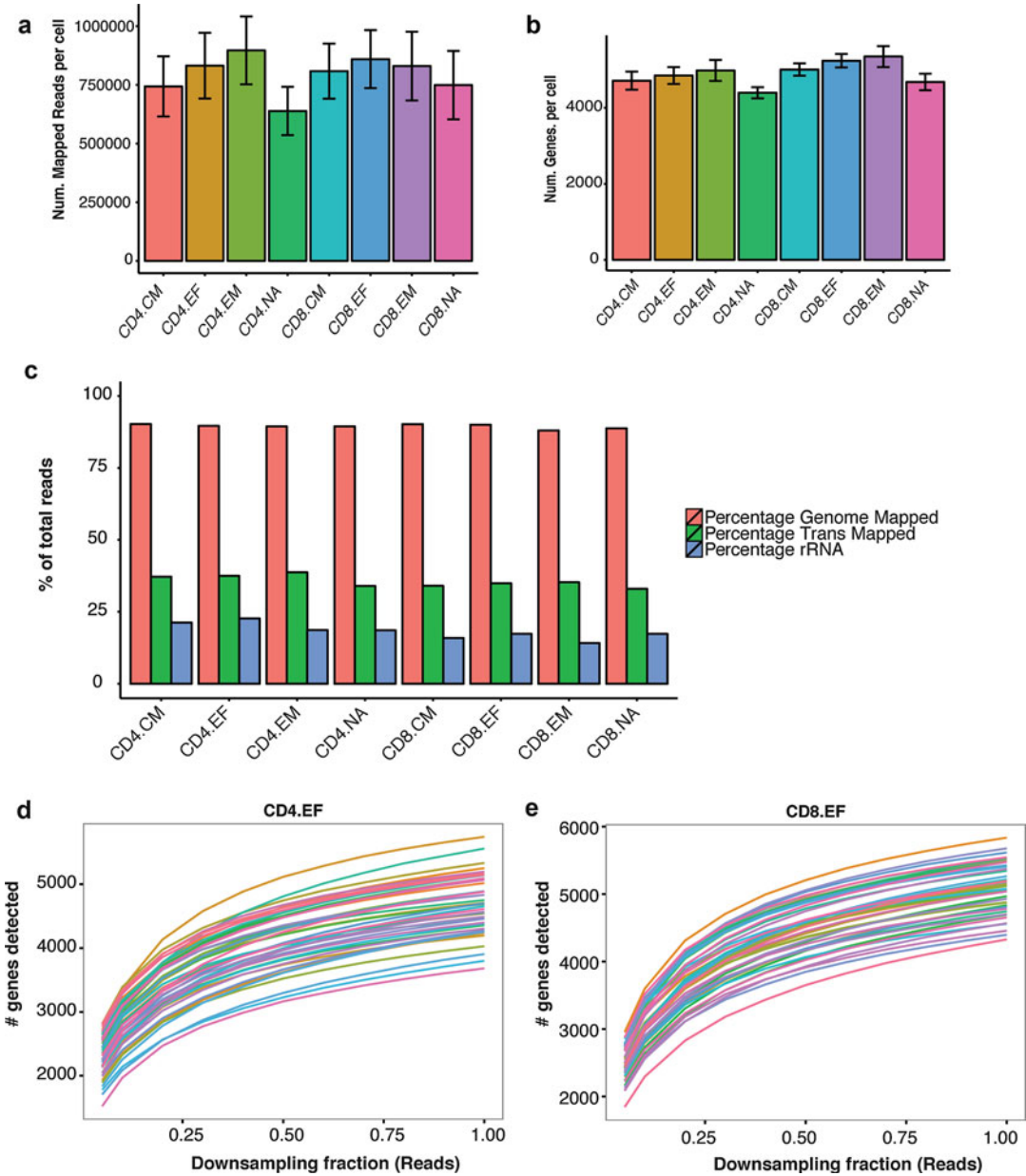


**Fig. 3** Visualizing quality controls in single cell RNA-sequencing data **a** and **b**. Barplots summarizing average number of reads mapped to the transcriptome per cell (**a**), and the average number of genes detected per cell (**b**) in each of the 8 subsets. (**c**) Barplots reporting summary statistics of the percentage of the genome-mapped (*red*), percentage of transcriptome-mapped (*green*) and percentage of ribosomal-RNA (*blue*) reads for each subset profiled, as a percentage of total sequenced reads. (**d**, **e**) Saturation curves for CD4<sup>+</sup> effector cells (CD4<sup>+</sup>CD62L<sup>-</sup> CD45RA<sup>+</sup>) and CD8<sup>+</sup> effector cells (CD8<sup>+</sup>CD62L<sup>-</sup> CD45RA<sup>+</sup>) reveal that deeper sequencing of these libraries can detect more genes. Briefly, every single-cell library is randomly “downsampled” to a certain proportion of the initial number of mapped reads 100 times, and the average number of detected genes is recorded. Performing this exercise at 20 values of downsampling proportions (5–98 %) yields a curve for every cell. The curves show that around 80 % of genes detected at full depth are detectable at 75 % of the sequencing depth, which is around two million reads per cell. The upward slope of the curves at fraction = 98 % suggests that deeper sequencing can be beneficial

sharply the number of detected genes falls as reads are removed. Figure 3d, e show the resulting “saturation curves” for CD4 and CD8 EF cells (computational procedure for downsampling is described in the figure legend. The code not be reproduced in this note because of space constraints).

- One can also plot the average expression of known marker genes within every group to verify whether their expression conforms to biological expectations. For example, when profiling T cells, one can look at: CD4 co-receptor (*CD4*, expressed only on CD4<sup>+</sup> T cells; Fig. 4a), CD8 co-receptor alpha chain (*CD8A*, expressed only in CD8<sup>+</sup> T cells, Fig. 4b), L-selectin (*SELL/CD62L*, a lymph node homing receptor predominantly expressed in naïve and central memory cells; Fig. 4c), and CD45 antigen/*PTPRC* (expressed in all T cells; Fig. 4d).

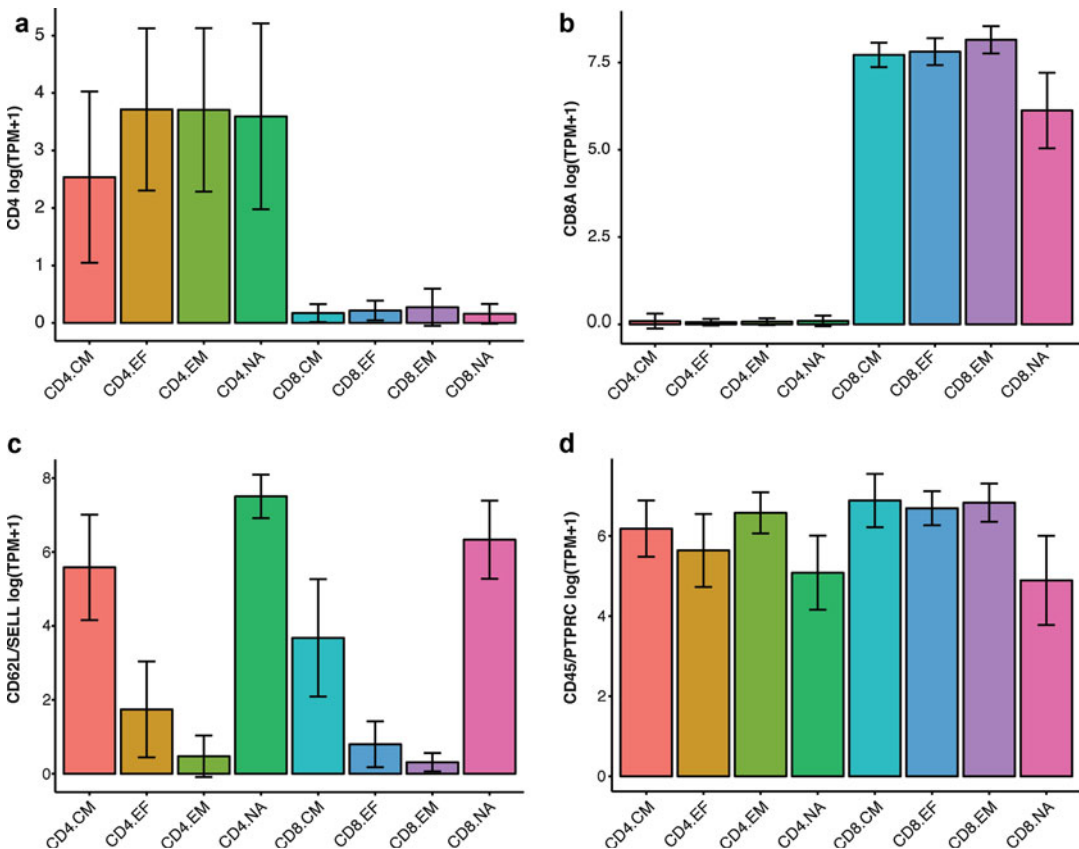


**Fig. 4** Expression of known T cell markers (a–d). Illustrative barplots showing the expression (average  $\pm$  SD log(TPM + 1)) of key marker genes across the 8 subsets. (a) *CD4*, gene encoding for CD4 co-receptor. (b) *CD8A*, gene encoding the alpha-subunit of the CD8 co-receptor. (c) *SELL*, gene encoding the lymph node homing receptor CD62L, expressed predominantly on circulating T cells. (d) *PTPRC*, gene encoding the CD45 antigen, expressed on all T cells

```

> logTPM_mat1=log(TPM_mat1+1)
> barplot_tcell(x=logTPM_mat1["CD4",], id=sample.ids, name="CD4
log(TPM+1) ")
> barplot_tcell(x=logTPM_mat1["CD8A",], id=sample.ids, name="CD8A
log(TPM+1) ")
>barplot_tcell(x=logTPM_mat1["SELL",], id=sample.ids,
name="CD62L/SELL log(TPM+1) ")
> barplot_tcell(x=logTPM_mat1["PTPRC",], id=sample.ids,
name="CD45/PTPRC log(TPM+1) ")

```

See Fig. 4a–d for these plots. It is common practice to log transform the TPM+1 values instead of using the raw TPMs. This causes the data points to more uniformly spread across their dynamic range, and also makes it easy to interpret differences between the transformed values as “fold changes.” The addition of 1 ensures that zero TPM values remain zero in the transformed units.

### Perform Principal Components Analysis (PCA)

6. PCA is a conceptually straightforward, yet an efficient and robust, approach [43] to perform unsupervised exploratory analysis on the data, and to identify structure within the single-cell data driven by the correlated expression of gene modules. It has been used successfully in a number of recent single-cell RNA-seq papers [44–47]. Here we apply PCA on the 357 cell-data while being completely blind to the cell-type labels of cells from the sorting procedure. We will then ask whether such an unbiased analysis is able to separate the different sorted populations. PCA takes as input an expression matrix, with rows as genes and columns as cells.
  - (a) *Selection of variable genes:* A typical practice is to perform PCA using only those genes that show appreciable variation within the data, and avoid genes that are poorly expressed. The following R code selects genes that are expressed by at least 40% of cells in any of the 8 samples at  $\log(\text{TPM}+1) > 4.5$ , and that have a coefficient of variation across all the cells higher than 0.5 (see **Note 18**):

```

> pca.genes=c()
> groups=unique(sample.ids)
> for (i in groups){
cells=grep(i, colnames(TPM_mat1), value=TRUE)
include.genes=apply(logTPM_mat1, 1, function(x) ((sum(x[cells]>4.5) /
length(cells)>0.4) & sd(x)/mean(x)>0.5))
pca.genes=union(pca.genes, rownames(TPM_mat1)[include.genes])
}
pca.genes comprises 678 genes, as can be checked by the length() func-
tion:
> length(pca.genes)
[1] 678

```

- (b) *PCA*: Use the log-transformed TPM matrix as input to PCA, but rescale its rows to have zero-mean and unit standard deviation. This normalization procedure, termed “z-scoring” or “standardizing,” ensures that relative expression variation in all genes is treated equally irrespective of their absolute expression levels. Standardizing can be turned on in the R function `prcomp`, which implements PCA.

```
> pca_result=prcomp(t(logTPM_mat1[pca.genes,]), center=TRUE,
scale=TRUE)
```

### Examine PCA Scores for the Presence of Cell-Subpopulations

7. Conceptually, PCA finds successive mutually independent linear combinations of genes that maximally capture correlated variation in the data. Such correlated variation might arise due to the presence of “gene modules”—groups of genes whose expression levels are highly correlated because of a common biological connection (e.g., response to T cell stimulation). Each linear combination of genes is called a “principal direction” and is ordered by the amount of variance in the data it captures (high to low). For every principal direction, the coefficient corresponding to every gene in the linear combination determines the extent to which that gene “drives” the variation captured by the principal direction, and is referred to as the gene’s “loading.” Genes whose loadings along a principal direction are high in magnitude and share the same sign are typically positively correlated within the data.

Each individual cell, which corresponds to a column in the expression matrix, can then be projected on to each of these principal directions yielding a vector of “scores” for *that* cell, and so on for all the cells. The vector of scores for all the cells along the first principal direction is referred to as the first “principal component” of the data (PC1), and so on. The matrices corresponding to the loadings (genes×PCs) and scores (cells×PCs) as column vectors may be directly extracted from the output of `princomp` as follows:

```
pca.loadings=data.frame(pca_result$rotation)
pca.scores=data.frame(pca_result$x)
```

With a PCA transformation in hand, a straightforward way to visualize subpopulation structures in the data is to make a 2D-scatter plot of cells based on the values of their PCs (*see Note 19* for scatter plot code).

```
> scatter_plot(X=pca.scores[,1:2], id=sample.ids, axis.labels=c("PC1", "PC2"))
> scatter_plot(X=pca.scores[,3:4], id=sample.ids, axis.labels=c("PC3", "PC4"))
```

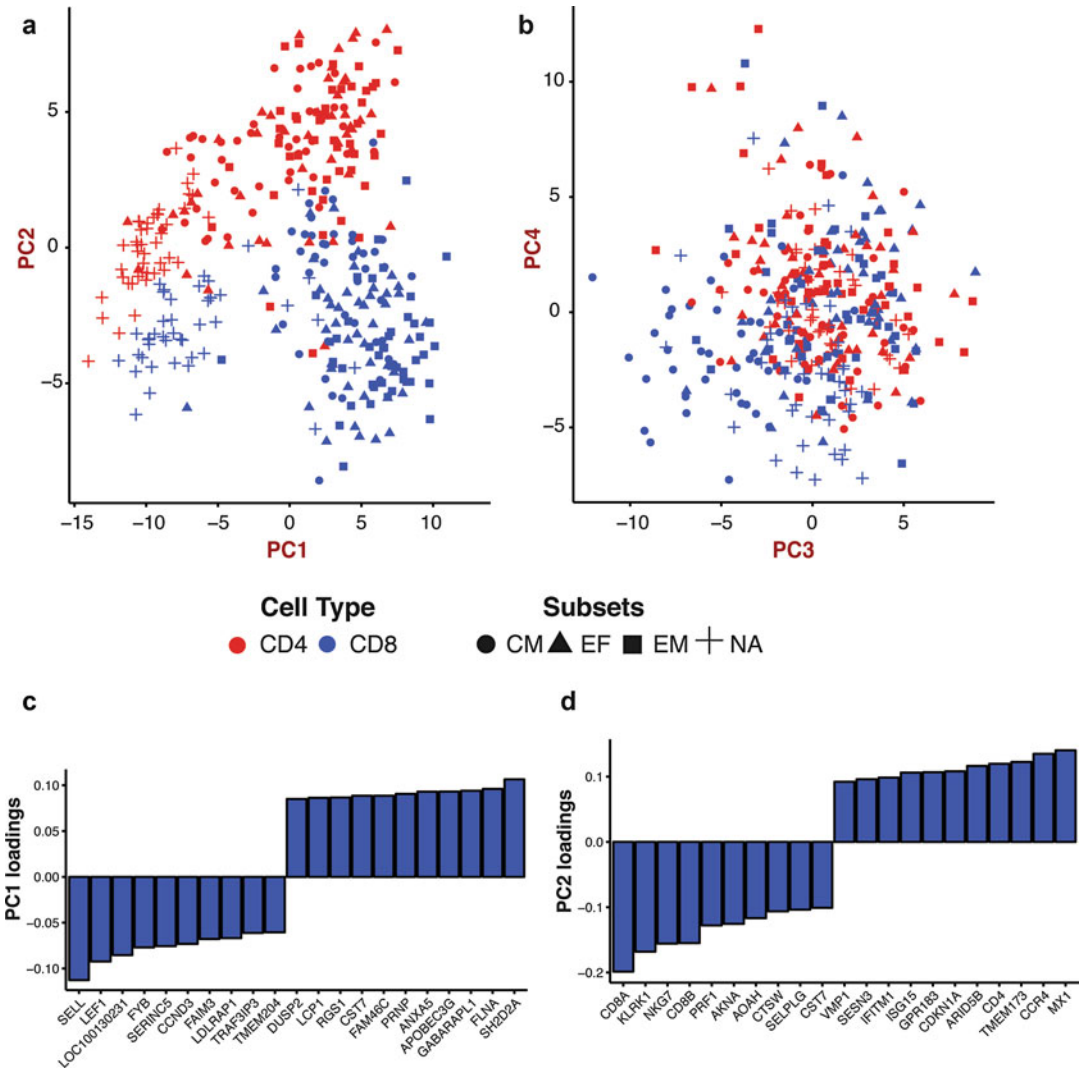


**Fig. 5** Unsupervised analysis using PCA separates cell-subsets **a** and **b**. Scatter plots of PCA-scores of single-cells, along PC1-PC2 (Panel **a**) and PC3-PC4 (Panel **b**). Each point is a cell with its location plotted as value of the “score” assigned by PCA along the corresponding PC. In Panel **a**, PC1 ( $x$ -axis) separates naïve cells (+ symbol) from the remaining subsets. PC2 ( $y$ -axis) separates CD4<sup>+</sup> T cells (*red*) from CD8<sup>+</sup> T cells (*blue*). (**c**, **d**) Top genes ( $x$ -axis) driving the variation captured by PC1 and PC2, and their relative weights or loadings ( $y$ -axis). Genes with high positive or negative loadings are the primary contributors. The gene with the most negative loading in PC1 (**c**) is *SELL* (also called L-selectin or CD62L), the lymph node homing receptor expressed in naïve and central memory cells but not effector and effector memory cells, while genes driving PC2 (**d**) include known CD8<sup>+</sup> T cell related genes such as *CD8A*, *CD8B*, and *PRF1*. This mirrors the observation in Panel **a** with PC1 ( $x$ -axis) separating naïve T cells from the other subsets, and PC2 ( $y$ -axis) separating CD8<sup>+</sup> T cells from CD4<sup>+</sup> T cells

The output of these commands, Fig. 5a, b, reveals that PCA separates the different subpopulations (Note that the PCA procedure was completely blind to the subpopulation identities of the T cells). PC1 in particular appears to separate

naïve from memory and effector cells, while PC2 separates CD4<sup>+</sup> from CD8<sup>+</sup> T cells. PC3, on the other hand separates central memory CD8<sup>+</sup> T cells from the rest. These figures also suggest that the naïve cells are transcriptionally more distinct than the effector and memory cells (CM and EM).

#### Examine PCA Loadings to Identify Key Genes That Drive Variation

8. Different principal directions (columns of the `pca.loadings`) are orthogonal vectors in multidimensional gene-expression space that describe prominent patterns of correlated variation. Genes with large positive values in a given loadings vector are positively correlated with each other along the direction of the vector, as are the genes with large negative values; however, these two groups of genes are anti-correlated with each other along that direction. It is usually very instructive to look at some of the top genes (positive and negative) driving individual principal directions using bar plots (*see Note 20* for code):

```
barplot_loadings(X=pca.loadings,pc.use=1,num.genes=10)
barplot_loadings(X=pca.loadings,pc.use=2,num.genes=10)
```

Figure 5c, d shows that a number of known T cell related genes feature among the top genes driving PC1 and PC2. The gene with the most negative loading in PC1 is *SELL* (also called L-selectin or CD62L), the lymph node homing receptor expressed in naïve and central memory cells but not effector and effector memory cells (Fig. 5c). Also featured is *LEF1*, a transcription factor that is essential for early T cell development [48]. This reflects the separation of naïve cells from the other cells along the PC1 axis in Fig. 5a. Genes driving PC2 (Fig. 5d) include known CD8<sup>+</sup> T cell related genes *CD8A*, *CD8B*, *PRF1* (perforin), *NKG7* (negative loadings), and CD4<sup>+</sup> T cell enriched genes *CD4*, *CCR4*, and *MX1* (positive loadings), which mirrors the separation of these cells along the PC2 axis in Fig. 5a [49].

We emphasize that these patterns were captured in a completely unsupervised manner by PCA from the list of highly variable genes, and were in no way “selected” based on their known biological roles.

#### Visualize PCA Results on a 2D Map Using t-Distributed Stochastic Neighbor Embedding (t-SNE)

9. Important modes of biological variation might manifest across multiple PCs, and thus incorporating multiple PCs into the analysis might be important to separate phenotypically/functionally distinct subpopulations of cells. A powerful way to visualize information contained in multiple PCs is to use the t-SNE algorithm [50], which performs nonlinear dimensionality reduction and generates a 2D scatter plot of cells, captur-

ing the essence of the variation contained across multiple PCs. The algorithm, implemented in the R-package `tsne`, needs as input a user-defined number of principal component values for all the cells.

There is no general answer to how many principal components one must consider, and describing tests for statistical significance of PCs is outside the scope of this protocol (see [51] for a review of this topic). Here we choose to keep the top 10 principal components in the data:

```
set.seed(10)
tsne.proj=data.frame(tsne(pca.scores[,1:10]),whiten=FALSE)
colnames(tsne.proj)=paste0("tsne_",c(1:2))
scatter_plot(X=tsne.proj, id=sample.ids, axis.labels=c("tSNE_1", "tSNE_2"))
```

Figure 6a shows the t-SNE plot. Compared to the PCA scatter, the distinction between multiple subsets now becomes much sharper now that we are incorporating more information (a total of 10 principal components in the visualization). Also note that while the CD4<sup>+</sup> and CD8<sup>+</sup> cells cluster separately, as do the naïve cells from the other subsets, the EF, CM and EM cells are spread within a single large cluster for both CD4<sup>+</sup> and CD8<sup>+</sup> cells, highlighting that the expression of very few genes contribute towards distinguishing these subsets.

Additionally one can also explore the presence of batch effects by coloring individual points on the PCA/t-SNE plots by their batch ID. Figure 6b shows that the cells cluster by their type (CD4<sup>+</sup> vs. CD8<sup>+</sup>) rather than their plate ID, suggesting that batch effects are absent/weak in our data. Alternatively one can also color points by their library quality metrics (e.g., number of genes detected and mapping rate) to explore whether technical effects drive the dominant modes of variation in the data. A number of computational strategies have been published to correct for batch effects (Table 2) [34, 52].

Typical downstream steps involve partitioning the cells into different discrete “subsets” using methods such as hierarchical, k-means or density based clustering, which we do not describe here. Many such methods, however, are available as R packages [53–55].

### Finding Differentially Expressed Genes

10. *Finding differentially expressed (DE) genes*: An important task in gene expression analysis is to find which genes are differentially expressed between two subsets of cells. Finding a set of DE genes might provide important clues regarding biological pathways that might be active in one subset compared to another, for example. Finding a set of reliable DE genes is a statistical exercise, and methods must take into account the

important sources of technical variability in the data (“noise”). One of the most important sources of uncertainty in scRNA-seq data is the low capture rates of transcripts during the reverse transcription step (*see Note 5*), which can lead to the “dropout” of genes in some libraries, even though they have non-zero expression in the biological sample [31]. Another source of technical noise is the differences in the quality of libraries that some cells produce because of upstream conditions (e.g., apoptosis in some cells, or RNA degradation). In any ordinary setting, these can confound true biological differences.

We use the R-package Single Cell Differential Expression (SCDE, Table 2) for performing differential expression analysis, which adopts a Bayesian approach to account for technical sources of variation typical in scRNA-seq [31]. SCDE may be invoked as follows for finding differentially expressed genes between CD4<sup>+</sup> naive cells and CD4<sup>+</sup> effector memory cells (*see Note 21*):

```
markers.CD4=scde_test(C=Counts_mat1, grp1="CD4.EM", grp2="CD4.NA",
min.fold=3)
nrow(markers.CD4)
[1] 733
```

The last output suggests that SCDE was able to detect 733 genes differentially expressed between naïve and effector memory T cells at an average log-fold change higher than 3 between the subsets. The heatmaps in Fig. 6 depict these results vividly, and were generated using the following commands:

```
CD4.NA.cells=sample.ids == "CD4.NA"
CD4.EM.cells=which(sample.ids == "CD4.EM")
A=t(scale(t(logTPM_mat1[rownames(markers.CD4[order(markers.CD4$mlc)],
c(CD4.NA.cells,CD4.EM.cells)]))))
aheatmap(A,color="-RdYlBu2:10", Rowv=NA, Colv=NA)
```

We repeated the above steps to find differentially expressed genes between naïve and effector memory CD8 positive T cells, which yielded 761 differentially expressed genes (Fig. 6c, d heatmap). Interestingly, 151 genes were common between the two sets, a result that was highly statistically significant ( $p < 10^{-42}$ , hypergeometric test).

---

## 4 Conclusions

Our aim in this chapter is to introduce the uninitiated T cell biologist to key experimental and computational steps in single cell RNA-sequencing analysis. Through our working example, we show that profiling of human T cells using scRNA-seq enables hypothesis-free evaluation of cellular expression states using

off-the-shelf computational methods. A key challenge for the future is to use this powerful technique to explore the causes and consequences of T cell heterogeneity in a number of contexts, ranging from function exhaustion in diseased states to the interplay between clonal dynamics and expression state during immune responses.

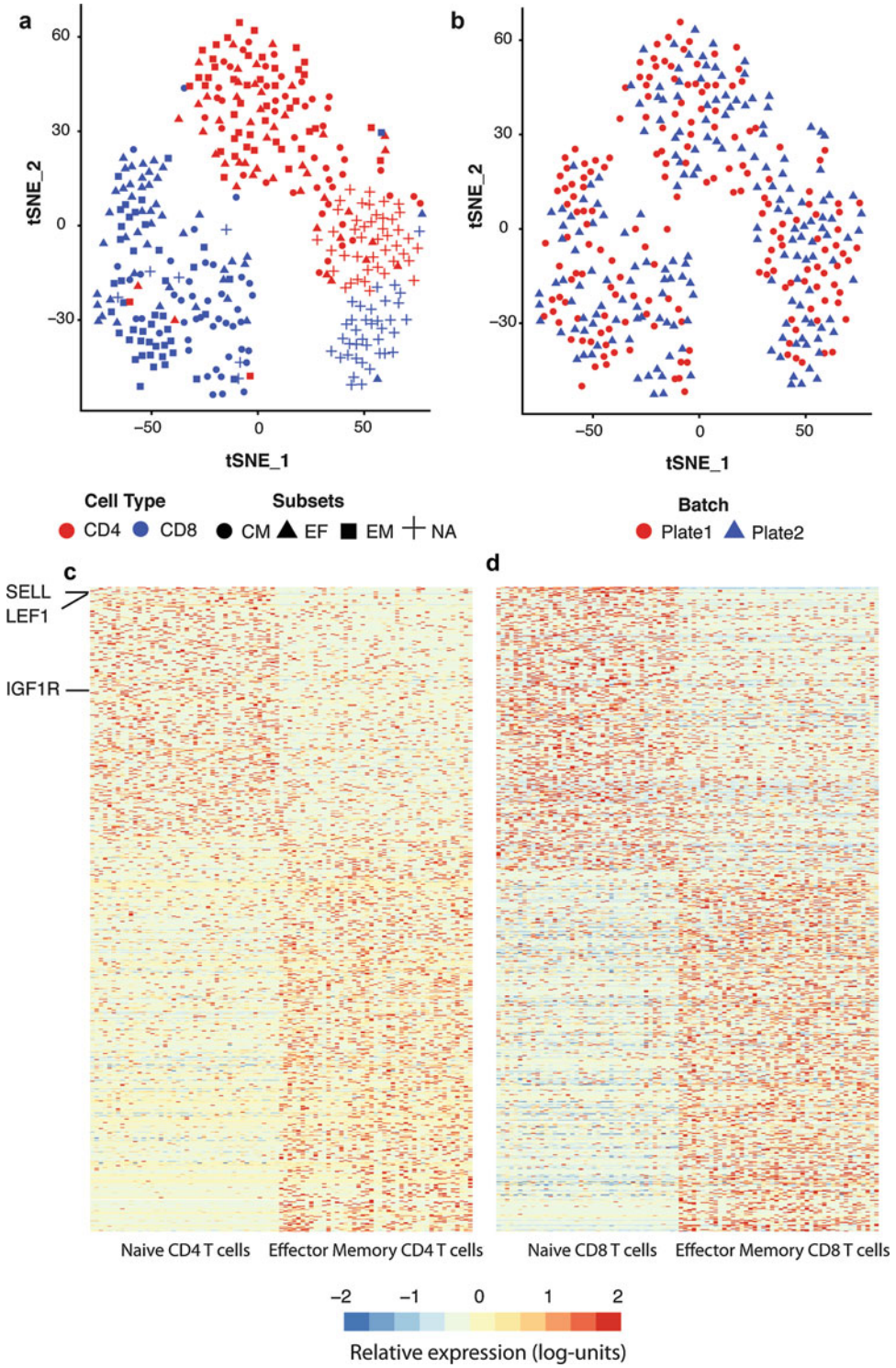
---

## 5 Notes

1. If this procedure is performed on a standard bench top (i.e., not in an RNA fume hood), keep the plate covered (e.g., using the lid from a fresh box of pipet tips, placed slightly ajar) to prevent dust and debris from falling into samples during procedure, thus limiting contamination.
2. The magnet described draws the beads to alternating sides of each column of the plate. It is therefore recommended to use a P200 eight-channel pipette to remove the supernatant.
3. Let the beads dry on the magnet to limit dried beads from leaving the wells and cross-contaminate adjacent wells. Furthermore, as beads are electrostatics, recovery will be improved if beads are dried on the magnet. Noteworthy, allowing beads to dry for too long (beyond 10 min) may impair recovery of RNA. Immediately proceed with protocol when visible cracks appear in the pellet of beads. If all residual ethanol was promptly removed, beads should crack within 10 min.
4. Once the beads are dried, it is best to deposit the 4  $\mu$ l of master mix on the bead pellet while the plate is still on the magnet to limit bead loss, which could otherwise easily escape the well once dried if not on the magnet because of their electrostatic properties. Then carefully move the plate away from the magnet and resuspend the 4  $\mu$ l with P20 multichannel and low retention tips. The solution should be homogeneous after resuspension; it is important to pipette slowly to limit the generation of bubbles.

---

**Fig. 6** Unsupervised clustering analysis of different T cell subsets. **(a)** tSNE scatter plot of 180 CD4<sup>+</sup> (*red*) and 177 CD8<sup>+</sup> (*blue*) T cells, which was generated using the top 10 principal components in the data. The subsets are highlighted by different symbols. **(b)** The data was generated through 2 experimental batches (2 batches of 96 CD4<sup>+</sup> and 96 CD8<sup>+</sup> cells each). The mixing of cells from the two batches (*red circles* and *blue squares*) in the tSNE plot in panel **b** suggests that no significant batch effects are observed across the 180 CD4<sup>+</sup> and 177 CD8<sup>+</sup> T cells analyzed. **(c, d)** Heatmaps were generated to illustrate the output from using SCDE software package. Heatmap in panel **(c)** highlights the 733 genes differentially expressed between naïve and effector memory CD4<sup>+</sup> T cells at an average log-fold change higher than 3 between the subsets. **(d)** Heatmap of the 761 differentially expressed genes expressed between naïve and effector memory CD8<sup>+</sup> T cells



5. For the reverse transcription (RT) step of the SS2 protocol, both Picelli et al. [25, 26], and Trombetta et al. [27] recommend using SuperScript II Reverse Transcriptase (ThermoFisher Scientific), while Satija et al. [75] reports using instead Maxima Reverse Transcriptase (ThermoFisher Scientific), which is significantly cheaper. As described above, the RT step can be inefficient with low capture rates of transcripts during the RT step, resulting in an important source of uncertainty in scRNA-seq data and leading to the “dropout” of genes in some libraries. If a low number of transcripts are detected, it is possible to troubleshoot the experimental system being used by trying different reverse transcription enzymes. Noteworthy, when using switching RT enzyme, it is important to adjust the optimal reaction temperature following the manufacturer’s recommendation (e.g., SuperScript II Reverse Transcriptase optimal reaction temperature is 42 °C, while Maxima Reverse Transcriptase’s is between 50 and 55 °C). In the case of T cells, both the SuperScript II Reverse Transcriptase and the Maxima Reverse Transcriptase work well at optimal reaction temperature. The data included in the figures of this protocol were generated using SuperScript II Reverse Transcriptase. Additionally, as originally reported by Picelli et al. [25, 26], trehalose and betaine may be added to the RT mix to limit the formation of RNA secondary structure (e.g., hairpins or loops) during the RT reaction, which might cause the enzyme terminating chain elongation owing to steric hindrance.
6. Reference transcriptomes are usually available as a FASTA file of transcript sequences, or as a tabular GTF file which indicates the positions of the transcripts along a reference genome. Reference genomes currently exist for many model and nonmodel organisms, and are available as FASTA files (*see Note 13*). In cases where a reference genome is available but not a reference transcriptome, it is possible to assemble it ab initio using reads mapped to a reference genome [56]. In cases where the genome of an organism has not been sequenced, it is possible to assemble a transcriptome de novo from bulk RNA-seq data [57].
7. As a general rule, it is implicit that the names of files in the commands specified here must include the full path to their location on the server or be available in the user’s current working directory.
8. SAM is an abbreviation for “Sequence Alignment Map” format. It is one of many standard formats in which commonly used genomics software output their results. It is a human readable tab-delimited text format, each line of which corresponds to the alignment of a single read. The alignment line

has 11 mandatory fields for important alignment information such as mapping position and mapping quality score, and a number of optional fields. The BAM format is a compressed version of the SAM format that is not directly human readable but can be efficiently read using programs like samtools (<https://samtools.github.io>), a suite of widely used tools for reading and manipulating SAM/BAM files. Full details of the SAM/BAM format are specified here, <https://samtools.github.io/hts-specs/SAMv1.pdf>.

9. RNA-SeQC [58] is a single java program built on the Picard API, which computes a series of quality control metrics for RNA-seq data using the BAM files as input, and outputs a series of HTML reports and tab delimited text files summarizing QC metrics. It can be downloaded from, <https://www.broadinstitute.org/cancer/cga/rna-seqc>. The RSeQC package [59] provides a number of useful scripts written in the python language that use the alignment BAM files as input to perform various individual tasks like calculating sequence quality, GC bias, and coverage uniformity. It can be downloaded from <http://rseqc.sourceforge.net>.
10. To visualize multiple sample alignments using minimal computer memory, convert the BAM files to the tiled data file (TDF) format, which summarizes the pileup of read counts along the genome. Instructions to convert BAM files to TDF format are provided in the IGV documentation, <https://www.broadinstitute.org/igv/>.
11. Alternative commonly used tools to perform transcript/gene quantification from reads aligned to a reference transcriptome include RNA-seq by Expectation Maximization (RSEM) [60] and Cufflinks [37].
12. Kallisto is a recently published program, and is based on the idea of “pseudoalignment,” wherein every read is queried for its compatibility with targets along the transcriptome without the need for an exact alignment. As demonstrated in Bray et al. [40] “pseudoalignment” not only computationally outperforms existing tools, but is also more robust to sequencing errors compared to techniques that involve exact alignment.
13. FASTA files use a standard text-based format for representing nucleotide sequences or protein sequences. The format also allows for sequence names and comments (meta-data) to precede the actual sequences as “headers.” FASTA is a simple format, which makes it easy for most bioinformatics tools and programming languages to manipulate and parse sequences. More information can be found at [https://en.wikipedia.org/wiki/FASTA\\_format](https://en.wikipedia.org/wiki/FASTA_format).

14. Here we used the Hg19 transcriptome (UCSC) reference annotation. The metadata files are available on request to the authors of the manuscript.
15. Because of differences in overall sequencing depth between samples and the difference in transcript lengths, the raw read counts of gene  $i$  in cell  $j$   $C_{ij}$  do not necessarily reflect the abundance of transcripts of gene  $i$  in cell  $j$ . It is common practice therefore to normalize the read counts, and multiple approaches exist. Here we use transcripts-per-million TPM $_{ij}$ , which is the expected number of transcripts of gene  $i$  in cell  $j$  per million transcripts, given the relative length of gene  $i$  and the abundances of all the other genes in cell  $j$ . As the name suggests, the TPM values for all the genes within a given cell sum to  $10^6$ . Kallisto automatically provides a column of calculated TPM values in the abundance.tsv file.
16. In R, these can be accomplished by repetitively using the read.table command, which reads individual tsv files as a vector, and applying the cbind command on these vectors to bind them into a matrix or a R data frame. The resulting matrix should have the genes as rows and individual single-cell samples as columns.
17. Barplot for visualizing library properties and genes. The following code can be copied and run in the console window in RStudio. This will make the function barplot\_tcell available to use. Note that sentences preceded by “#” are treated as comments and not executed by R,

```
barplot_tcell=function(x=NULL, id=NULL, name=NULL) {
  #Inputs:
  # x=numeric vector
  # id=factor, indicating sample ids with the same length and order as x
  # name=string, y-axis label
  #Outputs:
  # Bar plot
  df=data.frame(Value=as.numeric(x), id=as.character(id))
  means.sem=ddply(df, c("id"), summarise, mean=mean(Value),
sem=sd(Value))
  means.sem<- transform(means.sem, lower=mean-sem, upper=mean+sem)
  print(ggplot(means.sem, aes(x=id, y=mean, fill=factor(id))) +
geom_bar(stat="identity", color="black") +
  geom_errorbar(aes(ymax=upper,ymin=lower), position=position_
dodge(0.9), data=means.sem, width=0.3) +
  theme(axis.text.x=element_text(angle=45, hjust=1)) +
xlab("Sample")+ylab(name)+theme_bw())
}
```

18. The Coefficient of Variation (CV) is a measure of variability of the data and is defined as the ratio of the standard deviation by the mean.

19. Scatter plot for visualizing PCA projections of cells. The following code can be copied and run in the R terminal. This will make the function `scatter_plot` available to use. Note that sentences preceded by “#” are treated as comments and not executed by R.

```
scatter_plot=function(X=NULL, id=NULL, axis.labels=c("PC1","PC2")){
#Inputs:
# X - Any matrix with dimensions (cells X features. Here the features
are the PCA scores or the tSNE coordinates
# id ==factor, indicating sample ids with the same length and order
as the number of rows in X
# Axis labels=x- and y-axis labels for the plot
#Output:
# Barplot
df=as.data.frame(X)
colnames(df)=c("x","y")
df$sample=substr(id,5,6)
df$type=substr(id,1,3)
p=ggplot(df, aes(x,y))+geom_point(aes(shape=sample,
color=factor(type)), size=4)+scale_color_manual(values=c("red",
"blue"), name="Cell Type")+ylab(axis.labels[2])+xlab(axis.labels[1])
p<- p+theme(axis.title.x=element_text(face="bold", colour="#990000",
size=16), axis.text.x=element_text(angle=0, vjust=0.5, size=12))
p<- p+theme(axis.title.y=element_text(face="bold", colour="#990000",
size=16), axis.text.y=element_text(angle=0, vjust=0.5, size=12))
p<- p+theme(plot.title=element_text(size=12, face="bold"))+theme_
bw()
print(p)
}
```

20. Barplot for visualizing genes that drive PCs. The following code can be copied and run in the R terminal, and will make the function `barplot_loadings` available to use. Note that sentences preceded by “#” are treated as comments and not executed by R.

```
barplot_loadings=function(X=pca.loadings,pc.use=1, num.genes=8){
#Inputs :
# X=matrix (genes by PCs) of PCA loadings output by prcomp
# pc.use=The PC for which loadings are desired
# num.genes=The number of top+ve and -ve genes to plot
#Output :
# Barplot
ord=order(X[,pc.use]); vals=X[ord,pc.use]
genes.select=c(1:num.genes, (nrow(X)-num.genes):nrow(X))
vals=vals[genes.select];
names(vals)=rownames(X)[ord][genes.select];
df=data.frame(loadings=vals, genes=factor(names(vals), lev-
els=names(vals)))
print(ggplot(df, aes(x=genes, y=loadings))+geom_bar(position="iden-
tity", stat="identity", color="black",fill="blue") + +theme_bw() +
theme(axis.text.x=element_text(angle=45, hjust=1))+xlab("Gene")+ylab
(paste0("PC",pc.use," loadings")))
}
```

21. Invoking SCDE for differential expression analysis. The following code can be copied and run in the R terminal, and will make the wrapper function `scde_test` available to use. The following command can be copied and run in the R terminal, and will make the function `scatter_plot` available to the user:

```
scde_test=function(C=NULL, grp1=NULL, grp2=NULL, min.fold=3){
#Inputs:
#C - Counts matrix (genes x cells)
#grp1, grp2 - a character string indicating the sample names (e.g.,
CD4.NA, CD4.EM) that can be used to extract relevant cells.
#min.fold - minimum log-fold change between the two samples for a
marker to be considered for the differential expression test (Default
value 3)
#Output:
# Table showing differentially expressed genes, their inferred log-fold
changes and statistical score.
cells.1=grep(grp1,colnames(C),value=TRUE);
cells.2=grep(grp2,colnames(C),value=TRUE);
sg=factor(c(rep(grp1,length(cells.1)), rep(grp2, length(cells.2))),
levels=c(grp1,grp2))
names(sg)=c(cells.1, cells.2);
err.model=scde.error.models(counts=round(C[,c(cells.1,cells.2)]),
groups=sg, n.cores=8, verbose=1);
valid.cells=err.model$corr.a>0
err.model=err.model[valid.cells,];
prior<- scde.expression.prior(models=err.model,
counts=round(C[,valid.cells]), show.plot=F)
diff.exp=scde.expression.difference(err.model,
round(C[,valid.cells]), prior, groups=sg[valid.cells],
n.randomizations=100, n.cores=8, verbose=1)
diff.exp<- subset(diff.exp, ((lb>0 & ub>0) | (lb<0 & ub<0)) &
abs(mle)>min.fold)
return(diff.exp[,c("mle","Z")])}
```

---

## Acknowledgments

K. S. and A. C. V. thank Brian Haas, Dr. Timothy Tickle, Dr. Petter Brodin, Dr. Sara Garamszegi, Chris Rodman, and Noga Rogel for helpful comments and feedback on the content and organization of the manuscript. K. S. and A. C. V. thank Dr. Aviv Regev and Dr. Nir Hacohen for feedback and support.

## References

1. Lever M, Maini PK, van der Merwe PA et al (2014) Phenotypic models of T cell activation. *Nat Rev Immunol* 14(9):619–629. doi:[10.1038/nri3728](https://doi.org/10.1038/nri3728)
2. Yui MA, Rothenberg EV (2014) Developmental gene networks: a triathlon on the course to T cell identity. *Nat Rev Immunol* 14(8):529–545. doi:[10.1038/nri3702](https://doi.org/10.1038/nri3702)

3. Tschärke DC, Croft NP, Doherty PC et al (2015) Sizing up the key determinants of the CD8<sup>+</sup> T cell response. *Nat Rev Immunol* 15(11):705–716. doi:[10.1038/nri3905](https://doi.org/10.1038/nri3905)
4. Farber DL, Yudanin NA, Restifo NP (2014) Human memory T cells: generation, compartmentalization and homeostasis. *Nat Rev Immunol* 14(1):24–35. doi:[10.1038/nri3567](https://doi.org/10.1038/nri3567)
5. Geginat J, Paroni M, Maglie S et al (2014) Plasticity of human CD4<sup>+</sup> T cell subsets. *Front Immunol* 5:630. doi:[10.3389/fimmu.2014.00630](https://doi.org/10.3389/fimmu.2014.00630)
6. Zhu J, Paul WE (2010) Heterogeneity and plasticity of T helper cells. *Cell Res* 20(1):4–12. doi:[10.1038/cr.2009.138](https://doi.org/10.1038/cr.2009.138)
7. O’Shea JJ, Paul WE (2010) Mechanisms underlying lineage commitment and plasticity of helper CD4<sup>+</sup> T cells. *Science* 327(5969):1098–1102. doi:[10.1126/science.1178334](https://doi.org/10.1126/science.1178334)
8. O’Garra A, Vieira P (2007) T(H)1 cells control themselves by producing interleukin-10. *Nat Rev Immunol* 7(6):425–428
9. Zhou X, Bailey-Bucktrout S, Jeker LT et al (2009) Plasticity of CD4(+) FoxP3(+) T cells. *Curr Opin Immunol* 21(3):281–285. doi:[10.1016/j.coi.2009.05.007](https://doi.org/10.1016/j.coi.2009.05.007)
10. Chattopadhyay PK, Gierahn TM, Roederer M et al (2014) Single-cell technologies for monitoring immune systems. *Nat Immunol* 15(2):128–135. doi:[10.1038/ni.2796](https://doi.org/10.1038/ni.2796)
11. Stegle O, Teichmann SA, Marioni JC (2015) Computational and analytical challenges in single-cell transcriptomics. *Nat Rev Genet* 16(3):133–145. doi:[10.1038/nrg3833](https://doi.org/10.1038/nrg3833)
12. Raj A, Peskin CS, Tranchina D et al (2006) Stochastic mRNA synthesis in mammalian cells. *PLoS Biol* 4(10), e309
13. Wu AR, Neff NF, Kalisky T et al (2014) Quantitative assessment of single-cell RNA-sequencing methods. *Nat Methods* 11(1):41–46. doi:[10.1038/nmeth.2694](https://doi.org/10.1038/nmeth.2694)
14. Ozsolak F, Milos PM (2011) RNA sequencing: advances, challenges and opportunities. *Nat Rev Genet* 12(2):87–98. doi:[10.1038/nrg2934](https://doi.org/10.1038/nrg2934)
15. Tang F, Barbacioru C, Bao S et al (2010) Tracing the derivation of embryonic stem cells from the inner cell mass by single-cell RNA-Seq analysis. *Cell Stem Cell* 6(5):468–478. doi:[10.1016/j.stem.2010.03.015](https://doi.org/10.1016/j.stem.2010.03.015)
16. Tang F, Barbacioru C, Wang Y et al (2009) mRNA-seq whole-transcriptome analysis of a single cell. *Nat Methods* 6(5):377–382. doi:[10.1038/nmeth.1315](https://doi.org/10.1038/nmeth.1315)
17. Kurimoto K, Yabuta Y, Ohinata Y et al (2006) An improved single-cell cDNA amplification method for efficient high-density oligonucleotide microarray analysis. *Nucleic Acids Res* 34(5), e42
18. Hashimshony T, Wagner F, Sher N et al (2012) CEL-seq: single-cell RNA-seq by multiplexed linear amplification. *Cell* 2(3):666–673. doi:[10.1016/j.celrep.2012.08.003](https://doi.org/10.1016/j.celrep.2012.08.003)
19. Jaitin DA, Kenigsberg E, Keren-Shaul H et al (2014) Massively parallel single-cell RNA-seq for marker-free decomposition of tissues into cell types. *Science* 343(6172):776–779. doi:[10.1126/science.1247651](https://doi.org/10.1126/science.1247651)
20. Macosko EZ, Basu A, Satija R et al (2015) Highly parallel genome-wide expression profiling of individual cells using nanoliter droplets. *Cell* 161(5):1202–1214. doi:[10.1016/j.cell.2015.05.002](https://doi.org/10.1016/j.cell.2015.05.002)
21. Klein AM, Mazutis L, Akartuna I et al (2015) Droplet barcoding for single-cell transcriptomics applied to embryonic stem cells. *Cell* 161(5):1187–1201. doi:[10.1016/j.cell.2015.04.044](https://doi.org/10.1016/j.cell.2015.04.044)
22. Soumillon M, Cacchiarelli D, Semrau S et al (2014) Characterization of directed differentiation by high-throughput single-cell RNA-Seq. *BioRxiv*. doi: <http://dx.doi.org/10.1101/003236>
23. Islam S, Zeisel A, Joost S et al (2014) Quantitative single-cell RNA-seq with unique molecular identifiers. *Nat Methods* 11(2):163–166. doi:[10.1038/nmeth.2772](https://doi.org/10.1038/nmeth.2772)
24. Ramsköld D, Luo S, Wang YC et al (2012) Full-length mRNA-Seq from single-cell levels of RNA and individual circulating tumor cells. *Nat Biotechnol* 30(8):777–782
25. Picelli S, Björklund ÅK, Faridani OR et al (2013) Smart-seq2 for sensitive full-length transcriptome profiling in single cells. *Nat Methods* 10(11):1096–1098. doi:[10.1038/nmeth.2639](https://doi.org/10.1038/nmeth.2639)
26. Picelli S, Faridani OR, Björklund ÅK et al (2014) Full-length RNA-seq from single cells using Smart-seq2. *Nat Protoc* 9(1):171–181. doi:[10.1038/nprot.2014.006](https://doi.org/10.1038/nprot.2014.006)
27. Trombetta JJ, Gennert D, Lu D et al (2014) Preparation of single-cell RNA-seq libraries for next generation sequencing. *Curr Protoc Mol Biol* 107:4.22.1–4.22.17. doi:[10.1002/0471142727.mb0422s107](https://doi.org/10.1002/0471142727.mb0422s107)
28. Stubbington MJT, Lönnberg T, Proserpio V et al (2015) Simultaneously inferring T cell fate and clonality from single cell transcriptomes. *BioRxiv*. doi: <http://dx.doi.org/10.1101/025676>
29. Grün D, Kester L, van Oudenaarden A (2014) Validation of noise models for single-cell transcriptomics. *Nat Methods* 11(6):637–640. doi:[10.1038/nmeth.2930](https://doi.org/10.1038/nmeth.2930)
30. Grün D, van Oudenaarden A (2015) Design and analysis of single-cell sequencing experiments. *Cell* 163(4):799–810. doi:[10.1016/j.cell.2015.10.039](https://doi.org/10.1016/j.cell.2015.10.039)

31. Hicks SC, Teng M, Irizarry RA (2015) On the widespread and critical impact of systematic bias and batch effects in single-cell RNA-Seq data. *BioRxiv*. doi: <http://dx.doi.org/10.1101/025528>
32. Kharchenko PV, Silberstein L, Scadden DT (2014) Bayesian approach to single-cell differential expression analysis. *Nat Methods* 11(7):740–742. doi:[10.1038/nmeth.2967](https://doi.org/10.1038/nmeth.2967)
33. Luo H, Li J, Chia BKH et al (2014) The importance of study design for detecting differentially abundant features in high-throughput experiments. *Genome Biol* 15(12):527. doi:[10.1186/s13059-014-0527-7](https://doi.org/10.1186/s13059-014-0527-7). Johnson
34. Evan W, Li C et al (2007) Adjusting batch effects in microarray expression data using empirical Bayes methods. *Biostatistics* 8(1): 118–127. doi:[10.1093/biostatistics/kxj037](https://doi.org/10.1093/biostatistics/kxj037)
35. Leek JT, Scharpf RB, Bravo HC et al (2010) Tackling the widespread and critical impact of batch effects in high-throughput data. *Nat Rev Genet* 11(10):733–739. doi:[10.1038/nrg2825](https://doi.org/10.1038/nrg2825)
36. Qu K, Garamszegi S, Wu F, et al. (2016) Integrative genomic analysis by interoperation of bioinformatics tools in GenomeSpace. *Nat Methods*. doi: [10.1038/nmeth.3732](https://doi.org/10.1038/nmeth.3732)
37. Trapnell C, Roberts A, Goff L et al (2012) Differential gene and transcript expression analysis of RNA-seq experiments with TopHat and Cufflinks. *Nat Protoc* 7(3):562–578. doi:[10.1038/nprot.2012.016](https://doi.org/10.1038/nprot.2012.016)
38. Engström PG, Steijger T, Sipos B et al (2013) Systematic evaluation of spliced alignment programs for RNA-seq data. *Nat Methods* 10(12):1185–1191. doi:[10.1038/nmeth.2722](https://doi.org/10.1038/nmeth.2722)
39. Mortazavi A, Williams BA, McCue K et al (2008) Mapping and quantifying mammalian transcriptomes by RNA-Seq. *Nat Methods* 5(7):621–628. doi:[10.1038/nmeth.1226](https://doi.org/10.1038/nmeth.1226)
40. Bray N, Pimentel H, Melsted P et al (2015) Near-optimal RNA-seq quantification. *BioRxiv* 1505:02710
41. Trapnell C (2015) Defining cell types and states with single-cell genomics. *Genome Res* 25(10): 1491–1498. doi:[10.1101/gr.190595.115](https://doi.org/10.1101/gr.190595.115)
42. Gentleman RC, Carey VJ, Bates DM et al (2004) Bioconductor: open software development for computational biology and bioinformatics. *Genome Biol* 5(10):R80
43. Smith LI (2002) A tutorial on principal components analysis. *Cornell Univ* 51:52
44. Shalek AK, Satija R, Adiconis X et al (2013) Single-cell transcriptomics reveals bimodality in expression and splicing in immune cells. *Nature* 498(7453):236–240. doi:[10.1038/nature12172](https://doi.org/10.1038/nature12172)
45. Shalek AK, Satija R, Shuga J et al (2014) Single-cell RNA-seq reveals dynamic paracrine control of cellular variation. *Nature* 510(7505):363–369. doi:[10.1038/nature13437](https://doi.org/10.1038/nature13437)
46. Pollen AA, Nowakowski TJ, Shuga J et al (2014) Low-coverage single-cell mRNA sequencing reveals cellular heterogeneity and activated signaling pathways in developing cerebral cortex. *Nat Biotechnol* 32(10):1053–1058. doi:[10.1038/nbt.2967](https://doi.org/10.1038/nbt.2967)
47. Usoskin D, Furlan A, Islam S et al (2015) Unbiased classification of sensory neuron types by large-scale single-cell RNA sequencing. *Nat Neurosci* 18(1):145–153. doi:[10.1038/nn.3881](https://doi.org/10.1038/nn.3881)
48. Steinke FC, Yu S, Zhou X et al (2014) TCF-1 and LEF-1 act upstream of Th-POK to promote the CD4(+) T cell fate and interact with Runx3 to silence CD4 in CD8(+) T cells. *Nat Immunol* 15(7):646–656. doi:[10.1038/ni.2897](https://doi.org/10.1038/ni.2897)
49. Mingueneau M, Kreslavsky T, Gray D et al (2013) The transcriptional landscape of  $\alpha\beta$  T cell differentiation. *Nat Immunol* 14(6):619–632. doi:[10.1038/ni.2590](https://doi.org/10.1038/ni.2590)
50. Van der Maaten L, Hinton G (2008) Visualizing data using t-SNE. *J Mach Learn Res* 9:2579–2605
51. Peres-Neto PR, Jackson DA, Somers KM (2005) How many principal components? Stopping rules for determining the number of non-trivial axes revisited. *Comput Stat Data Anal* 49(4):974–997. doi:[10.1016/j.csda.2004.06.015](https://doi.org/10.1016/j.csda.2004.06.015)
52. Risso D, Ngai J, Speed TP et al (2014) Normalization of RNA-seq data using factor analysis of control genes or samples. *Nat Biotechnol* 32(9):896–902. doi:[10.1038/nbt.2931](https://doi.org/10.1038/nbt.2931)
53. Suzuki R, Shimodaira H (2013) Hierarchical clustering with P-values via multiscale bootstrap resampling. R package
54. Bodenhofer U, Kothmeier A, Hochreiter S (2011) APCluster: an R package for affinity propagation clustering. *Bioinformatics* 27(17):2463–2464. doi:[10.1093/bioinformatics/btr406](https://doi.org/10.1093/bioinformatics/btr406)
55. Fraley C, Raftery AE (2006) MCLUST version 3: an R package for normal mixture modeling and model-based clustering. Washington Univ Seattle Dept of Statistics
56. Trapnell C, Williams BA, Pertea G et al (2010) Transcript assembly and quantification by RNA-Seq reveals unannotated transcripts and isoform switching during cell differentiation. *Nat Biotechnol* 28(5):511–515. doi:[10.1038/nbt.1621](https://doi.org/10.1038/nbt.1621)

57. Grabherr MG, Haas BJ, Yassour M et al (2011) Full-length transcriptome assembly from RNA-seq data without a reference genome. *Nat Biotechnol* 29(7):644–652. doi:[10.1038/nbt.1883](https://doi.org/10.1038/nbt.1883)
58. DeLuca DS, Levin JZ, Sivachenko A et al (2012) RNA-SeQC: RNA-seq metrics for quality control and process optimization. *Bioinformatics* 28(11):1530–1532. doi:[10.1093/bioinformatics/bts196](https://doi.org/10.1093/bioinformatics/bts196)
59. Wang L, Wang S, Li W (2012) RSeQC: quality control of RNA-seq experiments. *Bioinformatics* 28(16):2184–2185. doi:[10.1093/bioinformatics/bts356](https://doi.org/10.1093/bioinformatics/bts356)
60. Li B, Dewey CN (2011) RSEM: accurate transcript quantification from RNA-Seq data with or without a reference genome. *BMC Bioinformatics* 12:323. doi:[10.1186/1471-2105-12-323](https://doi.org/10.1186/1471-2105-12-323)
61. Eberwine J, Yeh H, Miyashiro K et al (1992) Analysis of gene expression in single live neurons. *Proc Natl Acad Sci U S A* 89(7):3010–3014
62. Morris J, Singh JM, Eberwine JH (2011) Transcriptome analysis of single cells. *J Vis Exp* 50:e2634. doi:[10.3791/2634](https://doi.org/10.3791/2634)
63. Pan X, Durrett RE, Zhu H et al (2013) Two methods for full-length RNA sequencing for low quantities of cells and single cells. *Proc Natl Acad Sci U S A* 110(2):594–599. doi:[10.1073/pnas.1217322109](https://doi.org/10.1073/pnas.1217322109)
64. Kang Y, Norris MH, Zarzycki-Siek J et al (2011) Transcript amplification from single bacterium for transcriptome analysis. *Genome Res* 21(6):925–935. doi:[10.1101/gr.116103.110](https://doi.org/10.1101/gr.116103.110)
65. Islam S, Kjallquist U, Moliner A et al (2012) Highly multiplexed and strand-specific single-cell RNA 5' end sequencing. *Nat Protoc* 7(5):813–828. doi:[10.1038/nprot.2012.022](https://doi.org/10.1038/nprot.2012.022)
66. Pierson E, Yau C (2015) ZIFA: dimensionality reduction for zero-inflated single-cell gene expression analysis. *Genome Biol* 16:241. doi:[10.1186/s13059-015-0805-z](https://doi.org/10.1186/s13059-015-0805-z)
67. Trapnell C, Cacchiarelli D, Grimsby J et al (2014) The dynamics and regulators of cell fate decisions are revealed by pseudotemporal ordering of single cells. *Nat Biotechnol* 32(4):381–386. doi:[10.1038/nbt.2859](https://doi.org/10.1038/nbt.2859)
68. Buettner F, Natarajan KN, Casale FP et al (2015) Computational analysis of cell-to-cell heterogeneity in single-cell RNA-sequencing data reveals hidden subpopulations of cells. *Nat Biotechnol* 33(2):155–160. doi:[10.1038/nbt.3102](https://doi.org/10.1038/nbt.3102).Vallejos
69. Vallejos CA, Marioni JC, Richardson S (2015) BASiCS: Bayesian analysis of single-cell sequencing data. *PLoS Comput Biol* 11(6):e1004333. doi:[10.1371/journal.pcbi.1004333](https://doi.org/10.1371/journal.pcbi.1004333)
70. Fan J, Salathia N, Liu R et al (2016) Characterizing transcriptional heterogeneity through pathway and gene set overdispersion analysis. *Nat Methods*. doi: [10.1038/nmeth.3734](https://doi.org/10.1038/nmeth.3734)
71. Juliá M, Telenti A, Rausell A (2015) Sincell: an R/bioconductor package for statistical assessment of cell-state hierarchies from single-cell RNA-seq. *Bioinformatics* 31(20):3380–3382. doi:[10.1093/bioinformatics/btv368](https://doi.org/10.1093/bioinformatics/btv368)
72. Grün D, Lyubimova A, Kester L et al (2015) Single-cell messenger RNA sequencing reveals rare intestinal cell types. *Nature* 525(7568):251–255. doi:[10.1038/nature14966](https://doi.org/10.1038/nature14966)
73. Marco E, Karp RL, Guo G et al (2014) Bifurcation analysis of single-cell gene expression data reveals epigenetic landscape. *Proc Natl Acad Sci U S A* 111(52):E5643–E5650. doi:[10.1073/pnas.1408993111](https://doi.org/10.1073/pnas.1408993111)
74. Scater. <https://github.com/davismcc/scater>
75. Satija R, Farrell JA, Gennert D et al (2015) Spatial reconstruction of single-cell gene expression data. *Nat Biotechnol* 33(5):495–502. doi:[10.1038/nbt.3192](https://doi.org/10.1038/nbt.3192)

## Extensive Phenotypic Analysis, Transcription Factor Profiling, and Effector Cytokine Production of Human MAIT Cells by Flow Cytometry

Joana Dias, Johan K. Sandberg, and Edwin Leeansyah

### Abstract

The mucosa-associated invariant T (MAIT) cells are a large and relatively recently described innate-like antimicrobial T cell subset in humans. The study of human MAIT cells is still in its infancy, and many aspects of MAIT cell immunobiology in health and disease remain unexplored. Here, we describe methodological approaches and protocols to investigate the expression of a broad spectrum of surface receptors on human MAIT cells, and to examine their unique transcription factor profile, as well as their antimicrobial effector function using multicolor flow cytometry-based techniques. We provide specific guidance on protocols and describe potential pitfalls for each of the presented methodologies. Finally, we discuss future prospects and current limitations of multicolor flow cytometry-based approaches to the study of human MAIT cells.

**Key words** Human, Mucosa-associated invariant T cells, Immunophenotyping, Transcription factors, Cytokines, Cytolytic molecules, Multicolor flow cytometry, LEGENDScreen™

---

### 1 Introduction

Mucosa-associated invariant T (MAIT) cells are a newly described subset of innate-like antimicrobial T cells that are highly abundant in mucosal tissues, the liver, and circulation of healthy humans [1]. MAIT cells express the invariant T cell receptor (TCR) V $\alpha$ 7.2 segment coupled with restricted J $\alpha$  and V $\beta$  repertoires, which recognize antigens in complex with the major histocompatibility complex class I-related protein (MR1) [2–4]. The co-expression of the V $\alpha$ 7.2 TCR with high levels of the C-type lectin receptor CD161 or the IL-18 receptor  $\alpha$  subunit (IL-18R $\alpha$ ) defines this innate-like T cell population in humans [5, 6]. Recent advances have greatly facilitated our understanding of the role of MAIT cells in antimicrobial immunity in the human immune system, including the identification of microbial vitamin B<sub>2</sub> (riboflavin) metabolites as MR1-presented MAIT cell antigens [7–10], the regulation and

mechanisms of MAIT cell antimicrobial activity against a vast array of microbes [5, 11–17], and the involvement of MAIT cells in both infectious and noninfectious diseases [5, 12, 18–22]. In this Chapter, we present flow-cytometry based approaches to investigate human MAIT cells for a large number of cell surface markers, unique transcription factor profiles, and antimicrobial effector functions. Specifically, we describe how the surface immuno-proteome of MAIT cells can be screened for through the use of the BioLegend LEGENDScreen™ Human Cell Screening (PE) Kit. We also discuss strategies for how to analyze and compare the surface expression of these markers between different cell populations, such as MAIT cells and conventional CD4<sup>+</sup> and CD8<sup>+</sup> T cells. We describe how to investigate the human MAIT cell transcription factor profile in comparison to conventional CD4<sup>+</sup> and CD8<sup>+</sup> T cells. Furthermore, we also present methodologies to assess MAIT cell antimicrobial effector functions using the *Escherichia coli* bacteria as a model microbe. Throughout the chapter, we provide step-by-step guidelines on the practicalities and the need to follow standard operating procedures at certain critical steps to avoid potential pitfalls.

The protocols and methods described in detail herein allow us to extensively study the surface characteristics, transcription factor profile, as well as the functional responses of MAIT cells against microbes that harbor the riboflavin biosynthesis pathway. The protocols can with ease be applied to research questions concerning the development of MAIT cells, their functional specialization in different tissues, as well as their role during disease states that inflict morbidity and mortality in the human population. Nevertheless, these methods are limited in several ways. First, all these assays are dependent on the availability of monoclonal antibodies for proteins of interest. The surface and intracellular proteome which can be studied at the single cell level is thus restrained. Second, the cell numbers needed to perform these broad assays may not always be available. These limitations may potentially be alleviated by combining reagents in more complex multicolor panels for high-dimensional cytometry beyond 15 fluorescence parameters, or by using time-of-flight mass cytometry (CyTOF). Complementary approaches to increase our understanding of MAIT cells include cell sorting followed by whole-cell proteomic and transcriptomic analyses. These types of investigations can be guided by results obtained using the protocols described in the present chapter.

---

## 2 Materials

1. Bacteria freezing solution: (50% (v/v) glycerol with 50% (v/v) FBS); 0.22 µm filter-sterilized.
2. Phosphate-buffered saline (PBS) with 2 mM ethylenediamine-tetraacetic acid (EDTA).

3. Sodium diatrizoate density gradient solution (1.077 g/mL) for human peripheral blood mononuclear cell (PBMC) isolation, such as Lymphoprep™ (Axis-Shield) or Ficoll-Hypaque PLUS (GE Healthcare).
4. Peripheral blood
5. Complete R-10 medium: RPMI-1640 medium, 25 mM HEPES, 2 mM L-glutamine, 10% fetal bovine serum (FBS), 50–100 µg/mL gentamicin, and 100 µg/mL Normocin.
6. BD CellFIX™ Buffer (10×) (BD Biosciences): dilute to 1× by using distilled water.
7. FACS buffer: PBS, 2 mM EDTA, 2% FBS.
8. BD Pharmingen™ Transcription Factor (TF) Buffer Set (BD Biosciences).
9. BD Cytotfix/Cytoperm™ Fixation/Permeabilization Kit (BD Biosciences).
10. Anti-CD28 pure (clone: L293).
11. Fluorescently conjugated monoclonal antibodies (Tables 1 and 2).

**Table 1**

**Monoclonal antibodies used in the protocols of transcription factor (TF) and intracellular cytokine staining (ICS), including the fluorochrome, clone, and laser and filters suitable for data acquisition**

Marker	Fluorochrome	Clone	Laser and filter (nm)
Cocktail for surface pre-staining of PBMCs before ICS <sup>a</sup> or TF <sup>b</sup> staining (Subheading 3.5)			
CD3	AF700 <sup>a,b</sup>	UCHT1	639 (R 730/45)
CD4	BV711 <sup>a</sup> APC-H7 <sup>b</sup>	OKT-4 SK3	405 (V 710/50) 639 (R 780/60)
CD8	BV570 <sup>a,b</sup>	RPA-T8	405 (V 585/42)
Vα7.2	PE <sup>a</sup> PECy7 <sup>b</sup>	3C10	561 (YG 586/15) 561 (YG 780/60)
CD161	PECy5 <sup>a</sup> BV605 <sup>b</sup>	DX12 HP-3G10	561 (YG 661/20) 405 (V 610/20)
DCM	Near infrared <sup>a</sup> Aqua <sup>b</sup>	Not applicable	639 (R 780/60) 405 (V 525/50)
Cocktail for ICS <sup>a</sup> or TF staining <sup>b</sup> (Subheading 3.5)			
IL-22 <sup>a,d</sup> PLZF <sup>b</sup>	eFluor660 <sup>a</sup> APC <sup>b</sup>	22URTI 6318100	639 (R 670/30)
RORγt <sup>b</sup>	PE [BV421] <sup>b</sup>	Q21-559	561 (YG 586/15) [405 (V 450/50)] <sup>c</sup>

(continued)

**Table 1**  
**(continued)**

Marker	Fluorochrome	Clone	Laser and filter (nm)
IL-17A <sup>a</sup>	BV421 <sup>a</sup>	BL168	405 (V 450/50) [405 (V 710/50)]
T-bet <sup>b</sup>	BV421 [BV711] <sup>b</sup>	4B10	
Helios <sup>b,d</sup>	eFluor450 <sup>b</sup>	22F6	
Granzyme B <sup>a</sup>	FITC <sup>a, b</sup>	GB11	488 (B 530/30)
Eomes <sup>b,d</sup>		WD1928	
IFN $\gamma$ <sup>a</sup>	BV785 <sup>a</sup>	4S.B3	405 (V 780/60)
TNF <sup>a</sup>	PECy7 <sup>a</sup>	MAB11	561 (YG 780/60)
CD107a <sup>a,d,c</sup>		H4A3	

V violet laser, B blue laser, YG yellow-green laser, R red laser, BV Brilliant Violet™

<sup>a</sup>ICS

<sup>b</sup>TF staining

<sup>c</sup>Alternate fluorochrome and instrument settings

<sup>d</sup>Potential additional markers

<sup>e</sup>CD107a added at the beginning of the assay (see Subheading 3.4)

**Table 2**  
**Monoclonal antibodies used in the LEGENDScreen™ pre-staining protocol (see Subheading 3.6), including the fluorochrome, clone, and laser and filters suitable for data acquisition**

Marker	Fluorochrome	Clone	Laser and filter (nm)
CD3	BV785	OKT3	405 (V 780/60)
CD8	Qdot605	3B5	405 (V 610/20)
CD4	APC-H7	SK3	639 (R 780/60)
CD161	PECy5	DX12	561 (YG 661/20)
V $\alpha$ 7.2	PECy7	3C10	750 (YG 780/60)
CD127	BV650	A019D5	405 (V 670/30)
Amine-reactive live/dead cell marker (DCM)	Dump channel (FITC)	Not applicable	488 (B 530/30)
CD14		TÜK4	
CD19		HIB19	
CD20		2H7	
CD123		6H6	
Fc $\epsilon$ R1 $\alpha$		AER-37 (CRA-1)	
SLAN/M-DC8		DD-1	
BDCA-2		AC144	
LEGENDScreen™ surface marker	PE	See LEGENDScreen™ Data Sheet	561 (YG 586/15)

V violet laser, B blue laser, YG yellow-green laser, R red laser, BV Brilliant Violet™

12. Flow cytometry hardware and software: samples stained with the described antibody panels are suitable for acquisition in a LSRII Fortessa flow cytometer (BD Biosciences) equipped with 405, 488, 561, and 639 nm lasers, and by using FACSDiva™ (BD Biosciences) as a software platform and graphical user interface.
13. *Escherichia coli* strain D21 or DH5 $\alpha$ .
14. Phorbol 12-myristate 13-acetate (PMA) and ionomycin, such as the Leukocyte Activation Cocktail with GolgiPlug (BD Biosciences).
15. Protein transport inhibitors, such as monensin (GolgiStop, BD Biosciences) and brefeldin A (GolgiPlug, BD Biosciences).
16. LEGENDScreen™, Lyophilized Antibody Panel, Human Cell Screening (PE) Kit (BioLegend).
17. 10% intravenous immunoglobulin (IVIg) solution in 200 mM glycine pH 4.25 as stabilizer (Gamimune or Gamunex, Bayer): prepare working solution by diluting to 1% in PBS.
18. Anti-mouse IgG  $\kappa$  beads (BD™ CompBeads Set Anti-Mouse IgG  $\kappa$ ; BD Biosciences).

---

### 3 Methods

#### 3.1 Culture of *Escherichia coli*

1. Culture *E. coli* strain D21 or DH5 $\alpha$  in 1 L of Luria broth for 18 h at 37 °C with vigorous shaking.
2. Collect and centrifuge bacterial culture at 1500  $\times g$  for 20 min and at 4 °C with no brake.
3. Resuspend pellet in 10–20 mL of bacteria freezing solution, then aliquot, freeze, and store in –80 °C until needed.
4. Thaw a frozen aliquot of *E. coli* and determine the numbers of viable *E. coli* by total viable count (TVC) method on Luria agar. Express the numbers of viable *E. coli* cells as colony forming units per mL (CFUs/mL).

#### 3.2 Isolation of Human Peripheral Blood Mononuclear Cells from Peripheral Blood

1. Transfer the collected peripheral blood to 50 mL tubes and dilute in 2 mM EDTA-containing PBS (1:1 dilution).
2. Carefully layer 30 mL of diluted peripheral blood over 15 mL of density gradient medium, by slowly pipetting onto the medium with the 50 mL tube held at an angle of 45°.
3. Spin at 693  $\times g$  for 20 min at room temperature and with no brake.
4. Transfer the PBMC interface from each tube to new 50 mL tubes. Wash the cells three times by filling the tubes up with 2 mM EDTA-containing PBS, followed by spinning at 390  $\times g$  for 5 min.
5. After the third wash, resuspend the cells in complete R-10 medium and keep them on ice until further need (*see Note 1*).

### 3.3 Formaldehyde Fixation of *Escherichia coli*

1. Prepare 1× CellFIX solution using distilled water (*see Note 2*).
2. Thaw a frozen aliquot of *E. coli* and take  $5 \times 10^8$  CFUs (*see Note 3*). Wash once in 1 mL PBS in an Eppendorf tube, spin at  $5000 \times g$  for 3 min at 4 °C, and carefully aspirate supernatant completely.
3. Resuspend the bacteria in 500 µL of 1× CellFIX and incubate for 3–5 min at room temperature (*see Note 4*). Vortex vigorously for the first 60 s of fixation, followed by another vigorous vortex for the last 30 s of fixation.
4. Wash three times with 1 mL PBS at  $5000 \times g$  for 3 min at 4 °C. Resuspend bacteria at  $10^9$ /mL in complete R-10 medium, and vortex vigorously for at least 30 s. Keep fixed bacteria on ice while preparing cells. Do not freeze (*see Note 5*).

### 3.4 Activation of Human MAIT Cells

1. Thaw frozen PBMCs or prepare fresh PBMCs and resuspend them at  $5 \times 10^6$ /mL in complete R-10 medium in a 96-well round-bottom plate (*see Note 6*).
2. Culture cells in 200 µL per well (i.e.,  $10^6$  cells/well at  $5 \times 10^6$  cells/mL) (*see Note 7*).
3. Re-vortex bacteria at the highest speed for at least 1 min, then add bacteria at 1–10 CFUs per PBMC. Adjust the volume of bacterial suspension with complete R-10 medium so that exactly 10 µL of bacteria suspension is added per well. Mix thoroughly and incubate at 37 °C/5% CO<sub>2</sub> for 1 h (*see Note 8*).
4. After 1 h, add anti-CD28 to bacteria-PBMC wells at a final concentration of 1.25 µg/mL (*see Note 9*). Mix thoroughly and incubate for 23 h at 37 °C/5% CO<sub>2</sub>. Optional: to assess MAIT cell degranulation, add fluorochrome-conjugated anti-CD107a at a predetermined optimal concentration (0.4 µg/mL for anti-CD107a PECy7; *see Table 1*) at this step.
5. During the last 6 h of the assay, add brefeldin A-containing PMA/ionomycin (Leukocyte Activation Cocktail with GolgiPlug) at 1:500 and monensin (GolgiStop) at 1:1000 final concentrations to the corresponding PMA-control wells.
6. Add monensin (GolgiStop) and brefeldin A (GolgiPlug) each at 1:1000 final concentration to the rest of the wells. Mix well and further culture for 6 h at 37 °C/5% CO<sub>2</sub>.
7. Terminate experiment by transferring the cells to a V-bottom 96-well plate, and proceed to cell surface marker and intracellular cytokine staining (ICS) (*see Subheading 3.5*).

### 3.5 Phenotypic, TF Profiling, and Functional Analysis by Multicolor Flow Cytometry

1. After transferring the cells to a V-bottom 96-well plate, spin at  $604 \times g$  for 3 min at 4 °C. Discard supernatant and incubate the cells with the antibodies against the surface markers of interest for 20 min at 4 °C in the dark.
2. Wash cells once with 130 µL FACS buffer and spin at  $604 \times g$  for 2 min at 4 °C.

3. Optional: If a biotinylated antibody is used in **step 1**, Subheading **3.5**, incubate the cells with a streptavidin conjugate for 20 min at 4 °C and in the dark after **step 2**, Subheading **3.5**. Then wash the cells by repeating **step 2**, Subheading **3.5**.
4. Discard supernatant and proceed to cell fixation before data acquisition.
5. If proceeding with cell fixation for TF or cytokine analysis, prepare the working stock of buffer set by diluting the TF Fix/Perm or TF Perm/Wash solutions to 1× concentration using the TF Diluent Buffer or distilled water, respectively, and prepare the working stock of BD Perm/Wash buffer set by diluting to 1× concentration using distilled water.
6. After staining blood- or tissue-derived mononuclear cells with the cell surface markers of interest (*see* Subheading **3.5**, **steps 1–4**), fix the cells with 100 µL of BD CellFIX 1× for 10 min at room temperature in the dark if there will be no intracellular staining; 1× TF Fix/Perm for 40 min at 4 °C in the dark if staining for TF; BD Cytofix/Cytoperm for 30 min at 4 °C in the dark if staining for cytokines.
7. Wash away the fixative solution with 100 µL of FACS buffer if there will be no intracellular staining; 1× TF Perm/Wash if staining for TF; 1× BD Perm/Wash if staining for cytokines.
8. Spin at 755×*g* for 2 min at 4 °C and discard supernatant. Wash once more with 200 µL of the appropriate washing solution mentioned in **step 7**, Subheading **3.5**, repeat the centrifugation step, and discard the supernatant. If only surface staining is required, resuspend in 100–200 µL FACS Buffer and proceed to data acquisition.
9. Incubate the cells with mAbs against the TF of interest (*see* Table **1**) for 40 min at 4 °C in the dark, or against cytokines and cytolytic molecules (ICS) of interest (*see* Table **1**) for 30 min at 4 °C in the dark (*see* **Note 10**).
10. Wash once with 100 µL 1× TF Perm/Wash or 100 µL 1× BD Perm/Wash for TF or ICS, respectively. Spin at 755×*g* for 2 min at 4 °C.
11. Discard supernatant and resuspend in 100–200 µL FACS Buffer. Run the samples on the flow cytometer or store at 4 °C in the dark until needed (*see* **Note 11**).

**3.6 Extensive  
MAIT Cell  
Immunophenotyping  
by the LEGENDS-  
creen™ Kit**

The LEGENDScreen™ kit contains 332 phycoerythrin (PE)-conjugated monoclonal antibodies against cell surface markers and 10 immunoglobulin (Ig) isotype controls distributed throughout four 96-well plates, and can therefore be used to extensively screen PBMCs pre-stained for the cell populations of interest, such as the MAIT cells. Prepare the LEGENDScreen™ plates according to the manufacturer's

instructions (*see* LEGENDScreen™ Data Sheet available on the BioLegend website for more detailed information). Briefly:

1. Remove the plates from the aluminum pouches and spin them at  $470 \times g$  for 5 min at room temperature.
2. By holding the plate firmly, carefully remove the plate cover and discard it.
3. Reconstitute the lyophilized antibodies immediately with 25  $\mu$ L of deionized water per well using a multichannel pipette.
4. After reconstitution, use the plate sealers provided by the manufacturer to cover the plates. Wait for at least 15 min before proceeding to the staining procedure. Keep the plates in the dark.
5. Block the Fc receptors on the PBMC preparation by incubating the cells with 2 mL of 1% (v/v) intravenous immunoglobulin (IVIg) in a 50 mL tube for 10 min at room temperature.
6. Wash away the unbound IVIg by filling up the tube with FACS buffer and by spinning at  $390 \times g$  for 7 min at 4 °C.
7. Discard supernatant. Pre-stain PBMCs with the antibodies of interest for 20 min at 4 °C in the dark (*see* **Note 12** and **Table 2**).
8. Wash cells once by filling the tube up with FACS buffer and spin at  $390 \times g$  for 7 min at 4 °C. Discard supernatant.
9. Optional: incubate cells with streptavidin for 20 min at 4 °C in the dark. Repeat **step 8**, Subheading **3.6**.
10. Resuspend cells in 30 mL of cold FACS buffer.
11. Add 75  $\mu$ L of the pre-stained PBMC suspension (equivalent to  $10^6$  cells) to each well of the LEGENDScreen™ plates, and incubate the plates for 20 min at 4 °C in the dark.
12. Wash cells with 170  $\mu$ L FACS buffer and spin at  $604 \times g$  for 2 min at 4 °C.
13. Discard supernatant and fix cells in 100  $\mu$ L BD CellFIX 1 $\times$  for 10 min at room temperature in the dark. Wash cells with 170  $\mu$ L FACS buffer, spin at  $604 \times g$  for 2 min at 4 °C and discard supernatant.
14. Resuspend cells in 250  $\mu$ L FACS buffer and proceed to data acquisition. Keep the plates in the dark and at 4 °C prior to data acquisition.

### **3.7 Multicolor Flow Cytometry Compensation**

In order to correct the spectral overlap between the several fluorochromes used in the stainings, prepare single fluorochrome-stained controls using polystyrene microparticles (beads) (BD™ CompBeads Set Anti-Mouse Ig,  $\kappa$ ).

1. Add one drop of BD™ CompBeads Anti-Mouse IgG  $\kappa$  and one drop of BD™ CompBeads Negative Control per well in a V-bottom 96-well plate for each fluorochrome. Include a single well for an unstained bead control.
2. Add 0.5  $\mu$ L of each antibody to the wells and follow the same staining protocol as for the samples for which the compensation will be used (*see* Subheadings 3.5 and 3.6).

### 3.8 Multicolor Flow Cytometry Analysis

1. Use the FACSDiva software to export the acquired sample files in Flow Cytometry Standard (FCS) 3.0 files, required for further analysis in the FlowJo analysis software (TreeStar).
2. In FlowJo, use the *Compensation Wizard* tool to compensate the sample files with the bead files. A compensation matrix will be generated by FlowJo indicating the amount of spillover of one fluorochrome into the other, for all fluorochrome combinations in the panel used. This matrix might need to be adjusted, as explained below.
3. It is highly recommended to double-check the compensation applied to all fluorochrome combinations automatically set by the FlowJo software. For that, check the staining pattern of one fluorochrome against all the others in the lymphocyte gate.
4. Gate the acquired cells until the cell populations of interest. Fig. 1 illustrates our gating strategy for the MAIT cell population, and for the conventional CD4<sup>+</sup> and CD8<sup>+</sup> T cells.
5. Start by plotting the Time vs. any marker (it can be one of the readout markers or forward or side scatter—FSC or SSC, respectively) in order to check how stable the sample acquisition was.
6. Proceed to the single cells gating by plotting FSC-H vs. FSC-A and/or SSC-H vs. SSC-A.
7. Gate out the dead (or dump channel negative) cells by plotting Dump channel/DCM vs. FSC or SSC.
8. Plot FSC-A vs. SSC-A to gate the lymphocytes.
9. Gate T cells by using the CD3 vs. TCR V $\alpha$ 7.2 combination (*see* Note 13 and Subheading 3.11).
10. Gate the MAIT cell population by plotting CD161 vs. TCR V $\alpha$ 7.2 (*see* Note 14). Optional: in order to identify conventional CD4<sup>+</sup> and CD8<sup>+</sup> T cells, gate all the cells except the MAIT cells in the CD161 vs. TCR V $\alpha$ 7.2 plot and use the combination CD4 vs. CD8 to gate on the respective populations.

**3.9 LEGENDScreen™ Analysis**

The LEGENDScreen™ Kit is a highly useful tool to screen populations of interest for an extensive repertoire of surface markers. After gating on MAIT cells, it is possible to know the frequency of cells expressing every marker in the kit by using a histogram, and to compare with other cell populations, such as CD4+ and CD8+ conventional T cells (Fig. 1). However, it should be noted that this kit covers an extensive panel of markers with varying staining patterns, including those with clear negative and positive peaks, as well as weakly positive populations with no discernable peaks (i.e., shoulder populations). It might thus be useful to use a dot or contour plot with the LEGENDScreen™ marker in combination with another marker in order to understand the staining pattern and adequately set the gate. Also, other cell populations in the same sample, such as CD3+ cells, can be used as internal negative or positive controls for the marker in question. Importantly, the negative background of the markers varies across the kit, which is possibly due to a variation in the concentration of the antibodies within the LEGENDScreen™ kit. It is therefore highly recommended to go through the markers individually and set the gate adequately for each of the cell populations of interest. Fig. 1 shows the expression levels of CD26, one of the LEGENDScreen™ markers. As previously reported [23], all MAIT cells express high levels of CD26. This marker is also expressed, albeit at lower levels, by most conventional CD4+ T cells and by few conventional CD8+ T cells (Fig. 1).

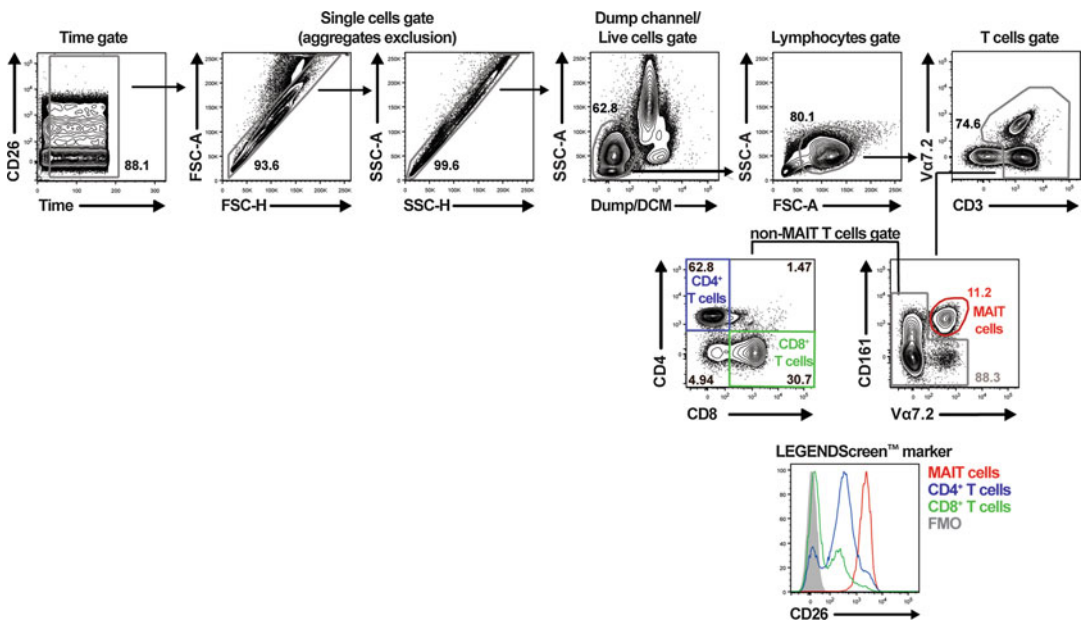


**Fig. 1** Gating strategy to identify MAIT cells and conventional CD4+ and CD8+ T cells by flow cytometry. Histogram shows the expression of the LEGENDScreen™ marker CD26 on MAIT cells and conventional CD4+ and CD8+ T cells. *FMO* fluorescence minus one control

Alternatively, or in combination with the frequency analysis, the geometric mean fluorescence intensity (geoMFI) of the markers within the cell populations of interest can be obtained through the *Statistics* tool in the FlowJo software.

Data from FlowJo can be exported to create heat maps, which facilitate the task of identifying distinct patterns of expression across populations. Data can also be used for cluster analysis in order to understand how close different cell populations are based on their expression levels of the different markers. JMP software offers different analysis tools for this type of data sets, such as principal component analysis and the possibility of combining heat maps and cluster analysis. Detailed instructions on how to perform such analyses have been published in previous issues of this series [24, 25].

### 3.10 Transcription Factor Profile Analysis

The identification and detailed profiling of the TFs that govern MAIT cell differentiation and effector function will undoubtedly contribute to our deeper understanding on MAIT cell immunobiology in health and disease. By analyzing just limited set of TFs, we can already determine that MAIT cells have a distinct TF profile, which is linked to MAIT cell antimicrobial effector functions when compared to conventional CD4<sup>+</sup> and CD8<sup>+</sup> T cells (Fig. 2) [16]. The range of commercially available mAbs directed against various TFs suitable for flow cytometry-based approaches is rapidly increasing. Thus, inclusion of a larger number of TFs in an analysis strategy similar to that described in Subheading 3.8 (Fig. 2) allows deeper investigation of the immunobiology of MAIT cells and their relationship with other immune cells both in health and in disease settings.

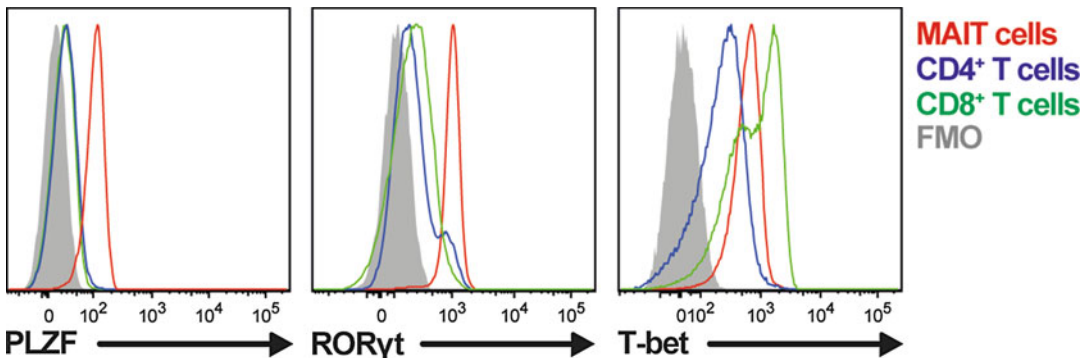


**Fig. 2** Representative example of the transcription factors PLZF, ROR $\gamma$ t, and T-bet in MAIT cells and conventional CD4<sup>+</sup> and CD8<sup>+</sup> T cells. *FMO* fluorescence minus one control

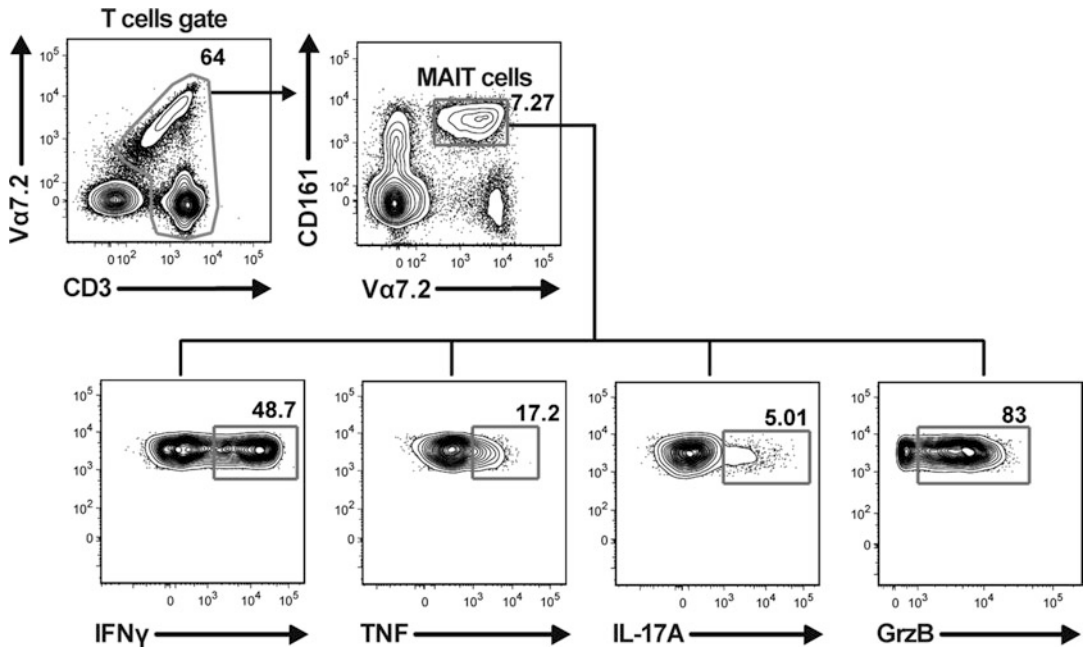


**Fig. 3** Representative flow cytometry plots of the CD3 and TCR Vα7.2 downregulation by MAIT cells and of the MAIT cell cytokine (IFN $\gamma$ , TNF, and IL-17A) and the cytolytic molecule Granzyme B (GrzB) production after 24 h stimulation with formaldehyde-fixed *E. coli*

### 3.11 Cytokine and Cytolytic Molecules Analysis

It is well known that the stimulation of T cells with cognate antigens will lead to strong downregulation of surface CD3 and TCR. Similar phenomenon is also observed when MAIT cells are stimulated by riboflavin-producing bacteria, such as *E. coli* (Fig. 3). It is therefore critical that the numbers of bacteria used are titrated by each operator to yield the optimal read-outs viz. a balance between down-regulation of surface CD3 and TCR Vα7.2 with measurable expression levels of the cytokines and cytolytic molecules of interest. Too high bacterial numbers will lead to strong downregulation of the CD3 and TCR Vα7.2 complex, rendering identification of MAIT cells from other lymphocytes in PBMC difficult, if not impossible. On the other hand, too low bacterial numbers lead to suboptimal cytokine or cytolytic molecules production. Refer to Fig. 3 and Note 13 for practical guidance on how to gate on MAIT cells that have been stimulated with *E. coli*. The use of anti-MR1 blocking mAb or pterin-based small molecules that competitively bind to MR1 and inhibit MAIT cell activation can also be included to assess the levels of MR1 dependency of MAIT cell activation [3, 13, 16, 26–28]. The overall methods described in this chapter and potential tools suitable for downstream data analyses are summarized in Fig. 4.

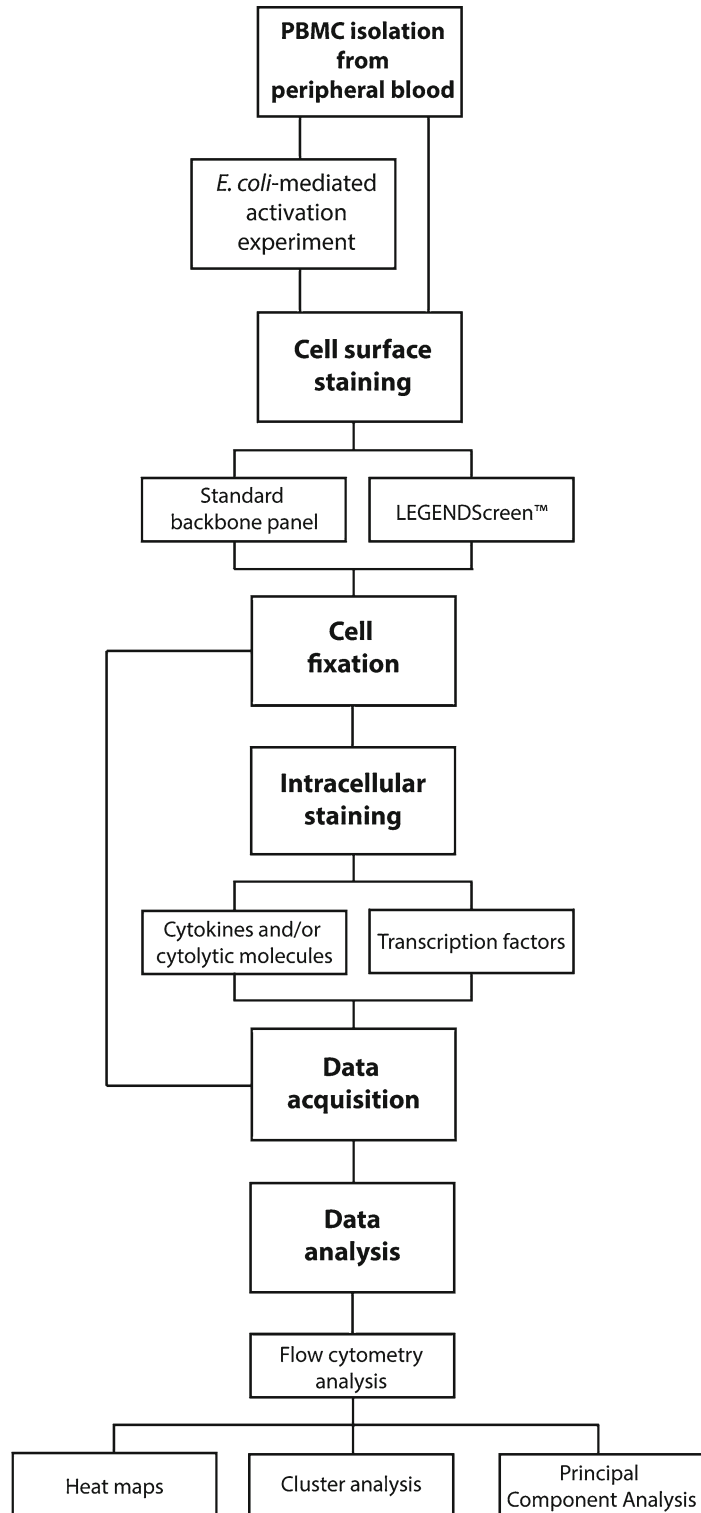


**Fig. 4** Flowchart of the methods described in this chapter and potential tools suitable for data analysis

---

## 4 Notes

1. Cells can be used after an overnight incubation on ice and at 4 °C for both phenotyping and functional assays.
2. Prepare a fresh 1× CellFIX solution after 1 month.
3.  $5 \times 10^8$  CFUs are the recommended minimum numbers of bacteria to use in order to have a decent size pellet.
4. Use a maximum amount of  $10^9$  CFUs per fixation.
5. Always use fresh preparation; do not keep bacteria on ice longer than 12 h.
6. Recommended wells: unstimulated wells, PMA-control wells, and bacteria-stimulated wells.
7. Do not exceed cell numbers or density. Make multiple wells of the same conditions if higher cell numbers are needed, then combine the cells at the end of the activation assay and before staining.
8. Titration of bacteria is recommended. 1–10 CFUs of *E. coli* strains D21 and DH5 $\alpha$  per cell was optimal for cytokine detection at 24 h.
9. Addition of anti-CD28 for co-stimulation increases the cytokine production by MAIT cells.
10. Because the expression levels of TFs by MAIT cells may vary and may not be as high as those of surface marker or cytokines, it is important to include a fluorescence minus one (FMO) control. An FMO control is where a staining panel contains all the fluorochromes except for the one that is being measured. An FMO control will therefore allow a proper measurement of the TF expression levels, especially when lowly expressed (*see* Fig. 2).
11. When possible, the samples should be run on the flow cytometer no later than 24 h after staining.
12. For this particular staining, 50  $\mu$ L of antibody cocktail was added per  $10^7$  cells, rather than per  $10^6$  cells. The dilution factors of the antibodies were adjusted when necessary.
13. The use of this combination rather than a CD3 histogram only is crucial when analyzing MAIT cell-stimulated samples to avoid excluding MAIT cells that have mildly downregulated CD3, before subsequently gating the *bona-fide* MAIT cells population using the conventional TCR V $\alpha$ 7.2 vs. CD161 combination (*see* Subheadings 3.8. and 3.11).
14. Apart from the CD161 vs. TCR V $\alpha$ 7.2 combination, MAIT cells can also be identified using the MRI tetramer loaded with MAIT cell antigens [9, 10]. However, these reagents are not available for most laboratories and their construction can be challenging, thus making the combination of CD161 and TCR V $\alpha$ 7.2 the widely used standard procedure to identify MAIT cells by flow cytometry.

## References

1. Le Bourhis L, Mburu YK, Lantz O (2013) MAIT cells, surveyors of a new class of antigen: development and functions. *Curr Opin Immunol* 25(2):174–180. doi:10.1016/j.coi.2013.01.005
2. Godfrey DI, Uldrich AP, McCluskey J et al (2015) The burgeoning family of unconventional T cells. *Nat Immunol* 16(11):1114–1123. doi:10.1038/ni.3298
3. Huang S, Martin E, Kim S et al (2009) MR1 antigen presentation to mucosal-associated invariant T cells was highly conserved in evolution. *Proc Natl Acad Sci U S A* 106(20):8290–8295. doi:10.1073/pnas.0903196106
4. Treiner E, Duban L, Bahram S et al (2003) Selection of evolutionarily conserved mucosal-associated invariant T cells by MR1. *Nature* 422(6928):164–169. doi:10.1038/nature01433
5. Le Bourhis L, Martin E, Peguillet I et al (2010) Antimicrobial activity of mucosal-associated invariant T cells. *Nat Immunol* 11(8):701–708. doi:10.1038/ni.1890
6. Martin E, Treiner E, Duban L et al (2009) Stepwise development of MAIT cells in mouse and human. *PLoS Biol* 7(3), e54. doi:10.1371/journal.pbio.1000054
7. Corbett AJ, Eckle SB, Birkinshaw RW et al (2014) T-cell activation by transitory neoantigens derived from distinct microbial pathways. *Nature* 509(7500):361–365. doi:10.1038/nature13160
8. Kjer-Nielsen L, Patel O, Corbett AJ et al (2012) MR1 presents microbial vitamin B metabolites to MAIT cells. *Nature* 491(7426):717–723. doi:10.1038/nature11605
9. Rahimpour A, Koay HF, Enders A et al (2015) Identification of phenotypically and functionally heterogeneous mouse mucosal-associated invariant T cells using MR1 tetramers. *J Exp Med* 212(7):1095–1108. doi:10.1084/jem.20142110
10. Reantragoon R, Corbett AJ, Sakala IG et al (2013) Antigen-loaded MR1 tetramers define T cell receptor heterogeneity in mucosal-associated invariant T cells. *J Exp Med* 210(11):2305–2320. doi:10.1084/jem.20130958
11. Chua WJ, Truscott SM, Eickhoff CS et al (2012) Polyclonal mucosa-associated invariant T cells have unique innate functions in bacterial infection. *Infect Immun* 80(9):3256–3267. doi:10.1128/iai.00279-12
12. Gold MC, Cerri S, Smyk-Pearson S et al (2010) Human mucosal associated invariant T cells detect bacterially infected cells. *PLoS Biol* 8(6), e1000407. doi:10.1371/journal.pbio.1000407
13. Kurioka A, Ussher JE, Cosgrove C et al (2015) MAIT cells are licensed through granzyme exchange to kill bacterially sensitized targets. *Mucosal Immunol* 8(2):429–440. doi:10.1038/mi.2014.81
14. Le Bourhis L, Dusseaux M, Bohineust A et al (2013) MAIT cells detect and efficiently lyse bacterially-infected epithelial cells. *PLoS Pathog* 9(10), e1003681. doi:10.1371/journal.ppat.1003681
15. Leeansyah E, Loh L, Nixon DF et al (2014) Acquisition of innate-like microbial reactivity in mucosal tissues during human fetal MAIT-cell development. *Nat Commun* 5:3143. doi:10.1038/ncomms4143
16. Leeansyah E, Svard J, Dias J et al (2015) Arming of MAIT cell cytolytic antimicrobial activity is induced by IL-7 and defective in HIV-1 infection. *PLoS Pathog* 11(8):e1005072. doi:10.1371/journal.ppat.1005072
17. Meierovics A, Yankelevich WJ, Cowley SC (2013) MAIT cells are critical for optimal mucosal immune responses during in vivo pulmonary bacterial infection. *Proc Natl Acad Sci U S A* 110(33):E3119–E3128. doi:10.1073/pnas.1302799110
18. Chua WJ, Kim S, Myers N et al (2011) Endogenous MHC-related protein 1 is transiently expressed on the plasma membrane in a conformation that activates mucosal-associated invariant T cells. *J Immunol* 186(8):4744–4750. doi:10.4049/jimmunol.1003254
19. Georgel P, Radosavljevic M, Macquin C et al (2011) The non-conventional MHC class I MR1 molecule controls infection by *Klebsiella pneumoniae* in mice. *Mol Immunol* 48(5):769–775. doi:10.1016/j.molimm.2010.12.002
20. Grimaldi D, Le Bourhis L, Sauneuf B et al (2014) Specific MAIT cell behaviour among innate-like T lymphocytes in critically ill patients with severe infections. *Intensive Care Med* 40(2):192–201. doi:10.1007/s00134-013-3163-x
21. Leung DT, Bhuiyan TR, Nishat NS et al (2014) Circulating mucosal associated invariant T cells are activated in *Vibrio cholerae* O1 infection and associated with lipopolysaccharide antibody responses. *PLoS Negl Trop Dis* 8(8), e3076. doi:10.1371/journal.pntd.0003076
22. Smith DJ, Hill GR, Bell SC et al (2014) Reduced mucosal associated invariant T-cells are associated with increased disease severity and *Pseudomonas aeruginosa* infection in cystic fibrosis. *PLoS One* 9(10), e109891. doi:10.1371/journal.pone.0109891
23. Sharma PK, Wong EB, Napier RJ et al (2015) High expression of CD26 accurately identifies

- human bacteria-reactive MR1-restricted MAIT cells. *Immunology* 145(3):443–453. doi:[10.1111/imm.12461](https://doi.org/10.1111/imm.12461)
24. Groth D, Hartmann S, Klie S et al (2013) Principal components analysis. *Methods Mol Biol* 930:527–547. doi:[10.1007/978-1-62703-059-5\\_22](https://doi.org/10.1007/978-1-62703-059-5_22)
25. Nugent R, Meila M (2010) An overview of clustering applied to molecular biology. *Methods Mol Biol* 620:369–404. doi:[10.1007/978-1-60761-580-4\\_12](https://doi.org/10.1007/978-1-60761-580-4_12)
26. Eckle SB, Birkinshaw RW, Kostenko L et al (2014) A molecular basis underpinning the T cell receptor heterogeneity of mucosal-associated invariant T cells. *J Exp Med* 211(8):1585–1600. doi:[10.1084/jem.20140484](https://doi.org/10.1084/jem.20140484)
27. Huang S, Gilfillan S, Kim S et al (2008) MR1 uses an endocytic pathway to activate mucosal-associated invariant T cells. *J Exp Med* 205(5):1201–1211. doi:[10.1084/jem.20072579](https://doi.org/10.1084/jem.20072579)
28. Soudais C, Samassa F, Sarkis M et al (2015) In vitro and in vivo analysis of the gram-negative bacteria-derived riboflavin precursor derivatives activating mouse MAIT cells. *J Immunol* 194(10):4641–4649. doi:[10.4049/jimmunol.1403224](https://doi.org/10.4049/jimmunol.1403224)

## Developmental and Functional Assays to Study Murine and Human $\gamma\delta$ T Cells

Julie C. Ribot, Karine Serre, and Bruno Silva-Santos

### Abstract

The key roles played by gamma-delta ( $\gamma\delta$ ) T cells in immunity to infection and tumors critically depend on their differentiation into effectors capable of secreting cytokines (such as interferon- $\gamma$  or interleukin-17), and killing infected or transformed cells. Here we detail the main methods used to investigate the differentiation of  $\gamma\delta$  T cells from murine or human origin. We describe developmental assays, such as thymic organ cultures (TOCs) and coculture of progenitors cells with OP9-DL1 stromal cells, as well as functional assays typically employed to evaluate  $\gamma\delta$  T cell cytotoxicity and cytokine production.

**Key words**  $\gamma\delta$  T cells, Thymic development, Thymic organ culture (TOC), Effector differentiation, Cytotoxicity, Cytokine production, Intracellular FACS staining

---

### 1 Introduction

$\gamma\delta$  T cells are multifaceted unconventional T cells that share innate and adaptive features and functions. They are endowed with potent cytotoxicity and produce large amounts of immunomodulatory cytokines, including interferon-gamma (IFN- $\gamma$ ), tumor necrosis factor-alpha (TNF- $\alpha$ ), interleukin (IL)-17, IL-10, IL-13, TGF- $\beta$ , and GM-CSF [1–6].  $\gamma\delta$  T cells sense changes in their microenvironment and respond to a variety of stress-inducible or pathogen-associated proteins or metabolites via their T cell receptor (TCR), cytokine receptors and natural cytotoxicity receptors (NCR) [7]. For all these reasons, they have been conceptualized as the first lymphoid line of immune defense [8, 9].

Mouse and human  $\gamma\delta$  T cells share many developmental and functional properties. However, whereas murine  $\gamma\delta$  T cells exit the thymus already predetermined to produce either IFN- $\gamma$  or IL-17 upon activation [2, 10], human  $\gamma\delta$  thymocytes are immature and selectively acquire their type 1/cytotoxic functions upon stimulation with IL-2 or IL-15 [11]. Infections of individuals leads to peripheral differentiation and circulating  $\gamma\delta$  T cells are mostly

mature effector cells, highly prone to produce IFN- $\gamma$  and TNF- $\alpha$ , and notably cytotoxic against viral-infected and transformed cells [12, 13]. The mechanisms regulating IL-17 production by human  $\gamma\delta$  T cells lags behind our understanding of the differentiation of mouse IL-17<sup>+</sup>  $\gamma\delta$  T cells. Similarities and differences between mouse and human are important to decipher, since in both species  $\gamma\delta$  T cells play critical role(s) in many aspects of immune responses including infection, cancer and tissue homeostasis and repair. In particular, given their potent antitumor properties [14] and the recent finding that intra-tumoral  $\gamma\delta$  T cells are the most significant favorable prognostic immune population [15],  $\gamma\delta$  T cells are increasingly attractive mediators of cancer immunotherapy [16]. However, such potent cells are also involved in pathogenic situations, often because they are a major source of IL-17 in animal models of autoimmune disorders including collagen-induced arthritis (CIA) and experimental autoimmune encephalomyelitis (EAE), as well as in human psoriasis [17], bacterial meningitis [18], and colon cancer [19]. Therefore, a better understanding of the mechanisms involved in the regulation of their activation and functional differentiation towards IFN- $\gamma$ - or IL-17-producers would greatly support the design of new clinical protocols to improve  $\gamma\delta$  T cell-mediated treatments [20].

The absence of genetic tools for selective targeting of  $\gamma\delta$  T cells *in vivo* has prevented the manipulation of molecular pathways in this specific cell lineage. Thus, studies on  $\gamma\delta$  T cell development and functional differentiation depend heavily on *in vitro* experiments. In this chapter we describe the main *in vitro* methods used to assess  $\gamma\delta$  T cell development and effector functions. We detail methods to study the development of  $\gamma\delta$  T cells from mouse and human thymocytes progenitors in either 3D thymic organ cultures or 2 D co-cultures with a mouse bone marrow stromal cell line (OP9-DL1). In addition, we present methods to assess the main effector functions of  $\gamma\delta$  T cells, *i.e.*, cytokine production and cytotoxicity (as measured by their ability to kill tumor cell lines), either starting from murine or human material ( $\gamma\delta$  T cells or their thymic progenitors).

---

## 2 Materials

All approaches require basic laboratory equipment including laminar flow hood, table centrifuge, pipettes, and plasticware.

### 2.1 *Sample Preparation and $\gamma\delta$ T Cell Isolation*

1. Dissection kit: regular dissection forceps, surgical scissors, needles.
2. Dissection microscope.
3. Flow cytometry activating cell sorter (FACS).
4. Petri dishes.

5. Falcon tubes.
6. 70  $\mu\text{m}$  cell strainers.
7. Nylon mesh.
8. Culture media: RPMI and DMEM completed with 10% fetal calf serum, 1 mM sodium pyruvate, nonessential amino acids, 10 mM Hepes, 100 IU/ml penicillin, 100  $\mu\text{g}/\text{ml}$  streptomycin, 50  $\mu\text{g}/\text{ml}$  gentamycin, 50  $\mu\text{M}$   $\beta$ -mercaptoethanol.
9. Heparin (stock concentration 5000 IU/ml).
10. Red blood cell lysis buffer.
11. Ficoll solution.
12. 0.8  $\mu\text{M}$  Isopore membranes.
13. MACS TCR $\gamma/\delta$ + T Cell Isolation Kit (Miltenyi Biotec).

## **2.2 Developmental Assays**

1. Bone marrow stroma cell line expressing Notch Ligand Delta-Like 1: OP9-DL1.
2. Falcon tubes.
3. Culture flasks.
4. 96-well plates.
5. 0.25% trypsin solution.
6. Irradiator.

## **2.3 Functional Assays**

1. FACS analyzer.
2. FACS tubes.
3. FACS buffer: PBS, 0.1% (w/v) sodium azide, 1% FCS, 2 mM EDTA.
4. 2 mg/ml phorbol 12-myristate 13-acetate (PMA) stock solution.
5. 2 mg/ml ionomycin stock solution.
6. 2 mg/ml brefeldin A stock solution.
7. CellTrace Far Red DDAO-SE.
8. Recombinant mouse cytokines: IL-1 $\beta$ , IL-23, IL-7.
9. Recombinant human cytokines: IL-2, IL-7, IL-15, Flt3-L.
10. Fc Block solution of anti-Fc Receptor 24G2 rat antibody.
11. 10 $\times$  Annexin V buffer (eBioscience).
12. Annexin V-FITC.
13. Anti human TCR $\gamma\delta$  MicroBead Kit (Miltenyi).
14. Foxp3 eBioscience kit.
15. Murine antibodies: anti-TCR $\delta$  (GL3), anti-CD3 $\epsilon$  (145-2C11), anti-CD4 (RM4-5), anti-CD8 (53-6.7), anti-CD25 (PC61 5.3), anti-CD28 (37-51), anti-IFN $\gamma$  (XMG1.2), anti-IL-17A (TC11-18H10; 17B7).

16. Human antibodies: anti-PanTCR $\gamma\delta$  (SA6E9), anti-CD3 (UCHT1), anti-CD4 (RPA-T4), anti-CD8 (HIT8a), anti-IFN $\gamma$  (B27).

---

### 3 Methods

Carry out all procedures at room temperature unless otherwise specified.

#### 3.1 Preparation of Single Cell Suspensions of $\gamma\delta$ T Cells

##### 3.1.1 Isolation of $\gamma\delta$ T Cells from Murine Organs

All procedures are processed in the laminar flow hood in sterile conditions.  $\gamma\delta$  T cells are harvested either from thymus ( $\gamma\delta$  thymocytes) or from secondary lymphoid organs. In both cases manipulation is similar.

1. Remove thymus or secondary lymphoid organs. The later include spleen, and the following lymph nodes popliteal, inguinal, axillary, brachial, cervical, mesenteric, periaortic. Process thymus or secondary lymphoid organs separately.
2. Put organs in a 70  $\mu\text{m}$  cell strainer placed in a Petri dish containing complete RPMI.
3. Make single cell suspensions for lymph nodes and spleen separately. Use 1 ml plastic syringe tip to dilacerate the organs with repetitive circular movements ( $\sim 20\times$ ) through the mesh of the strainer.
4. For thymus or lymph nodes filter on a new 70  $\mu\text{m}$  cell strainer to obtain a cell suspension. Centrifuge at  $453\times g$  for 5 min. Discard supernatant and resuspend in complete RPMI.
5. For spleen, filter on a new 70  $\mu\text{m}$  cell strainer to obtain a cell suspension. Centrifuge at  $453\times g$  for 5 min. Discard supernatant and resuspend in red blood cell lysis (500  $\mu\text{l}$  per spleen). Centrifuge at  $453\times g$  for 5 min. Discard supernatant and resuspend in complete RPMI.
6. Mouse  $\gamma\delta$  thymocytes are isolated from thymus while peripheral  $\gamma\delta$  T cells are isolated from spleen and lymph nodes, in both cases by FACS as CD3 $^+$  TCR $\delta^+$  cells. Refer to your facility specialist to perform FACS sorting.

##### 3.1.2 Isolation of $\gamma\delta$ T Cells from Human Thymus

1. Human thymic specimens are collected when excision of this organ is unavoidable in children undergoing corrective cardiac surgery (*see* **Note 1**). In a sterile Petri dish, cut the organ using sterile #7 forceps and scissors into pieces of  $\sim 5\text{ mm}^3$ .
2. Place a nylon cell strainer (70  $\mu\text{m}$ ) atop a 50 ml Falcon tube and transfer tissue and media (complete RPMI) directly onto strainer.

3. With the wide tip a plastic plunger (from a 5 ml syringe), gently but firmly press thymic tissue with a circular motion ( $\sim 30\times$ ) through the strainer.
4. Pass 20 ml additional media through the screen while continuing to mash with plunger; this will dislodge any cells caught in the strainer.
5. Centrifuge at  $453\times g$  for 10 min. Discard supernatant and resuspend in complete RPMI.

### 3.1.3 Isolation of $\gamma\delta$ T Cells from Human Peripheral Blood

1. Collect human peripheral blood on a tube containing heparin (final concentration 50 IU/ml). If using human thymocytes, proceed directly to **step 3**.
2. Gently mix anticoagulated blood with an equal volume of PBS.
3. With a sterile pipet, place 10 ml of the Ficoll solution into a 50 ml Falcon tube.
4. Slowly layer the diluted blood or thymocyte cell suspension over the Ficoll solution by gently pipetting the sample down the side of the tube.
5. Centrifuge 30 min at  $500\times g$ , RT, without brake.
6. Using a sterile Pasteur pipet, carefully remove the mononuclear cells, located at the interface between the plasma or media (upper layer) and the Ficoll (bottom).
7. Transfer the aspirated mononuclear cells to a 15 ml conical tube. Add 10 ml complete RPMI and mix thoroughly. Centrifuge at  $453\times g$  for 10 min.
8. Discard the supernatant and repeat wash with complete RPMI.
9. In both cases, (i.e., cell suspension from human blood or thymus), purify  $\gamma\delta$  T cells using the MACS TCR $\gamma/\delta$ +T Cell Isolation Kit (Miltenyi Biotec), following the manufacturer's recommendations.

## 3.2 Preparation of $\gamma\delta$ T Cells for Thymic Organ Cultures (TOCs)

### 3.2.1 Sample Collection from Murine Embryos

All procedures should be performed in sterile conditions in a cell culture hood. Wash surgical material (regular dissection #7 forceps and surgical scissors) in 70% ethanol and keep in complete RPMI.

1. Prepare 100-mm sterile petri dishes, each containing 20 ml of culture.
2. Sacrifice timed pregnant mice (at gestational age E14.5 or E15.5: *see Note 2*) by CO<sub>2</sub> asphyxiation.
3. Wipe abdomens with 70% ethanol and make an abdominal incision using scissors and forceps, remove fetus-filled uteri.
4. Transfer uteri to an empty petri dish.
5. Using scissors and forceps, remove fetuses from the uteri and transfer them to a new dish containing complete RPMI.

6. Wash out the blood by transferring fetuses to new dishes containing fresh complete RPMI.
7. Place a dissecting microscope in the cell culture hood.
8. Prepare a surgery dish by wetting a sterile compress in a petri dish.
9. Place a fetus in the supine position in a petri dish under the microscope.
10. Gently open the chest (*see Note 3*) and locate the two lobes of the thymus.
11. The thymus lobes are removed from the body by raising them with sterile #7 forceps so that the whole lobes are lifted. The isolated lobes are placed in a 1.5 ml eppendorf filled with complete RPMI.

### 3.2.2 Sample Collection from Human Thymic Biopsies

1. Prepare a petri dish filled with complete RPMI on ice under a dissecting microscope.
2. Cut thymic tissue into 1–2 mm<sup>3</sup> pieces in complete RPMI using sterile #7 forceps and surgical scissors.
3. Collect TOCs in a U-bottom 96-well plate with 150 µl/well of complete RPMI.

### 3.2.3 TOCs

1. Prepare a 6-well plate with 3 ml/well of complete RPMI.
2. Place 3–4 0.8 µM Isopore membranes (bright side up) in each well of a 6-well plate, floating on the media (*see Note 4*).
3. By using forceps, transfer the murine fetal thymuses or human thymic pieces (up to 5/membrane) (*see Note 5*).
4. Place the culture plate in a 37 °C, 5% CO<sub>2</sub> incubator for 7–14 days.
5. Replace half the medium every 3–4 days.
6. Apply a drop of the suspension buffer (100 µl) at the center of the lid of a 30 mm dish.
7. Transfer thymus lobes into the drop with #7 forceps.
8. Place a small (approximately 5 mm × 5 mm) piece of nylon mesh on the drop.
9. Attach 26-gauge needle to 1-ml syringe. Using forceps, bend the tip (top 5 mm, 90° angle) of needles.
10. Gently tease the lobes under the small piece of nylon mesh by softly pressing them with the needle. This procedure will release the thymocytes.
11. Transfer the cell suspension to a plastic tube and determine the cell number. Use the cell suspension for further examination of γδ T cell development by flow cytometry analysis.

### 3.3 $\gamma\delta$ T Cell Differentiation on a OP9-DL1 Monolayer

#### 3.3.1 OP9-DL1 Culture

1. Culture OP9-DL1 cells in a T25 flask in complete DMEM. The cells should be kept in the pre-confluent (up to 80%) condition, by the passage of one-fifth cells every 3 days (*see Note 6*).
2. To split the cells, discard culture medium and wash the flask with 4 ml of PBS.
3. Discard the PBS.
4. Trypsinize the cells with 4 ml of 0.25% trypsin solution, and incubate the cells for 5 min at 37 °C.
5. Disaggregate the cells from the plastic by pipetting them up and down, and transfer the cell suspension into a 15 ml Falcon tube containing 6 ml of complete DMEM.
6. Centrifuge the cells at  $453 \times g$  for 5 min. Discard the supernatant, resuspend the pellet in 10 ml of complete DMEM and transfer one-fifth of the cell suspension into a new T25 flask filled with complete DMEM.

#### 3.3.2 $\gamma\delta$ Progenitors/OP9-DL1 Cocultures

1. One day prior to the seeding of progenitors cells, trypsinize and wash the OP9-DL1 cells as mentioned in Subheading 3.3.1, **step 4**.
2. Count cells and resuspend at  $2 \times 10^4$  cells/ml in a Falcon tube.
3. Irradiate at 1000 rad.
4. Culture  $10^4$  OP9-DL1 cells in 500  $\mu$ l of complete DMEM/well of a 48-well plate.
5. The following day (*see Note 7*), isolate  $\gamma\delta$  thymocyte progenitors by flow cytometry, as follows: murine as CD3<sup>-</sup> CD4<sup>-</sup> CD8<sup>-</sup>  $\gamma\delta$ <sup>-</sup> CD25<sup>+</sup> (DN2/3) thymocytes; human as CD3<sup>-</sup> CD4<sup>-</sup> CD8<sup>-</sup>  $\gamma\delta$ <sup>-</sup> thymocytes.
6. Seed 100,000–200,000  $\gamma\delta$  thymocyte progenitors in 500  $\mu$ l of complete DMEM/well containing the OP9-DL1 monolayers. Add Flt-3 ligand and IL-7 solutions to a final concentration of 5 ng/ml each.
7. Incubate the culture at 5% CO<sub>2</sub> and 37 °C for 7–14 days.
8. Refresh the cocultures by transferring onto freshly prepared OP9-DL1 cells every 4–5 days. Cells can be removed by gentle pipetting and collected by centrifugation at  $453 \times g$  for 5 min. Use the cell suspension for further examination of  $\gamma\delta$  T cell development, by flow cytometry analysis.

### 3.4 Polarization of Mouse IFN- $\gamma$ -Producing $\gamma\delta$ T Cells

1. Prepare a coating solution of anti-CD3 $\epsilon$  (145.2C11) plus anti-CD28 mAb (37.51) (both at 2  $\mu$ g/ml) in PBS. Distribute 50  $\mu$ l per well of in 96-well plate (round bottom) and incubate at 4 °C overnight (*see Note 9*).
2. Remove the coating solution and wash each well with 200  $\mu$ l of complete RPMI.

3. Add 50,000 (*see Note 10*) purified  $\gamma\delta$  T cells in 200  $\mu\text{l}$  of complete RPMI and incubate at 37 °C for a period of 16–72 h.

### **3.5 Polarization of Mouse IL-17-Producing $\gamma\delta$ T Cells**

1. Prepare a cytokine solution of murine IL-1 $\beta$  (100 ng/ml) plus IL-23 (100 ng/ml) in complete RPMI (*see Note 11*).
2. Distribute 100  $\mu\text{l}$  of the cytokine solution in 96-well plate (round bottom), then top up with 100  $\mu\text{l}$  containing 50,000  $\gamma\delta$  T cells and incubate at 37 °C for a period of 16–72 h.

### **3.6 Polarization of Human IFN- $\gamma$ -Producing $\gamma\delta$ Thymocytes (See Note 12)**

1. Culture isolated  $\gamma\delta$  T cells at 10<sup>6</sup> cells/ml in complete RPMI with IL-2 or IL-15 (10 ng/ml each) in round bottom 96-well plates during 15–20 days.
2. Monitor cell density and pass cells when necessary (typically one third cells every 3–4 days).

### **3.7 Cytotoxicity Assay**

The culture of target cell line(s) (*see Note 13*) should be started at least 1 week prior to the experiment. Monitor cell density and perform regular passage to avoid confluency.

1. Activate mouse or human  $\gamma\delta$  T cells in the culture condition promoting IFN- $\gamma$  production, as mentioned above.
2. Count  $\gamma\delta$  T cells after culture.
3. Wash target cells twice in PBS.
4. Resuspend at 2  $\times$  10<sup>6</sup> of target cells in 200  $\mu\text{l}$  of PBS (10  $\times$  10<sup>6</sup>/ml). Add 200  $\mu\text{l}$  of 2  $\mu\text{M}$  CellTrace Far Red 7-hydroxy-9H-(1,3-dichloro-9,9-dimethylacridin-2-one-succinimidyl ester, DDAose, diluted in PBS).
5. Incubate for 10 min at 4 °C in the dark.
6. Wash twice in complete RPMI.
7. Count target cells.
8. Mix targets with  $\gamma\delta$  T cells at defined titrated ratios in complete RPMI, in 96-well plates (round bottom). Keep a control condition without  $\gamma\delta$  T cells to check for the background of spontaneous death.
9. If required, add anti-CD3 (1  $\mu\text{g}/\text{ml}$ ) to promote redirected lysis.
10. Incubate at 5% CO<sub>2</sub> and 37 °C for 4 h.
11. Wash the cells in PBS.
12. Resuspend in 100  $\mu\text{l}$  of Annexin V buffer.
13. Add 2  $\mu\text{l}$  of Annexin V-FITC.
14. Incubate for 15 min at room temperature, in the dark.
15. Without washing, transfer samples into FACS tubes and add 200  $\mu\text{l}$  of Annexin buffer.
16. Analyze by flow cytometry.

## 4 Notes

1. The human biopsies are from 0- to 5-year-old donors. They can be kept in complete RPMI at 4 °C until processing, up to 3 days post-surgery.
2. Timed pregnancies in mice are achieved as follows: place two females and one male in a cage in the evening (7 p.m.), and separate them in the morning (9 a.m.). Gestational age is designated by assigning the day when mice are separated as E0.5, and is confirmed on the day of the experiment according to the size and developmental features of fetuses. Generally, eight fetuses are expected from a pregnant C57BL/6 mouse.
3. To locate embryonic thymus may require practice. Fetuses and fetal thymuses are easiest to handle at gestational age E15.5.
4. It is important to make sure that: (a) the membrane is floating, (b) the samples are not in contact with each others, and (c) the samples are not covered by a drop of medium.
5. Determination of the signaling pathways participating in  $\gamma\delta$  T cell development can be assessed and manipulated at this stage by adding blocking antibodies or selective drugs.
6. The OP9-DL1 culture should be started ~1 week prior to initiating cocultures. It is important to keep cells less than 80–90% confluent. Monitor cell density to avoid exceeding this level of confluency, otherwise cells will stop proliferating and will start differentiating into adipocytes. Although the presence of some adipocytic cells will not affect the culture, large numbers will have a negative impact.
7. OP9-DL1 can be plated at least 6 h before being seeded with isolated progenitors.
8. It is important to choose different fluorochromes to purify  $\gamma\delta$  T cells and detect cytokines.
9. Alternatively, it is possible to coat wells with anti-CD3 $\epsilon$  and anti-CD28 Abs by incubating the antibodies solution for at least 4 h at 37 °C. However, for comparable results between experiments it is best to utilize always the same protocol.
10. 20,000 cells/well in 200  $\mu$ l is the minimum number of  $\gamma\delta$  T cells to be added.
11. Another alternative to stimulate IL-17-producing  $\gamma\delta$  T cells is the combination of plate-bound anti-CD3 $\epsilon$  plus anti-CD28 antibodies in the presence of 50 ng/ml IL-7 [21].
12. Circulating  $\gamma\delta$  T cells show a typical type 1/cytotoxic differentiated profile [13].
13. The P815 cell line is commonly used to assess murine  $\gamma\delta$  T cell cytotoxicity, in the redirected lysis condition. A panel of 20

human  $\gamma\delta$  T cell-susceptible and -resistant tumor cell lines of hematopoietic origin has been screened and described previously in the following review [20].

## Acknowledgement

This work was supported by the European Research Council (CoG\_646701 to B.S.-S.); and the Investigator FCT (to J.C.R. and K.S.) programme of Fundação para a Ciência e Tecnologia.

## References

- Jensen KD, Su X, Shin S et al (2008) Thymic selection determines gammadelta T cell effector fate: antigen-naive cells make interleukin-17 and antigen-experienced cells make interferon gamma. *Immunity* 29(1):90–100. doi:10.1016/j.immuni.2008.04.022
- Ribot JC, deBarros A, Pang DJ et al (2009) CD27 is a thymic determinant of the balance between interferon-gamma- and interleukin 17-producing gammadelta T cell subsets. *Nat Immunol* 10(4):427–436. doi:10.1038/ni.1717
- Strid J, Sobolev O, Zafirova B, Polic B, Hayday A (2011) The intraepithelial T cell response to NKG2D-ligands links lymphoid stress surveillance to atopy. *Science* 334(6060):1293–1297. doi:10.1126/science.1211250
- Rhodes KA, Andrew EM, Newton DJ, Tramonti D, Carding SR (2008) A subset of IL-10-producing gammadelta T cells protect the liver from Listeria-elicited, CD8(+) T cell-mediated injury. *Eur J Immunol* 38(8):2274–2283. doi:10.1002/eji.200838354
- Seo N, Tokura Y, Takigawa M, Egawa K (1999) Depletion of IL-10- and TGF-beta-producing regulatory gamma delta T cells by administering a daunomycin-conjugated specific monoclonal antibody in early tumor lesions augments the activity of CTLs and NK cells. *J Immunol* 163(1):242–249
- Lukens JR, Barr MJ, Chaplin DD, Chi H, Kanneganti TD (2012) Inflammasome-derived IL-1beta regulates the production of GM-CSF by CD4(+) T cells and gammadelta T cells. *J Immunol* 188(7):3107–3115. doi:10.4049/jimmunol.1103308
- Correia DV, Lopes A, Silva-Santos B (2013) Tumor cell recognition by gammadelta T lymphocytes: T-cell receptor vs NK-cell receptors. *Oncoimmunology* 2(1):e22892. doi:10.4161/onci.22892
- Hayday AC (2000) [gamma][delta] cells: a right time and a right place for a conserved third way of protection. *Annu Rev Immunol* 18:975–1026. doi:10.1146/annurev.immunol.18.1.975
- Hayday AC (2009) Gammadelta T cells and the lymphoid stress-surveillance response. *Immunity* 31(2):184–196. doi:10.1016/j.immuni.2009.08.006
- Schmolka N, Serre K, Grosso AR et al (2013) Epigenetic and transcriptional signatures of stable versus plastic differentiation of proinflammatory gammadelta T cell subsets. *Nat Immunol* 14(10):1093–1100. doi:10.1038/ni.2702
- Ribot JC, Ribeiro ST, Correia DV, Sousa AE, Silva-Santos B (2014) Human gammadelta thymocytes are functionally immature and differentiate into cytotoxic type 1 effector T cells upon IL-2/IL-15 signaling. *J Immunol* 192(5):2237–2243. doi:10.4049/jimmunol.1303119
- DeBarros A, Chaves-Ferreira M, d'Orey F, Ribot JC, Silva-Santos B (2011) CD70-CD27 interactions provide survival and proliferative signals that regulate T cell receptor-driven activation of human gammadelta peripheral blood lymphocytes. *Eur J Immunol* 41(1):195–201. doi:10.1002/eji.201040905
- Dieli F, Poccia F, Lipp M et al (2003) Differentiation of effector/memory Vdelta2 T cells and migratory routes in lymph nodes or inflammatory sites. *J Exp Med* 198(3):391–397. doi:10.1084/jem.20030235
- Silva-Santos B, Serre K, Norell H (2015) gammadelta T cells in cancer. *Nat Rev Immunol* 15(11):683–691. doi:10.1038/nri3904
- Gentles AJ, Newman AM, Liu CL et al (2015) The prognostic landscape of genes and infiltrating immune cells across human cancers. *Nat Med* 21(8):938–945. doi:10.1038/nm.3909
- Gomes AQ, Martins DS, Silva-Santos B (2010) Targeting gammadelta T lymphocytes for cancer immunotherapy: from novel mechanistic insight to clinical application. *Cancer Res* 70(24):10024–10027. doi:10.1158/0008-5472.CAN-10-3236

17. Cai Y, Shen X, Ding C et al (2011) Pivotal role of dermal IL-17-producing gammadelta T cells in skin inflammation. *Immunity* 35(4):596–610. doi:[10.1016/j.immuni.2011.08.001](https://doi.org/10.1016/j.immuni.2011.08.001)
18. Caccamo N, La Mendola C, Orlando V et al (2011) Differentiation, phenotype, and function of interleukin-17-producing human Vgamma9Vdelta2 T cells. *Blood* 118(1):129–138. doi:[10.1182/blood-2011-01-331298](https://doi.org/10.1182/blood-2011-01-331298)
19. Wu P, Wu D, Ni C et al (2014) gammadeltaT17 cells promote the accumulation and expansion of myeloid-derived suppressor cells in human colorectal cancer. *Immunity* 40(5):785–800. doi:[10.1016/j.immuni.2014.03.013](https://doi.org/10.1016/j.immuni.2014.03.013)
20. Gomes AQ, Correia DV, Grosso AR et al (2010) Identification of a panel of ten cell surface protein antigens associated with immunotargeting of leukemias and lymphomas by peripheral blood gammadelta T cells. *Haematologica* 95(8):1397–1404. doi:[10.3324/haematol.2009.020602](https://doi.org/10.3324/haematol.2009.020602)
21. Michel ML, Pang DJ, Haque SF et al (2012) Interleukin 7 (IL-7) selectively promotes mouse and human IL-17-producing gammadelta cells. *Proc Natl Acad Sci U S A* 109(43):17549–17554. doi:[10.1073/pnas.1204327109](https://doi.org/10.1073/pnas.1204327109)

# INDEX

## A

- Activation..... 2, 6–8, 10, 19, 23, 33, 49, 63, 64,  
66–72, 74, 75, 77–80, 83, 105, 109, 112, 114–115,  
117, 120, 121, 123, 125, 127, 132, 135, 136, 140,  
154, 158, 245, 246, 252, 254, 257, 258
- Adoptive cell transfer.....32
- Allergy..... 139, 203
- AMPK..... 121, 122
- Antibody..... 36–38, 42, 43, 45, 52, 57, 58,  
67–70, 74, 80, 85, 87–91, 98, 106, 109, 112–114,  
117, 122–124, 130, 131, 133, 159, 168, 210, 245,  
247, 249, 254, 259
- Antibody-conjugated beads..... 130, 133
- Antigen..... 1, 23, 31, 49, 63, 83, 93, 103,  
111, 120, 139, 154, 203, 241
- Antigen presenting cell (APC).....2, 3, 8, 9, 24, 34,  
40–42, 63, 64, 66, 72–78, 83, 85, 95, 97–99, 103,  
130, 133, 203
- Apoptosis..... 2, 5, 190, 229
- Autoimmunity..... 10, 22, 203

## B

- Bioinformatics.....155, 166, 167, 176,  
208, 214, 215, 219, 233
- Biopsy.....262
- Bi-specific T cell engagers (BITE).....111

## C

- Calcium flux.....77–78
- Cancer immunotherapy.....258
- Carboxyfluorescein succinimidyl ester (CFSE)..... 46, 56,  
84–86, 89–91, 140, 141, 146–150
- Cell cycle.....7
- Cell sorting.....32, 46, 194–195, 209–212, 242  
fluorescence activated cell sorting (FACS)..... 136,  
188, 209  
magnetic activated cell sorting  
(MACS)..... 121, 259, 261
- Checkpoint-blockade.....111
- Chemokine.....154
- Chemokine receptor..... 33, 109, 154  
CCR4..... 20, 227  
CCR5.....24

- CCR7..... 4, 10, 32–34, 36, 38, 42, 44, 45,  
53, 84, 85, 87, 88, 105–108, 190
- CCR10
- CXCR3.....20
- CXCR5.....192
- Chimeric antigen receptor (CAR)..... 111, 112, 118
- ChIP-seq.....174
- Clinical trials.....112
- Cluster analysis..... 181, 192, 251
- Combinatorial tetramer staining.....11
- Computational.....182, 208, 214, 215,  
219, 221, 228, 229
- Conventional T cells..... 140, 250
- Costimulatory molecules.....2, 9  
CD27..... 10, 32–34, 38, 44, 45, 84,  
85, 87, 88, 123, 125
- CD28.....10, 12, 64, 66, 67, 70–74, 80, 104, 106,  
108, 109, 117, 123, 125, 128–137, 156, 159–160
- CD137/4-1BB  
OX40..... 140–142, 144
- CTLA-4.....23
- Cytokine..... 2–7, 9, 11–13, 19–21, 23, 24, 32,  
35, 83–85, 87, 89, 104, 105, 108, 109, 127–130,  
132–135, 137, 154, 190, 241–254, 257, 258, 264
- IFN-g.....20
- IL-2..... 4, 12, 20–24, 50, 53, 84, 85,  
87, 104–106, 108, 115, 117, 118, 130, 133, 135,  
137, 139, 154, 156, 160, 257, 259, 264
- IL-4.....20, 23, 128, 130–133
- IL-7.....104–106, 108, 259, 263, 265
- IL-10..... 20, 22–25, 257
- IL-12.....3, 20, 21, 104–106, 108, 127, 128, 130–132
- IL-15.....104–106, 108, 257, 259, 264
- IL-17.....21, 24, 128, 129, 136, 154, 257, 258, 264, 265
- TNF.....20, 21, 24, 84, 85, 87, 91, 251, 257, 258
- Cytotoxic T cell..... 31, 44
- Cytotoxicity assay.....264–265

## D

- Differentiation..... 1, 19, 33, 49, 103, 125,  
127, 153, 173, 203, 251, 257
- DNA damage response.....119
- DNA replication.....119
- Drosha.....153

**E**

Effector differentiation ..... 8, 49  
 Effector function ..... 2, 4, 242, 251, 258  
 Epigenetic ..... 19, 20, 174, 203  
 Exhaustion ..... 10, 11, 13, 83–87, 89–91, 230

**F**

Ficoll ..... 35, 84, 104, 105, 114, 123,  
 130, 131, 136, 155, 157–159, 210, 243, 259, 261  
 Fluorescence compensation ..... 37  
 Fluorescence minus one control ..... 250

**G**

Gamma delta ( $\gamma\delta$ ) T cells ..... 257–266  
 Gating strategy ..... 43–45, 98–100, 106, 107,  
 143, 144, 148, 210, 211, 220, 250  
     boolean ..... 94, 98  
 Gene delivery ..... 2  
 Gene-transfer ..... 112, 116–118  
 Granzyme ..... 13, 24, 53, 244, 252

**H**

Heatmap ..... 179, 199, 229  
 Heterogeneity ..... 2, 4, 19, 32, 144, 187, 204,  
 208, 214, 218, 219, 230

**I**

Immune response ..... 2, 5, 23, 63, 153, 154,  
 187, 203, 204, 230, 258  
 Immunological synapse ..... 3, 65, 71–73  
 Immunosuppression ..... 23  
 Infection  
     bacterial ..... 12, 21  
     fungal ..... 21  
     viral ..... 2, 6, 32, 103, 125, 258  
 Inflammation ..... 3, 4, 22, 61, 154  
 Inhibitory receptor ..... 33, 83, 84, 87, 88  
     CD160 ..... 83–85, 87, 88  
     CTLA-4 ..... 23  
     PD-1 ..... 7, 83–85, 87, 88  
     TIM-3 ..... 24

Intracellular cytokine  
     staining ..... 84–87, 134, 243–244, 246  
 Isotype controls ..... 43, 86, 89, 247

**L**

Labeling ..... 11, 49, 140, 150, 195  
 Lentivirus ..... 122, 123  
 Library ..... 76, 158, 164–168, 171, 176,  
 206, 207, 209, 214, 215, 220–222, 228, 234  
 Lineage relationship ..... 215  
 Living drug ..... 111  
 Long noncoding RNAs ..... 173–178, 180–183  
 Long term persistence ..... 4

**M**

MAIT cells ..... 241, 242, 245–252, 254  
 Memory T cell ..... 2–7, 10–13, 24, 31–35,  
 43–45, 103–106, 108, 109, 128, 229  
 Metabolism ..... 7  
 Microarray ..... 204  
 Microchip ..... 165, 187, 188  
 Microfluidics ..... 187–191, 193–197, 199–201, 205  
 Microscopy  
     confocal ..... 63, 64, 66–72, 74, 75, 77–80  
     intravital ..... 49–59, 61  
     real time ..... 75–77  
 Migration ..... 2, 10, 20, 49, 56, 168  
 Mitochondria ..... 7, 66, 73–77, 80  
 mTOR ..... 121, 122  
 Multicolor ..... 37–39  
 Multiplexing ..... 93, 95–98, 101, 170,  
 187–191, 193–197, 199–201, 207

**N**

Naïve T cell ..... 2, 7, 10, 19, 20, 23, 24, 49,  
 103, 104, 127, 128, 131, 136, 203  
 Next-generation sequencing ..... 155, 158, 164–166, 173,  
 175–178, 180–183  
 Northern blot ..... 155–158, 160–163, 169

**O**

OP9-DL1 ..... 258, 259, 263, 265  
 Organ ..... 23, 31, 49, 56, 64, 127, 260  
     bone marrow ..... 66, 258, 259  
     liver ..... 49–61, 168, 241  
     lungs ..... 6, 168  
     spleen ..... 4, 50, 53, 54, 56, 66, 112, 113, 117, 260  
 Organ cultures ..... 258, 261–262  
 OT-I ..... 50  
 OT-II ..... 79

**P**

Panel ..... 5, 8, 9, 32, 34, 36, 38, 41, 43,  
 46, 95, 97, 140, 144, 148–149, 188, 190–194, 200,  
 242, 245, 249, 250, 254  
 PD-L1 ..... 83, 86, 89, 90  
 Peptide ..... 5, 11, 53, 67, 84–91, 93, 95, 96, 98–101  
 Peptide-MHC (pMHC) ..... 11, 35, 84, 203  
 Perforin ..... 13, 24, 154, 227  
 Peripheral blood ..... 10, 12, 105, 108, 114,  
 125, 128, 155, 158, 168, 209, 210, 243, 245, 261  
 Peripheral blood mononuclear cell (PBMC) ..... 33, 84,  
 104, 114, 123, 209, 210, 243, 245  
 pMHC tetramer ..... 84  
 Polychromatic flow cytometry ..... 32  
 Precursors ..... 2–4, 10, 20, 66, 103–106,  
 108, 109, 127–130, 132–136, 155

Principal component analysis ..... 179, 251  
 Programmed death-1 (PD-1) ..... 7, 83  
 Pro-inflammatory ..... 22, 24  
 Proliferation ..... 9, 12, 24, 83, 84, 90,  
 109, 120, 128, 140, 143, 146–150, 154

**R**

Reference genome ..... 164, 167, 178, 182,  
 214, 216, 217, 232  
 Regulatory T cell (Treg) ..... 22–25, 139–143, 145–148, 150  
 Retronectin ..... 115, 117  
 Reverse transcription (RT) ..... 158, 164, 169,  
 188, 190, 191, 194–195, 200, 204–206, 209–210,  
 212–214, 229, 232  
 RNA extraction ..... 156, 160  
 RNA interference ..... 160  
 (RNA sequencing) RNAseq ..... 175  
 RPM11640 ..... 189

**S**

Self-renewal ..... 6  
 Senescence ..... 10, 120–122  
 Sequence ..... 57, 79, 119, 120, 164, 166–168,  
 174, 176–178, 180, 182, 190, 204–208, 217, 218,  
 221, 222, 232, 233  
 Sequencing reads ..... 166, 167, 214–218  
 Single cell ..... 32, 35, 41, 49,  
 140, 187–201, 203–236, 242, 249, 260, 261  
 Single-cell RNA-sequencing (scRNA-seq) ..... 203, 204,  
 206, 208–210, 212–214, 216–221, 223–225,  
 227–229, 232–236  
 Single cell sorting ..... 209, 210, 212  
 Single-stained control ..... 39  
 Smart-seq ..... 204–210, 212  
 Spreading error ..... 41  
 Stem cell ..... 4–6, 23, 104, 105, 109  
 Stem cell memory ..... 4–7, 104  
 Stimulation ..... 3, 11, 20, 24, 32, 84, 86,  
 87, 90, 91, 104–109, 117, 125, 127, 128, 130,  
 132–137, 154, 159–160, 225, 252, 254  
 Subsets ..... 19, 20, 32, 33, 41–46, 123, 125,  
 127, 128, 135, 140, 153–164, 166–171, 206, 210,  
 211, 222, 223, 226, 228–230

Surface marker ..... 4, 10, 24, 32, 72, 84, 140,  
 142, 242, 244, 246, 247, 250, 254

**T**

T cell receptor (TCR) ..... 2, 4, 6, 8, 9, 20, 24,  
 31, 50, 53, 63, 64, 66, 79, 93, 104, 109, 112, 127,  
 128, 136, 154, 210, 241, 249, 252, 254, 257  
 TCR affinity ..... 8–10  
 TCR avidity ..... 8–10  
 T-Distributed Stochastic Neighbor Embedding  
 (t-SNE) ..... 227, 228  
 Telomerase ..... 119–124  
 Telomere erosion ..... 120  
 T<sub>EMRA</sub> ..... 11–13  
 Termed central memory (T<sub>CM</sub>) ..... 4–6, 10–12, 33, 44  
 Termed effector memory (T<sub>EM</sub>) ..... 4–6, 10–13, 33, 44, 45  
 Tetramer ..... 11  
 Th2 ..... 20–23, 127–129, 131–133, 154  
 Th17 ..... 20–24, 127–129,  
 133–134, 136, 154  
 T helper cell ..... 19–24, 127–130, 132–136  
 T helper type 1 (Th1) ..... 20–24, 127–129, 131–133, 154  
 Thymus ..... 12, 23, 31, 128, 257, 260–262, 265  
 Titration ..... 32, 35–37, 41, 43, 97, 106, 109, 136, 254  
 T memory stem cells (T<sub>SCM</sub>) ..... 4–7, 10, 33,  
 35, 44, 45, 104, 106–109  
 Transcription factors ..... 6, 7, 24, 103, 120, 127,  
 128, 133, 140, 190, 227, 241, 242, 245–251, 254  
 Eomes ..... 7, 8  
 FoxP3 ..... 21–24, 139, 140, 142, 144, 148–150, 259  
 GATA-3 ..... 20, 21, 127, 133  
 PLZF ..... 251  
 RORC ..... 128, 133  
 T-bet ..... 7, 8, 20, 127, 133  
 Transduction ..... 111–117, 123, 125, 190  
 Transfection ..... 113, 116  
 Tumor antigen ..... 13, 112

**U**

Umbilical cord blood ..... 128, 129

**W**

Western blot ..... 125